GEOCHEMISTRY OF BONINITES

AND OTHER LOW TiO_2 ISLAND ARC VOLCANIC ROCKS

by

ROSEMARY LOUISE HICKEY

B.S., Hofstra University
(1977)

Submitted to the Department of
Earth and Planetary Sciences
in Partial Fulfillment of the
Requirements of the
Degree of

DOCTORATE IN PHILOSOPHY

at the

MASSACHUSETTS INSTITUTE OF TECHNOLOGY

June 1983

© Massachusetts Institute of Technology

Signature of author: _____
Department of Earth and Planetary Sciences

Certified by: _____
Thesis Supervisor

Accepted by: _____
Chairman, Departmental Committee

MASSACHUSETTS INSTITUTE OF TECHNOLOGY
WITHDRAWN
JUN 15 1983
FROM
Lindgren

GEOCHEMISTRY OF BONINITES

AND OTHER LOW TiO_2 ISLAND ARC VOLCANIC ROCKS

by

ROSEMARY LOUISE HICKEY

Submitted to the Department of Earth and Planetary Sciences
on April 11, 1983 in partial fulfillment of the requirements
for the Degree of Doctor of Philosophy in Geology

ABSTRACT

Boninites are unusual island arc volcanic rocks with high MgO (>9%), high SiO_2 (>55%) contents, and exceptionally low TiO_2 (<0.4%) contents. High MgO contents, MgO/(MgO + ΣFeO), Ni, Cr and Co contents indicate that boninites have equilibrated with mantle peridotite. Experimental petrologic studies and high Cr/(Cr + Al) in spinels in boninites suggest that they have separated from extremely refractory residual peridotite. Based on this information and low ratios of Ti/V and Ti/Sc in boninites, which are characteristic of depleted peridotites, it is concluded that the low content of Ti and other moderately incompatible elements in boninites reflect a peridotite source which has been depleted in incompatible elements by a previous melting event. Boninites usually have high chondrite normalized LREE (light rare earth element) abundances relative to HREE (heavy rare earth element) or intermediate REE, and La/Sm ratios increase with decreasing $^{143}Nd/^{144}Nd$. Similar to other island arc volcanics, Ba and Sr are enriched relative to LREE, but K/Ba and Rb/Ba ratios in boninites are higher than in other arc volcanic rocks. These features are not consistent with derivation from depleted peridotite. A two-stage geochemical model is proposed to explain the geochemical characteristics of boninites: 1) modification of a depleted peridotite source, residual from the generation of MORB, by LREE-enriched, mantle derived fluids or melts with low $^{143}Nd/^{144}Nd$, and 2) enrichment of the source in K, Rb and to a lesser extent Sr and Ba by fluids released from subducted oceanic crust which are dominated by a component with trace element and isotopic characteristics of seawater.

The Facpi Formation, Guam consists of MgO-rich arc volcanics with low TiO_2 contents comparable to boninites, including tholeiitic basalts and boninite-like lavas with slightly lower SiO_2 contents than boninites. Abundance patterns of Ti, Sc and HREE in Facpi Formation lavas are virtually identical to boninites. Based on this observation and other similarities between Facpi Formation lavas and boninites it is concluded that low abundances of Ti and other moderately incompatible elements in Facpi Formation lavas also reflect derivation from depleted mantle peridotite. LREE/HREE ratios in Facpi Formation lavas increase with decreasing $^{143}Nd/^{144}Nd$. A LREE-enriched sample has $^{207}Pb/^{204}Pb$ similar to Pacific Ocean basalts and higher $^{206}Pb/^{204}Pb$ than Pacific Ocean sediments,

while a LREE-depleted sample has similar $^{207}Pb/^{204}Pb$, but lower $^{206}Pb/^{204}Pb$. A mantle metasomatic origin for LREE-enrichment in Facpi Formation lavas as well as boninites is supported by this data. In addition to lower SiO_2 content, boninite-like Facpi Fm. lavas differ from boninites in their lower K/Ba and Rb/Ba ratios. Basaltic Facpi Fm. lavas have lower K/Ba and Rb/Ba than the boninite-like lavas, like the majority of island arc basalts. A model is proposed to explain these major and trace element differences in which SiO_2-rich boninites originate at shallow depths within the subarc mantle, where material derived from subducted oceanic crust is dominated by K and Rb-rich fluids released by dehydration of basaltic alteration products. Basaltic Facpi Fm. lavas are generated at greater depths, where material released by subducted oceanic crust is poorer in K and Rb compared to Ba and Sr, and boninite-like Facpi Fm. lavas are generated at intermediate depths. Shallow level melting, which is consistent with the siliceous composition of boninites, can thus be related to their trace element characteristics.

Lavas from Manam Island, Bismarck Arc are low TiO_2 island arc basalts. Manam lavas have lower MgO, Ni and Cr contents than boninites, and may have evolved from a more primitive magma which equilibrated with mantle peridotite. Relative abundances of Sc, V, HREE and Ti in Manam lavas are nearly identical to boninites, and on this basis a depleted peridotite source is inferred for these low TiO_2 basalts. Enrichments in K, Rb, Ba, Sr and Pb relative to REE in Manam lavas are among the highest found in island arcs. $^{87}Sr/^{86}Sr$, $^{143}Nd/^{144}Nd$ and $^{207}Pb/^{204}Pb$ ratios are not significantly different from oceanic volcanics, which do not show this enrichment. Relative abundances of K, Rb, Ba and Sr to LREE, and Ba to K, Rb, and Sr increase with increasing $^{87}Sr/^{86}Sr$. Decreasing $^{143}Nd/^{144}Nd$ correlates with increasing LREE-enrichment, but does not correlate with abundance ratios of K, Rb, Ba, Sr or $^{87}Sr/^{86}Sr$. Extrapolation of possible mixing relationships leads to the conclusion that the peridotite sources of Manam lavas have been modified by two materials with high K, Rb, Ba and Sr abundances relative to REE. Inferred Sr and Pb-isotopic and trace element characteristics of these materials are consistent with their derivation from subducted MORB and sediment.

Based on similarities in trace element abundance patterns and isotopic ratios in boninites, and low TiO_2 island arc volcanics from the Facpi Fm. and Manam Island, a general model for development of sources for low TiO_2 volcanics is proposed: 1) refractory peridotite residual from MORB generation within the oceanic upper mantle is enriched in LREE by mantle derived fluids or partial melts, incorporated into the upper plate of a subduction zone; and 2) materials enriched in K, Rb, Ba and Sr relative to REE, derived from subducted oceanic crust, are added to the overlying peridotite. Materials released at shallow depths have higher K/Ba and Rb/Ba than materials released at greater depth. SiO_2-rich boninites are generated by partial melting of peridotite at shallow depths and have high K/Ba and Rb/Ba, while basaltic arc volcanics are generated by partial melting of deeper level peridotite and have lower K/Ba and Rb/Ba.

TABLE OF CONTENTS

LIST OF TABLES

Table

LIST OF FIGURES

Figure

ACKNOWLEDGEMENTS

First and foremost, I would like to thank Dr. F. A. Frey for his support and confidence during my time at M.I.T..

I am grateful to Drs. A. Meijer, R. A. Coish, R. W. Johnson and Mark Reagan for sharing my interest in boninites and low TiO_2 rocks, for donating samples and unpublished data for use in this thesis, and for sharing their ideas and perspectives.

I am also grateful to Drs. D. H. Green and G. A. Jenner for donating the ten boninites which initiated my interest in this research, and for the use of their unpublished data and experimental results.

Thanks to Dr. S. R. Hart for teaching me about isotope geochemistry, and for unrestricted use of his laboratories.

I would like to thank C. Y. Chen, M. Roden, H. W. Stockman, B. J. Pegram, and D. Sherman for their willingness to discuss everything, and for helping me to discover when the dumb questions were really the hard ones.

Ultimo y mas importante gracias especial por mi marido Hector por venir de Chile para ayudarme.

CHAPTER 1: INTRODUCTION

OBJECTIVES AND SCOPE

This thesis is a geochemical study of basaltic or MgO-rich island arc volcanic rocks with exceptionally low TiO_2 contents. An important rock type studied are boninites, which are found in several western Pacific island arcs. The unusual geochemical features of boninites are their high SiO_2 (>55%) and high MgO (>9%) contents, and their low TiO_2 contents (<0.4%). The potential importance of boninites to the understanding of island arc volcanism was first noted by D. H. Green. In 1973 and 1976 Green performed partial melting experiments on peridotite, designed primarily to determine if andesites could be derived from mantle peridotite under particular pressure, temperature and P-H_2O conditions. In the course of these experiments Green produced high SiO_2, high MgO liquids similar to boninites by high degrees of partial melting (~35%) of pyrolite under low pressure (10 kbar), water-saturated conditions. Liquids produced at higher pressures under water-saturated conditions were basaltic. Green concluded that typical orogenic andesites could not be derived directly by partial melting of peridotite, but that boninites could be primary island arc magmas derived by high degrees of partial melting of mantle peridotite at low to moderate pressures under water-saturated conditions.

The exceptionally low TiO_2 contents of boninites were of secondary interest to Green's experiments, however, the low TiO_2 contents of primitive island arc volcanics in general compared to MORB's (mid-ocean ridge basalts) is a long-standing geochemical problem. Sun and Nesbitt (1978a) suggested that extremely low TiO_2 basalts found in ophiolites were formed in island arc regimes, where partial melting of refractory

peridotite, depleted in Ti and other moderately incompatible elements (e.g., HREE (heavy rare earth elements) and Y) and highly incompatible elements (e.g., LREE (light rare earth elements), K, Rb and Ba) by a previous episode of melt extraction at mid-ocean ridges, might be initiated by the introduction of water from subducted oceanic crust. They suggested that boninites, which also have extremely low TiO_2 contents and are definitely arc related, were derived by this process and that their existence supported the occurrence of melting of refractory peridotite in subduction zones. For island arc volcanics in general, two basic models have been proposed to account for their low TiO_2 contents compared to MORB's: 1) that they are derived wholly or in part from mantle peridotite which has been depleted in Ti by a prevous partial melting episode (Green, 1973; 1976; Kay, 1980), similar to the model proposed by Sun and Nesbitt (1978a) for boninites and low TiO_2 ophiolitic basalts, or 2) that they are derived by partial melting of subducted MORB in the presence of residual Ti-retaining minerals (e.g., Hellman and Green, 1979). The existence of extremely low TiO_2 island arc volcanics with characteristics of primary liquids derived from peridotite lends support to the depleted peridotite source model, and indicates that study of boninites could be potentially useful in explaining some of the geochemical characteristics of other island arc volcanics.

Although the low TiO_2 contents of boninites suggest a source with unusually low abundances of incompatible and moderately incompatible elements (i.e., a depleted peridotite), early REE (rare earth element) analyses by Sun and Nesbitt (1978a) and Hickey and Frey (1979) showed that boninites are typically enriched in the highly incompatible LREE relative to the more compatible intermediate REE and HREE. This feature led to

theories of secondary metasomatic modification of the depleted peridotite sources of boninites by materials enriched in LREE and other incompatible elements (Sun and Nesbitt, 1978a; Hickey and Frey, 1979; Hickey et al., 1980; Hickey and Frey, 1982). The purposes for studying the geochemical characteristics of boninites as part of this thesis were: 1) to determine if the trace element and isotopic characteristics of boninites were consistent with their derivation from a refractory peridotite, formed as a residue from the generation of MORB's; 2) to evaluate if the metasomatic model is a suitable explanation for the enrichment of incompatible elements in boninites, and to determine as exactly as possible the geochemical characteristics and sources of incompatible element enriched materials which may have interacted with the peridotite sources; and 3) to determine if the geochemical characteristics of boninites from different geographic areas supported a single model for boninite generation.

Since a refractory peridotite source is suggested for boninites and since boninites are MgO-rich lavas containing predominantly orthopyroxene phenocrysts, relative abundances of highly incompatible and moderately incompatible elements in these rocks may reflect closely those of their peridotite sources, i.e., little modification by partial melting and fractional crystallization processes. Therefore, information about the trace element and isotopic composition of boninites could help to identify and characterize source materials for island arc volcanics in general.

Extremely low TiO_2 contents occur in some MgO-rich island arc volcanics other than boninites. Arc volcanics with these characteristics were identified by Meijer (1980), and include basalts and basaltic andesites from the Facpi Formation, Guam; Tafahi Island, Tonga; and the islands of Karkar, Manam, Kadovar and Blup Blup in the western Bismarck Arc. A

natural extension of the study of boninites is geochemical research on basaltic low TiO_2 arc volcanics. The purpose for studying these rocks was to determine if their trace element and isotopic characteristics indicated a mode of origin similar to that proposed for boninites, in particular, if a depleted peridotite source could also be proposed for these low TiO_2 volcanic rocks. The implication of such a result would be that the unusual major element composition of boninites (i.e., high SiO_2 and high MgO) is largely a result of partial melting conditions rather than source composition, and would further support a depleted source peridotite to account for the low Ti contents in arc volcanics compared to MORB's.

Trace element analyses of low TiO_2 lavas from the Facpi Formation, Guam (Chapter 4) and Manam Island, Bismarck Arc (Chapter 5) revealed that these rocks, like boninites, are enriched in highly incompatible elements relative to moderately incompatible elements. Although rocks from the Facpi Formation and Manam Island are more differentiated than boninites (e.g., 4 - 10% MgO vs 9 - 17% MgO in boninites), and contain phenocrysts of clinopyroxene and plagioclase, their relative abundances of highly incompatible elements could also be useful in characterising and identifying material added to the subarc mantle.

Most boninites and low TiO_2 island arc volcanics, as well as low TiO_2 basalts found in ophiolites, are associated spatially with lavas having higher TiO_2 contents. An additional objective of this research is to compare the tectonic settings of low TiO_2 island arc volcanics and their position within sequences including other volcanic rock types, in order to determine the tectonic requirements for the generation of low TiO_2 arc magmas. This information, in turn, may better constrain the tectonic environment of ophiolites containing low TiO_2 lavas.

RELATIONSHIP TO OTHER RESEARCH

The low TiO_2 volcanic rocks studied in this thesis were obtained through collaboration with other scientists interested in other aspects of these rocks. Boninite samples from the Bonin Islands, Mariana Trench Site 1403, and Cape Vogel, Papua New Guinea (Chapter 3) were obtained from D.H. Green and G. Jenner, who were performing petrologic experiments on these rocks (Jenner and Green, in prep.), and were later interested in the trace element geochemistry of samples from Cape Vogel (Jenner, 1981). Boninites from DSDP Site 458 (Chapter 3) were obtained from A. Meijer, who was studying the petrography and petrology of volcanic rocks cored at the Mariana fore-arc sites of DSDP Leg 60 (Meijer et al., 1981), and had a general interest in boninites and their significance to island arc volcanism (Meijer, 1980). Samples from the Facpi Formation, Guam (Chapter 4) were provided by A. Meijer and M. Reagan, who were studying the geology of Guam and the geochemistry of Guam volcanics (Reagan and Meijer, 1982; Reagan et al., 1981; Hickey and Reagan, 1981). Volcanics from Manam Island (Chapter 5) were provided by R. W. Johnson, as part of a detailed geochemical project on volcanics from the Bismarck Arc (Johnson et al., 1981). Major element analyses and some trace element analyses for samples discussed in this thesis were performed by these researchers and are noted in tables in each chapter. Samples from the Betts Cove Ophiolite for Nd-isotopic analysis were donated by R.A. Coish.

The major objective of this thesis is to compare boninites and low TiO_2 island arc volcanics from diverse geographic locations, so that geochemical and tectonic regularities, if present, can be identified and incorporated into general models for island arc volcanism. The results of

this research are organized as follows: in Chapter 2, the major element and petrographic features of boninites and low TiO_2 arc volcanics are compared to each other and to existing definitions of boninite, and a general classification scheme for these rocks is proposed. In Chapters 3, 4, and 5, the geochemical characteristics of boninites and low TiO_2 lavas from the Facpi Formation, Guam and Manam Island, Bismarck Arc are presented, and geochemical models for each area are discussed. In Chapter 6, geochemical characteristics of low TiO_2 lavas from the Betts Cove Ophiolite and the Troodos Ophiolite and Arakapas Fault Belt, Cyprus are reviewed and compared to boninites and low TiO_2 island arc lavas. In Chapter 7, geochemical and tectonic regularities between low TiO_2 lavas noted in earlier chapters are discussed and used to develop a general model for the sources and generation of low TiO_2 volcanics and their position in the development of island arcs, and to constrain geochemical models for island arc volcanism. In Chapter 8, the results of this research are summarized and major conclusions presented.

CHAPTER 2: CLASSIFICATION AND DESCRIPTION OF LOW TiO_2 VOLCANIC ROCKS

Until recently the rock name "boninite" was relatively obscure in the geological literature. In response to the large number of "boninite-like" volcanic rocks discovered within the past 25 years, Cameron et al. (1979) and Meijer (1980) suggested definitions for boninite based on the petrographic and geochemical characteristics of these rocks. On the basis of these definitions, associations between boninites and other volcanic rocks were proposed. In this chapter the petrographic and major element features of boninites and volcanic rocks associated with them are compared, and a new criterion for classification of these rocks is suggested.

BONINITES FROM THE BONIN ISLANDS, JAPAN

The term boninite was introduced by Petersen (1891) to describe chemically and petrographically unusual rocks from the Bonin Islands, Japan. According to Johanssen (1937), Petersen described boninite as a glass-rich rock containing phenocrysts of olivine, bronzite and clinopyroxene, but virtually no plagioclase. Earlier descriptions and chemical analyses of rocks from the Bonin Islands were published by Kikuchi (1890). These analyses and Petersen's are given in Table 2.1. Currently, analysis (1) (Table 2.1) of Kikuchi (1890) is widely accepted as a "typical" boninite. This analysis was chosen by Troger (1935) in his compilation of volcanic rocks to represent boninite, and a similar composition (Average boninite, Table 2.1) was chosen by Shiraki and Kuroda (1977) as a possible parental composition from which less MgO-rich Bonin Island rocks, similar to analyses (2) and (3) of Table 2.1, could be derived by fractional crystallization of olivine and bronzite.

TABLE 2.1: MAJOR ELEMENT ANALYSES OF BONINITES FROM THE BONIN ISLANDS AND BONINITE-LIKE ROCKS FROM THE WESTERN PACIFIC

	Kikuchi (1890) (1)	Kikuchi (1890) (2)	Petersen (1891) (3)	Average[1] Boninite
SiO_2	54.4	53.18	53.92	58.0
TiO_2	--	--	--	0.27
Al_2O_3	12.9	16.18	17.98	13.9
Fe_2O_3	7.08	10.30	--	--
FeO	--	--	4.88	7.73
MnO	--	--	--	0.19
MgO	12.75	6.72	4.57	9.64
CaO	5.12	10.12	7.59	7.50
Na_2O	2.06	1.85	3.92	1.99
K_2O	0.35	0.35	1.14	0.60
H_2O	5.54	1.65	4.64	--

Bonin Island boninites: 30-70% glass, 35-56% augite, 10-20% orthopyroxene, <7% olivine (Kuroda and Shiraki, 1975)

	Mariana Trench[2] Dredge Site 1403	Cape Vogel[2] PNG	DSDP Site 458[2] Mariana Fore-arc
SiO_2	57.33	57.9	57.18
TiO_2	0.14	0.43	0.24
Al_2O_3	9.75	11.5	13.48
Fe_2O_3	--	2.39	--
FeO	9.06	7.34	8.78
MnO	0.13	0.16	--
MgO	15.19	12.6	7.56
CaO	5.86	5.96	10.84
Na_2O	1.59	1.26	1.59
K_2O	0.93	0.43	0.30
P_2O_5	0.16	0.13	--

Mariana Trench: enstatite phenocrysts with chromite inclusions, in a matrix of glass, and enstatite, pigeonite and augite microphenocrysts (Dietrich et al., 1978).

Cape Vogel: phenocrysts of enstatite, bronzite and chromite in a matrix of glass, and ortho- and clinopyroxene microlites (Dallwitz et al., 1966).

Site 458: glass and microphenocrysts of clinopyroxene and rare bronzite with Cr-spinel inclusions. Plagioclase as spherulitic quench crystals with clinopyroxene (Meijer et al., 1981).

(1) Average boninite (Shiraki and Kuroda, 1977): a possible parental composition calculated by averaging four Bonin Island boninites with 7 to 13% MgO.
(2) Table 3.1, this study.

BONINITE-LIKE ROCKS FROM OTHER WESTERN PACIFIC AREAS

Since 1966, rocks which are petrographically and compositionally similar to boninites have been found in many areas in the western Pacific Ocean: Cape Vogel, Papua New Guinea (Dallwitz et al., 1966; Dallwitz, 1968); the inner Mariana Trench wall at dredge Site 1403 near Guam (Dietrich et al., 1978; Sharaskin et al., 1979) and at three dredge sites between Guam and 18° N (Hawkins et al., 1979; Bloomer et al., 1979); and at DSDP Site 458 in the Mariana fore-arc at 18° N (Meijer, 1980; Meijer et al., 1981). Several names have been used for these rocks. Sun and Nesbitt (1978a), Hickey and Frey (1979) and Jenner (1981), following Green (1973), used the term "high-Mg andesite" for samples from Cape Vogel, the Bonin Islands and Site 1403. Hawkins et al. (1979) and Bloomer et al. (1979) used the term boninite to describe their rocks, and noted that the wide variation of SiO_2 and MgO contents in their samples defined a "boninite series", consisting of MgO-rich lavas petrographically similar to boninites from the Bonin Islands, and differentiated members containing plagioclase, amphibole and quartz (Bloomer et al., 1979). Sharaskin et al. (1979) suggested that clinoenstatite-bearing samples, like those from Cape Vogel and Site 1403, be called "marianites", and orthopyroxene-bearing samples be called boninites.

Typical analyses and modes of rocks from these sites are given in Table 2.1. Except for samples from DSDP Site 458, which are similar to Bonin Island rocks with low (<8%) MgO contents, lavas from Cape Vogel and the Mariana region are very similar in composition and petrographic features to each other, and to boninites from the Bonin Islands. In addition, all of these rocks have exceptionally low TiO_2 contents (<0.4%),

a characteristic of boninites that was not evident from the early analyses which lacked TiO_2.

BONINITES AND LOW TiO_2 OPHIOLITIC BASALTS

In 1979, Cameron et al. defined boninite as: "a highly magnesian but relatively siliceous, glassy rock containing one or more varieties of pyroxene, some or all of which have a morphology of rapid growth, accessory magnesiochromite, and commonly, minor amounts of olivine. Laths of amphibole or plagioclase microlites are rare." Consequently, the previously described rocks from Cape Vogel and the Mariana Region were classed as boninites. Because the petrographic definition included olivine and stressed the textural features of boninites, Cameron et al. (1979) extended the term boninite to include low TiO_2 ophiolitic basalts from the Troodos Ophiolite and Arakapas Fault Belt, Cyprus, which were texturally similar to boninite, but generally contained a higher modal proportion of olivine, and were less SiO_2-rich. Compositional similarity, particularly low TiO_2, between these ophiolite lavas and boninites (high-Mg andesites) was also noted by Sun and Nesbitt (1978a). Sun and Nesbitt (1978a) and Cameron et al. (1979) also noted similarity between boninites and low TiO_2 basalts from the Betts Cove and Rambler, Newfoundland ophiolites, although the original mineralogy of these lavas has been destroyed by alteration and metamorphism. A third similar feature between boninites and low TiO_2 ophiolitic basalts is the high Cr/(Cr + Al) of their chromites (0.74 - 0.91 in boninites, Cameron et al., 1979; Jenner and Green, in prep; 0.65 - 0.9 in low TiO_2 basalts from Cyprus, Cameron et al., 1979; and 0.79 - 0.85 in low TiO_2 basalts from Betts Cove, Coish and Church, 1979).

THE BONINITE SERIES

Boninite-like lavas from DSDP Site 458 include two distinct mineralogical compositions. Lavas from the upper 40 meters of the volcanic section are glassy pillow lavas, with orthopyroxene and clinopyroxene microphenocrysts exhibiting quench textures and rare plagioclase as quench microlites (Meijer et al., 1981). These lavas are boninites according to Cameron et al.'s definition (Meijer, 1980). Lavas from the underlying 55 meters, although compositionally identical to the upper lavas (Meijer, 1980; Wood et al., 1981), are glass-poor and have plagioclase as a groundmass phase intergrown with clinopyroxene (Meijer et al., 1981). Meijer (1980) suggested that these differences were the result of differences in cooling rate or H_2O content, and proposed a classification scheme for boninites based on normative mineralogy. Since the low TiO_2 content of boninites from Site 458 is the most important feature distinguishing these relatively low MgO samples from other island arc volcanic rocks, Meijer (1980) proposed a classification based on normative quartz, enstatite and ilmenite contents (Fig. 2.1a). Rocks which plot toward the low ilmenite side of a line drawn between boninites from the Bonin Islands, Cape Vogel and Site 1403, and other arc volcanics were defined as members of a "boninite series" of island arc volcanics. On this diagram, petrographically different samples from Site 458 plot close to one another and close to MgO-poor boninites from the Bonin Islands.

Volcanic rocks from several areas which were not previously recognized as boninites plot within Meijer's boninite series. These include lavas from the Facpi Formation, Guam; lavas from the western Bismarck Arc islands of Karkar, Manam, Kadovar and Blup Blup, and lavas from Tafahi Island, Tonga (Meijer, 1980). Volcanic rocks from the Facpi Fm., Manam Island,

FIGURE 2.1a: Plot of normative (cation norm) quartz, enstatite and ilmenite components in boninites from Cape Vogel, Dredge Site 1403, DSDP Site 458 and the Bonin Islands, after Meijer (1980). Fe_2O_3/FeO recalculated to 0.15. Compositions with lower ilmenite content than curve are members of a "boninite series" (Meijer, 1980). Data from Table 3.1, this study; Shiraki and Kuroda (1977); and Dietrich et al. (1978).

FIGURE 2.1b: Lavas from the low TiO_2 Facpi Formation and overlying Alutom Formation, Guam on the projection quartz - enstatite - ilmenite x 10. Fe_2O_3/FeO recalculated to 0.15. Data from Table 4.1, this study; and Reagan and Meijer (1982).

FIGURE 2.1c: Lavas from Tafahi Island, Tonga and Manam Island, Bismarck Arc on the projection quartz - enstatite - ilmenite x 10. Fe_2O_3/FeO in Tafahi lavas recalulated to 0.15. Fe_2O_3/FeO in Manam lavas: (1) measured values (~1.0), and (2) recalulated to 0.15. Data from Table 5.1, this study; and Ewart et al. (1977).

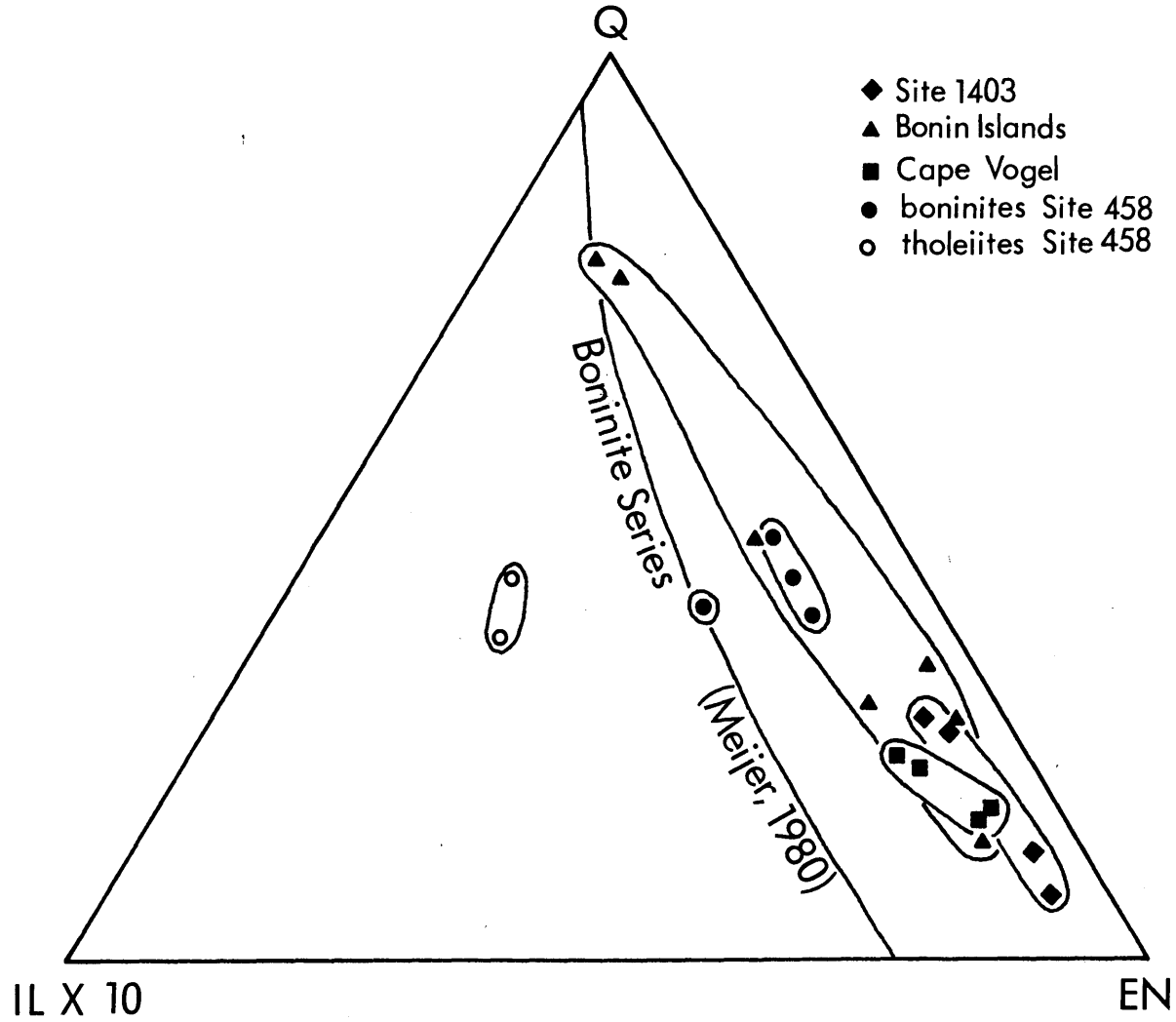
Q
IL X 10
EN
Site 1403
Bonin Islands
Cape Vogel
boninites Site 458
tholeiites Site 458
Boninite Series
(Meijer, 1980)

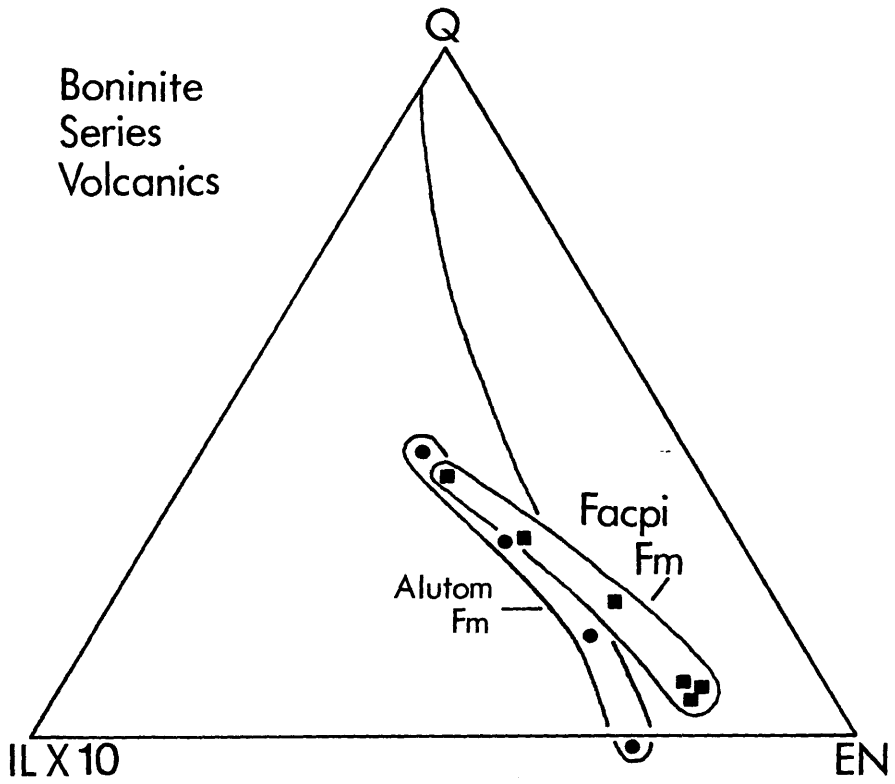
Boninite
Series
Volcanics
Q
Facpi
Fm
Alutom
Fm
IL X 10
EN

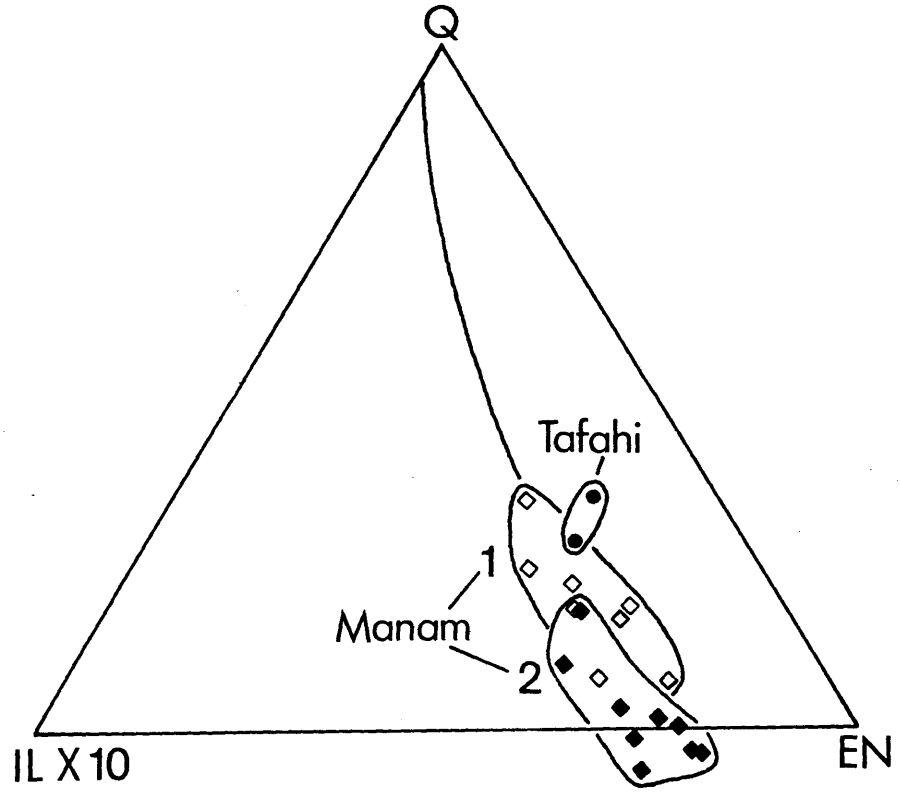
Q
Tafahi
1
Manam
2
IL X 10
EN

and Tafahi Island are shown on the boninite series projection in Figs. 2.1b and c. MgO-rich lavas from the Facpi Fm. plot within the boninite series, but more differentiated Facpi lavas (lower En content) plot outside the boninite series field. Lavas from the overlying Alutom Formation (Fig. 2.1b), which are desribed as calc-alkaline and arc tholeiitic volcanics (Reagan et al., 1981; Reagan and Meijer, 1982), have only slightly higher normative ilmenite contents than the Facpi Fm.

Meijer (1980) showed that lavas from western Bismarck Arc islands plot within the boninite series, and in Fig. 2.1c, lavas from Manam Island, Bismarck Arc overlap with the boninite series field. However, these rocks have exceptionally high (~1) Fe_2O_3/FeO ratios compared to those measured in boninites (~0.2 - 0.3, Table 3.1). If Fe_2O_3/FeO ratios in Manam lavas are recalculated to a constant value similar to boninites (e.g., Fe_2O_3/FeO = 0.15, used in Figs. 2.1a and b), many samples do not plot in the boninite series and several are not quartz normative (Fig. 2.1c). Since Fe_2O_3/FeO ratios in rocks are susceptible to post-eruptive changes, it is unclear whether recalculation to a constant value (this study) or use of measured values when available (Meijer, 1980) is best for comparison of different rocks. If differences in Fe_2O_3/FeO between these rocks result from post-eruptive alteration, then recalculation of values is probably better, and Manam lavas would not plot in the boninite series. If the high Fe_2O_3/FeO in Manam Island lavas compared to boninites is an igneous feature, then this indicates a significant difference in magma composition between these rocks and boninites.

COMPARISON OF BONINITES WITH MEMBERS OF THE BONINITES SERIES AS DEFINED BY MEIJER (1980)

In Fig. 2.2a, composition of boninite series lavas are plotted on the projection quartz - olivine - plagioclase. Several differences between boninites and boninite series lavas, as defined in Fig. 2.1, can be seen on this diagram. First, boninites have a much lower plagioclase component content than lavas from the Facpi Fm., Tafahi Island and Manam Island. Compared to the 1 atm. clinopyroxene-saturated liquidus boundaries determined for MORB's (Stolper, 1980), boninites which do not contain plagioclase do not plot within the plagioclase primary phase volume. All other boninite series lavas identified on the basis of the quartz - enstatite - ilmenite projection (Fig. 2.1) plot within the plagioclase field. Boninites which do contain plagioclase, such as samples from Site 458 and differentiated lavas from the Bonin Islands, also plot within the plagioclase primary phase volume, but have higher quartz component contents. This phase diagram may not be rigorously applicable to boninites or other arc volcanics because of the compositional differences between these rocks and MORB's. However, the presence and absence of plagioclase in these rocks corresponds to their position on the diagram, and suggests that the presence of plagioclase in lavas from the Facpi Fm., Tafahi Island and Manam Island, but not in boninites, is the result of major differences in magma composition.

A second petrographic difference between boninites and boninite series lavas can also be explained in terms of this phase diagram. A characteristic feature of boninites is the early appearance of orthopyroxene, preceeding clinopyroxene and plagioclase. In low TiO_2

FIGURE 2.2a: Boninites and "boninite series" lavas identified in Figs. 2.1a, b and c on the projection quartz - olivine - plagioclase. Boninite symbols are identified in Fig. 2.1a. Projection calculation is given in Grove et al. (1982). 1 atm clinopyroxene saturated liquidus for MORB's (Stolper, 1980) is also shown. Boninites have lower plagioclase component and higher quartz component contents than "boninite series" lavas.

FIGURE 2.2b: Calc-alkaline (Medicine Lake) and tholeiitic (Tonga) arc volcanics on the projection quartz - olivine - plagioclase. Lavas from the Facpi Formation, Guam; Manam Island, Bismarck Arc; Tafahi Island, Tonga; and differentiated boninites (e.g., some Bonin Island samples and samples from DSDP Site 458) plot in the same area as these arc volcanics. Projection calculation and Medicine Lake data from Grove et al. (1982). Tonga data from Ewart et al. (1973) and (1977).

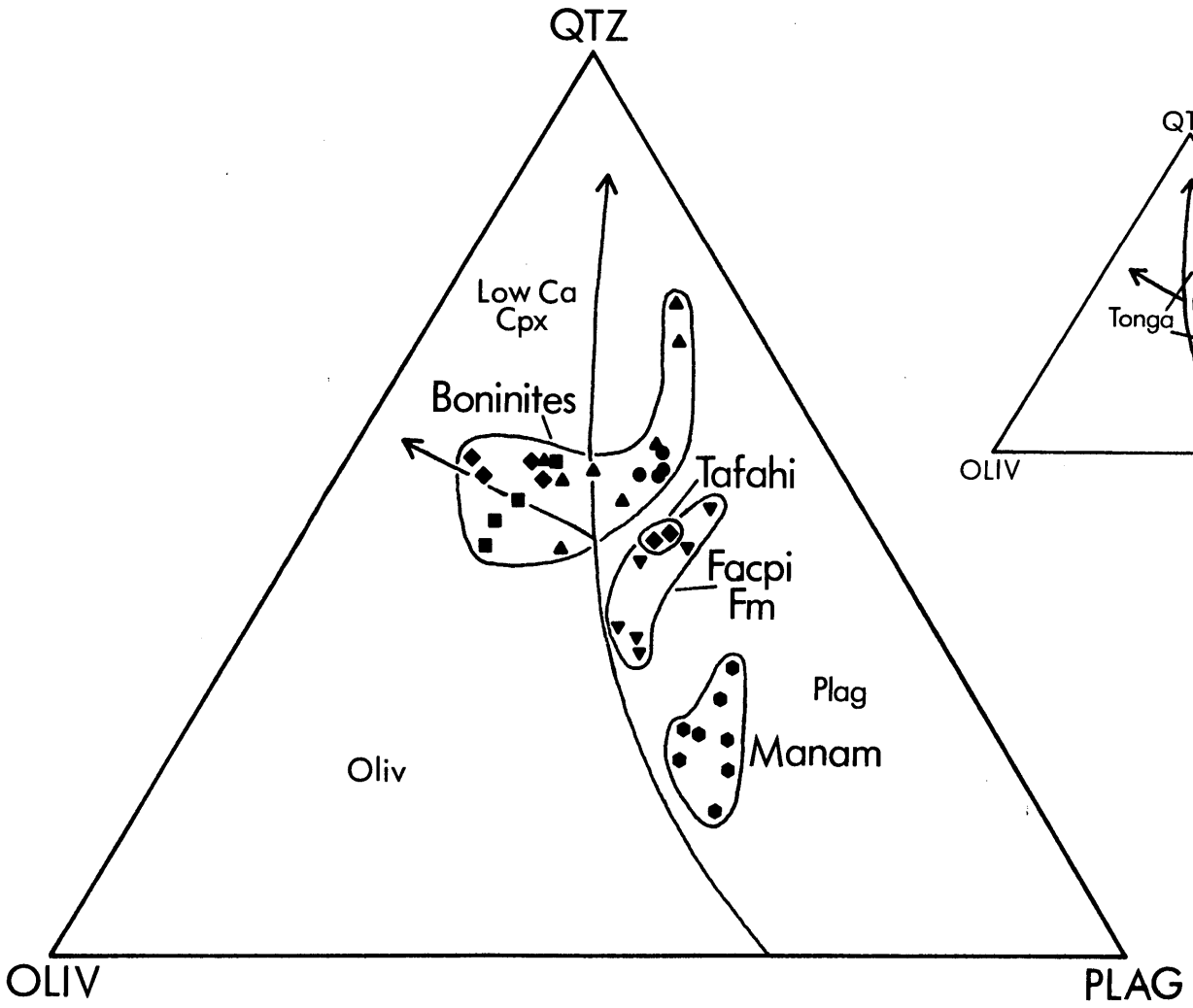
QTZ
Low Ca
Cpx
Boninites
Tafahi
Facpi
Fm
Plag
Manam
Oliv
OLIV
PLAG

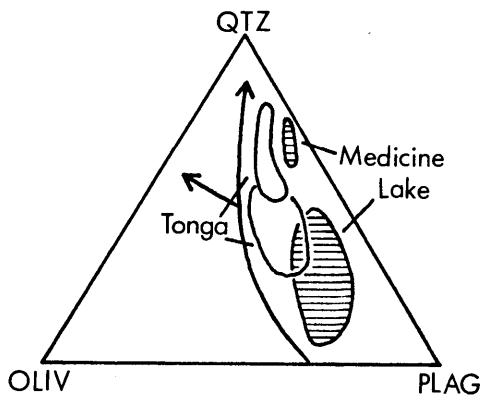
QTZ
Medicine
Lake
Tonga
OLIV
PLAG

volcanics from the Facpi Fm. and Manam Island (Chapters 4 and 5), orthopyroxene follows olivine and clinopyroxene. According to the experimental phase relationships in Fig. 2.2a, liquids with the composition of boninites will crystallize low-Ca pyroxene, either as the primary phenocryst or following crystallization of olivine. Boninite series lavas from the Facpi Fm. and Manam Island, which contain less quartz component than boninites (Fig. 2.2a), should crystallize olivine and clinopyroxene followed by plagioclase and low-Ca pyroxene, which is consistent with their mineralogy.

On the quartz - olivine - plagioclase projection (Fig. 2.2a), boninite series lavas which are petrographically different from boninites are indistinguishable from calc-alkaline and tholeiitic arc volcanics (Fig. 2.2b). In this projection, the boninite series of Meijer (1980) does not appear to represent a distinct magma series in the sense of grouping only rocks of similar parental magma composition and fractional crystallization history. Since boninites, represented by samples from the Bonin Islands, Cape Vogel, Dredge Site 1403 and Drill Site 458, have similar compositions and petrographic features which are distinct from the calc-alkaline and tholeiitic arc series (Figs. 2.2a and b), the name boninite should be reserved for these rocks. In contrast, low TiO_2 lavas from the Facpi Fm., Guam; Manam Island, Bismarck Arc; and Tafahi Island, Tonga, are more appropriately classed as low TiO_2 members of the tholeiitic or calc-alkaline island arc series, rather than as members of a "boninite series". However, the low TiO_2 contents of these lavas, shown on the quartz - enstatite - ilmenite diagram, suggests that they have a common petrogenetic factor, which is discussed in following chapters.

Distinguishing fractionated (i.e., low MgO) boninites from SiO_2-rich members of other island arc series on the basis of normative mineralogy may be impossible (e.g., Figs. 2.2a and b). Major element data for the "boninite series" from Mariana Trench dredge sites, described by Bloomer et al. (1979), could be helpful in this respect.

COMPARISON OF BONINITES WITH LOW TiO_2 OPHIOLITIC BASALTS

Representative samples of low TiO_2 ophiolitic basalts from the Troodos Ophiolite and Arakapas Fault Belt, Cyprus, and the Betts Cove Ophiolite, Newfoundland are plotted on the quartz - enstatite - ilmenite projection in Fig. 2.3a. On this diagram Arakapas lavas and some Troodos lavas are similar to MgO-rich boninites. Other Troodos lavas have higher normative ilmenite contents than boninites with similar MgO and SiO_2 contents. Lavas from the Betts Cove Ophiolite have very low normative ilmenite contents, like boninites, but some samples are not quartz normative.

In Fig. 2.3b, these low TiO_2 ophiolitic basalts are plotted on the projection quartz - olivine - plagioclase. The samples plotted were chosen to span the range in MgO, SiO_2, and TiO_2 contents for each area, in order to reveal fractionation trends, if present. The trends formed by these samples do not match the trend shown by boninites and their fractionated derivatives. For example, lavas from Troodos show increasing plagioclase component enrichment with decreasing SiO_2 and MgO, and the plagioclase-rich lavas have the highest normative ilmenite (Fig. 2.3a). Lava compositions from the Betts Cove Ophiolite are scattered on this diagram, possibly as the result of major element changes caused by metamorphism of the rocks.

FIGURE 2.3a: Low TiO_2 lavas from the Upper Pillow Lavas, Troodos Ophiolite and Arakapas Fault Belt, Cyprus, and the Betts Cove Ophiolite, Newfoundland on the projection quartz - enstatite - ilmenite x 10. Fe_2O_3/FeO recalulated to 0.15. Data from Smewing and Potts (1976), Simonian and Gass (1978) and Coish et al. (1982).

FIGURE 2.3b: Low TiO_2 lavas from the Upper Pillow Lavas, Troodos Ophiolite and Arakapas Fault Belt, Cyprus, and the Betts Cove Ophiolite, Newfoundland on the projection quartz - olivine - plagioclase. Projection calculation from Grove et al. (1982). Some Cyprus lavas overlap with the boninite field. Betts Cove lava labelled 101 is a possible parental composition chosen by Coish and Church (1979), and is less quartz rich than boninites. Data from Smewing and Potts (1976), Simonian and Gass (1978) and Coish et al. (1982).

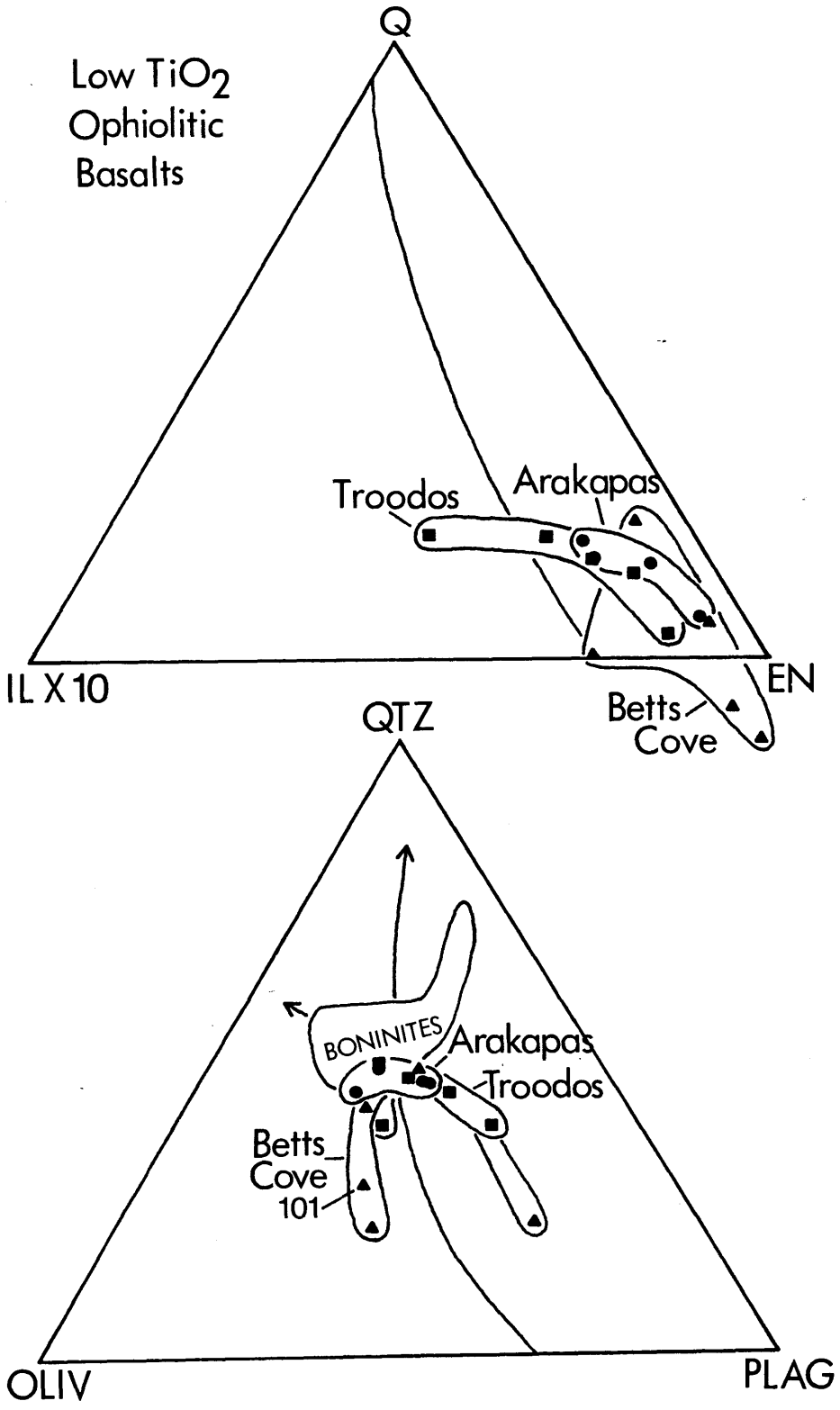
Low TiO_2
Ophiolitic
Basalts
Q
Troodos
Arakapas
IL X 10
EN
Betts
Cove
QTZ
BONINITES
Arakapas
Troodos
Betts
Cove
101
OLIV
PLAG

Some Troodos Upper Pillow Lavas, and all Arakapas Fault Belt lavas shown in Fig. 2.3b plot close to or within the boninite field. On this basis, as well as their petrographic features, these rocks are probably boninites. The compositional variation shown by the Troodos Upper Pillow Lavas in Fig. 2.3b suggests this sequence may include other types of low TiO_2 volcanics, in addition to boninites.

SiO_2-rich lavas from the Betts Cove Ophiolite also plot close to boninites in Fig. 2.3b. However, in interpreting the composition of these rocks Coish (1977) concluded that their high SiO_2 contents could be the result of secondary silicification. An MgO-rich, low SiO_2 sample (labelled 101, Fig. 2.3b) was chosen by Coish and Church (1979) as a primitive liquid composition from which other Betts Cove lavas could be derived. This composition is not boninitic, but could by fractional crystallization of olivine, yield low TiO_2 derivatives similar in composition to the non-boninitic low TiO_2 lavas included in Meijer's "boninite series".

SUMMARY

The petrographic definition of boninite given by Cameron et al. (1979) is an accurate description of boninites from the Bonin Islands, and similar rocks from Cape Vogel, Papua New Guinea and the Mariana Trench. These rocks can be distinguished from other volcanic rocks on the basis of their high quartz and low plagioclase contents on a plot of quartz, olivine and plagioclase components (Figs. 2.2a and b). Low TiO_2 rocks of the "boninite series" defined by Meijer (1980) on the basis of normative quartz, enstatite and ilmenite, which are not petrographically like boninites, are indistinguishable from calc-alkaline and arc tholeiitic rocks on the quartz - olivine - plagioclase projection and probably do not constitute a

separate island arc series. Fractionated boninite derivatives from the Bonin Islands and DSDP Site 458 also overlap with other arc volcanics on this diagram, thus further work is required to define a boninite series consisting of rocks related to boninite by fractional crystallization.

Low TiO_2 ophiolitic basalts from the Arakapas Fault Belt, Cyprus and some lavas from the Upper Pillow Lavas, Troodos Ophiolite, Cyprus, which are petrographically like boninites, are also similar to boninites on the quartz - olivine - plagioclase projection. Low TiO_2 lavas from the Betts Cove Ophiolite are probably more MgO-rich than boninites, but could by crystallization of olivine, produce liquids similar in composition to the non-boninitic low TiO_2 lavas included in the "boninite series" of Meijer (1980).

CHAPTER 3: GEOCHEMISTRY OF BONINITES

Occurrences of boninite, as defined in Chapter 2, within island arc environments are restricted to Tertiary arcs in the western Pacific Ocean: the Mariana - Bonin Arc system and southeastern Papua New Guinea. Recently, boninites have also been reported in the Zambales Ophiolite, Philippines (Hawkins et al., 1982).

This chapter is a comparative study of the geochemical features of boninites from the Bonin Islands, DSDP Site 458 in the Mariana fore-arc, Mariana Trench dredge Site 1403, and Cape Vogel, Papua New Guinea (Fig. 3.1). The similar major element and petrographic features of boninites from these areas suggests they have a similar mode of origin. The purpose of this chapter is to determine if the trace element and isotopic characteristics of boninites are also consistent with a common petrogenetic history, and to explain these characteristics. Since MgO-rich boninites have geochemical traits expected of primary magmas in equilibrium with mantle peridotite (e.g., $Mg/(Mg + \Sigma Fe) = 0.67 - 0.83$, Ni = 111 - 450 ppm, Cr = 540 - 1800 ppm), and since orthopyroxene is the dominant fractionating mineral, relative abundances of highly incompatible and moderately incompatible trace elements in boninites should be very similar to those in their sources. Therefore, the trace element and isotopic characteristics of boninites may be useful in defining processes which occur in the subarc mantle, and may provide information about the sources of island arc volcanics in general.

GEOLOGICAL BACKGROUND

Mariana - Bonin Arc System: Boninites have been found in three areas of the Mariana - Bonin Arc System (Fig. 3.1): the islands of Chichi Jima and

Muko Jima in the Bonin Islands, at DSDP Site 458 in the Mariana fore-arc at 18° N, and at Mariana Trench dredge sites along the arc wall between Guam and 18° N.

Bonin Islands: The Bonin Ridge is located in a fore-arc position, about 130 km from the Bonin Trench axis, and about 150 km east of the currently active Volcano Islands. Chichi Jima and Muko Jima, Bonin Islands, on the Bonin Ridge, are the only subaerially exposed boninite occurrences in the Mariana - Bonin Arc System. Chichi Jima is composed of pillow lavas, overlain or intercalated with volcanic breccias, and subordinate sedimentary rocks of Oligocene - Miocene age which overlie the volcanics (Kuroda and Shiraki, 1975). The pillow lavas are mainly boninite (MgO-rich boninite) and bronzite andesite, while the volcanic breccias are hypersthene andesite and dacite (Shiraki and Kuroda, 1977). A K/Ar date of 26-30 m.y. was determined on a hypersthene andesite (Kaneoka et al., 1970). On Muko Jima, 80 km north of Chichi Jima, clinoenstatite bearing boninites occur as pillow lavas and volcanic breccia (Shiraki et al., 1979). Haha Jima, 50 km south of Chichi Jima, contains no boninite, but small amounts of olivine tholeiitic pillow lava of Eocene age occur (Kuroda and Shiraki, 1975).

DSDP Site 458: At DSDP Site 458 (17° 52'N, 120 km west of the Mariana Trench), 210 meters of volcanic basement rocks were penetrated beneath early Oligocene sediments. The volcanic rock sequence consisted of 160 meters of boninite flows and pillows, divided at 120 meters by 10 meters of arc tholeiitic basalts, which also comprised the lower 40 meters of the hole. An $^{40}Ar/^{39}Ar$ age of 34 m.y. was obtained from a boninite lava from the top of Site 458 (Takigami and Ozima, 1981). At DSDP Site 459, 50 km east of Site 458, volcanic basement rocks are exclusively arc tholeiitic

FIGURE 3.1: Map of the western Pacific Ocean showing boninite locales represented in this study.

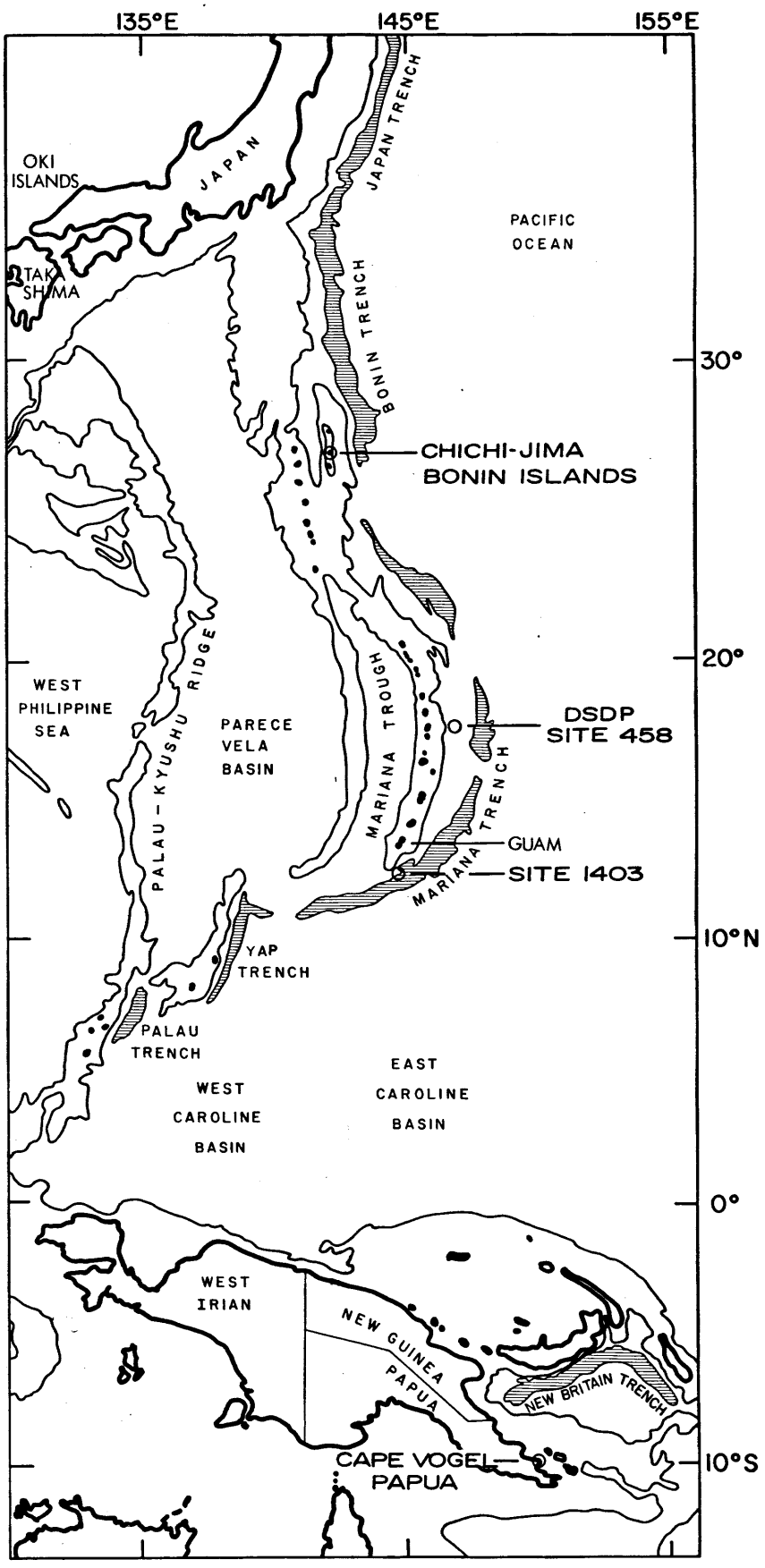
135°E
145°E
155°E
30°
20°
10°N
0°
10°S
OKI ISLANDS
JAPAN
JAPAN TRENCH
PACIFIC OCEAN
TAKA SHIMA
BONIN TRENCH
CHICHI-JIMA
BONIN ISLANDS
WEST PHILIPPINE SEA
PALAU - KYUSHU RIDGE
PARECE VELA BASIN
MARIANA TROUGH
DSDP SITE 458
GUAM
SITE 1403
MARIANA TRENCH
YAP TRENCH
PALAU TRENCH
WEST CAROLINE BASIN
EAST CAROLINE BASIN
WEST IRIAN
NEW GUINEA
PAPUA
NEW BRITAIN TRENCH
CAPE VOGEL
PAPUA

lavas, overlain by late Eocene sediments.

Dredge Site 1403: Dredge station 1403 of the 17th Cruise of the R/V "Dmitry Mendeleev" was located on the lower part of the island arc slope of the Mariana Trench about 100 km south of Guam. The igneous rocks recovered included peridotites, gabbros, basalts and boninites, and therefore include the components of an ophiolitic suite (Dietrich et al., 1978). Similar ophiolitic rock assemblages have been recovered at other arc-wall Mariana Trench dredge sites (Hawkins et al., 1979; Bloomer, 1981). At Dredge Site 1404, on the trench - slope break, basalts and dolerites were recovered. Basaltic rocks from both sites are low K_2O tholeiities and have geochemical characteristics intermediate between island arc tholeiites and MORB's (Dietrich et al., 1978; Beccaluva et al., 1980). A K/Ar age from a basalt from Site 1404 is 28 m.y. (Beccaluva et al., 1980).

The position of boninites in the tectonic development of the Philippine Basin region is a critical feature in interpreting the causes of boninite volcanism and their relationship to other arc volcanics (Chapter 7). The development of the Philippine Sea by repeated episodes of arc rifting and back-arc spreading was proposed by Karig (1971; 1975). Recently, K/Ar ages obtained from samples dredged and drilled at numerous sites in the Philippine Basin have improved time constraints on Karig's model. Syntheses of this information have been presented by Crawford et al. (1979); Scott et al. (1980); and Meijer et al. (1982), and include the following features: subduction of the Pacific Ocean crust beneath the Philippine Sea began approximately 45 m.y.b.p. as a result of a change in Pacific plate motion from northward to westward. Arc volcanism began along the Palau-Kyushu Arc (Fig. 3.1) and continued from 45 to 34 m.y.p.b.. Rifting of this arc and formation of the Parece Vela Basin by

back-arc spreading began approximately 32 m.y.b.p. and ceased approximately 20 m.y.b.p.. Arc volcanism began along the West Mariana Ridge (Fig. 3.1) between 32 and 20 m.y.b.p., and the arc was rifted by formation of the Mariana Trough at approximately 6 m.y.b.p.. Arc volcanism has occurred along the presently active Mariana Arc for at least 2 m.y..

The ages of boninites from the Mariana - Bonin Arc (28 - 34 m.y.) correspond to the latest period of arc volcanism along the Palau-Kyushu Arc or to the earliest stage of back-arc spreading of the Parece Vela Basin. They have apparently been moved through one or more periods of back-arc spreading to their present fore-arc or trench wall positions.

Cape Vogel, Papua New Guinea: Boninites from Cape Vogel (Fig. 3.1) form part of a sequence of submarine flows and pillow lavas called the Dabi Volcanics, which include, in addition to boninites, tholeiitic lavas ranging from basaltic to dacitic compositions (Smith and Davies, 1976). The volcanics are exposed along faults on the Cape Vogel Peninsula, and are overlain unconformably by early Miocene sediments (Smith and Davies, 1976). A K/Ar age of 28 m.y. (middle Oligocene) was obtained from one boninite.

The position of the Dabi Volcanics in the tectonic evolution of southeastern Papua is undetermined. The Cape Vogel Peninsula is bounded on the south by sections of the Papuan Ultramafic Belt (PUB). The Oligocene age of the volcanics indicates that they were erupted after the emplacement of the PUB in the early Eocene (Davies, 1977). Oligocene volcanics are not exposed elsewhere in southeastern Papua. Based on chemical similarities between the Dabi Volcanics and Eocene volcanics and intrusions in other areas of the PUB, Jaques and Chappell (1980) suggested that the Dabi Volcanics are also Eocene in age and were erupted in an island arc regime immediately prior to the emplacement of the PUB.

MAJOR ELEMENT CHARACTERISTICS AND SAMPLE DESCRIPTIONS

Major element compositions for boninites discussed in this chapter are listed in Table 3.1. Detailed petrographic descriptions, experimental petrological results and phenocryst compositions of samples from the Bonin Islands, Cape Vogel and Mariana Trench Site 1403 are given in Jenner (1981) and Jenner and Green (in prep.). Petrographic descriptions and phenocryst compositions for the DSDP Site 458 samples are given by Meijer et al. (1981).

Bonin Islands: Samples from the Bonin Islands include three MgO-rich boninites (samples 2981, 2982 and 2983) which range in SiO_2 from 57.2 to 58.5%, MgO from 9.4 to 12.3% and have TiO_2 contents of <0.15%. Sample 1129-4 is a bronzite andesite containing 59.7% SiO_2, 5.7% MgO and 0.3% TiO_2, and sample 1127-5 is a perlitic dacite containing 69.6% SiO_2, 1.7% MgO and 0.3% TiO_2. Samples 2981, 2982 and 2983 contain phenocrysts of orthopyroxene and a smaller amount of clinopyroxene; plagioclase occurs only in the less magnesian samples 1129-4 and 1127-5.

Cape Vogel: Four samples from Cape Vogel range in SiO_2 content from 56.8 to 57.9%, MgO from 12.6 to 17.1%, and have TiO_2 contents <0.43%. Three samples (2985, 2986 and 2987) contain clinoenstatite as the major phenocryst, while sample 2984 contains only bronzite. Boninite lavas from Cape Vogel vary from 12 to 25% MgO within a narrow range of SiO_2 contents (56.4 to 58.3%), and the most magnesian members of this series contain up to 70% clinoenstatite (Dallwitz, 1968; Jenner, 1981).

Mariana Region: Sample 2980, from Dredge Site 1403 contains 57.3% SiO_2, 15.2% MgO and 0.14% TiO_2. Other boninites from this site range from 7 to 21% MgO, 53 to 57% SiO_2 and have <0.3% TiO_2 (Dietrich et al., 1978; Sharaskin et al., 1979).

TABLE 3.1: MAJOR ELEMENT ABUNDANCES IN BONINITES FROM THE WESTERN PACIFIC AND AN ARC THOLEIITE FROM DSDP SITE 458

	CHICHI JIMA, BONIN ISLANDS, JAPAN				
	2981(1)	2982(1)	2983(1)	1129-4(2)	1127-5(2)
SiO_2	58.46	57.23	58.43	59.69	69.56
TiO_2	0.10	0.12	0.15	0.29	0.33
Al_2O_3	13.37	10.61	11.35	14.44	13.26
Fe_2O_3	--	--	--	1.67	0.87
FeO	8.27	8.8	8.57	6.73	5.16
MnO	--	--	0.12	0.23	0.12
MgO	9.39	12.27	11.40	5.71	1.65
CaO	8.11	9.69	7.76	8.38	4.80
Na_2O	1.59	0.87	1.74	2.28	3.27
K_2O	0.70	0.33	0.51	0.51	0.95
P_2O_5	--	--	--	0.07	0.04
Cr_2O_3	0.14	0.18	0.19	--	--
H_2O^+(6)	3.92	3.11	3.78	3.65	4.88
$\frac{Mg}{Mg + \Sigma Fe}$	0.67	0.71	0.70	0.55	0.33

	CAPE VOGEL PAPUA NEW GUINEA				MARIANA TRENCH SITE 1403
	2984(3)	2985(3)	2986(3)	2987(3)	2980(1)
SiO_2	56.8	57.9	57.6	57.58	57.33
TiO_2	0.33	0.43	0.33	0.25	0.14
Al_2O_3	11.9	11.5	9.15	8.50	9.75
Fe_2O_3	1.73	2.39	2.61	2.74	--
FeO	7.1	7.34	6.95	7.41	9.06
MnO	0.16	0.16	0.17	0.22	0.13
MgO	12.6	12.6	16.8	17.10	15.19
CaO	7.89	5.96	4.92	5.11	5.86
Na_2O	1.05	1.26	1.10	0.64	1.59
K_2O	0.41	0.43	0.22	0.37	0.93
P_2O_5	0.03	0.13	0.08	0.06	0.16
H_2O^+(6)	2.65	4.35	2.65	4.34	4.27
$\frac{Mg}{Mg + \Sigma Fe}$	0.72	0.70	0.76	0.76	0.75

TABLE 3.1 (CONT'D): MAJOR ELEMENT ABUNDANCES IN BONINITES FROM THE WESTERN PACIFIC AND AN ARC THOLEIITE FROM DSDP SITE 458

DSDP SITE 458, MARIANA FORE-ARC

	BONINITE				THOLEIITE
	28-1(4) (136-139)	30-1(4) (45-49)	39-1(4) (23-26)	43-2(5) (34-37)	46-1(4) (100-106)
SiO_2	57.99	57.88	57.18	58.64	59.28
TiO_2	0.23	0.22	0.24	0.52	0.88
Al_2O_3	14.48	13.63	13.48	15.38	15.16
Fe_2O_3	--	--	--	--	--
FeO	8.03	8.14	8.78	8.02	10.61
MnO	--	--	--	0.12	--
MgO	6.71	6.34	7.56	4.56	3.06
CaO	10.47	10.39	10.84	8.74	7.63
Na_2O	1.87	1.83	1.59	1.84	3.10
K_2O	0.35	0.35	0.30	0.35	0.35
P_2O_5	--	--	--	0.17	--
H_2O^+(6)	2.52	2.01	2.06	2.43	2.18
$\frac{Mg}{Mg + \Sigma Fe}$	0.60	0.58	0.61	0.50	0.34

(1) Volatile free whole rock microprobe analyses, provided by G. Jenner.
(2) Wet chemical whole rock analyses recalculated volatile free to 100%, Shiraki and Kuroda (1977).
(3) Wet chemical whole rock analyses recalculated volatile free to 100%, Dallwitz (1968).
(4) Volatile free whole rock microprobe analysis, Meijer (1980).
(5) Microprobe analysis of interstitial glass in pillow rind, Meijer (1980).
(6) Whole rock analyses, technique given in Hickey and Frey (1981).

Four boninite samples from DSDP Site 458 were analyzed. Three samples (28-1, 30-1, and 39-1, Table 3.1) are from the upper 120 meters (Units I and III, Meijer et al., 1981) and have 57.2 to 58.0% SiO_2, 6.3 to 7.6% MgO and <0.24% TiO_2. Sample 43-2 is a boninite from the lower part of Site 458 (Unit IVB, Meijer et al., 1981) and has 58.6% SiO_2, 4.6% MgO and 0.52% TiO_2. Boninite lavas from this unit have consistently higher TiO_2 contents than the upper lavas, but other major element features are the same (Wood et al., 1981). As a group Site 458 boninites are less magnesian than other boninites, and petrographically they resemble the bronzite andesite (Bonin Island sample 1129-4). Sample 46-1 (Table 3.1) is an arc tholeiitic andesite from the lower 40 meters of Site 458.

Alteration: All samples from the Bonin Islands, Cape Vogel and Site 1403 were provided as powders by D. H. Green, therefore the exact degree of alteration of each sample is not known. Thin sections were provided for samples 2982, 2983, 2985, 2986 and 2987. Bonin Island samples (2982 and 2983) are relatively fresh, with alteration restricted to replacement of olivine by iddingsite and devitrification of glass in some areas. Altered glass is more abundant in Cape Vogel samples (2985, 2986 and 2987), and vesicles filled with zeolites were also present in sample 2987.

Site 458 samples were obtained as rock chips. The four boninites analyzed were glassy pieces of pillow rinds, and alteration effects included devitrification of glass and the presence of zeolites and clay in numerous vesicles, which were avoided during sample preparation (Appendix I). Arc tholeiite 46-1 was more strongly altered, as are all rocks from the lower part of Site 458. Much of the groundmass was replaced by clays, but vesicles were unfilled in this sample.

SUMMARY OF MAJOR ELEMENT CHARACTERISTICS

The key major element features of boninites are outlined in Chapter 2. Compared to other MgO-rich island arc volcanics, boninites are distinguished by their higher SiO_2 and lower Al_2O_3 contents. The wide variation in MgO contents, but relatively constant SiO_2 contents in boninites (e.g., Cape Vogel and Dredge Site 1403 boninites, above), result from low pressure fractionation, principally of orthopyroxene (Jenner, 1981; Howard and Stolper, 1981). CaO and Al_2O_3 contents increase regularly with decreasing MgO contents, as expected for orthopyroxene controlled fractionation, and are similar, at a particular MgO content, in boninites from different geographic areas (Table 3.1). The most distinct major element difference between boninites from different areas is their TiO_2 content. Sun and Nesbitt (1978a) noted that some boninites, like low TiO_2 basalts from ophiolites, have very high Al_2O_3/TiO_2 and CaO/TiO_2 ratios compared to MORB's and chondrites (Fig. 3.2). However, Al_2O_3/TiO_2 and CaO/TiO_2 ratios in boninites are extremely variable (Fig. 3.2) as a result of variation in TiO_2 content, and boninites from Cape Vogel are notable in that they have CaO/TiO_2 ratios which are chondritic or less than chondritic, despite their low TiO_2 contents.

FIGURE 3.2: Variation of CaO/TiO_2 and Al_2O_3/TiO_2 ratios with TiO_2 content in boninites, island arc tholeiites from DSDP Site 458 and MORB's. Boninite data from Table 3.1, this study, Shiraki and Kuroda (1977), Dallwitz (1968), Dietrich et al. (1978), Sun and Nesbitt (1978a) and Wood et al. (1981). Data for tholeiites from Wood et al. (1981), and MORB fields after Sun and Nesbitt (1978a). Dashed lines indicate chondritic ratios.

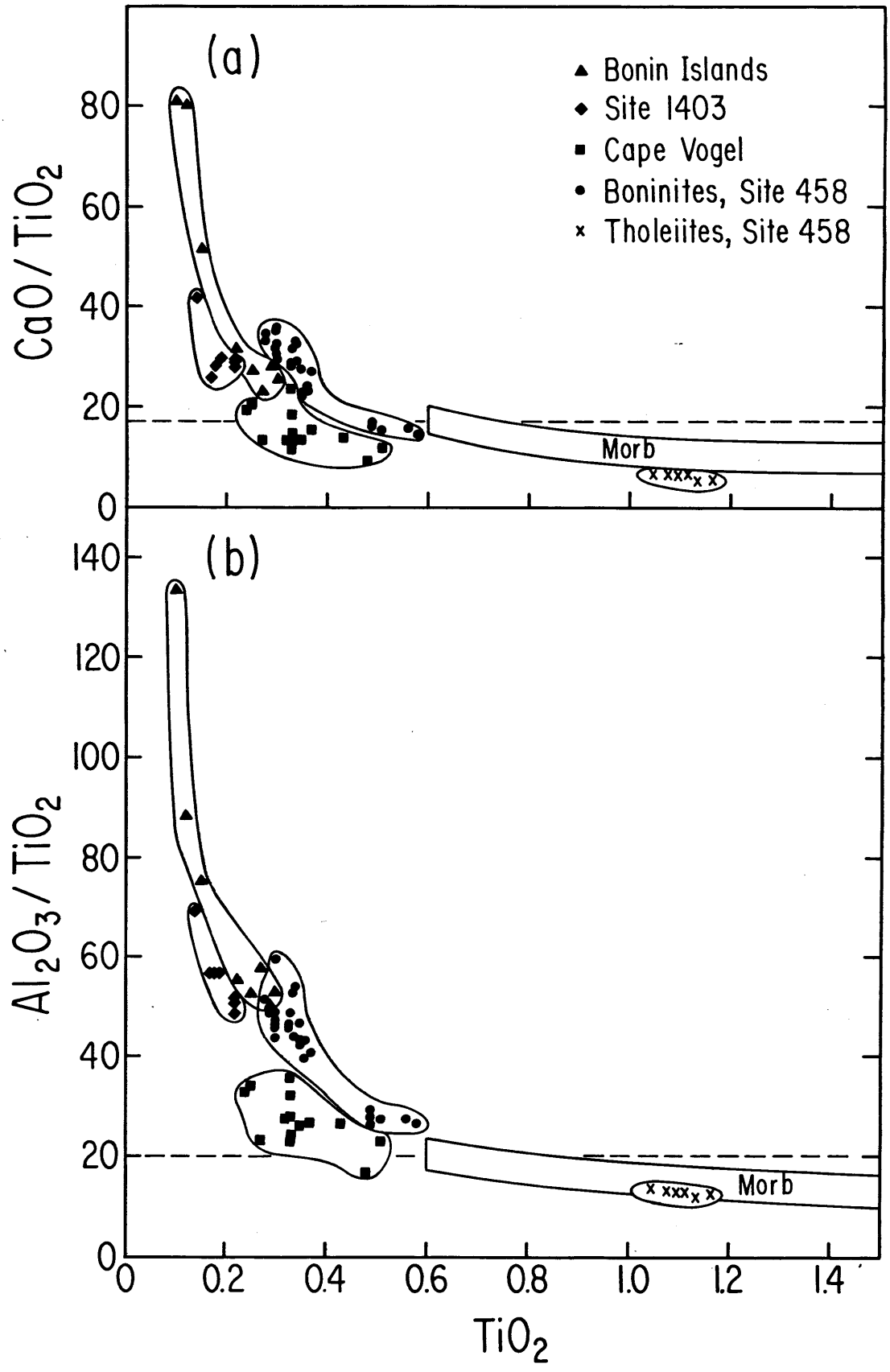
(a)
(b)
▲ Bonin Islands
◆ Site 1403
■ Cape Vogel
• Boninites, Site 458
× Tholeiites, Site 458
Morb
Morb
CaO / TiO2
Al2O3 / TiO2
TiO2
0
20
40
60
80
100
120
140
0.2
0.4
0.6
0.8
1.0
1.2
1.4

RESULTS: TRACE ELEMENTS

Trace element abundances for boninites are given in Table 3.2.

Sc and First Series Transition Elements:

With the exception of Ti, absolute abundances of Sc and first series transition elements in magnesian boninites are similar to those in MgO-rich basalts from other tectonic regimes (Fig. 3.3). Cr, Co and Ni abundances decrease regularly with decreasing MgO content, and vary from 37-60 ppm Co, 100-450 ppm Ni and 500-1800 ppm Cr in samples with 12-19% MgO. The high Cr contents of boninite liquids are verified by the Cr-rich (50-70% Cr_2O_3) spinels occurring as inclusions in phenocrysts and the relatively high Cr content of the pyroxene phenocrysts (Jenner and Green, in prep.). The high Cr/(Cr + Al) (0.8 - 0.9) of the spinels overlap and exceed the ratios in alpine peridotites and ocean floor peridotites (Dick and Bullen, in press).

Ratios of Ti to the adjacent transition metals Sc and V (Fig. 3.4) are lower in boninites than in oceanic basalts, and for samples from the Bonin Islands and Site 1403, Ti/Sc and Ti/V ratios are less than chondritic. Some samples from Cape Vogel have similar Ti/V ratios to those in komatiites (Nesbitt and Sun, 1976), but lower Ti/Sc ratios. Differences in Ti/V and Ti/Sc ratios in boninites correspond to geographic region, as do their Al_2O_3/TiO_2 and CaO/TiO_2 ratios, but do not covary with MgO, Ni or Cr content or other indicators of mafic mineral fractionation. In contrast, V/Sc ratios in boninites from all areas are relatively constant, ranging from 3.2 to 5.4, with all but two samples between 4.2 and 5.1. These values are typical of primitive MORB's (Fig. 3.4).

TABLE 3.2: TRACE ELEMENT ABUNDANCES IN BONINITES FROM THE WESTERN PACIFIC AND AN ARC THOLEIITE FROM DSDP SITE 458

	CHICHI JIMA, BONIN ISLANDS, JAPAN				
	2981	2982	2983	1129-4	1127-5
Sc(1)	36.2	45.1	37.4	35.9	22.0
Ti(2)	600	740	1011	1601	1525
V	174	145	164	--	--
Cr	538	888	832	208	<5
Mn	1020	1150	1080	--	--
Co	37.3	46.1	41.7	31.6	12.4
Ni	140	111	205	--	--
Rb	12.2	7.5	10.5	11.1	20.0
Sr	97.2	58.7	68.3	85.7	113.5
Ba	30.0	20.2	28.2	27.9	55.8
Y	4.9*	2	5	8	7
Zr	25.4*	11	19	30	44
Hf	0.69	0.31	0.54	0.88	1.34
La	1.27	0.71	0.95	1.13	1.82
Ce	2.57	1.62	2.16	2.69	3.96
Nd	1.65	0.97	1.47	1.95	2.69
Sm	0.426	0.266	0.429	0.623	0.769
Eu	0.146	0.107	0.150	0.231	0.268
Tb	0.099	0.078	0.109	0.160	0.188
Yb	0.591	0.480	0.663	0.894	1.08
Lu	0.103	0.084	0.115	0.149	0.186
Rb/Sr	0.13	0.13	0.15	0.13	0.18
K/Rb	480	390	420	380	370
Ba/La	23.6	28.5	29.6	24.7	30.7
Ti/Zr	24	67	53	53	35
Zr/Hf	37	35	35	35	33
Ti/Y	120	370	200	200	220
$(La/Yb)_{e.f.}$	1.45	1.00	0.97	0.85	1.14
$(La/Sm)_{e.f.}$	1.88	1.69	1.40	1.14	1.49
Zr/Nb	58	--	--	--	--
La/Nb	2.9	--	--	--	--

(1) Data for Sc, Co, Cr and Hf by INAA. Precision and accuracy given in Appendix II, and Hickey and Frey (1982). REE by RNAA. Precision and accuracy given in Appendix II, and Hickey and Frey (1981). Rb, Sr and Ba by isotope dilution (Appendix II).

TABLE 3.2 (CONT'D): TRACE ELEMENT ABUNDANCES IN BONINITES FROM THE WESTERN PACIFIC AND AN ARC THOLEIITE FROM DSDP SITE 458

	CAPE VOGEL PAPUA NEW GUINEA				MARIANA TRENCH SITE 1403
	2984	2985	2986	2987	2980
Sc(1)	34.9	33.7	27.9	30.6	31.3
Ti(2)	1978	2757	2008	1600	840
V	187	165	132	145	132
Cr	715	664	1790	1615	1386
Mn	1140	1140	1190	1270	1230
Co	47.3	47.5	59.0	60.3	53.4
Ni	154	199	334	334	258
Rb	8.3	9.4	4.7	6.0	15.2
Sr	338.6	90.7	76.2	84.1	106.8
Ba	39.5	30.6	26.9	42.7	22.5
Y	7*	7	6	3	4.6*
Zr	29.5*	55	49	36	36*
Hf	0.58	1.30	1.24	0.81	0.79
La	1.47	4.80	4.57	3.11	1.27
Ce	3.51	9.49	9.16	6.48	2.93
Nd	2.09	4.72	4.44	2.95	1.85
Sm	0.602	1.13	0.972	0.689	0.508
Eu	0.210	0.392	0.326	0.234	0.171
Tb	0.144	0.221	0.178	0.130	0.115
Yb	0.809	0.820	0.653	0.521	0.602
Lu	0.133	0.131	0.108	0.087	0.104
Rb/Sr	0.025	0.10	0.064	0.072	0.14
K/Rb	410	380	360	510	510
Ba/La	26.9	6.38	5.89	13.7	17.7
Ti/Zr	67	50	41	44	23
Zr/Hf	51	42	40	44	46
Ti/Y	280	390	330	530	180
$(La/Yb)_{e.f.}$	1.23	3.95	4.73	4.03	1.42
$(La/Sm)_{e.f.}$	1.54	2.68	2.96	2.84	1.58
Zr/Nb	34	--	--	--	50
La/Nb	1.7	--	--	--	1.8

(2) Data for V, Mn and Ni by A.A.. Y, Zr and Ti by XRF, except for starred values by SSMS. This data and Nb values provided by G. Jenner. Precision and accuracy given in Jenner (1981).

TABLE 3.2 (CONT'D): TRACE ELEMENT ABUNDANCES IN BONINITES FROM THE WESTERN PACIFIC AND AN ARC THOLEIITE FROM DSDP SITE 458

	DSDP SITE 458, MARIANA FORE-ARC					
	BONINITE				THOLEIITE	NORMALIZING[4]
	28-1	30-1	39-1	43-2	46-1	VALUES
Sc[1]	33.3	41.3	41.0	36.2	33.6	7.9
Ti[2]	(1679)[3]	(1799)	(1679)	(2998)	(6954)	620
V	--	--	--	--	--	74
Cr	197	253	224	202	3	3490
Mn	--	--	--	--	--	2610
Co	29.9	37.3	36.6	34.6	35.9	710
Ni	--		--	--	--	14400
Rb	8.5	8.2	8.5	7.1	5.6	0.35
Sr	89.1	87.1	89.6	106.9	123.8	11
Ba	26.8	26.4	26.9	25.4	25.8	3.5
Y	(7)	(5)	(6)	(11)	(26)	2.2
Zr	(28)	(27)	(29)	(48)	(68)	5.6
Hf	0.62	0.66	0.68	1.12	1.69	0.18
La	0.75	0.80	0.80	1.19	2.04	0.311
Ce	2.10	2.29	2.27	3.41	6.12	0.810
Nd	1.72	1.88	1.76	2.93	5.41	0.602
Sm	0.574	0.633	0.604	1.00	1.99	0.196
Eu	0.226	0.250	0.235	0.384	0.766	0.0737
Tb	0.160	0.176	0.166	0.269	0.525	0.0476
Yb	0.736	0.816	0.781	1.20	2.36	0.210
Lu	0.120	0.132	0.127	0.190	0.373	0.0318
Rb/Sr	0.095	0.094	0.095	0.066	0.045	
K/Rb	340	350	290	410	520	
Ba/La	35.9	32.8	33.6	21.3	12.6	
Ti/Zr	(60)	(67)	(58)	(62)	(102)	
Zr/Hf	--	--	--	--	--	
Ti/Y	(240)	(360)	(280)	(270)	(270)	
$(La/Yb)_{e.f.}$	0.68	0.66	0.70	0.66	0.58	
$(La/Sm)_{e.f.}$	0.82	0.80	0.84	0.75	0.64	

(3) XRF data for sample from same core and section, or average of adjacent sections (43-2), Wood et al. (1981).

(4) Normalizing values for transition metals and refractory elements Sc, Y, Hf and Sr are taken from abundances for ordinary chondrites Mason (1979). Values for REE are those of Evensen et al. (1978) multiplied by 1.27 to fit absolute abundances given by Haskin et al. (1970). Normalizing values for K and Rb are values for the bulk earth estimated by Sun et al. (1979).

FIGURE 3.3: Range of chondrite normalized Sc and transition metal abundances in Mg-rich boninites (>9% MgO) (shaded) and least-differentiated basalts from the ocean floor, oceanic islands and continents. Boninite data from Table 3.2, this study, Dietrich et al. (1978) and Sun and Nesbitt (1978a). Basalt field after Langmuir et al. (1977). Normalizing values given in Table 3.2.

FIGURE 3.4: Variation of Ti/V and Ti/Sc ratios in boninites, MORB's and komatiites. Boninite data from Table 3.2, this study, Dietrich et al. (1978) and Sun and Nesbitt (1978a). MORB data from Frey et al. (1974), Sun et al. (1979) and Langmuir et al. (1977). Komatiite data from Nesbitt and Sun (1976) and Sun and Nesbitt (1978b). Dashed lines indicate chondritic ratios.

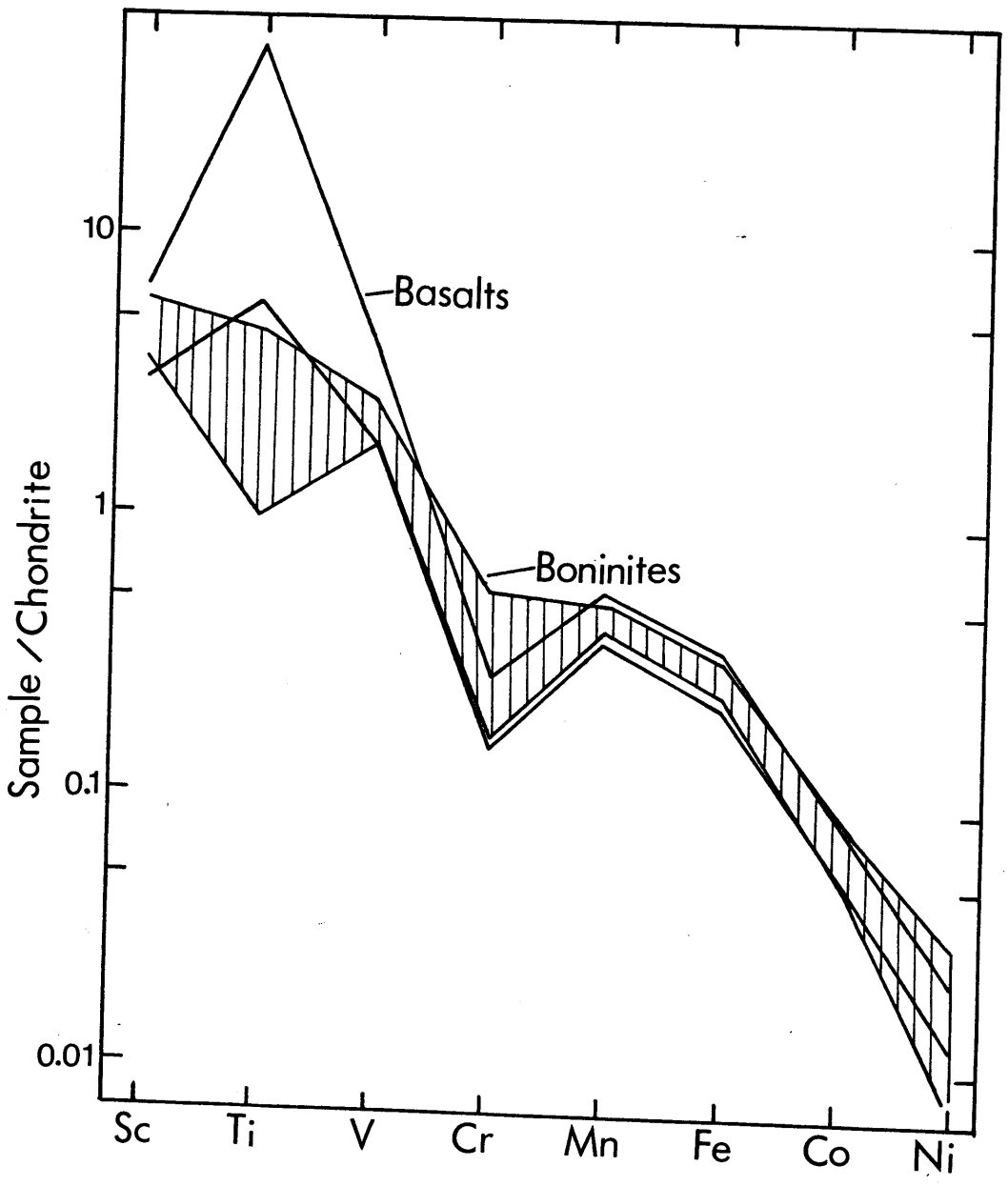
10
1
0.1
0.01
Sample / Chondrite
Basalts
Boninites
Sc
Ti
V
Cr
Mn
Fe
Co
Ni

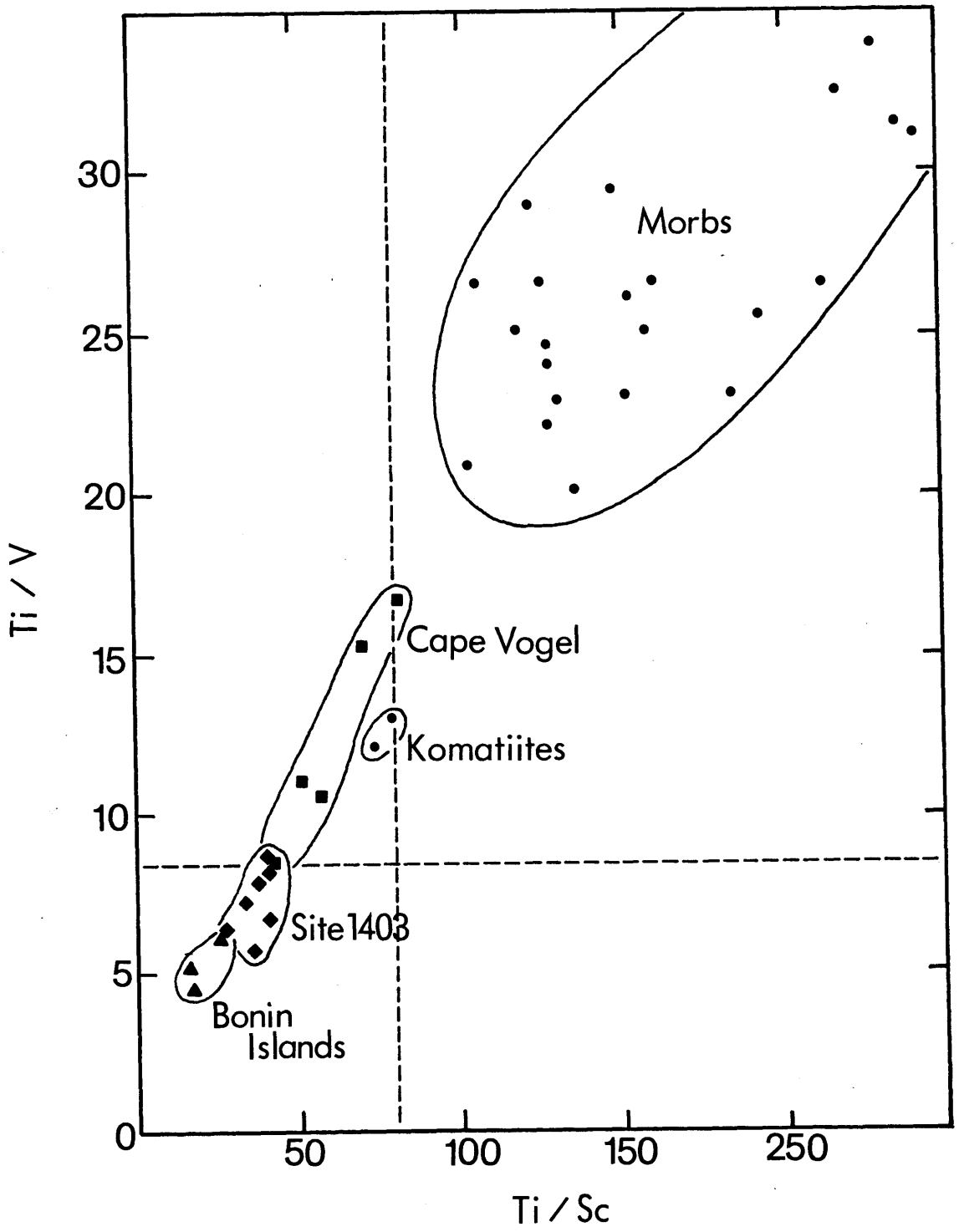
Morbs
Cape Vogel
Komatiites
Site 1403
Bonin
Islands
Ti / V
Ti / Sc
0
5
10
15
20
25
30
50
100
150
250

Rare Earth Elements:

Chondrite normalized REE abundances for boninite samples are plotted in Figs. 3.5a - d. Most samples from Cape Vogel (Fig. 3.5a) are significantly LREE-enriched ($(La/Yb)_{e.f.}$ = 3.9 - 4.7), and have concave upward REE patterns. One sample (2984) has an unusual "U-shaped" REE pattern, with $(La/Yb)_{e.f.}$ = 1.5. This pattern type is characteristic of boninites from Site 1403 and the Bonin Islands (Figs. 3.5b and c). The Bonin Island samples range in $(La/Yb)_{e.f.}$ from 0.85 to 1.4 and $(La/Sm)_{e.f.}$ varies from 1.1 to 1.9. Boninites from DSDP Site 458 (Fig. 3.5d) are relatively depleted in LREE compared to chondrites, and range in $(La/Yb)_{e.f.}$ from 0.66 to 0.70. Sample 43-2, from Unit IV, has systematically higher REE abundances than boninites from Unit I, consistent with its high TiO_2 content (Table 3.1). A common feature of boninites from all areas is their low HREE abundances of 2 to 5 times chondrites.

Trace Element Abundance Patterns in Boninites
Compared to MORB's and Island Arc Tholeiites:

In Figs. 3.6a - e, normalized abundances of K, Ba, Rb, La, Sr, Hf, Zr, Sm, Ti, Y and Sc are plotted in approximate order of their increasing bulk solid/melt partition coefficients for peridotite mineral assemblages.

The most prominent feature of the trace element distributions in boninites is the marked enrichment of K and Rb relative to REE and HFS (high field strength) elements. Compared to the distribution of these elements in MORB's (Fig. 3.6b), boninites have higher alkali contents, but significantly lower HREE and HFS element concentrations. Island arc basalts typically show enrichment in alkalis and depletion in HFS elements relative to MORB's (e.g., Perfit et al., 1980; Kay, 1980), but these

FIGURE 3.5: Chondrite normalized REE abundances in boninites. Data from Table 3.2, this study. Dashed lines indicate samples 331/540 and 482/12 analyzed by Sun and Nesbitt (1978a). Normalizing values given in Table 3.2.

FIGURE 3.6: Abundances of trace elements in boninites, normalized to a bulk earth composition. Normalizing values given in Table 3.2. Data for boninites and arc tholeiite 46-1 (e) are from Table 3.2, this study; sample 482/12 (b) from Sun and Nesbitt (1978a). MORB pattern (b) is an average of 5 normal MORB's from Frey et al. (1974) and Sun et al. (1979).

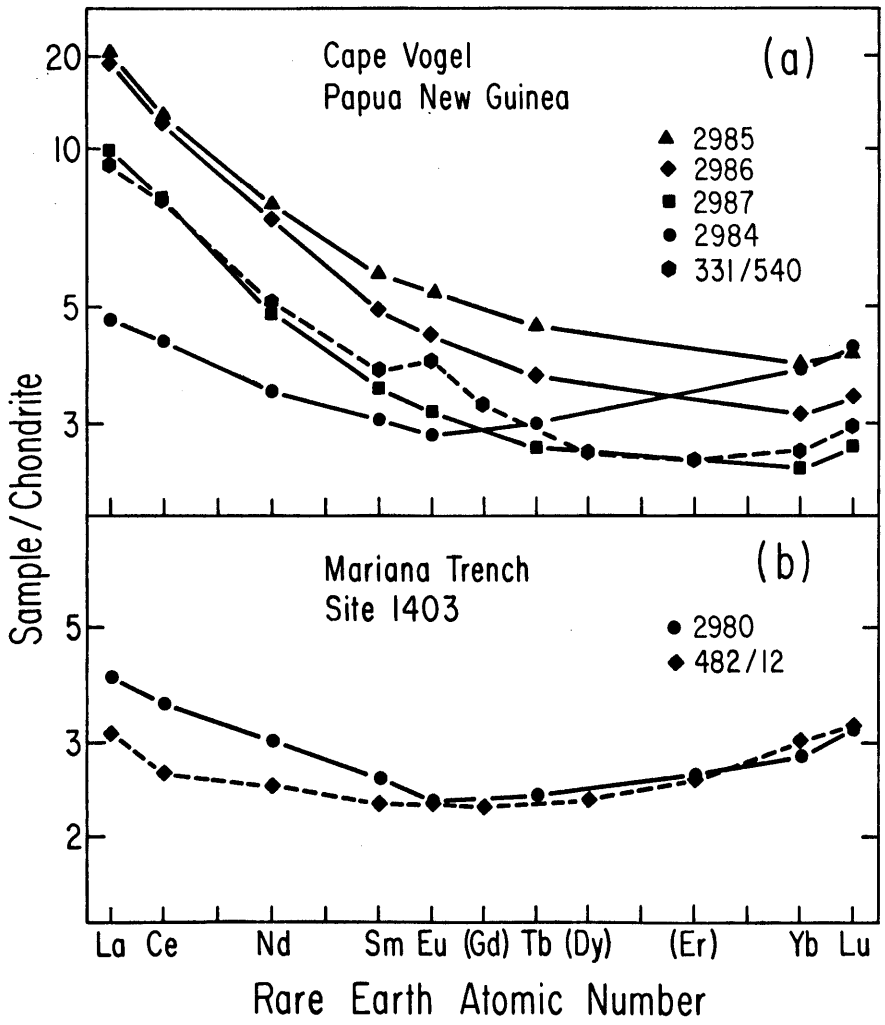
Cape Vogel
Papua New Guinea
(a)
2985
2986
2987
2984
331/540
Mariana Trench
Site 1403
(b)
2980
482/12
Sample / Chondrite
20
10
5
3
2
La Ce Nd Sm Eu (Gd) Tb (Dy) (Er) Yb Lu
Rare Earth Atomic Number

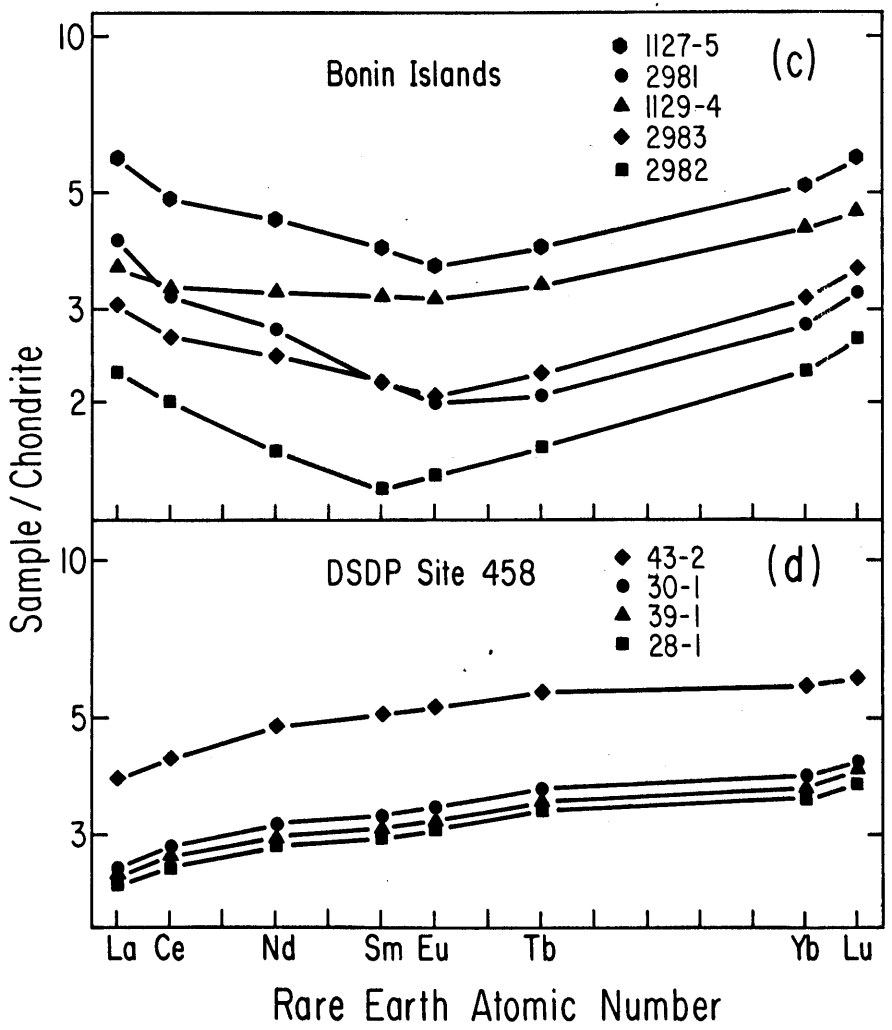
Bonin Islands
(c)
1127-5
2981
1129-4
2983
2982
DSDP Site 458
(d)
43-2
30-1
39-1
28-1
Sample / Chondrite
10
5
3
2
La Ce Nd Sm Eu Tb Yb Lu
Rare Earth Atomic Number

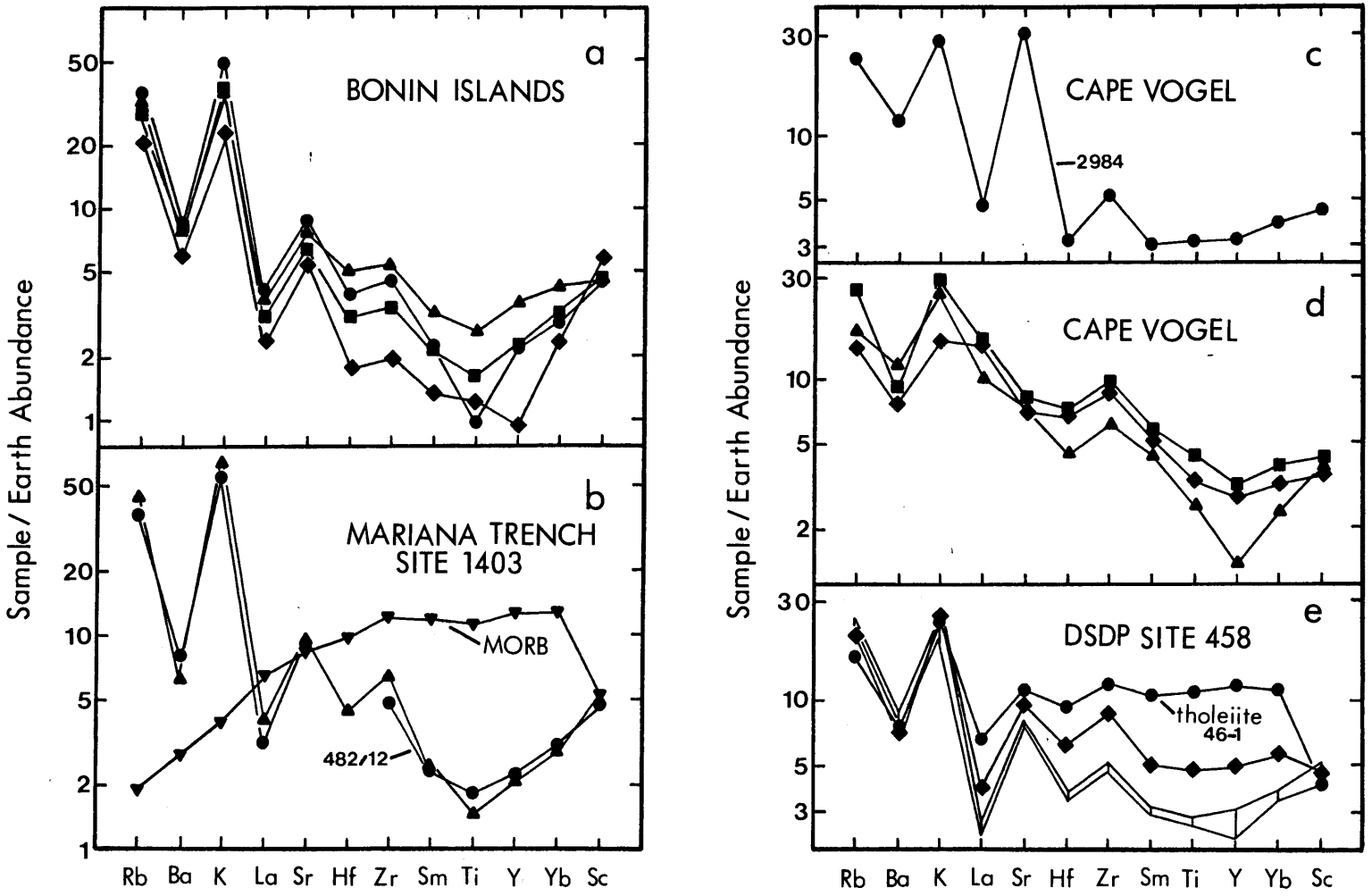
a
BONIN ISLANDS
b
MARIANA TRENCH
SITE 1403
MORB
482/12
c
CAPE VOGEL
2984
d
CAPE VOGEL
e
DSDP SITE 458
tholeiite
46-1
Sample / Earth Abundance
50
20
10
5
2
1
30
3
Rb Ba K La Sr Hf Zr Sm Ti Y Yb Sc

differences are accentuated for boninites, e.g., K/Ti ratios in these samples vary from 1 to 10, while those in island arc basalts rarely exceed 2. Rb concentrations (5-15 ppm), K_2O contents (0.2-0.9%), and K/Rb ratios (290-510) in boninites are not unusual for island arc volcanics.

Ba and Sr abundances and Sr/Ba ratios in boninites are typical of those in primitive island arc basalts (Ba = 20-43 ppm, Sr = 59-107 ppm, Sr/Ba = 2 - 5, except for Cape Vogel sample 2984, Sr = 339 ppm, Sr/Ba = 8.6, Table 3.2). Like K and Rb, normalized abundances of Ba and Sr are higher than REE and HFS element concentrations (Table 3.2, Figs. 3.6a - e), except in high La/Yb boninites from Cape Vogel (Table 3.2, Fig. 3.6d). Ba/La ratios in boninites increase with decreasing La/Sm, as is characteristic of island arc basalts (Kay, 1980), and boninites plot in the lower range of Ba/La values reported for arc volcanics at a particular La/Sm value (Fig. 3.7). Strongly LREE-enriched boninites have Ba/La ratios like those in oceanic basalts (Fig. 3.7).

The enrichment of K and Rb compared to Sr and particularly Ba in boninites (Figs. 3.6a - e), is not typical of island arc volcanics. K/Ba (86-340) and Rb/Ba (0.15-0.7) ratios in boninites exceed those in most arc lavas by a factor of 2 to 5 (Fig. 3.8), and the range of Rb/Sr (0.03 - 0.15) and K/Sr (10-70) ratios in boninites also extend to values which are higher than those in primitive arc basalts with similar Sr and Ba concentrations. Variations in K/Ba, Rb/Ba, Rb/Sr and K/Sr ratios do not correlate with variations in relative LREE enrichment in boninites or other ratios of the REE and HFS elements, but K/Ba, Rb/Ba, K/Sr and Rb/Sr are strongly correlated (Fig. 3.8).

FIGURE 3.7: Plot of $(Ba/La)_{e.f.}$ vs $(La/Sm)_{e.f.}$ in boninites. Data from Table 3.2, this study and Sun and Nesbitt (1978a). Fields for island arc basalts and oceanic basalts from Kay (1980).

FIGURE 3.8: K/Ba and Rb/Ba ratios in boninites and other arc volcanics. Area labelled arc volcanics contains samples from the active Mariana arc (Dixon and Batiza, 1979); the Aleutians (Kay, 1977); New Britain (Johnson and Chappell, 1979); Tonga and Kermadec (Ewart et al, 1973; Ewart et al., 1977); the New Hebrides (Gorton, 1977); the Banda Arc (Whitford and Jezek, 1979); and the Antilles (Arculus, 1976). Arc tholeiites from DSDP Site 458 (Table 3.2, this study; Wood et al., 1981) plot with boninites. "Boninite series" and tholeiite series lavas from the Facpi Formation, Guam (Chapter 4) are also shown.

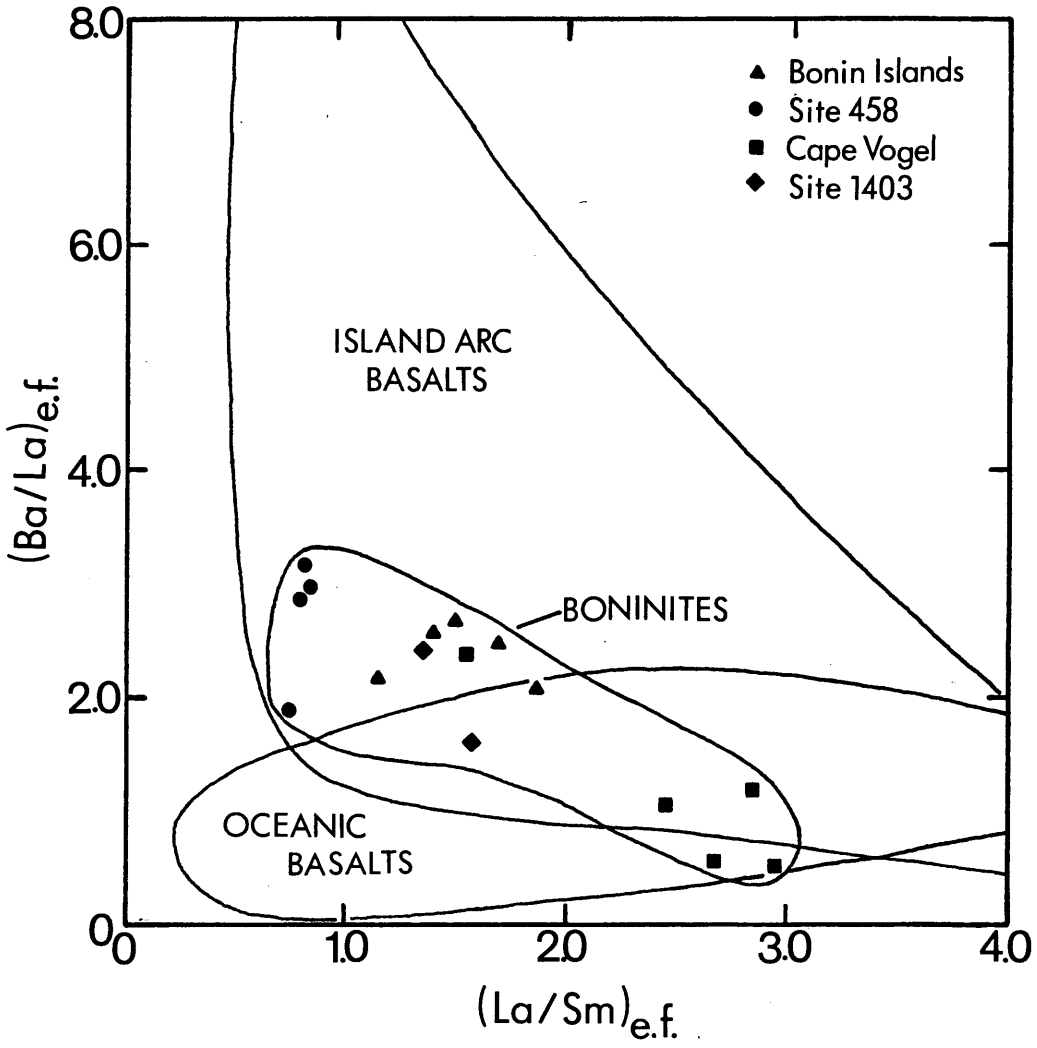
8.0
6.0
4.0
2.0
0
0
1.0
2.0
3.0
4.0
(Ba/La)e.f.
(La/Sm)e.f.
Bonin Islands
Site 458
Cape Vogel
Site 1403
ISLAND ARC
BASALTS
BONINITES
OCEANIC
BASALTS

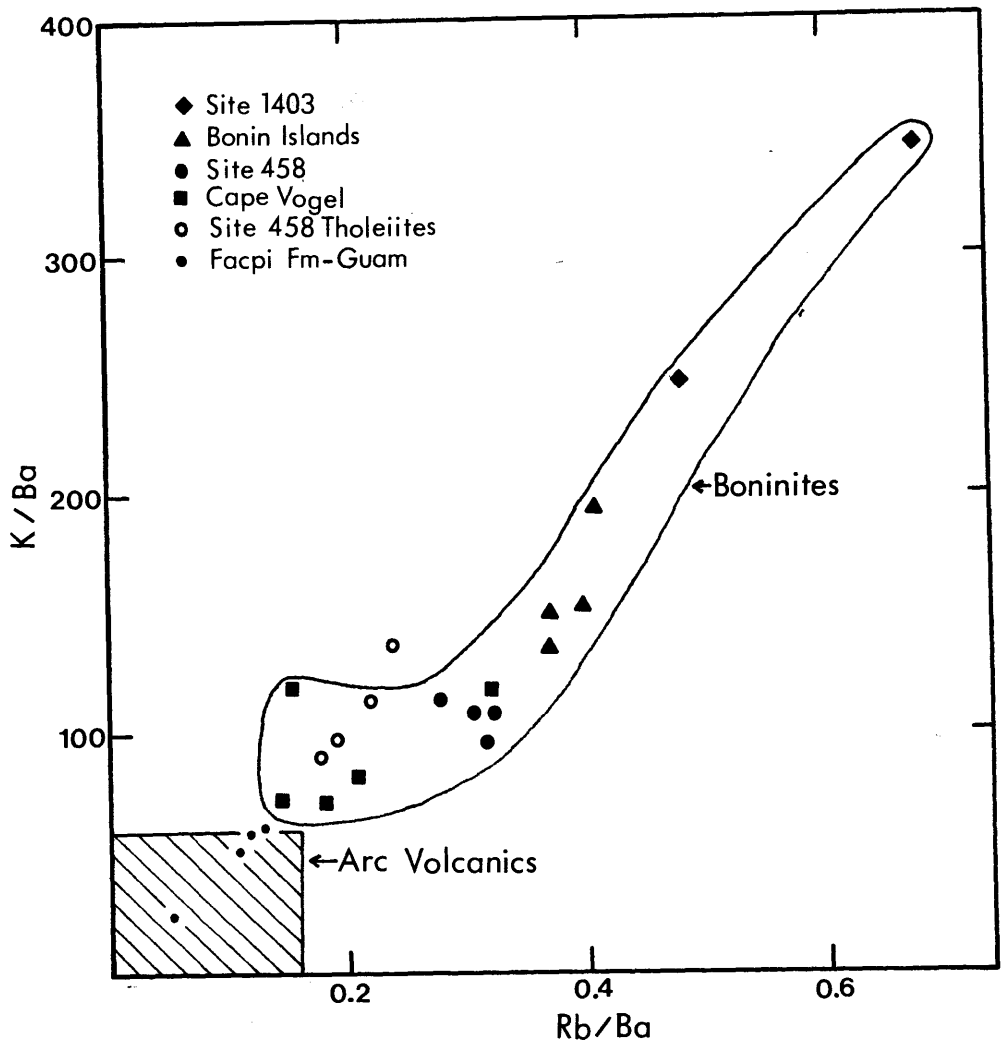
400
300
200
100
K / Ba
0.2
0.4
0.6
Rb / Ba
◆ Site 1403
▲ Bonin Islands
● Site 458
■ Cape Vogel
o Site 458 Tholeiites
• Facpi Fm-Guam
←Boninites
←Arc Volcanics

The distribution of HFS elements Ti, Zr, Hf and Y in boninites is complex compared to the regular pattern displayed by normal MORB's (Fig. 3.6b). All boninites studied are enriched in Zr relative to the intermediate and heavy REE (Fig. 3.6). Ti/Zr ratios in these samples range from 23 to 67, as compared to an average of 110 for oceanic and island arc basalts (Sun et al., 1979; Wood et al., 1981). Ti/Zr ratios vary among boninite samples from a single geographic area, and samples from the Mariana - Bonin Arc (Bonin Islands, DSDP Site 458 and dredge Site 1403) and Cape Vogel form separate trends of increasing Ti/Zr with decreasing La/Sm (Fig. 3.9). Zr/Hf ratios in boninites vary from 33 to 51 and are within or slightly higher than the range found in oceanic basalts (39 $\pm$ 5) and chondrites (30 - 40) (Bougault et al., 1980). Zr/Nb ratios in boninites vary from values higher than those found in MORB's in boninites from the Bonin Islands and Site 1403 (Table 3.2; Sun and Nesbitt, 1978a) to values lower than MORB's in LREE-enriched samples from Cape Vogel (Jenner, 1981; Sun and Nesbitt, 1978a), therefore enrichment in Nb follows enrichment in LREE. However, La/Nb ratios in boninites range from 1.7 to 2.9 (Table 3.2; Jenner, 1981; Sun and Nesbitt, 1978a) and are higher than values of 0.6 - 1.1 reported for oceanic basalts (Bougault et al., 1980).

Relative abundances of the elements Sc, Yb and Y in boninites (Figs. 3.6a - e) decrease systematically from Sc to Y. Ti/Y ratios, like Zr/Nb ratios, vary from values less than those in MORB's in samples from the Bonin Islands and Site 1403, to values greater than MORB's in LREE enriched samples from Cape Vogel.

FIGURE 3.9: Variation of Ti/Zr and $(La/Sm)_{e.f.}$ in boninites and an arc tholeiite from DSDP Site 458. Data from Table 3.2, this study and Sun and Nesbitt (1978a).

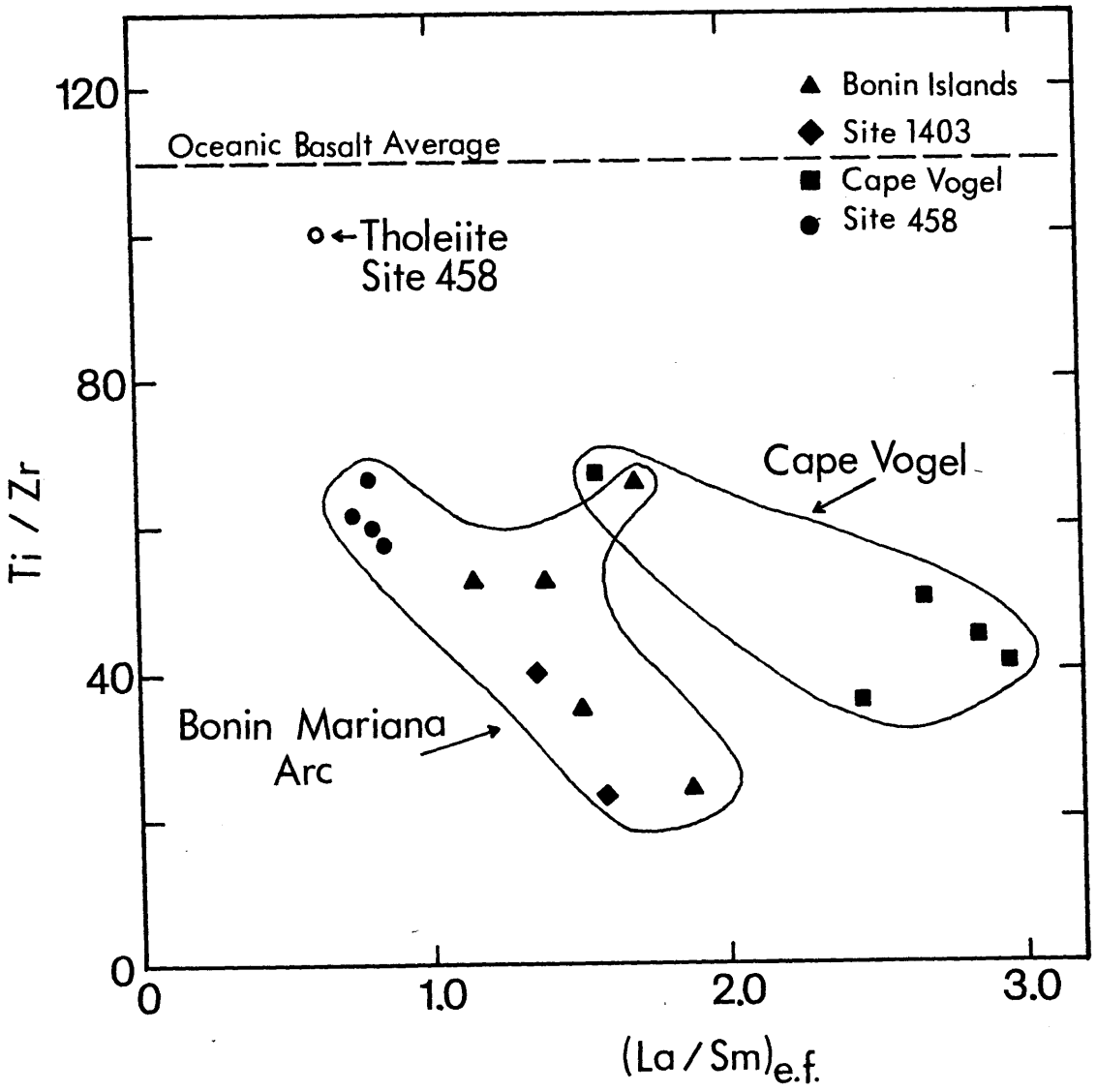
120
80
40
0
Ti / Zr
0
1.0
2.0
3.0
(La / Sm)e.f.
Oceanic Basalt Average
Tholeiite
Site 458
Bonin Islands
Site 1403
Cape Vogel
Site 458
Cape Vogel
Bonin Mariana
Arc

RESULTS: ISOTOPIC DATA

The large variation in relative LREE abundances in boninites indicates that their Nd-isotopic ratios may be an important constraint for interpreting their complex trace element distributions. Nd-isotopic data for the boninites studies are listed in Table 3.3. $^{143}Nd/^{144}Nd$ ratios in these samples have an extremely large range and include some of the lowest values reported for intra-oceanic island arcs. Four samples from the Bonin Islands vary from $(^{143}Nd/^{144}Nd)_o$ = 0.51259 to 0.51290, and form a line with positive slope when plotted against Sm/Nd (Fig. 3.10). Samples from Site 1403 and Site 458 plot near this line. Four samples from Cape Vogel have $(^{143}Nd/^{144}Nd)_o$ = 0.51279 to 0.51287 and also show a positive correlation with Sm/Nd. Like Ti/Zr ratios, $^{143}Nd/^{144}Nd$ ratios in boninites vary with relative LREE-enrichment such that samples from the Mariana - Bonin Arc and Cape Vogel form separate trends.

Because some boninite samples were visibly altered, their measured Sr-isotope values (Table 3.3) may reflect exchange with seawater. Early in the research, leaching experiments were performed in which powdered samples were heated in 2N HCl for 6-24 hours, recovered from the leachate, rinsed and analyzed for $^{87}Sr/^{86}Sr$. These experiments were discontinued because it was believed that measured $^{87}Sr/^{86}Sr$ values on such material had no precise scientific meaning, and the data was discarded. However, in the experiments (e.g., for Site 458 samples 28-1 and 39-1, and Cape Vogel sample 2984), $^{87}Sr/^{86}Sr$ ratios never changed significantly from the value measured in the unleached sample. This can be interpreted to indicate that the values measured on unleached material did not result from post-eruptive

TABLE 3.3: Sr AND Nd ISOTOPIC COMPOSITIONS IN BONINITES AND TRACE ELEMENT PARAMETERS

	Sm/Nd	$(^{143}Nd/^{144}Nd)_o$(1)	$(\varepsilon_{Nd})_o$	Rb/Sr	$(^{87}Sr/^{86}Sr)_o$(2)	$(\varepsilon_{Sr})_o$	Sr/Nd
BONIN ISLANDS:							
2981	0.270	0.512587 ± 17	-0.3 ± 0.3	0.126	0.70510 ± 7	+6.2 ± 0.9	58.9
2982	0.283	0.512643 ± 24	+0.8 ± 0.5	0.128	--	--	60.5
2983	0.298	0.512763 ± 15	+3.1 ± 0.3	0.154	0.70508 ± 4	+6.0 ± 0.5	46.5
1129-4	0.316	0.512889 ± 19	+5.6 ± 0.4	0.130	0.70472 ± 3	+0.9 ± 0.4	43.9
1127-5	0.290	--	--	0.176	--	--	42.2
CAPE VOGEL:							
2984	0.289	0.512874 ± 17	+5.3 ± 0.3	0.025	0.70735 ± 4	+38.2 ± 0.5	162.0
2985	0.241	0.512808 ± 16	+4.0 ± 0.3	0.104	0.70431 ± 3	-5.0 ± 0.4	19.2
2986	0.235	0.512787 ± 15	+3.6 ± 0.3	0.062	--	--	17.2
2987	0.235	0.512804 ± 17	+3.9 ± 0.3	0.071	--	--	28.5
SITE 1403:							
2980	0.275	0.512698 ± 15	+1.9 ± 0.3	0.142	0.70613 ± 4	+20.9 ± 0.5	57.7
SITE 458:							
28-1	0.353	0.512921 ± 16	+6.2 ± 0.3	0.095	0.70381 ± 4	-12.1 ± 0.4	51.8
39-1	0.350	0.512904 ± 16	+5.9 ± 0.3	0.095	0.70376 ± 4	-12.8 ± 0.4	50.9
30-1	0.356	--	--	0.094	0.70385 ± 4	-11.5 ± 0.4	46.3
43-2	0.351	--	--	0.066	0.70365 ± 4	-14.3 ± 0.4	36.5
46-1	0.363	0.513016 ± 16	+8.1 ± 0.3	0.045	0.70354 ± 4	-15.9 ± 0.4	22.9

(1) $^{143}Nd/^{144}Nd$ ratios normalized to $^{146}Nd/^{144}Nd = 0.7219$, and to BCR-1, $^{143}Nd/^{144}Nd = 0.51263$. Initial ratios calculated for 30 m.y.b.p.. Initial ε_{Nd} calculated relative to present day chondritic $^{143}Nd/^{144}Nd = 0.51264$ and $^{147}Sm/^{144}Nd = 0.1936$.

(2) $^{87}Sr/^{86}Sr$ ratios normalized to $^{86}Sr/^{88}Sr = 0.1194$ and to Eimer and Amend $SrCO_3 = 0.7080$. Initial ε_{Sr} calculated relative to present day bulk earth $^{87}Sr/^{86}Sr = 0.7047$ and $^{87}Rb/^{86}Sr = 0.085$.

FIGURE 3.10: Variation of $(^{143}Nd/^{144}Nd)_o$ with Sm/Nd for boninites. Data from Table 3.3.

Maximum and minimum $^{143}Nd/^{144}Nd$ values for model LREE enriched and depleted mixing endmembers (see discussion), indicated by vertical tics at ends of lines, are derived from intercepts in Figs. 3.12a, b and c. The possible LREE-depleted endmembers for Bonin Island samples extend to Sm/Nd = 0.45 and ε_{Nd} = +23.

FIGURE 3.11: Initial $^{87}Sr/^{86}Sr$ and $^{143}Nd/^{144}Nd$ ratios in boninites compared to the oceanic mantle array. Numbers in parentheses are Sr/Nd ratios (Table 3.3).

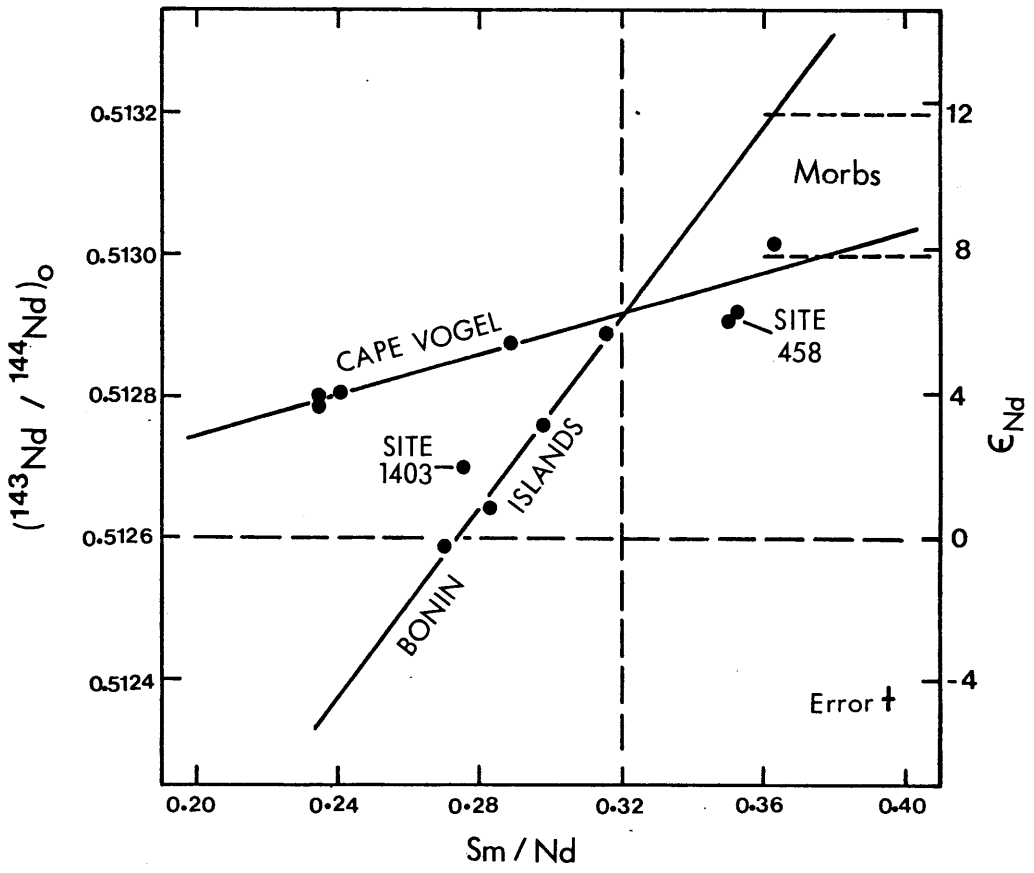
0.5132
0.5130
0.5128
0.5126
0.5124
12
8
4
0
-4
Morbs
CAPE VOGEL
SITE
458
SITE
1403
ISLANDS
BONIN
Error ±
0.20
0.24
0.28
0.32
0.36
0.40
Sm / Nd
$(^{143}Nd / ^{144}Nd)_o$
ϵ_{Nd}

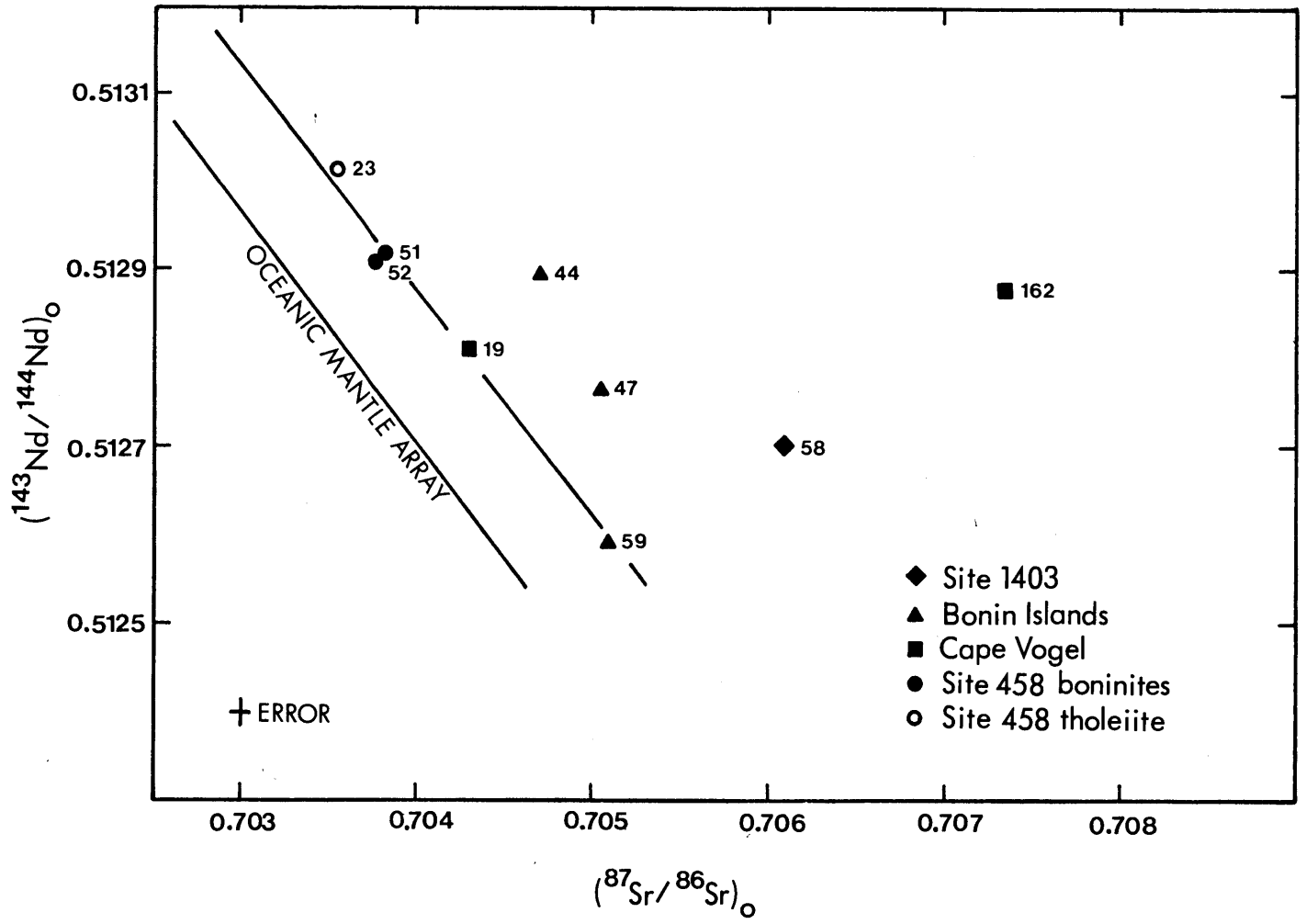
0.5131
0.5129
0.5127
0.5125
$(^{143}Nd/^{144}Nd)_o$
0.703
0.704
0.705
0.706
0.707
0.708
$(^{87}Sr/^{86}Sr)_o$
OCEANIC MANTLE ARRAY
23
51
52
19
59
44
47
58
162
+ ERROR
Site 1403
Bonin Islands
Cape Vogel
Site 458 boninites
Site 458 tholeiite

alteration. Alternatively, it could indicate that $^{87}Sr/^{86}Sr$ values in altered and fresh material were homogenized during the heating, or that the alteration products were not soluble in HCl.

Except for Site 458 sample 46-1, samples which appeared freshest in thin section were analyzed for Sr-isotopes. Three geochemically identical boninites from Site 458 chosen for their freshness yielded identical $^{87}Sr/^{86}Sr$ ratios (Table 3.3). This may be a measure of the reliablity of the Sr-isotope data, since significant increases in these values through interaction with seawater would also be expected to create variation in the values. However, it is also possible that these samples have been altered to the same degree.

Initial $^{87}Sr/^{86}Sr$ ratios in boninites from the Bonin Islands, Cape Vogel and Site 1403 range from 0.7043 to 0.7074, and these samples do not plot within the mantle array on a Sr -Nd isotope correlation diagram (Fig. 3.11). $^{87}Sr/^{86}Sr$ values in the two Cape Vogel samples are inversely correlated with Rb/Sr (Table 3.3) and their displacement from the mantle array corresponds to their relative Sr/Nd values (Fig. 3.11). Three Bonin Islands samples form a near vertical trend at high $^{87}Sr/^{86}Sr$ relative to the mantle array (Fig. 3.11). Rb/Sr does not correlate with $^{87}Sr/^{86}Sr$ (Table 3.3), and Sr/Nd decreases in these samples with increasing displacement from the mantle array (Fig. 3.11). Four boninites and the tholeiitic andesite from Site 458 have a small range of $^{87}Sr/^{86}Sr$ (0.7034-0.7036) and plot at slightly higher $^{87}Sr/^{86}Sr$ than the mantle array (Fig. 3.11). The arc tholeiite has lower $^{87}Sr/^{86}Sr$, Rb/Sr and Sr/Nd and higher $^{143}Nd/^{144}Nd$ ratios than the boninites (Table 3.3).

SUMMARY OF TRACE ELEMENT AND ISOTOPIC CHARACTERISTICS IN BONINITES

The important geochemical characteristics common to boninites from the four areas studied are:

1) High concentrations of compatible elements Ni, Cr and Co, similar to those in MORB's, but low concentrations of Ti and depletion of Ti relative to Sc and V (Figs. 3.3 and 3.4).

2) High abundances of K, Rb and Ba compared to abundances of these elements in MORB's, and high ratios of alkali metals and Ba to REE and HFS elements, which is a characteristic of island arc volcanics, but exceptionally high abundances of K and Rb relative to Ba and Sr, which is not characteristic of other arc volcanics (Figs. 3.6, 3.7 and 3.8).

3) Low abundances of REE and HFS elements compared to MORB's, but variable ratios of these elements, such as La/Sm and Ti/Zr (Figs. 3.5, 3.6, and 3.9).

4) The positive correlation of $(^{143}Nd/^{144}Nd)_o$ and with Sm/Nd in boninites from the Mariana - Bonin Arc and Cape Vogel (Fig. 3.10).

5) The high and widely variable $(^{87}Sr/^{86}Sr)_o$ values compared to oceanic volcanics with similar $^{143}Nd/^{144}Nd$ (Fig. 3.11).

DISCUSSION

NATURE OF SOURCE PERIDOTITE

A major question in the petrogenesis of island arc volcanics is the relative role of mantle peridotite and subducted oceanic crust as sources of the magmas. For boninites the situation appears less ambiguous: the high MgO contents, Mg/(Mg + ΣFe), and high Ni, Cr and Co contents in boninites are similar to or higher than most oceanic basalts, therefore a dominantly ultramafic source material is inferred for boninites. Experimental results indicate that SiO_2-saturated liquids can be derived from peridotite under conditions in which orthopyroxene melts incongruently, i.e., at low to moderate pressures under H_2O-saturated conditions, and at low pressure under anhydrous conditions (Kushiro, 1969; 1971; Nicholls and Ringwood, 1973). Liquids similar to boninites have been experimentally derived from peridotite under H_2O-saturated, low pressure conditions, at high degrees of partial melting (27-35%, Green, 1973; 1976). Recent petrologic experiments on natural boninites have further constrained the conditions required for their generation. The results of Jenner and Green (in prep.) suggest that boninite magmas form at >1200° C and low pressures (<5-10 kbar), but that the initial melts are not H_2O-saturated. The results of Howard and Stolper (1981) indicate that the residuum from boninite generation does not contain clinopyroxene or an Al-rich phase, consistent with the high degrees of partial melting suggested by Green (1973; 1976).

Although an ultramafic source is inferred for boninites, abundances of Ti, Y and HREE in fertile peridotites are similar to and in some cases greater than those in these lavas. In order to derive boninites from

peridotite, these elements must have been present in unusually low concentrations in the source peridotite, or they must have been retained in residual minerals, such as clinopyroxene, amphibole or garnet, during partial melting. Several lines of evidence argue against the retention of these elements in residual minerals:

1) the experimental studies which suggest that boninites formed by high degrees of partial melting, leaving an extremely refractory residue consisting only of olivine and orthopyroxene;

2) the less than chondritic Ti/Sc and Ti/V ratios in some boninites which are not consistent with residual clinopyroxene, amphibole or garnet, because Sc and V are retained preferentially to Ti by these minerals (Gill, 1978; Irving, 1978); and

3) the covariation of highly incompatible/moderately incompatible element ratios such as La/Sm and Zr/Ti with Nd-isotopic composition in boninites, which suggests mixing of materials with different trace element and isotopic compositions, rather than the fractionation of these elements by residual minerals.

The most straightforward interpretation of the data is therefore that boninites are derived from a depleted source peridotite, with initially low concentrations of highly incompatible and moderately incompatible elements as a result of previous melt removal, which subsequently has been enriched in K, Rb, Sr, Ba, Zr and LREE. The compositions of mantle peridotite inclusions in alkalic basalts ofter reflect mixing of an incompatible element rich component with refractory peridotite (Frey and Green, 1974; Kurat et al., 1980; Stosch and Seck, 1980; Frey, 1982). Moreover, concave upward REE patterns, which are rare in volcanic rocks other than boninites, are also found in harzburgites occurring in ophiolites and as xenoliths in

alkalic basalts (Stosch and Seck, 1980; Tanaka and Aoki, 1981; Frey, 1982). Therefore some mantle peridotites have geochemical features similar to those required in the peridotite sources of boninites.

COMPARISON OF CaO, Al_2O_3, Ti, Sc and V ABUNDANCES IN BONINITES AND DEPLETED PERIDOTITES

In Figs. 3.2 and 3.4, CaO/TiO_2, Al_2O_3/TiO_2, Sc/Ti and V/Ti ratios in some boninites are shown to be exceptionally high compared to values in MORB's and chondrites. This result is consistent with a refractory peridotite source for boninites because Ti is less compatible than Sc or V in peridotite minerals and would be removed preferentially to these elements, and CaO and Al_2O_3 during an earlier melting episode. The CaO/TiO_2, Al_2O_3/TiO_2, Sc/Ti and V/Ti ratios in boninites must also be lower than those in their refractory peridotite sources.

CaO/TiO_2, Al_2O_3/TiO_2, Sc/Ti and V/Ti ratios are extremely variable in boninites, but generally are similar for samples from a particular boninite locale (Figs. 3.2 and 3.4). This variation could be attributed either to variations in the fertility of source peridotites in different areas, or alternatively, to differences in the amount of Ti introduced into the depleted peridotite source by secondary enrichment. Data for the Cape Vogel boninites suggests that most of this variation results from secondary enrichment in Ti, since these boninites have low TiO_2 abundances (0.3 - 0.5%), but have Y/Ti (Fig. 3.6d) and CaO/TiO_2 (Fig. 3.2) ratios which are less than chondritic. Variability in the amount of secondary Ti-enrichment in boninite sources, rather than source fertility, also explains their relatively constant V/Sc ratios (Fig. 3.4), because in peridotites this ratio generally varies with modal clinopyroxene contents, $MgO/(MgO + \Sigma Fe)$,

and other measures of peridotite fertility vs depletion (Frey and Green, 1974; Frey and Suen, 1982). Since Ti may have been added to the sources of some boninites, the highest Al_2O_3/TiO_2, CaO/TiO_2, Sc/Ti and V/Ti ratios found in boninites are probably most indicative of those required for their peridotite sources.

Table 3.4 lists the highest values for these ratios in boninites from Tables 3.1 and 3.2, compared to analyses of refractory peridotites. Peridotites which are satisfactory sources for boninites are rare, but are more common when Ti has been analyzed as a trace element, therefore, part of the problem may be analytical. Peridotites with characteristics required in boninite sources (Table 3.4) are harzburgitic (<3% clinopyroxene), and most frequently tectonized harzburgites from alpine peridotites (e.g., Papua, Josephine, and Ronda), as opposed to peridotite inclusions in alkalic basalts.

The low clinopyroxene content of these peridotites suggests that boninites must be derived by relatively small degrees of partial melting. For example, Frey and Suen (1982) demonstrated that Ronda sample 771 (Table 3.4) could be the residuum of a primitive MORB-like melt, through about 28% partial melting of a more fertile peridotite. About 3% partial melting of this residual peridotite (Table 3.4) with melting proportions of 50 cpx : 50 opx (i.e., at low pressure or high P-H_2O) will yield a melt with Ti, Sc and V contents, and Ti/Sc and Ti/V ratios similar to those in the most Ti-poor boninites.

TABLE 3.4: COMPARISON OF INFERRED BONINITE SOURCES AND PERIDOTITES

	ppm Ti	Ti/Sc	V/Sc	Al_2O_3/TiO_2	CaO/TiO_2	Modal cpx
BONINITE(1) SOURCE:	<600	<16.6	<4.8	>134	>81	--
PAPUAN(2) U.M. BELT:	3-13	1.0-3.3	2.3-3.0	23-60	18-80	--
JOSEPHINE(3) PERIDOTITE:						
J42C	24	--	--	160	208	--
KHAN TAISHIR(4) OPHIOLITE:						
GA910/2	9	1.6	7.1	350	280	--
VICTORIA,(5) AUSTRALIA:						
2669	"30"	4.4	3.3	172	152	2.8
RONDA:(6)						
771	30	3.8	3.4	272	244	1.3
893	60	8.6	3.4	80	70	2.0
856	180	18.0	4.2	68	56	3.1
3% MELT OF(7) RONDA 771:	652	18.8	4.7	$\leq$272	$\leq$244	--

(1) Values for boninite sample 2981 (Table 3.2).

(2) Jaques and Chappell (1980), samples 720, 715, 716 and 714.

(3) Stockman (unpublished data).

(4) Zonenshain and Kuzmin (1978).

(5) Frey and Green (1974). Reported TiO_2 = 0.00 for this sample, 0.005 used for calculation.

(6) Frey and Suen (1982).

(7) 3% nonmodal melt of Ronda 771, using $D_o^V = 0.15$ and $D_o^{Sc} = 0.23$ from Frey and Suen (1982) and $D_o^{Ti} = 0.19$ calculated using modal proportions for R771 and mineral/melt partition coefficients from Sun et al. (1979). Melting proportions: 50 opx : 50 cpx, $P^V = 0.45$, $P^{Sc} = 0.95$ and $P^{Ti} = 0.100$, using mineral/melt partition coefficients from Sun et al. (1979).

Nd ISOTOPES AND REE AND HFS ELEMENT ABUNDANCES IN BONINITE SOURCE MATERIALS

Because only olivine and orthopyroxene are likely residual and early fractionating phases during boninite petrogenesis, abundance ratios of highly incompatible and moderately incompatible elements should not be affected by partial melting and crystallization processes related to the generation of boninite magma. Since relative abundances of these elements in boninites are not those expected in an incompatible element depleted peridotite, either the peridotite sources of boninites or primitive boninite magmas must have been enriched in these elements by mixing with other materials.

The covariation of Ti/Zr and $^{143}Nd/^{144}Nd$ with relative LREE enrichment in boninites is evidence that their relative abundances of REE and HFS elements were produced by mixing of isotopically and compositionally distinct materials. For Bonin Island boninites, the variation of Sm/Nd with $^{143}Nd/^{144}Nd$ is linear (Fig. 3.10) and this suggests that mixing of two components, each having constant relative LREE abundances, is responsible for the variation. The variation of other Nd-normalized ratios of REE and HFS elements with Sm/Nd is shown in Figs. 3.12a -d, for boninites from all areas. Ratios of La/Nd and Ti/Nd also form linear trends with Sm/Nd (Figs. 3.12a and b), Yb/Nd vs Sm/Nd is more scattered (Fig. 3.12c), and Zr/Nd (Fig. 3.12d) does not correlate with Sm/Nd at all. These variations are consistent with mixing of two components, each with constant relative LREE and Ti abundances, but with variable contents of Yb and Zr, or with modification of Yb and Zr abundances by other components which did not affect LREE or Ti.

If the trends in Figs. 3.12a - c are interpreted as mixing lines, the relative REE and Ti abundances in possible endmembers which were mixed to

FIGURE 3.12: Variation of normalized La/Nd (a), Ti/Nd (b), Yb/Nd (c) and Zr/Nd (d) with normalized Sm/Nd in boninites.
Data from Tables 3.2 and 3.3, this study, and Sun and Nesbitt (1978a). Regression lines in (a) and (b) are calculated for Cape Vogel and Bonin Island samples; Bonin Island sample 2982 was not included in the calculation for (b). Regression line in (c) is calculated for Cape Vogel samples only.

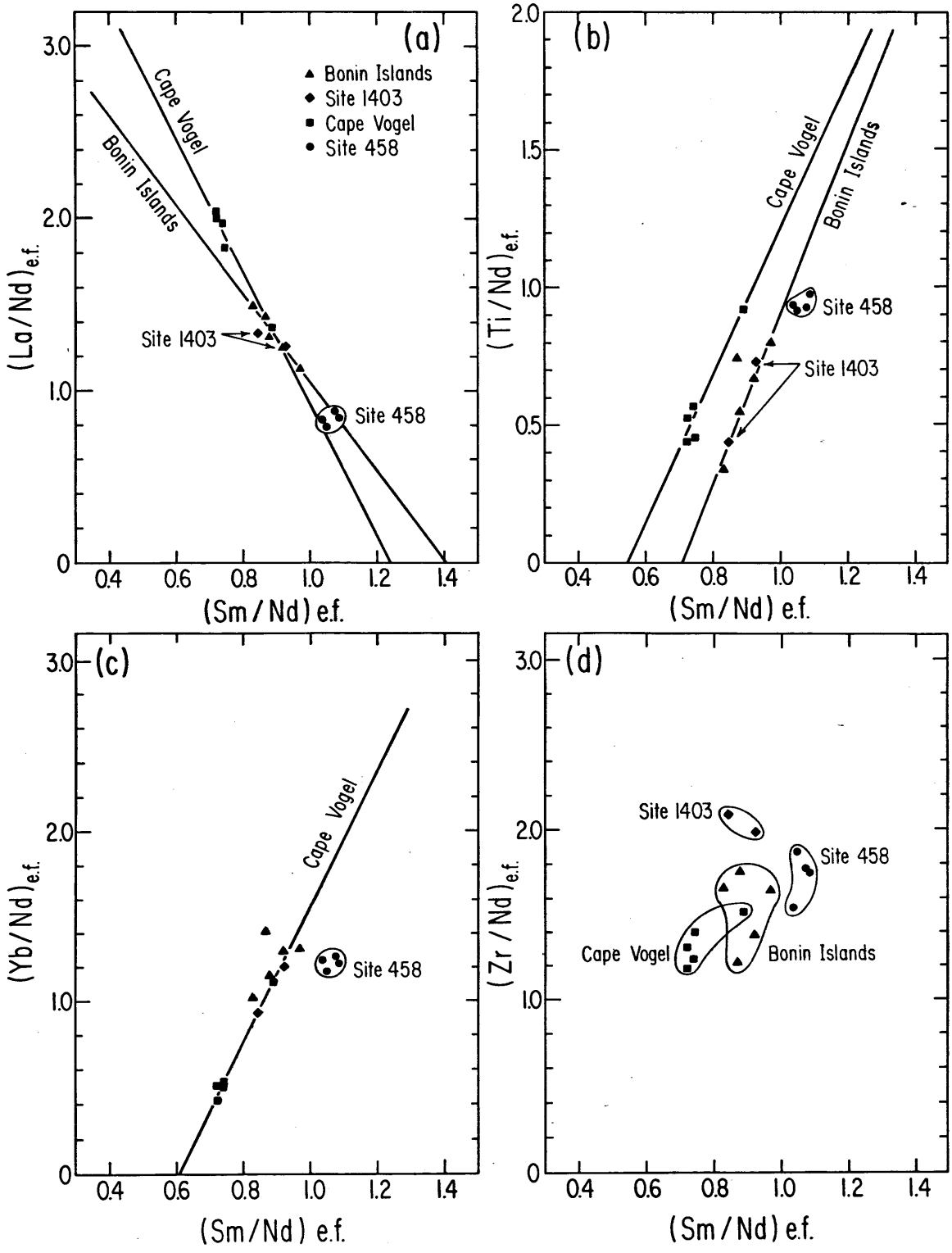
(a)
Bonin Islands
Site 1403
Cape Vogel
Site 458
Cape Vogel
Bonin Islands
Site 1403
Site 458
(La/Nd)e.f.
(Sm/Nd) e.f.
(b)
Cape Vogel
Bonin Islands
Site 458
Site 1403
(Ti/Nd)e.f.
(Sm/Nd) e.f.
(c)
Cape Vogel
Site 458
(Yb/Nd)e.f.
(Sm/Nd) e.f.
(d)
Site 1403
Site 458
Cape Vogel
Bonin Islands
(Zr/Nd)e.f.
(Sm/Nd) e.f.

FIGURE 3.13: Normalized relative abundances of La, Sm, Yb and Ti in model mixing endmembers for boninites. These relative abundances are derived from Fig. 3.12 by extrapolating to $(Sm/Nd)_{e.f.}$ values greater and less than those for samples, and calculating corresponding $(La/Nd)_{e.f.}$, $(Ti/Nd)_{e.f.}$ and $(Yb/Nd)_{e.f.}$ values from the regression lines. Each set of ratios is divided by $(Ti/Nd)_{e.f.}$, and abundances of La, Sm and Yb are plotted relative to Ti = 1. Sm/Nd ratios given next to each line are the un-normalized values of the ratios used in Fig. 3.12, and are also used in Fig. 3.10 to relate Sm/Nd to ε_{Nd}. Because of the poor correlation of $(Sm/Nd)_{e.f.}$ and $(Yb/Nd)_{e.f.}$ for Bonin Island samples (Fig. 3.12c),the regression line for Cape Vogel samples was used for both areas. Data points for Bonin Island samples cluster around this line, and those for Site 1403 lie directly on it.

Dashed lines in the range for boninites indicate relative abundances of La, Sm, Yb and Ti in samples from Table 3.2. Dashed lines labelled peridotite represent two LREE-depleted peridotites from Ronda (Frey and Suen, 1982) and Lizard (Frey, 1969). Dashed line labelled MORB is DSDP sample 3-14-10-1 (Frey et al., 1974).

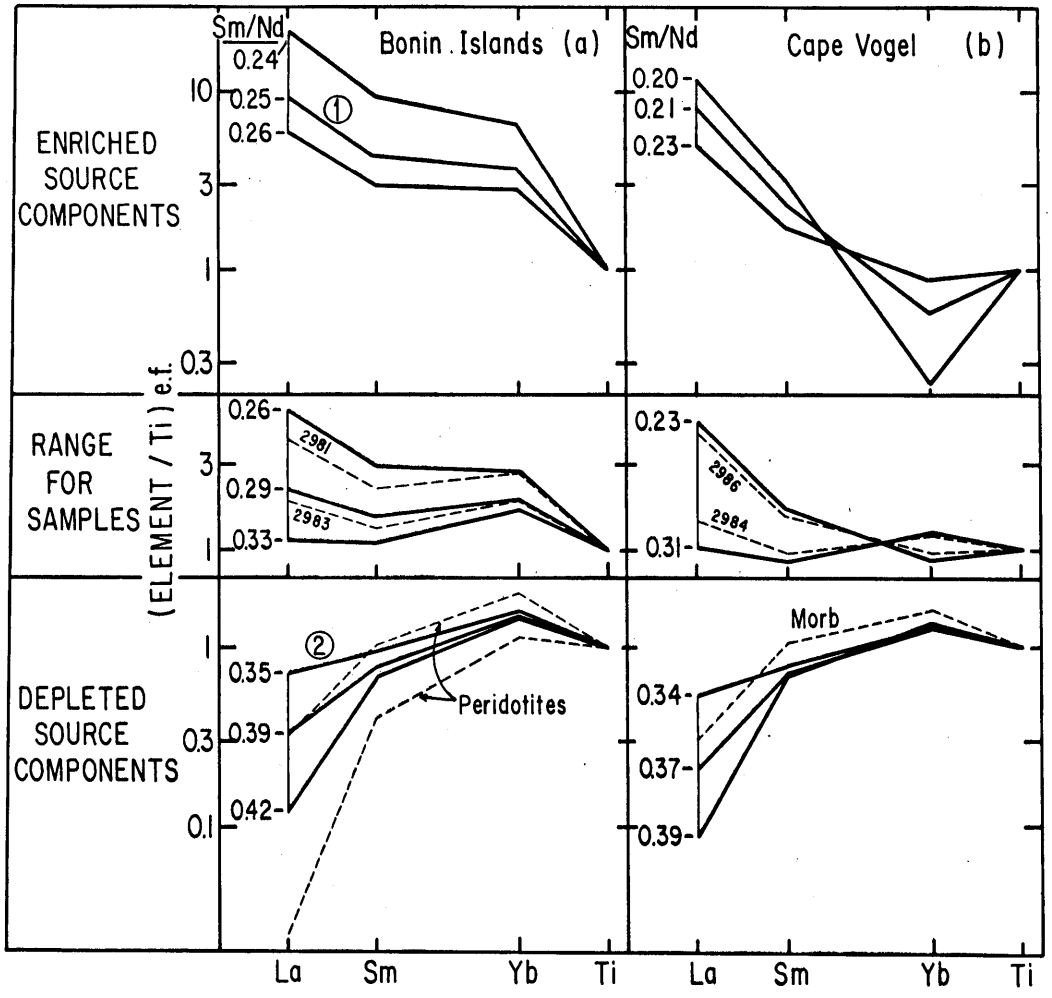
Sm/Nd
Bonin Islands (a)
Sm/Nd
Cape Vogel (b)
ENRICHED SOURCE COMPONENTS
RANGE FOR SAMPLES
DEPLETED SOURCE COMPONENTS
(ELEMENT / Ti) e.f.
0.24
0.25
0.26
0.20
0.21
0.23
10
3
1
0.3
①
2981
2983
2986
2984
0.29
0.33
0.31
②
0.35
0.39
0.42
0.34
0.37
0.1
Peridotites
Morb
La
Sm
Yb
Ti

form the Bonin Island and Cape Vogel boninites or their sources can be inferred. For example, in Fig. 3.12c the minimum $(Sm/Nd)_{e.f.}$, i.e., at $(Yb/Nd)_{e.f.} = 0$, is 0.61 (Sm/Nd = 0.20) for Cape Vogel boninites, and in Fig. 3.12b, the minimum $(Sm/Nd)_{e.f.}$, at $(Ti/Nd)_{e.f.} = 0$, is 0.72 (Sm/Nd = 0.45) for Bonin Island boninites. Maximum $(Sm/Nd)_{e.f.}$ values, at $(La/Nd)_{e.f.} = 0$, are 1.23 (Sm/Nd = 0.40) for Cape Vogel, and 1.40 (Sm/Nd = 0.45) for the Bonin Islands.

Relative abundances of REE and Ti in possible mixing endmembers for boninites, inferred from Fig. 3.12 between these minima and maxima, are shown in Fig. 3.13. For Cape Vogel and the Bonin Islands, the relative abundances and variation of these elements in the lavas can be explained by mixing of LREE-enriched and LREE-depleted endmembers. Possible LREE-depleted endmembers are similar for the two areas, and have REE and Ti abundances similar to those of LREE-depleted peridotites and primitive MORB's (Fig. 3.13). Possible LREE-enriched endmembers inferred for the two areas have different relative abundances of REE and Ti (Fig. 3.13). Both LREE-enriched endmembers have high La/Ti and Sm/Ti ratios (10-20 and 3-10 x chondrites, respectively), but the LREE-enriched endmember for Cape Vogel boninites is depleted in Yb relative to Ti, and has much higher La/Yb ratios (30 vs 3 x chondrites for Bonin Island boninites). However, for both areas the concave upward REE patterns distinctive of boninites are generated by approximately equal contributions of REE (i.e., total REE) from the LREE-enriched and LREE-depleted materials.

Nd-isotopic characteristics of the LREE-enriched and LREE-depleted source materials can be inferred from Fig. 3.10. For example, a line drawn through samples from Cape Vogel extrapolates into the MORB field, and, at the maximum Sm/Nd value of 0.40 inferred for the LREE-depleted endmember,

the maximum ε_{Nd} value is +8.5. The high Sm/Nd value is consistent with derivation of the LREE-depleted endmember from a strongly LREE-depleted peridotite, and is consistent with previous arguments for a refractory peridotite source for boninites. The high ε_{Nd} suggests that this peridotite was the residue of MORB or arc magma generation. During mixing with the LREE-enriched endmember, this component may have been a solid (i.e., metasomatism of a depleted peridotite by LREE-enriched fluids, with subsequent melting to form boninites), or a melt (i.e., partial melting of a depleted peridotite followed by mixing of the melt with a LREE-enriched material).

A line drawn through samples from the Bonin Islands toward high Sm/Nd values also extrapolated into the MORB field, but does not reach high Sm/Nd values expected in a refractory peridotite within the range of ε_{Nd} normally measured in oceanic rocks (Fig. 3.10). At Sm/Nd = 0.40 an ε_{Nd} of +15 is indicated, and a peridotite with this Sm/Nd would require 2.5 b.y. to evolve this ε_{Nd}. Within the range of ε_{Nd} values commonly measured in MORB's (+10 to +12), a maximum Sm/Nd of 0.33 to 0.36 is indicated for the LREE-depleted endmember, and peridotites with these Sm/Nd values would require more than 4 b.y. to evolve ε_{Nd} = +10 to +12. The source for the LREE-depleted endmember for Bonin Island boninites could be a refractory peridotite with an extremely long history of LREE-depletion (>2.5 b.y.). Alternatively, the LREE-depleted endmember could be derived from a peridotite residue from MORB generation which has undergone an episode of LREE enrichment before that recorded by the boninites.

Using the minimum Sm/Nd ratios inferred from Fig. 3.12, ε_{Nd} values in the LREE-enriched end-members are constrained to ε_{Nd} = +2 to +3 for boninites from Cape Vogel, and ε_{Nd} = -6 to 0 for boninites from the Bonin

Islands (Fig. 3.10). These values are consistent with derivation of the LREE-enriched endmembers from oceanic mantle sources (i.e., sources like those for most oceanic island lavas for Cape Vogel boninites, and sources like those for "anomalous" oceanic islands with $\varepsilon_{Nd} < 0$ like Kerguelen (Dosso and Murthy, 1980) and Tristan da Cuhna (O'Nions et al., 1977) for Bonin Island boninites), or from subducted sediment sources (i.e., young, arc-derived sediment for Cape Vogel boninites, and older, continentally derived sediment for Bonin Island boninites).

The relative REE and Ti abundances inferred for the LREE-enriched endmembers (Fig. 3.13) do not distinguish between sedimentary vs oceanic mantle sources for these materials. For example, Fig. 3.14 shows that relative abundances of REE and Ti in both sediments and metasomatized mantle peridotite nodules are similar to the LREE-enriched endmembers. The high La/Ti and Sm/Ti ratios in the LREE-enriched endmembers (and the high La/Nb in boninites, Table 3.2) could result if these materials had equilibrated as melts with a Ti-rich mineral (i.e., oceanic mantle sources), or had been derived from a material which had fractionated a Ti-mineral (i.e., silicic detrital sediment). The low Yb/Ti and high La/Yb ratios in the Cape Vogel LREE-enriched endmember could be explained by the presence of abundant garnet in its residue, as opposed to a garnet-poor residue for the Bonin Island LREE-enriched endmember. This is also supported by the higher Ti/Y and lower Zr/Nb ratios in Cape Vogel boninites compared to Bonin Island boninites (Table 3.2). However, garnet could be present either in mantle peridotite or a high pressure sediment mineral assemblage.

The enrichment of Zr relative to Ti and Sm in boninites is their most unusual geochemical feature. Zr abundances in boninites are not explicable

FIGURE 3.14: Relative abundances of REE and Ti in the maximum LREE-enriched mixing endmembers for Bonin Island and Cape Vogel boninites (Fig. 3.13) compared to abundances in sediments and metasomatized mantle peridotites. Sediment data from Turekian and Wedepohl (1961) and Shimokawa et al. (1972). Peridotite data from Frey and Green (1974), Ridley and Dawson (1975) and Frey and Prinz (1978).

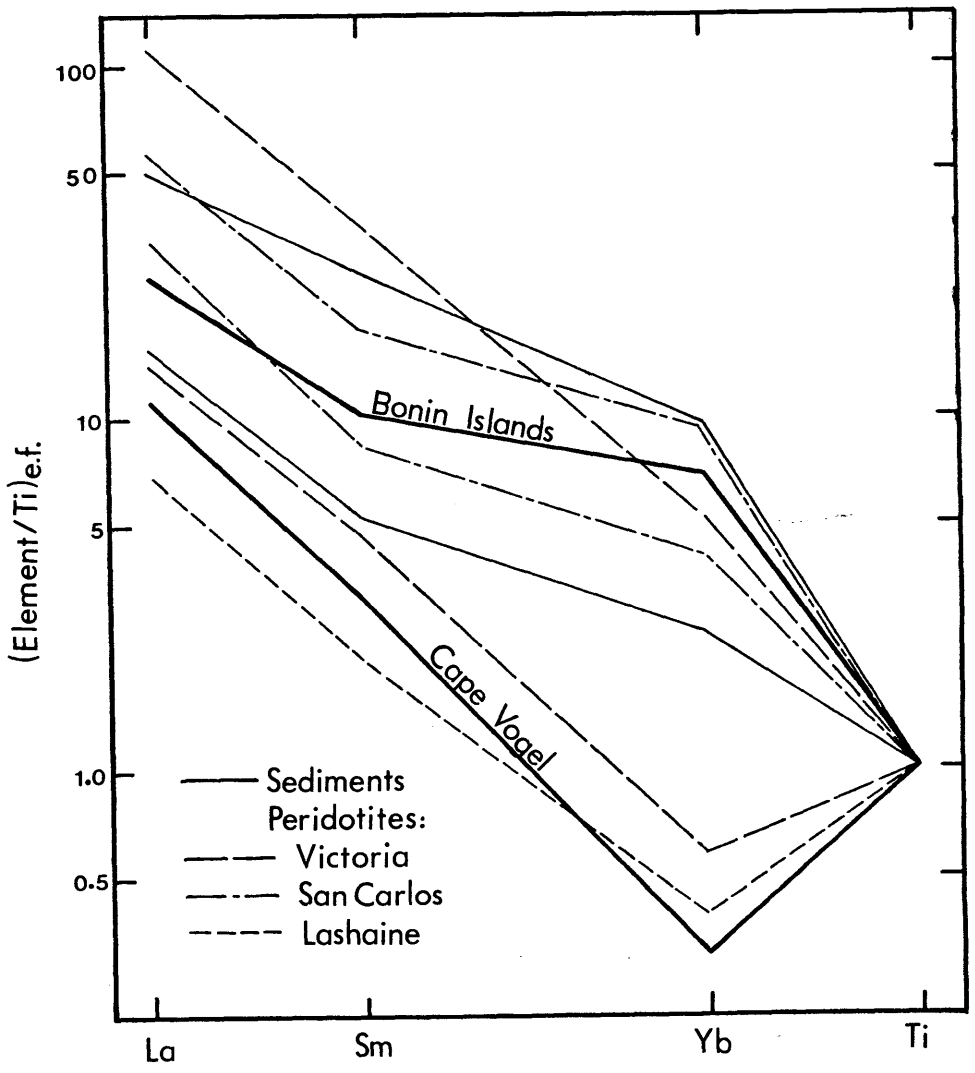
100
50
10
5
1.0
0.5
(Element/Ti)e.f.
Bonin Islands
Cape Vogel
Sediments
Peridotites:
Victoria
San Carlos
Lashaine
La
Sm
Yb
Ti

by two component mixing (Fig. 3.12d), however, the correlation of decreasing Ti/Zr with increasing La/Sm (Fig. 3.9) indicates that Zr-enrichment may be related to LREE-enrichment. Low Ti/Zr ratios like those in boninites are characteristic of highly differentiated rocks (e.g., rhyolites, Pearce and Norry, 1979), which have fractionated Fe-Ti oxides, and also detrital sediments (e.g., deep-sea clay and shale, Turekian and Wedepohl, 1961). Low Ti/Zr ratios are also found in some kimberlites (Kable et al., 1975; Fesq et al., 1975), and may result from residual garnet and clinopyroxene since these minerals have higher mineral/melt partition coefficients for Ti and Zr (see Chapters 5 and 7). However, enrichment in Zr relative to the intermediate REE, which is always present in boninites (Fig. 3.6), is not a characteristic of most differentiated rocks, sediments or kimberlites (Chapter 7). Enrichment in Zr relative to intermediate REE in boninites could be explained if the LREE-enriched endmembers equilibrated with a mineral with higher partition coefficients for intermediate REE than Zr. If their mineral/melt partition coefficients for Zr are low, possible residual minerals are amphibole or sphene, which have high partition coefficients for intermediate REE (Hellman and Green, 1979; Nicholls and Harris, 1980).

The similarity of relative REE and HFS element abundances in the LREE-enriched endmembers for boninites from the Bonin Islands and Cape Vogel is a good indication that they are derived from similar sources, particularly since they have a characteristic (high Zr/Sm) which is unusual in other rocks. Although oceanic mantle or subducted sediment sources are possible sources for the LREE-enriched endmember, an oceanic mantle source is considered most likely because the Cape Vogel boninites (i.e., the most LREE-enriched boninites) have the least trace element and

Nd-isotopic evidence for sediment involvement (e.g., low Ba/La, Fig. 3.7; $\varepsilon_{Nd} > 0$, Fig. 3.10).

SOURCES FOR K, Rb, Ba AND Sr IN BONINITES

The lack of correspondence between abundances of K, Rb, Ba and Sr in boninites and abundances of REE and HFS elements (Figs. 3.6, 3.7 and 3.8), and the lack of correlation between Sr and Nd isotopes (Fig. 3.11) indicates that these two groups of elements are derived from different sources. Decoupling and enrichment of K, Rb, Ba and Sr relative to REE and HFS elements in a common feature of arc volcanics, therefore, the source for K, Rb Ba and Sr in boninites has implications for other arc volcanics.

EVIDENCE FOR SEAWATER INVOLVEMENT:

A distinctive feature of boninites compared to other island arc volcanics is their enrichment in K and Rb relative to Ba (Fig. 3.8). This feature, along with the high and variable $^{87}Sr/^{86}Sr$ found in some boninites, suggests a contribution from seawater in boninites. For example, in Table 3.5, ratios of K, Rb, Sr and Ba in seawater, basalt alteration products resulting from seawater interaction, several types of sediments and arc lavas with possible Nd and Sr-isotopic evidence for sediment involvement are compared with those in boninites. Extremely high abundances of K and Rb relative to Ba are characteristic of seawater, and palagonites and smectites separated from altered MORB's. Sediments, which also can produce high $^{87}Sr/^{86}Sr$ as a source for arc lavas, do not have high K/Ba and Rb/Ba ratios, nor do lavas from the Banda Arc with high $^{87}Sr/^{86}Sr$ (Whitford and Jezek, 1979), which are believed to contain a sediment component (Whitford et al., 1980). A seawater component in boninites is also indicated by a $^{3}He/^{4}He$ ratios of 1.5 x atmospheric, reported in a

TABLE 3.5: RATIOS OF K, Rb, Ba and Sr IN SEAWATER, SEAWATER ALTERED BASALTS, BASALTIC ALTERATION PRODUCTS, SEDIMENTS, BANDA ARC LAVAS AND BONINITES

	BONINITES(1)	SEAWATER(2)	ALTERED(3) BASALTS	PALAGONITE(4)	SMECTITE(5)	AVERAGE(2) SEDIMENT	PACIFIC(6) SEDIMENTS	BANDA ARC(7) VOLCANICS
K/Ba	158	15,200	333	375	--	11	15	26
Rb/Ba	0.40	4.8	0.41	0.79	--	0.04	0.04	0.11
K/Rb	406	3,000	983	629	444	242	380	232
Sr/Ba	2.91	320	13.0	5.3	--	0.47	0.16	0.79
Rb/Sr	0.13	0.015	0.02	0.11	0.52	0.09	0.25	0.14
K/Sr	55	48	15.7	56	155	21	94	33

(1) Average of four Bonin Island boninites (Table 3.2).

(2) Kay (1980).

(3) Hart et al. (1974) and Staudigel et al. (1978).

(4) Staudigel et al. (1978).

(5) Staudigel et al. (1981).

(6) Church (1973).

(7) Four Banda Arc lavas with $^{87}Sr/^{86}Sr > 0.707$, Whitford and Jezek (1979) and Whitford et al. (1981).

boninite dredged from the Mariana Trench (Bloomer et al., 1979).

Therefore, three geochemical features of boninites suggest that they contain a component from seawater: their high K/Ba and Rb/Ba ratios, their high and variable $^{87}Sr/^{86}Sr$ ratios, and a near atmospheric $^{3}He/^{4}He$ value measured on one sample. Since the boninites studied also had some visible evidence for seawater alteration (e.g., devitrification of glass, formation of palagonite and clay), these features could be attributed to post eruptive processes. Several lines of evidence suggest that these geochemical features of boninites are primary, igneous characteristics:

1) All boninites have high K/Ba and Rb/Ba ratios compared to other arc volcanics. As noted earlier, boninites from the locales studied exhibited a wide range in extent of alteration: Bonin Island samples are relatively fresh, some Cape Vogel samples contain zeolites, and some Site 458 samples contain palagonite. If the high K/Ba and Rb/Ba in boninites results from post eruptive alteration, these ratios should correlate with the relative degree of alteration (particularly the presence of palagonite or clay). This is not the case (Fig. 3.8), in fact, Cape Vogel and Site 458 boninites have the lowest K/Ba and Rb/Ba ratios of boninites studied. In addition, K/Ba and Rb/Ba ratios in boninites from a single locale are similar (Fig. 3.8). In contrast, K/Ba and Rb/Ba ratios in altered MORB basalts from DSDP cores may vary by an order of magnitude between fresh and altered samples (Staudigel et al., 1978), the most altered samples having values like boninites (Table 3.5). If the high K/Ba and Rb/Ba ratios in boninites result from post eruptive alteration, greater variation in these values would be expected in samples from a single area, particularly since visible alteration effects varied among samples from individual areas.

2) $^{87}Sr/^{87}Sr$ ratios did not change during acid leaching experiments. Although acid leaching probably will not recover the original $^{87}Sr/^{86}Sr$ value of an altered rock (Staudigel et al., 1978), the lack of any change in $^{87}Sr/^{86}Sr$ suggests that the values measured in unleached samples could be the original values. If not, this result implies that fresh glass, altered glass and alteration products in the leached samples had exactly the same HCl solubility.

3) According to Bloomer et al. (1979), He concentration data (presumably high compared to seawater) precluded post eruptive seawater alteration as a source of the atmospheric $^{3}He/^{4}He$ value measured in their boninite sample.

These observations support the conclusion that the high K/Ba and Rb/Ba, high and variable $^{87}Sr/^{86}Sr$ ratios, and atmospheric $^{3}He/^{4}He$ ratio in boninites result from addition of a seawater component to their sources, rather than following their eruption.

Addition of a "seawater" component with high Rb/Ba, K/Ba and $^{87}Sr/^{86}Sr$ to the mantle sources of boninites could take place either by direct addition of subducted seawater or by addition of H_2O-rich fluids released by dehydration of basaltic clays with these chemical characteristics. Since unbound seawater is unlikely to be carried very far, if at all, into the mantle, addition of this component by dehydration of hydrous minerals is a more likely process.

ANOTHER SOURCE FOR Sr in BONINITES: MANTLE OR OCEANIC CRUST

The enrichment of Sr and Ba relative to REE and HFS elements, which is characteristic of boninites and most other arc volcanics, cannot be explained directly by addition of a hydrous component derived from subducted altered MORB, as suggested above for K and Rb, because unlike K and Rb, abundances of Sr and Ba in MORB's generally do not increase significantly relative to REE and HFS elements during alteration (Staudigel et al., 1978; Hart, 1971; Hart et al., 1974). Carbonate precipitation during alteration can result in Sr enrichment in MORB's but such carbonates generally have the Sr-isotopic composition of seawater (Staudigel et al., 1978). Addition of Sr with the isotopic composition of seawater cannot account quantitatively for the $^{87}Sr/^{86}Sr$ ratios in most boninites and their high Sr/Nd ratios.

For example, Table 3.6a lists the $^{87}Sr/^{86}Sr$ value required for a high Sr/Nd material ("anomalous Sr") which when added to "mantle" sources for boninites (i.e., Sr/Nd = 20, $^{87}Sr/^{86}Sr$ corresponding to $^{143}Nd/^{144}Nd$ in the mantle array) will produce their measured Sr/Nd and $^{87}Sr/^{86}Sr$ ratios. Except for boninites from Cape Vogel (Table 3.6a), these $^{87}Sr/^{86}Sr$ values are lower than that for seawater. Therefore, most boninites require a source for "anomalous Sr" (enriched relative to Nd when compared to chondrites and oceanic basalts) which has lower $^{87}Sr/^{86}Sr$ ratios than seawater. Because of their wide range, the calculated $^{87}Sr/^{86}Sr$ values for "anomalous Sr" in boninites (Table 3.6a) do not constrain the source for this Sr in boninites, except to indicate that a source with $^{87}Sr/^{86}Sr$ lower than seawater is required. Such sources could be the mantle sources of oceanic island volcanics, subducted MORB, or mixtures of these sources with detrital sediment and the "seawater" component.

TABLE 3.6: MIXING CALCULATIONS FOR Sr IN BONINITES

	(A) Sr derived from mantle and oceanic crust							(B) Sr derived from 2 mantle components and seawater Sr			
	(1) $^{87}Sr/^{86}Sr$	(2) Sr ppm	(3) Mantle Sr	(4) Anomalous Sr	(5) Mantle $^{87}Sr/^{86}Sr$	Anomalous $^{87}Sr/^{86}Sr$	% Sr Anomalous	(6) Mantle Sr	Seawater Sr	(7) Mantle $^{87}Sr/^{86}Sr$	(8) Mantle Sr/Nd
BONIN ISLANDS:											
2981	0.70510	97.2	30.1	67.1	0.7048	0.7052	69	88.1	9.1	0.7048	53
1983	0.70508	68.3	26.9	41.4	0.7042	0.7057	61	59.2	9.1	0.7046	40
1129-4	0.70472	85.7	35.6	50.1	0.7036	0.7055	58	76.6	9.1	0.7043	39
SITE 1403:											
2980	0.70613	106.8	33.8	73.0	0.7044	0.7069	68	55.5	51.3	0.7044	30
SITE 458:											
28-1	0.70381	89.1	31.4	57.7	0.7036	0.7040	65	83.0	6.1	0.7036	48
39-1	0.70376	89.6	32.2	57.4	0.7035	0.7039	64	86.3	3.3	0.7035	48
CAPE VOGEL:											
2984	0.70735	338.6	38.2	300.4	0.7037	0.7078	89	334.1	4.5	0.7073	158
2985	0.70431	90.7	86.2	4.5	0.7040	0.7103	5	86.2	4.5	0.7040	18

(1) Table 3.3.
(2) Table 3.2.
(3) Sr concentration assuming Sr/Nd = chondrites.
(4) Total Sr minus mantle Sr.
(5) $^{87}Sr/^{86}Sr$ values corresponding to $^{143}Nd/^{144}Nd$ for samples within the mantle array (Fig. 3.11).
(6) Sr contributed by mantle components assuming a constant contribution from seawater Sr.
(7) $^{87}Sr/^{86}Sr$ calculated for mantle Sr using 0.7080 for seawater Sr at 30 m.y.b.p. (Peterman et al., 1970).
(8) Sr contributed by mantle components divided by Nd in sample.

Except for the "seawater" component, Sr must be fractionated from REE and HFS elements by some process for any of these materials to serve as sources for Sr enrichment in boninites.

The suitability of potential sources for Sr in boninites can be evaluated to some extent using Pb isotopic data on boninites obtained by A. Meijer (personal communication, 1980). Because the Pb concentration of seawater is very low (~1 ng/kg, Quinby-Hunt and Turekian, 1983), and because seawater alteration does not result in changes in Pb-isotopic composition, the Pb-isotopic compositions of other potential boninite source materials may be more easily detected by their Pb-isotopic compositions.

Fig. 3.15 shows Pb isotopic compositions of boninites from the Bonin Islands and DSDP Site 458. Boninites from DSDP Site 458 have $^{206}Pb/^{204}Pb$ ratios similar to Pacific Ocean basalts, but lower $^{207}Pb/^{204}Pb$ ratios. Arc tholeiites from this site have Pb-isotopic compositions within error of the boninites. These values are unlike most measured in pre-Miocene Mariana Arc lavas (Fig. 3.15), and therefore are not likely to reflect assimilation of arc derived sediments or crust. A low $^{207}Pb/^{204}Pb$ ratio similar to the Site 458 boninites was measured by Meijer (1976) in a Cretaceous (?) basalt from the Pacific Ocean side of the Mariana Trench (Fig. 3.15; Meijer, personal communication). This supports a contribution from subducted MORB in these boninites, but could also reflect similarity in the Pb-isotopic composition of mantle sources on either side of the trench.

Pb-isotope compositions of two Bonin Island boninites (samples 1129-4 and 2982) have $^{206}Pb/^{204}Pb$ of 17.97-17.98, and $^{207}Pb/^{204}Pb$ of 15.52-15.53 (Fig. 3.15; Meijer, personal communication). These data were not published

FIGURE 3.15: Pb - Pb isotope diagram showing values for boninites from the Bonin Islands, and boninites and tholeiites from DSDP Site 458 (A. Meijer, personal communication). Data for Mariana Arc from Meijer (1976) and Table 4.2, this study. Data for Japan from Tatsumoto (1969).

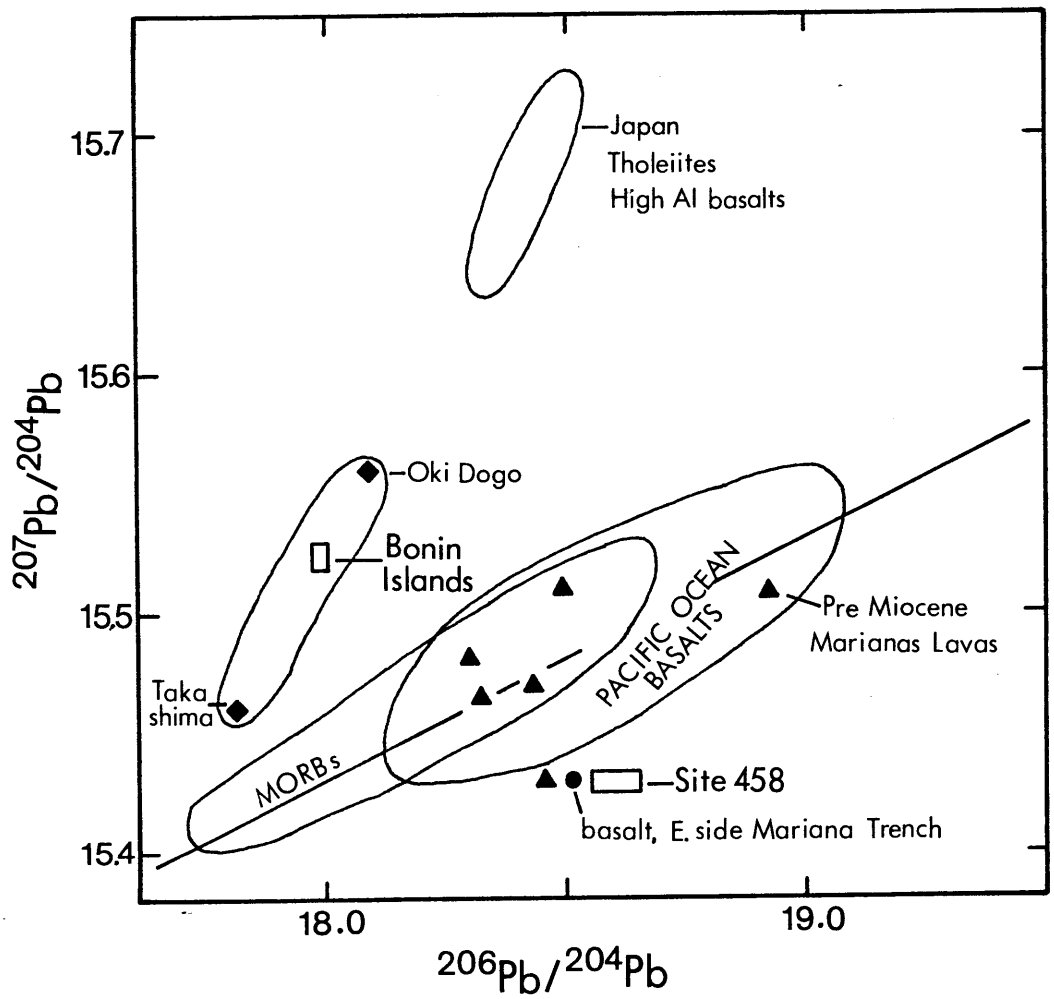
15.7
15.6
15.5
15.4
18.0
19.0
$^{207}Pb/^{204}Pb$
$^{206}Pb/^{204}Pb$
Japan
Tholeiites
High Al basalts
Oki Dogo
Bonin
Islands
Taka
shima
MORBs
PACIFIC OCEAN
BASALTS
Pre Miocene
Marianas Lavas
Site 458
basalt, E. side Mariana Trench

because the unusual values and possibly low Pb concentrations suggested that the samples could have been contaminated by Precambrian Pb during crushing in agate (Appendix I; Meijer, personal communication). However, very similar Pb-isotopic values were measured in alkalic basalts from Takashima and Oki Islands, southwestern Japan (Tatsumoto, 1969), which are adjacent to the northern extension of the Palau Kyushu Ridge, where the Bonin Islands probably originated (Fig. 3.1). These Takashima and Oki Island lavas have near-chondritic Sr and Nd-isotopic compositions (Allegre et al., in prep.), and were interpreted as derivatives from a chondritic "subcontinental" mantle source beneath southwestern Japan (Allegre et al., in prep.). Tholeiitic and high Al-lavas from Japan have more radiogenic Pb-isotope compositions (Fig. 3.15).

The variation in Pb isotopic composition in the Japan lavas was interpreted by Tatsumoto (1969) to reflect mixing between and mantle source (Takashima lavas) and sedimentary Pb (tholeiitic and high-Al lavas) from the subducted oceanic crust. The similarity of Pb and Nd isotope ratios in the Japanese alkalic basalts and boninites suggests that the Pb and Nd-isotopic composition of the boninites dominantly reflect chondritic characteristics of the mantle in this area, or metasomatism by a material derived from a nearby chondritic mantle source. For Sr, the Pb data could indicate derivation of a Sr-enriched, relatively low $^{87}Sr/^{86}Sr$ material from mantle sources. However, the Oki Island and Takashima lavas, like most alkalic basalts, do not have high Sr/Nd ratios, indicating that Sr-enrichment is not a characteristic of the mantle in this area. Since MORB's have low Pb/Sr ratios and $^{206}Pb/^{204}Pb$ ratios similar to the Bonin Island boninites, a component from subducted MORB could also be a source for Sr enrichment in Bonin Island boninites, without significantly

affecting their Pb-isotopic composition. Unlike Site 458 boninites, a small subducted sediment component is also permitted by the Pb isotopic data for Bonin Island boninites, therefore a Sr-enriched, intermediate $^{87}Sr/^{86}Sr$ component in Bonin Island boninites could be derived from subducted oceanic crust, including a sediment component.

Pb-isotopic data for boninites from DSDP Site 458 and the Bonin Islands are consistent with mantle sources or subducted oceanic crustal sources for enrichment in Sr. For Site 458 boninites, a oceanic crustal component cannot include subducted sediment, while for Bonin Island boninites a sediment component is permissible. Therefore, the enrichment in Sr relative to REE and HFS elements in boninites could result in two possible ways:

1) derivation of a high Sr/Nd component from mantle sources (possibly along with LREE and Zr), followed by addition of a "seawater" component with high K/Ba, Rb/Ba and $^{87}Sr/^{86}Sr$ derived from basaltic alteration products and carbonate, or
2) derivation of the high Sr/Nd component from oceanic crustal sources alone, including Sr from MORB, "seawater" and for Bonin Island boninites, possibly subducted detrital sediments.

MANTLE SOURCES FOR ENRICHMENT IN SR

Fig. 3.16a and Table 3.6b show possible mixtures of mantle and "seawater" component Sr which could explain the $^{87}Sr/^{86}Sr$, $^{143}Nd/^{144}Nd$ and Sr/Nd ratios in boninites. A constant contribution of "seawater" Sr is assumed for samples from a single area (Table 3.6b, column 2), consistent with their similar K/Ba and Rb/Ba ratos (Fig. 3.8), equal to the amount required to explain the displacement in $^{87}Sr/^{86}Sr$ of the sample with the

lowest $^{143}Nd/^{144}Nd$ from the mantle array. Calculated $^{87}Sr/^{86}Sr$ and Sr/Nd ratios without the "seawater" component (Table 3.6b, columns 7 and 8), should represent these values in the mantle sources of the boninites if this model is correct.

For boninites from the Bonin Islands, the calculated Sr/Nd ratios decrease with increasing $^{143}Nd/^{144}Nd$. Sm/Nd ratios in Bonin Island boninites also increase with increasing $^{143}Nd/^{144}Nd$ (Fig. 3.10), and earlier this was interpreted as indicating mixing between a LREE-depleted peridotite with high $^{143}Nd/^{144}Nd$ and a LREE-enriched mantle derived fluid or melt with low $^{143}Nd/^{144}Nd$. As shown in Fig. 3.16a, the variation in $^{87}Sr/^{86}Sr$, $^{143}Nd/^{144}Nd$ and Sr/Nd in Bonin Island boninites can be explained by mixing of a depleted peridotite with high $^{143}Nd/^{144}Nd$ and low or chondritic Sr/Nd, and a mantle derived metasomatic material with low $^{143}Nd/^{144}Nd$ and high Sr/Nd, followed by addition of equal amounts of a "seawater" Sr component. The calculated sources for these boninites, before addition of "seawater" Sr, are displaced from the mantle array (Fig. 3.16a), and mixing curves projected through these points from the source for sample 2981 (lowest $^{143}Nd/^{144}Nd$) intersect the mantle array at high MORB-like $^{143}Nd/^{144}Nd$ ratios, and near chondritic Sr/Nd ratios. Calculated mantle sources for boninites from Site 1403 and DSDP Site 458 do not plot on these mixing curves (Table 3.6b, Fig. 3.16a), but could lie on similar mixing curves with different endmember compositions. Therefore, mixing of two mantle components, specifically, a LREE-depleted peridotite with high $^{143}Nd/^{144}Nd$ and a LREE-enriched, low $^{143}Nd/^{144}Nd$, high Sr/Nd fluid or melt, followed by interaction of this mixed source with a "seawater" component from the subducted oceanic crust, could explain the K, Rb, Sr and LREE

abundances, and Sr and Nd isotopic characteristics of boninites from the Mariana-Bonin Arc.

For boninites from Cape Vogel (Table 3.6b), a constant contribution from the "seawater" component is not consistent with this model, because the sample with lower $^{143}Nd/^{144}Nd$ also has lower Sr/Nd and $^{87}Sr/^{86}Sr$. For these boninites, the contribution from the "seawater" component must be different in the sources for the two samples in order for mixing of two mantle components to explain their $^{87}Sr/^{86}Sr$, $^{143}Nd/^{144}Nd$ and Sr/Nd ratios.

The major problem with this model is that Sr-enrichment is rarely observed in mantle derived magmas or metasomatized peridotites. Near chondritic Sr/Nd ratios are characterisitic of oceanic basalts (DePaolo and Wasserburg, 1979), and as noted earlier earlier, the Takashima and Oki Island alkalic basalts, which are isotopically similar to Bonin Island boninites, have chondritic Sr/Nd ratios (Allegre et al., in prep.). LREE-enriched peridotites from Victoria, Australia (Chen, unpublished data; Burwell, 1976); Dreiser Weiher, West Germany (Jagoutz et al., 1978); and most peridotites from Lashaine, Tanzania (Ridley and Dawson, 1975) also have Sr/Nd ratios of only 9-19, although they have REE and Ti abundances like those in the LREE-enriched endmembers of boninites (Fig. 3.14). In general, high Sr/Nd ratios in mantle derived materials are restricted to carbonatites and some peridotites found in them (Allegre et al., 1971; Ridley and Dawson, 1975).

FIGURE 3.16: Sr - Nd correlation diagrams showing possible mixing schemes for low Sr/Nd and high Sr/Nd source components for boninites.

a) Mixing of a mantle derived component with high Sr/Nd and low $^{143}Nd/^{144}Nd$, with MORB-residue peridotite, followed by addition of a constant amount of "seawater" Sr. The amount of "seawater" Sr required to displace sample 2981 from the mantle array is used for the other two samples (Table 3.6b). Mixing curves projected from the mantle source for 2981 through mantle sources for the other samples intersect the mantle array at high $^{143}Nd/^{144}Nd$ ratios and near chondritic Sr/Nd ratios appropriate for a MORB-residue peridotite.

b) Mixing of Sr derived from oceanic crust (MORB, sediment and "seawater") with an oceanic mantle source with chondritic Sr/Nd and variable $^{143}Nd/^{144}Nd$ for Bonin Island boninites. Sr/Nd in the oceanic crustal component is assumed to be extremely high. Percentages to left of large dots are % Sr of total derived from the oceanic crust (Table 3.6a).

c) Mixing of Sr derived from subducted oceanic crust with an oceanic mantle source with chondritic Sr/Nd and variable $^{143}Nd/^{144}Nd$ for boninites from Cape Vogel, Dredge Site 1403, and DSDP Site 458. The average Sr isotope composition of the oceanic crustal component varies from area to area but is similar for samples from each area (Table 3.6a).

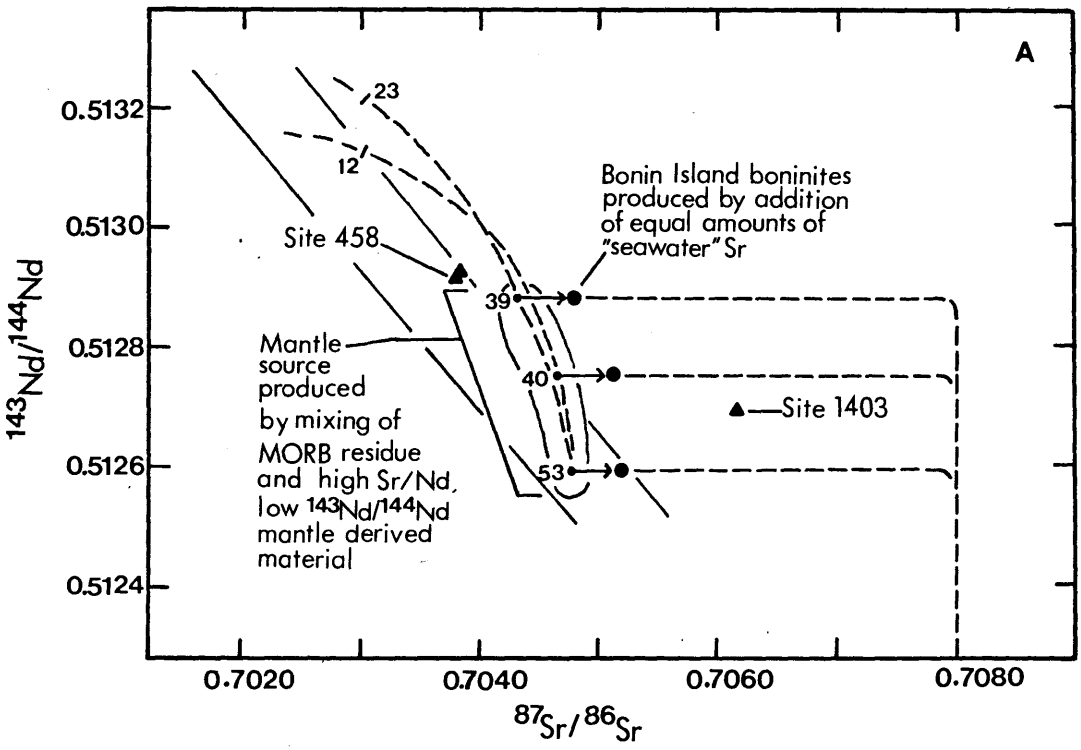
A
0.5132
0.5130
0.5128
0.5126
0.5124
$^{143}Nd/^{144}Nd$
0.7020
0.7040
0.7060
0.7080
$^{87}Sr/^{86}Sr$
23
12
Site 458
Bonin Island boninites produced by addition of equal amounts of "seawater" Sr
39
40
53
Site 1403
Mantle source produced by mixing of MORB residue and high Sr/Nd, low $^{143}Nd/^{144}Nd$ mantle derived material

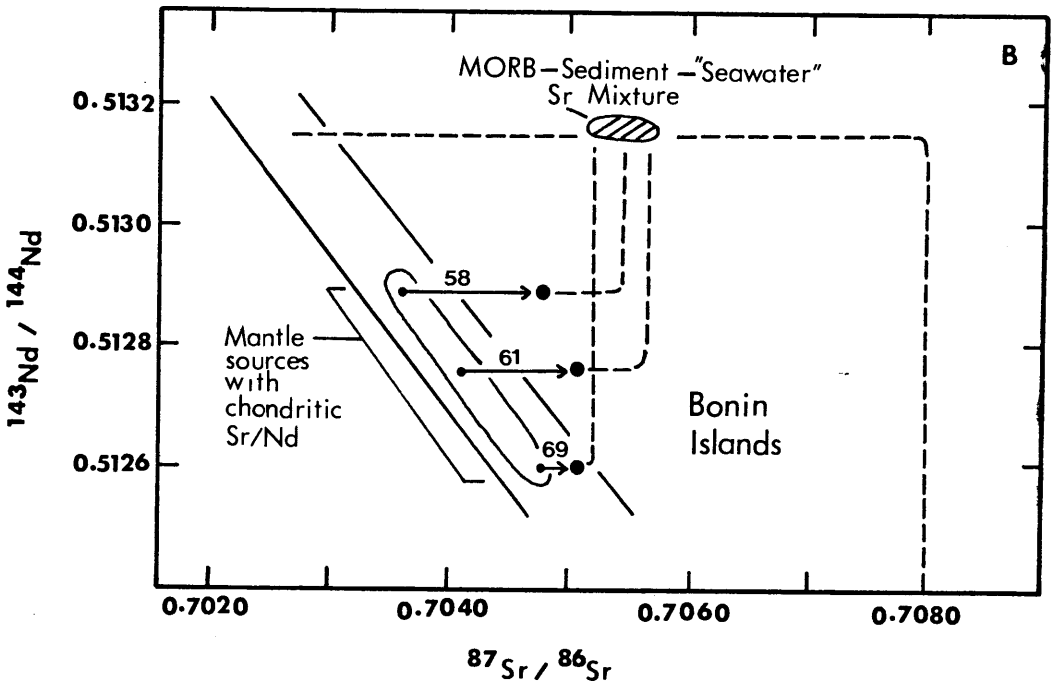
B
MORB–Sediment–"Seawater"
Sr Mixture
0.5132
0.5130
0.5128
0.5126
$^{143}Nd / ^{144}Nd$
58
61
69
Mantle
sources
with
chondritic
Sr/Nd
Bonin
Islands
0.7020
0.7040
0.7060
0.7080
$^{87}Sr / ^{86}Sr$

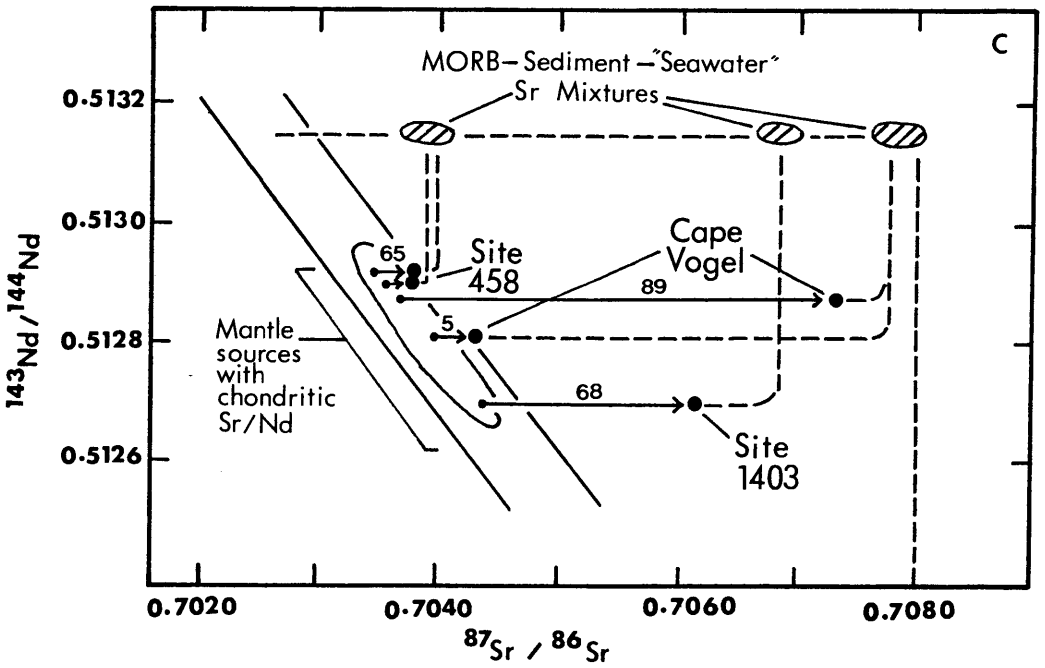
C
MORB–Sediment–"Seawater"
Sr Mixtures
0.5132
0.5130
0.5128
0.5126
$^{143}Nd / ^{144}Nd$
65
Site
458
Cape
Vogel
89
5
68
Site
1403
Mantle
sources
with
chondritic
Sr/Nd
0.7020
0.7040
0.7060
0.7080
$^{87}Sr / ^{86}Sr$

OCEANIC CRUSTAL SOURCES FOR Sr IN BONINITES

The second possible source for Sr-enrichment in boninites is the subducted oceanic crust. Since all boninites appear to contain a "seawater" component with high K/Ba, Rb/Ba and $^{87}Sr/^{86}Sr$, derivation of Sr from other components of the oceanic crust may be indicated. In this case, the average $^{87}Sr/^{86}Sr$ for "anomalous" Sr in boninites (Table 3.6a) may represent a mixture of MORB, "seawater" component, and possibly sedimentary Sr from the oceanic crust, which is added to the refractory, LREE-metasomatized mantle peridotite source for boninites.

As noted earlier, such a source for Sr requires a mechanism by which Sr is fractionated from REE and HFS elements, because MORB's and detrital sediments usually have near chondritic Sr/Nd. The "seawater" component in boninites may be K, Rb and H_2O-rich fluids released by dehydration of basaltic alteration products. At atmospheric pressure Sr is enriched relative to Nd in seawater which is in equilibrium with basalt, silicate and carbonate sediment. If this relationship continues to low to moderate pressure (<10 kbar, the pressures determined experimentally for boninite generation), then it is possible that H_2O-rich fluids released from the subducted oceanic crust may also be enriched in Sr relative to REE and HFS elements, and have a Sr-isotopic composition reflecting equilibration with altered basalt and sediment.

A possible mixing model for enrichment in Sr in boninites from oceanic crustal sources is shown in Figs. 3.16b and c. In this model the anomalous $^{87}Sr/^{86}Sr$ calculated in Table 3.6a is used as the Sr-isotopic composition of the oceanic crustal component, and the Nd-isotopic composition of MORB is used. Since relative amounts of MORB vs "seawater" vs sediment Sr cannot be calculated, the Nd-isotopic composition of an oceanic crustal component

is unknown. However, since no detrital sediment contribution is indicated by Pb-isotopic data for DSDP Site 458 boninites and only a small contribution from sediment is indicated by Pb data for Bonin Island boninites, a MORB-like $^{143}Nd/^{144}Nd$ may be reasonable. Mixing lines between the Sr-enriched oceanic crustal component and the mantle sources of boninites are drawn in Figs. 3.16b and c assuming an extremely high Sr/Nd in the oceanic crustal component.

As shown in Table 3.6a, the Sr-isotopic composition of the oceanic crustal component is similar in boninites from a given area. For boninites from Cape Vogel, different Sr/Nd and $^{87}Sr/^{86}Sr$ values in the two samples correspond to different amounts of the oceanic crustal component added. For boninites from the Bonin Islands, variation in Sr/Nd and $^{87}Sr/^{86}Sr$ also results from variations in the amount of this component added to their mantle sources. The lack of correlation between Sr/Nd and displacement of $^{87}Sr/^{86}Sr$ from mantle array values in these samples (Fig. 3.11) can be explained by the fact that the $^{87}Sr/^{86}Sr$ indicated for their oceanic crustal component (0.7055) is similar to that in their mantle sources. For example, sample 2981 has the highest Sr/Nd and requires the largest amount of the oceanic crustal component (69%, Table 3.6a), but has a mantle $^{87}Sr/^{86}Sr$ of 0.7048, therefore its displacement from the mantle array is smaller than other Bonin Island samples, which have lower $^{87}Sr/^{86}Sr$ ratios in their mantle Sr components (Table 3.6a).

For boninites from the Mariana-Bonin Arc increasing $^{87}Sr/^{86}Sr$ in the oceanic crustal component corresponds to their relative K/Ba and Rb/Ba ratios, e.g., Site 458 boninites have the lowest $^{87}Sr/^{86}Sr$ in their oceanic crustal component and the lowest K/Ba and Rb/Ba ratios (Fig. 3.8), while the Dredge Site 1403 boninite has the highest $^{87}Sr/^{86}Sr$ in its oceanic

crustal component and the highest K/Ba and Rb/Ba. This suggests that the "seawater" component may be the major source of high $^{87}Sr/^{86}Sr$ in these boninites. For Cape Vogel boninites this is not the case (i.e., they have high $^{87}Sr/^{86}Sr$ in their oceanic crustal component, but low K/Ba and Rb/Ba). Therefore, more detailed Sr and Pb isotopic study of boninites from each area is required to resolve these complexities.

Thus two general models for boninite generation can be outlined:

1) mixing of two mantle components, a LREE-depleted peridotite with high $^{143}Nd/^{144}Nd$ and a LREE-enriched, low $^{143}Nd/^{144}Nd$ fluid or melt with high Sr/Nd, followed by interaction of this mixed source with fluids derived from the subducted oceanic crust having high K/Ba, Rb/Ba and Sr/Nd, and the Sr-isotopic composition of seawater; or
2) mixing of two mantle components, a LREE-depleted peridotite with high $^{143}Nd/^{144}Nd$ and a LREE-enriched, low $^{143}Nd/^{144}Nd$ fluid or melt with chondritic Sr/Nd, followed by interaction of this mixed source with fluids derived from the subducted oceanic crust with high K/Ba, Rb/Ba and Sr/Nd, and an intermediate Sr-isotopic composition reflecting equilibration with subducted MORB, seawater and possibly detrital sediment.

Both models can explain the variation of Sr/Nd and $^{87}Sr/^{86}Sr$ in boninites, and both models rely on an unknown process which fractionates Sr from Nd. In mantle derived materials enrichment in Sr compared to Nd is rare, whereas high Sr/Nd is a characteristic of seawater. Based on this observation and that Sr-enrichment relative to REE and HFS elements is generally restricted to island arc volcanics, which supports a subduction related source for Sr-enrichment, a subducted oceanic crustal source Sr-enrichment in boninites is preferred.

CONCLUSIONS AND SUMMARY

The trace element and isotopic characteristics of boninites from the Mariana - Bonin Arc and Cape Vogel, Papua New Guinea support a common mode of origin for these rocks, as suggested by their similar major element compositions. The high Mg/(Mg + ΣFe), Ni, Cr and Co abundances, but low Ti contents and low Ti/V and Ti/Sc ratios in boninites from these areas indicate that boninite magma is derived by partial melting of refractory mantle peridotite, which has been depleted in highly and moderately incompatible elements, possibly as the result of a previous partial melting episode.

Abundances of highly incompatible elements, such as K, Rb, Ba, Sr, La and Zr in boninites are high relative to HREE and Ti contents, and are not consistent with a depleted peridotite source. Nd, Sr and Pb isotopic ratios in boninites are highly variable, and can be correlated with variations in trace element ratios. These features indicate that the incompatible element characteristics of boninites reflect mixing or metasomatism of their depleted peridotite sources with incompatible element enriched materials. Based on geochemical similarities between boninites from different areas, and variations within individual areas, two types or stages of incompatible element enrichment can be identified:

1) mixing of a refractory peridotite having MORB-like $^{143}Nd/^{144}Nd$ with a LREE-enriched, low $^{143}Nd/^{144}Nd$ mantle derived fluid or melt with high Zr abundances compared to intermediate REE (i.e., high Zr/Sm). For boninites from the Bonin Islands, Nd and Pb isotopic data suggest this material was derived from a chondritic or LREE-enriched mantle source, while for boninites from Cape Vogel, a mantle source similar to those

for most oceanic island volcanics (i.e., Sm/Nd < chondrites, but $\varepsilon_{Nd} > 0$) is indicated. This stage of incompatible element enrichment may not be related to subduction.

2) enrichment of this mixed mantle source in K, Rb and to a lesser extent Sr and Ba by H_2O-rich fluids released from the subducted oceanic crust. The trace element imprint of this material is similar to seawater (e.g., high K/Ba and Rb/Ba), and its Sr-isotopic composition reflects equilibration with MORB, seawater and possibly detrital sediment. That boninites from all areas have evidence for a "seawater" component suggests that the presence of water in their refractory peridotite sources may be critical for boninite generation.

Compared to other island arc volcanics, boninites are similar in that they are enriched in K, Rb, Ba and Sr relative to REE and HFS elements. High K/Ba, Rb/Ba, Zr/Sm and Zr/Ti ratios, and U-shaped REE patterns in some samples distinguish boninites from other arc lavas. Therefore, the specific boninite model is probably not applicable to arc volcanics in general. However, it is unlikely that the oceanic crust or mantle-derived materials proposed as components of boninites would be restricted to a particular area of the sub-arc mantle. These materials may be present in other types of arc volcanics, but be geochemically less evident because of the presence of additional components such as more fertile mantle peridotite, or partial melts of subducted oceanic crust.

CHAPTER 4: ISOTOPE AND TRACE ELEMENT GEOCHEMISTRY OF LOW TiO_2 LAVAS FROM THE FACPI FORMATION, AND OTHER VOLCANIC ROCKS FROM GUAM, MARIANA ARC

GEOLOGICAL BACKGROUND

Guam is the southernmost island of the Mariana Frontal Arc (Fig. 3.1). The geology of Guam and the geochemistry of volcanic rocks from Guam were described by Stark (1963) and Tracey et al. (1964), and more recently by Reagan and Meijer (1982). Based on K/Ar ages of volcanic rocks, Reagan and Meijer (1982) revised the stratigraphic relationships proposed by Tracey et al. (1964), and divided rocks from Guam into three time units (Fig. 4.1), the Facpi Formation (late -middle Eocene), the Alutom Formation (late Eocene to early Oligocene), and the Umatac Formation (Miocene).

Volcanic rocks from the Facpi Formation are predominantly low TiO_2 (<0.5% TiO_2 in samples with >8% MgO) pillow lavas and pillow breccias. One sample has a K/Ar age of 43.8 $\pm$ 1.5 m.y. (Meijer et al., 1982). In the Alutom Formation, volcanic rocks are breccias, lava flows and sills, and have calc-alkaline and tholeiitic characteristics. Calc-alkaline Alutom volcanics are found in central Guam, while tholeiitic Alutom volcanics predominate in northern Guam (Reagan and Meijer, 1982). K/Ar ages on breccia clasts from the Alutom Formation range from 34 to 36 m.y. (Meijer et al., 1982). Volcanic rocks from the Umatac Formation include flows and pyroclastics, and are calc-alkaline to alkaline rocks. One sample has a K/Ar age of 13 m.y. (Meijer et al., 1982).

According to the historical outline of the Mariana Arc - Philippine Sea region (Chapter 3), the low TiO_2 Facpi Formation lavas correspond in age to the earliest period of volcanism of the Palau-Kyushu Arc, following

FIGURE 4.1: Stratigraphic column for Guam: a) from Tracey et al. (1964); b) revised by Reagan and Meijer (1982). From Reagan and Meijer (1982).

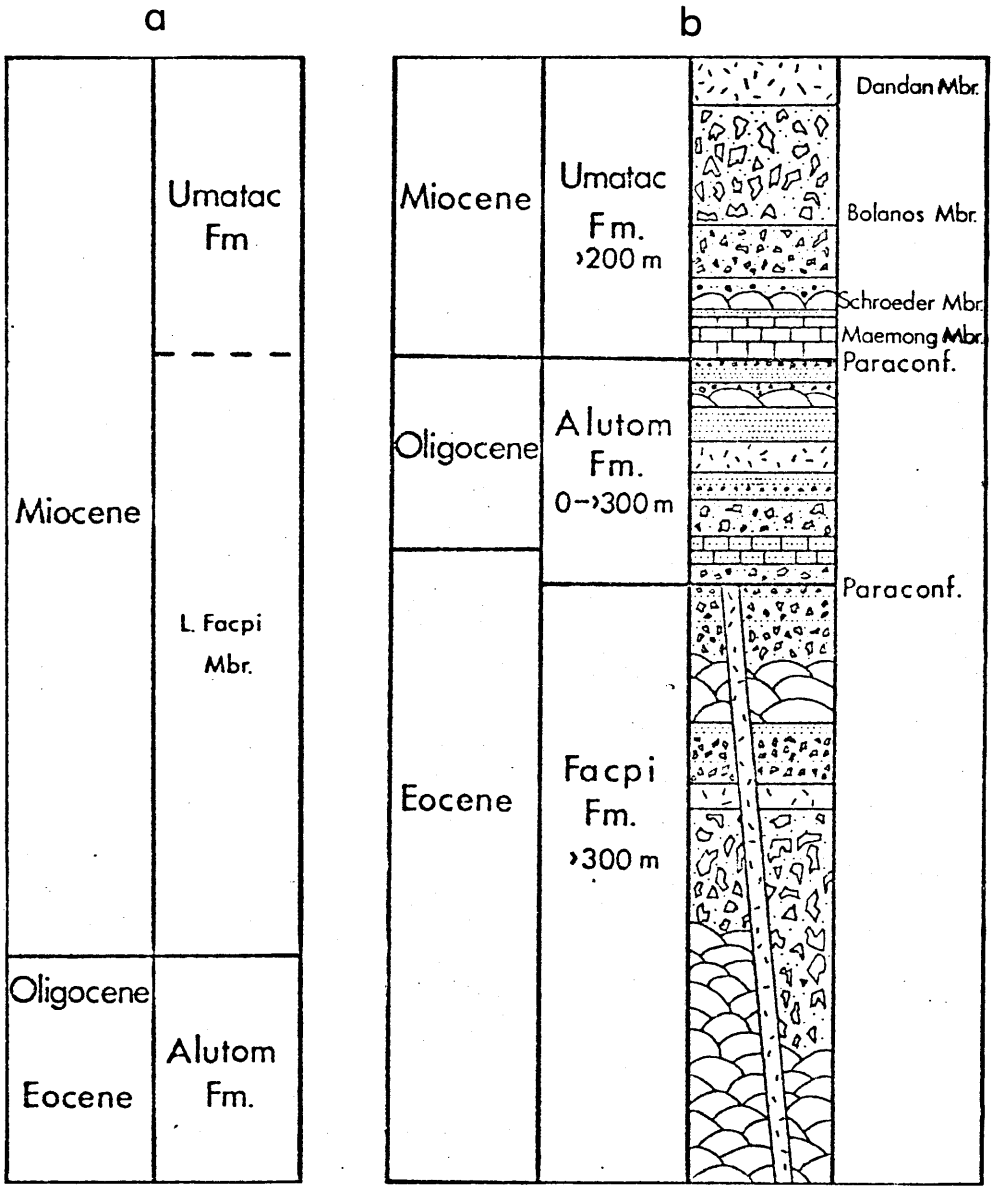
a
Miocene
Umatac Fm
L. Facpi Mbr.
Oligocene
Eocene
Alutom Fm.
b
Miocene
Umatac Fm. >200 m
Dandan Mbr.
Bolanos Mbr.
Schroeder Mbr.
Maemong Mbr.
Paraconf.
Oligocene
Alutom Fm. 0–>300 m
Paraconf.
Eocene
Facpi Fm. >300 m

Pacific plate subduction under the Philippine Basin. They are at least 10 m.y. older than boninites from the Bonin Islands, DSDP Site 458 and Dredge Site 1403, based on a combination of K/Ar and stratigraphic dating. Alutom Formation volcanics represent a later period of volcanism in the same position (Palau-Kyushu Arc), and are also older than boninites. The Umatac Formation corresponds in age to volcanism along the West Mariana Arc, following rifting of the Palau-Kyushu Arc and development of the Parece Vela back-arc basin, and is younger than boninites.

MAJOR ELEMENT GEOCHEMISTRY AND PETROGRAPHY

Whole rock and phenocryst compositions for lavas from the Facpi and Alutom Formations, including samples analyzed for trace elements and isotopes in this study, are discussed in detail by Reagan and Meijer (1982). Rocks from these two formations are categorized by Reagan and Meijer (1982) as members of the "boninite series", arc tholeiite series, and calc-alkaline series based on TiO_2 content (i.e., normative ilmenite, Fig. 2.1b), inferred crystallization sequence, and Fe-enrichment trends as shown on an AFM diagram.

The Facpi Formation consists of "boninite series" (analyses 1-4, Table 4.1) and arc tholeiite series (analysis 5, Table 4.1) lavas. Arc tholeiites cap the unit in one area of southwestern Guam and occur as dikes intruding "boninite series" pillow lavas (Reagan and Meijer, 1982). Both Facpi rock types have low TiO_2 contents in MgO-rich samples (0.32-0.45% TiO_2 at 8-13% MgO in the "boninite series", and 0.34-0.52% TiO_2 at 8-11% MgO in the arc tholeiite series, Reagan and Meijer, 1982), and plot in the "boninite series" area of Fig. 2.1b. "Boninite series" Facpi lavas typically are glassy and contain less than 10% phenocrysts, mainly olivine

TABLE 4.1: MAJOR ELEMENT COMPOSITIONS OF VOLCANIC ROCKS FROM GUAM

	FACPI FORMATION					ALUTOM FORMATION			UMATAC FORMATION	
	"BONINITE SERIES"				THOLEIITE -SERIES-	THOLEIITE -SERIES-		CALC-ALKALINE -SERIES-		
	(1)	(2)	(3)	(4)	(5)	(6)	(7)	(8)	(9)	(10)
	GM-68	GUM 79-11	GUM 79-19	GUM 80-39	GUM 79-6	GSR 3	GUM 79-2	GM-75	71781-A1	GM 65-3
SiO_2	54.44	55.42	56.05	58.30	51.80	54.61	58.47	66.26	60.27	54.29
TiO_2	0.34	0.45	0.52	0.77	0.36	0.55	0.64	0.34	0.89	1.04
Al_2O_3	15.05	15.34	16.37	14.04	16.83	17.60	17.14	15.16	16.29	15.21
FeO	7.81	7.91	8.46	8.63	8.26	8.79	7.25	5.02	8.06	13.26
MnO	0.19	0.16	0.15	0.15	0.14	0.15	0.09	0.09	0.23	0.22
MgO	9.71	8.58	5.65	2.72	9.81	5.31	3.51	3.51	1.87	3.85
CaO	9.32	9.10	8.76	6.41	10.85	10.21	8.36	5.66	5.32	8.84
Na_2O	2.36	2.09	2.48	2.85	1.64	2.10	2.89	2.73	3.73	2.25
K_2O	0.62	0.54	0.75	1.08	0.12	0.36	0.95	0.73	2.74	0.90
P_2O_5	0.05	0.07	0.08	--	0.05	0.08	0.10	0.08	0.52	0.26

Samples 1 through 9 are major element microprobe analyses from Reagan and Meijer (1982), and Reagan (personal communication). Sample 10 is an XRF analysis, this study. Fe for sample 10 is Fe_2O_3.

and clinopyroxene in MgO-rich samples. Olivine cores range from Fo 92 to 85, and chromites, occurring as inclusions in olivines and rarely in clinopyroxene, have Cr/(Cr + Al) ratios of 0.6 to 0.85 which overlap the range found in boninites (Reagan and Meijer, 1982). Orthopyroxene phenocrysts occur only in more differentiated Facpi "boninite series" lavas (e.g., analyses 2 through 4, Table 4.1), and have En contents of 79 to 65 (Reagan and Meijer, 1982). Plagioclase follows orthopyroxene crystallization (e.g., analyses 3 and 4, Table 4.1), and ranges from An 81 to 73 (Reagan and Meijer, 1982).

The inferred crystallization sequence based on petrography for Facpi "boninite series" lavas is consistent with trends formed by the four samples used in this study on the projections quartz - olivine - clinopyroxene (Fig. 4.2a) and quartz - olivine - plagioclase (Fig. 4.2b). In Fig. 4.2a, Facpi "boninite series" samples form a linear trend of nearly constant olivine - clinopyroxene ratio, displaced toward higher olivine component and lower clinopyroxene component content than plagioclase saturated, olivine - clinopyroxene cotectics determined by Grove et al. (1982) and Walker et al. (1979), for calc-alkaline lavas and MORB's respectively. This trend could be produced by fractional crystallization of olivine and clinopyroxene, followed by orthopyroxene and clinopyroxene, as suggested by Reagan and Meijer (1982), at several kbar P-H_2O, based on the position of the 1 kbar P-H_2O curve inferred by Grove et al. (1982). In Fig. 4.2b, Facpi "boninite series" lavas define a trend suggesting dominant olivine crystallization relative to plagioclase, although all the lavas plot within the 1 atm plagioclase primary field determined by Stolper (1982) for MORB's. Since the trend shown in Fig. 4.2a suggests high P-H_2O crystalliztion, which would also decrease the field of plagioclase

FIGURE 4.2: a) Four Facpi Formation "boninite series" lavas on the projection Olivine - Quartz - Clinopyroxene, showing plagioclase, clinopyroxene and olivine multiple saturation curves determined by Grove et al. (1982) for calc-alkaline lavas and Walker et al. (1979) for MORB's, and the field for boninites.

b) Four Facpi Formation "boninite series" lavas on the projection Olivine - Quartz - Plagioclase, showing a plagioclase, olivine and clinopyroxene multiple saturation curve determined by Stolper (1980) for MORB's, and the field for boninites.

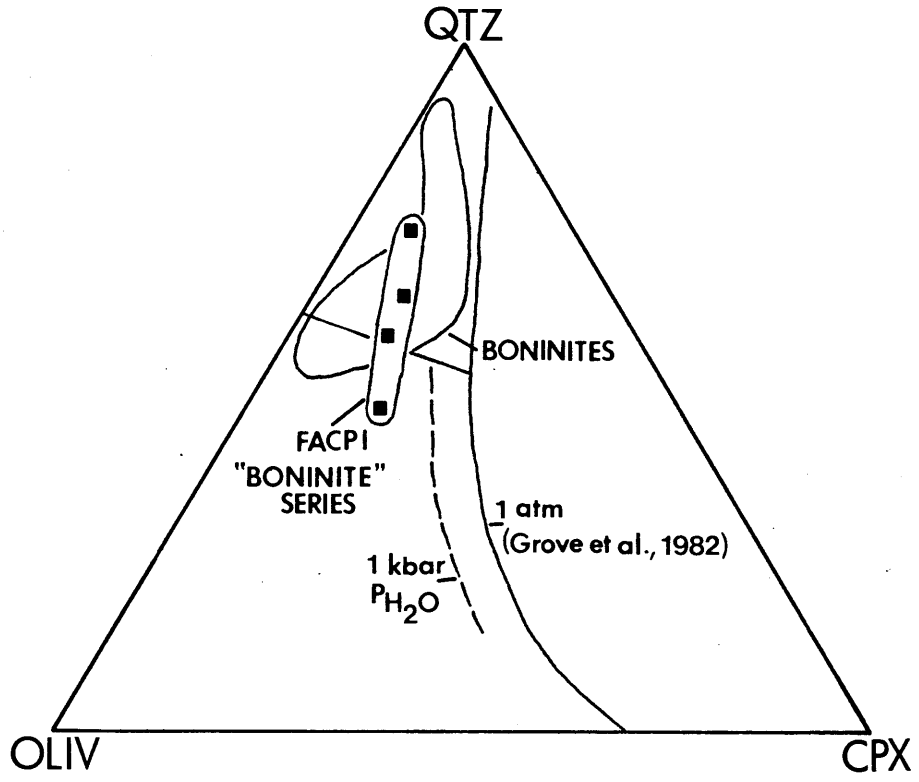
QTZ
BONINITES
FACPI
"BONINITE"
SERIES
1 atm
(Grove et al., 1982)
1 kbar
P_{H_2O}
OLIV
CPX

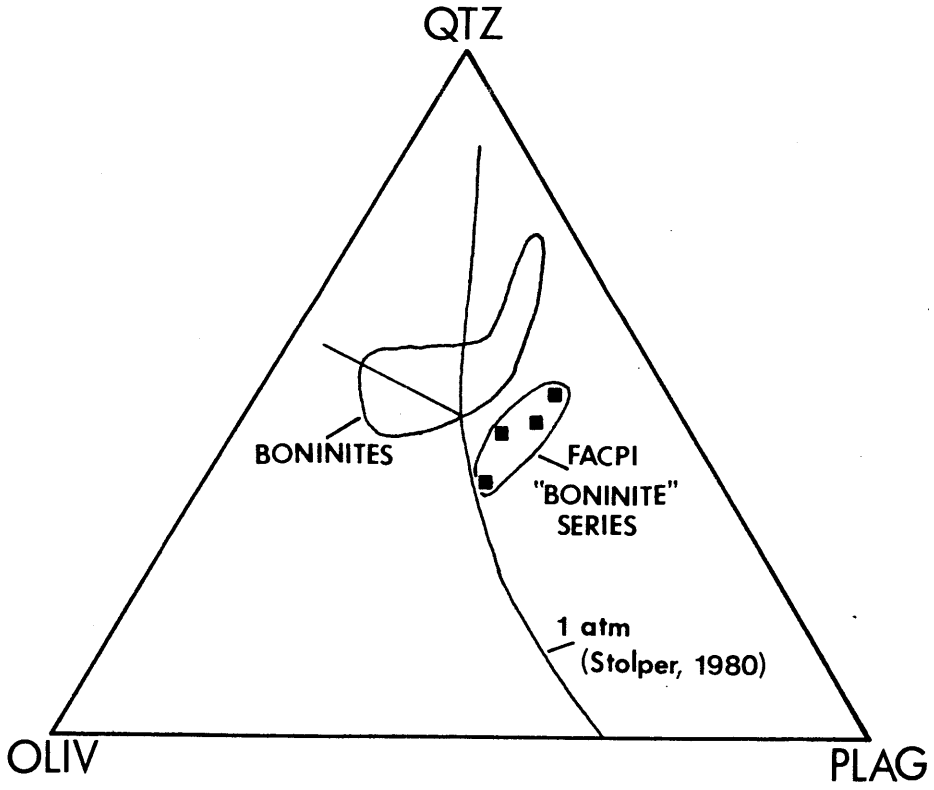
QTZ
BONINITES
FACPI
"BONINITE"
SERIES
1 atm
(Stolper, 1980)
OLIV
PLAG

stability relative to olivine, plagioclase crystallization in the Facpi "boninite series" may have been inhibited by high P-H_2O, increasing their petrographic resemblance to boninites. However, compared to boninites, Facpi "boninite series" lavas are distinguished petrographically by the late appearance of orthopyroxene, following clinopyroxene and olivine, and chemically by their higher content of plagioclase component (Fig. 4.2b).

Facpi Formation arc tholeiites differ from "boninite series" lavas in their lower SiO_2 contents, higher Al_2O_3 and CaO contents at a given MgO content, lower K_2O, and higher modal abundance of plagioclase (analysis 5, Table 4.1; Reagan and Meijer, 1982). The inferred crystallization sequence for Facpi arc tholeiites is olivine plus plagioclase, followed by clinopyroxene and orthopyroxene (Reagan and Meijer, 1982).

Rocks from the Alutom Formation can be divided into arc tholeiite and calc-alkaline series based on Fe-enrichment trends, and correspond to different geographic locations on Guam (Reagan and Meijer, 1982). Three Alutom samples were analyzed, a tholeiitic basaltic andesite and andesite (analyses 6 and 7, Table 4.1) and a calc-alkaline andesite (analysis 8, Table 4.1). Because MgO-rich tholeiitic and calc-alkaline lavas from Guam have similar major element compositions and similar Rb, Sr, Ba and Zr abundances, Reagan and Meijer (1982) concluded that these two groups evolved from similar parental magmas, the arc tholeiites through early crystallization of olivine, plagioclase and clinopyroxene, followed by orthopyroxene and magnetite, and the calc-alkaline lavas through fractionation of hornblende, plagioclase, clinopyroxene, orthopyroxene and magnetite, combined with magma mixing.

The Umatac Formation samples analyzed are two andesites (analyses 9 and 10, Table 4.1). Sample 9 is from the Schroeder Flow Member of the Umatac (Fig. 4.1) and Sample 10 is from the Bolanos Member. Sample 10 has 6.4% $Na_2O + K_2O$ at 60% SiO_2, would be classified as an alkaline lava in the scheme of Kuno (1966). The samples are glassy or extremely fine-grained rocks, with less than 10% plagioclase phenocrysts and minor clinopyroxene.

ALTERATION AND SAMPLE PREPARATION

Facpi and Alutom Formation samples (analyses 1 through 8, Table 4.1) are altered to some extent. Olivines are usually represented by pseudomorphs of alteration products, while clinopyroxene, orthopyroxene and plagioclase are usually fresh appearing. Fresh appearing glass or groundmass material was present in all samples at least in small quantities. Sample preparation techniques are described in detail in Appendix I. INAA, RNAA and Nd-isotope analyses were done on powders prepared from least altered appearing rock, separated as small chunks, based on the freshness of phenocrysts, and groundmass clarity and color. Sr-isotope analyses were done on plagioclase separates for samples 3, 6, 7, 8, 9 and 10. Comparisons of plagioclase and whole rock Sr-isotope analyses are given in Appendix I. $^{87}Sr/^{86}Sr$ values for plagioclase separates are 0.00003 to 0.00020 lower than whole rock values. For samples lacking plagioclase (samples 1, 2, and 4), or containing very fine grained plagioclase (sample 5), Sr-isotope and Rb and Sr concentrations were determined on freshest appearing rock (predominantly groundmass or glass) separated after fine crushing (Appendix I).

TRANSITION METAL ABUNDANCES IN FACPI LAVAS

Trace element abundances in volcanics from Guam are listed in Table 4.2. Normalized abundances of transition metals in an MgO-rich Facpi "boninite series" lava and arc tholeiite series lava (both 10% MgO) are shown in Fig. 4.3, superimposed on the field for boninites. Like boninites, MgO-rich Facpi lavas have high Cr, Ni and Co abundances (134-199 ppm Ni, 36-42 ppm Co; 462-827 ppm Cr in the two samples), which overlap the range found in primitive basalts from non-island arc environments (Fig. 4.3). The two lavas have lower than chondritic Ti/Sc ratios (48-49), similar to those in boninites from Cape Vogel (Ti/Sc = 40-80, Table 3.2), but they have Sc and Ti contents near the upper range of boninites (Fig. 4.3). The MgO-rich Facpi lavas also have higher than chondritic Al_2O_3/TiO_2 and CaO/TiO_2 ratios (44-47 and 27-30 respectively), which are within the range for these ratios in boninites (CaO/TiO_2 = 10-80; Al_2O_3/TiO_2 = 18-130, Fig. 3.2). Less MgO-rich samples (e.g., samples 3 and 4, Table 4.1) have lower than chondritic CaO/TiO_2 and Sc/Ti ratios.

INCOMPATIBLE TRACE ELEMENT ABUNDANCES IN FACPI LAVAS COMPARED TO BONINITES

In Fig. 4.4, normalized abundances of highly incompatible and moderately incompatible elements in two MgO-rich "boninite series" Facpi Formation lavas are shown along with normalized trace element abundances in a boninite from the Bonin Islands. Relative abundances of Sr, REE and HFS elements in the two Facpi lavas are similar to those in boninites. In particular, the Facpi "boninite series" lavas have characteristics of boninites such as depletion in Ti relative to Y and Yb, low Ti/Zr ratios (44-51), enrichment in Zr relative to intermediate REE (Zr/Sm = 1.2-1.5 x chondrites), and high Sr/Nd (24-40).

TABLE 4.2: TRACE ELEMENT ABUNDANCES IN VOLCANIC ROCKS FROM GUAM

	FACPI FORMATION					ALUTOM FORMATION			UMATAC FORMATION	
	--------"BONINITE SERIES"----------				THOLEIITE --SERIES-					
	(1)	(2)	(3)	(4)	(5)	(6)	(7)	(8)	(9)	(10)
Sc[1]	41.3	32.8	--	28.9	44.9	--	17.3	16.2	17.9	35.2
Cr	697	827	--	46.9	462	--	148	112	0.9	6.1
Co	36.5	38.3	--	25.5	42.4	--	31.4	18.8	15.8	33.0
Ni[2]	199	196	67	--	134	24	38	48	16	--
Rb[3]	10.6*	9.97*	13	--	1.95*	8	24.0	11	77	18.4
Sr	145.3*	126.4*	139	--	122.0*	145	130	124	573	443.0
Ba	83.2*	77	122	--	37	62	93	101	515	--
Y	10	34	20	--	10	28	22	38	--	46
Zr	46	53	68	--	30	51	73	82	126	57
Hf	1.04	1.19	--	--	0.57	--	1.35	2.22	4.7	1.82
La[4]	2.72	3.55	4.03	4.94	1.01	3.16	6.19	3.67	31.4	10.4
Ce	6.45	7.55	9.09	11.2	2.89	9.07	10.3	8.37	61.7	22.3
Nd	3.57	4.82	5.78	6.43	2.44	7.71	7.07	6.17	31.1	13.8
Sm	1.08	1.63	1.84	2.01	0.99	2.81	2.07	1.91	6.79	3.78
Eu	0.426	0.613	0.63	0.698	0.428	1.01	0.746	0.714	1.74	1.37
Tb	0.272	0.438	0.468	0.492	0.272	0.697	0.483	0.482	1.03	0.69
Yb	1.29	2.10	2.08	2.34	1.27	2.51	2.09	2.40	3.60	2.74
Lu	0.206	0.336	0.335	0.365	0.202	0.391	0.336	0.378	0.556	0.411

(1) Sc, Cr, Co and Hf by INAA (this study).
(2) Ni, Y, and Zr by XRF from Reagan and Meijer (1982).
(3) Rb, Sr and Ba by XRF from Reagan and Meijer (1982), except for starred values by isotope dilution (this study).
(4) REE for samples 1, 2, 4, 7, 8, 9 and 10 by INAA, samples 3, 5 and 6 by RNAA (this study).

FIGURE 4.3: Chondrite normalized transition metal abundances in a MgO rich Facpi Formation "boninite series" lava (circle) and tholeiite series lava (diamond), compared to boninites and primitive basalts from non-island arc environments. Normalizing values given in Table 3.2.

FIGURE 4.4: a) Normalized trace element abundances in two Fapci Formation "boninite series" lavas compared to a boninite from the Bonin Islands. Normalizing values given in Table 3.2.
b) Normalized trace element abundances in a Facpi Formation tholeiite series lava (sample 5, Table 4.2) compared to a Facpi "boninite series" lava (sample 1, Table 4.2).

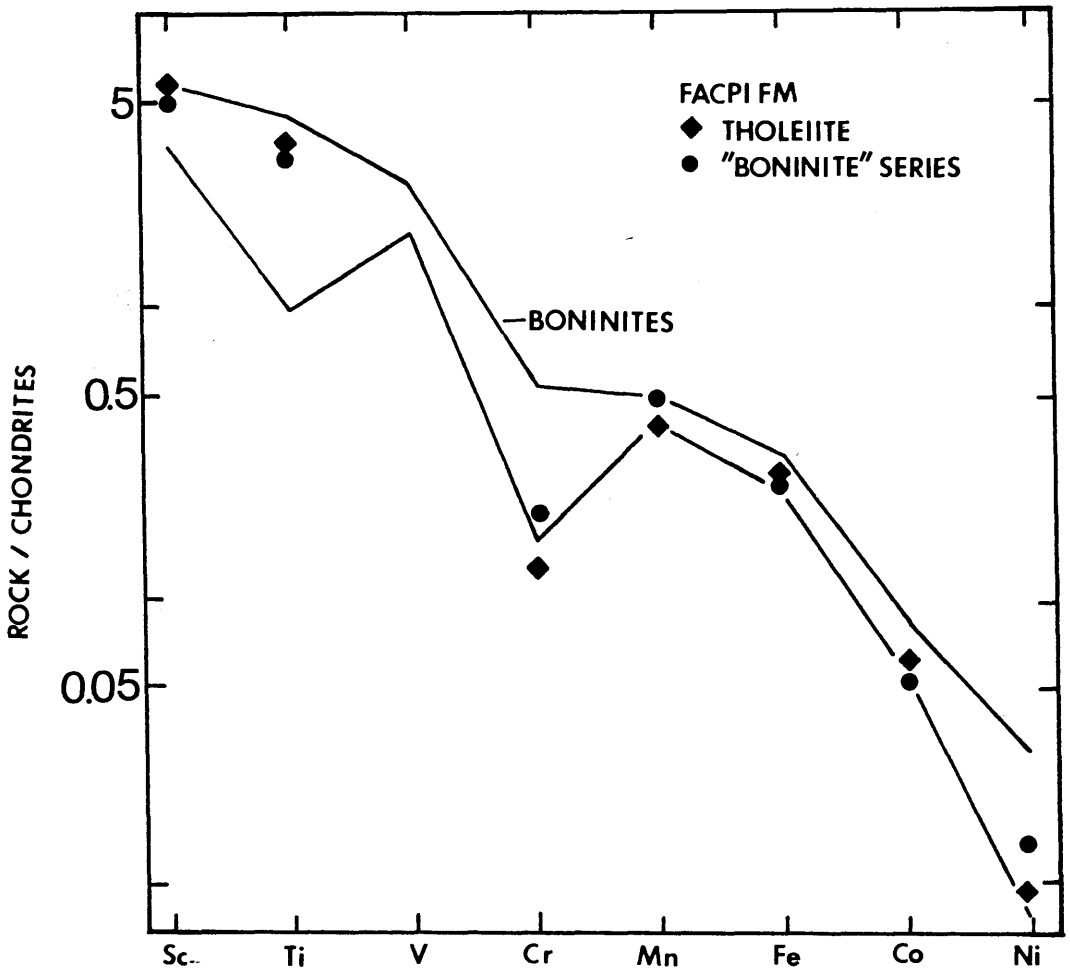
FACPI FM
THOLEIITE
"BONINITE" SERIES
BONINITES
ROCK / CHONDRITES
5
0.5
0.05
Sc
Ti
V
Cr
Mn
Fe
Co
Ni

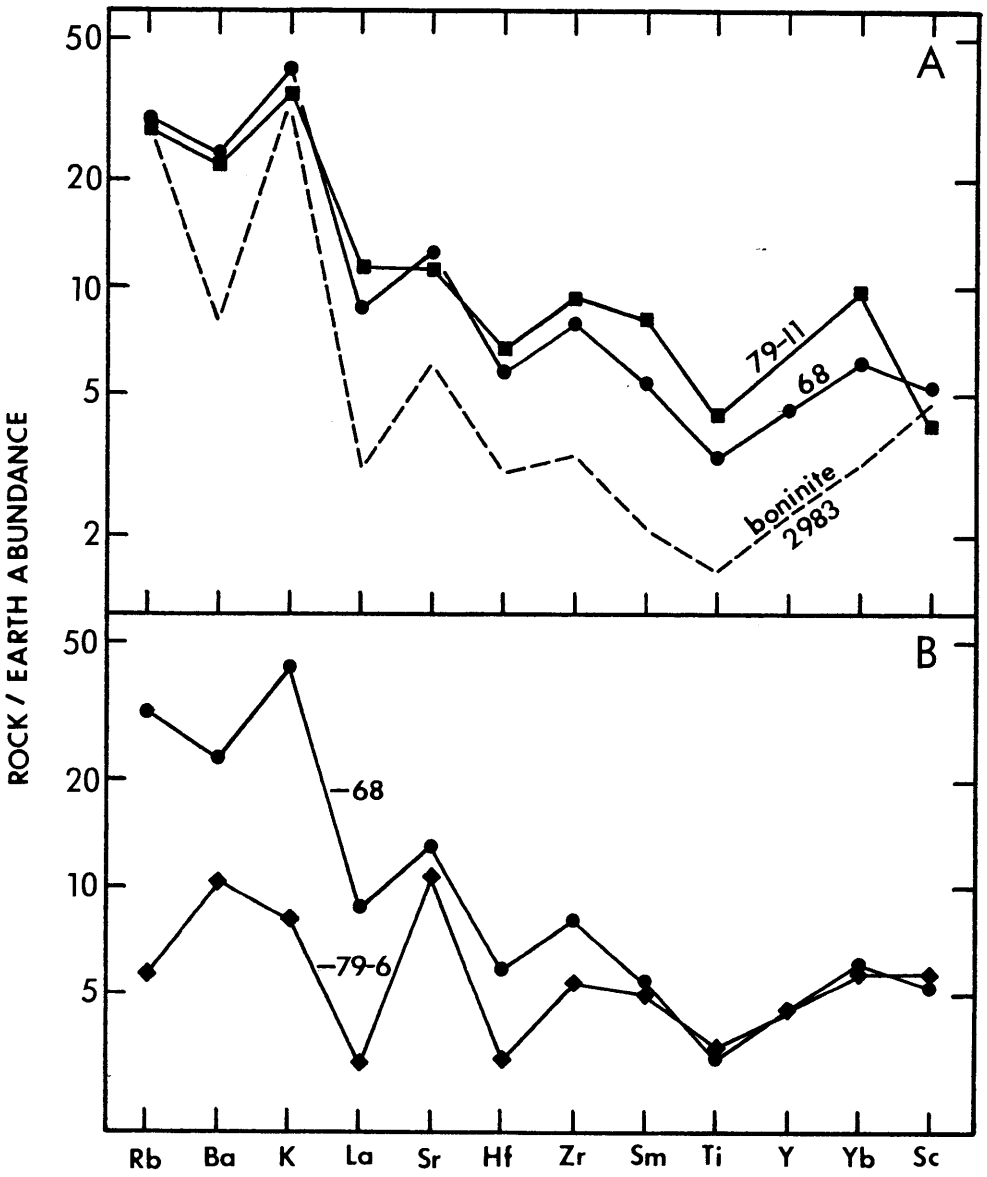
ROCK / EARTH ABUNDANCE
50
20
10
5
2
A
79-11
68
boninite
2983
B
68
79-6
Rb
Ba
K
La
Sr
Hf
Zr
Sm
Ti
Y
Yb
Sc

Fig. 4.5 shows chondrite normalized REE abundances in "boninite series" Facpi lavas compared to boninites, and normalized REE abundances in other volcanics from Guam. Absolute REE abundances in Facpi "boninite series" lavas (5-16 x chondrites) are systematically higher than those in boninites from the Bonin Islands (1-5 x chondrites), but, like boninites, these Facpi lavas have concave upward REE patterns which are enriched in LREE and HREE relative to intermediate REE. $(La/Sm)_{e.f.}$ ranges from 1.37 to 1.58 and $(La/Yb)_{e.f.}$ ranges from 1.14 to 1.43. In contrast, the tholeiitic Facpi Formation sample (Fig. 4.5b) is LREE-depleted, with $(La/Sm)_{e.f.}$ of 0.65 and $(La/Yb)_{e.f.}$ of 0.55.

Andesitic lavas from the Alutom and Umatac Formations on Guam have variable REE abundances and normalized abundance patterns. The three Alutom Formation lavas (Fig. 4.5d) have similar REE abundances of 10-20 x chondrites. Two samples from the tholeiitic Alutom series have different REE pattern types; one sample is LREE-enriched and has a concave upward pattern, while the other is LREE-depleted and has a concave downward pattern. A calc-alklaine Alutom sample has a U-shaped REE pattern that is much flatter than those in the Facpi "boninite series" lavas ($(La/Sm)_{e.f.}$ = 1.2, $(La/Yb)_{e.f.}$ = 1.0). Two Umatac Formation samples (Fig. 4.5c) are strongly LREE-enriched ($(La/Yb)_{e.f.}$ = 2.6 and 5.9), and have HREE abundances of 13-18 x chondrites.

In Fig. 4.4b, normalized trace element abundances in the LREE-depleted Facpi tholeiite series lava is compared to a "boninite series" lava with similar MgO content (9.7 and 9.8% MgO). As noted earlier, both samples have low TiO_2 contents and plot in the "boninite series" of Meijer (1980) (Fig. 2.1b). In fact, the two lavas have nearly identical absolute and relative abundances of Ti, Y, Yb and Sc (Fig. 4.4b). The LREE-depleted

FIGURE 4.5: Chondrite normalized REE abundances in: a) Facpi Formation "boninite series" lavas; b) a Facpi Formation tholeiite series lava; c) two lavas from the Umatac Formation; and d) lavas from the calc-alkaline and tholeiitic series of the Alutom Formation, Guam. Data from Table 4.2, normalizing values in Table 3.2.

FIGURE 4.6: Ti/Zr plotted vs $(La/Sm)_{e.f.}$ for Facpi Formation lavas compared to values in boninites from the Mariana - Bonin Arc and Cape Vogel, PNG.

FIGURE 4.7: $(Ba/La)_{e.f.}$ plotted vs $(La/Sm)_{e.f.}$ for Facpi Formation lavas and Alutom and Umatac Formation lavas, compared to boninites, island arc and oceanic basalts. Fields for island arc and oceanic basalts from Kay (1980).

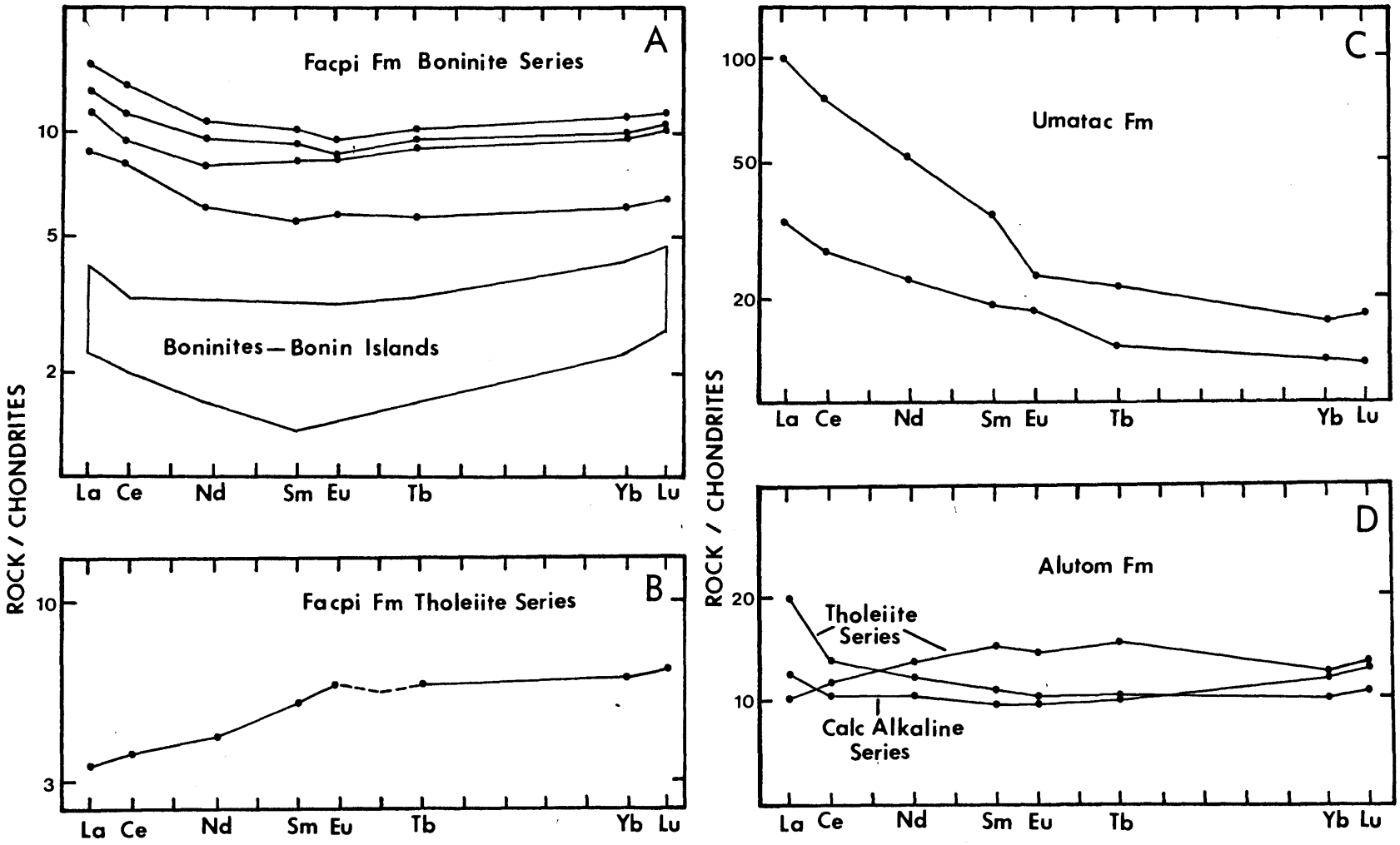
A
Facpi Fm Boninite Series
Boninites—Bonin Islands
B
Facpi Fm Tholeiite Series
C
Umatac Fm
D
Alutom Fm
Tholeiite Series
Calc Alkaline Series
ROCK / CHONDRITES
ROCK / CHONDRITES
La Ce Nd Sm Eu Tb Yb Lu
10
5
2
3
100
50
20

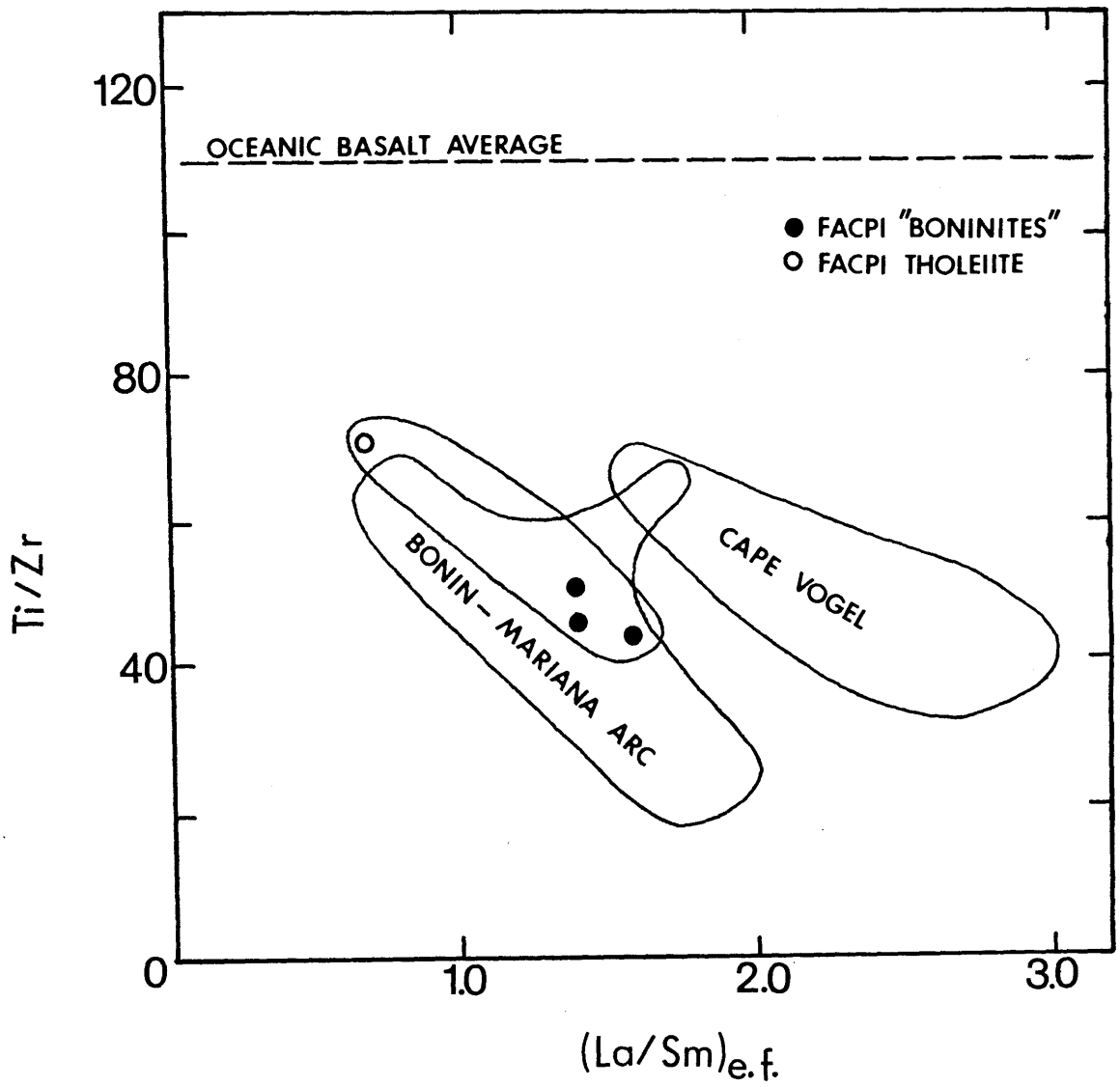
120
80
40
0
Ti/Zr
OCEANIC BASALT AVERAGE
● FACPI "BONINITES"
○ FACPI THOLEIITE
CAPE VOGEL
BONIN-MARIANA ARC
1.0
2.0
3.0
(La/Sm)e.f.

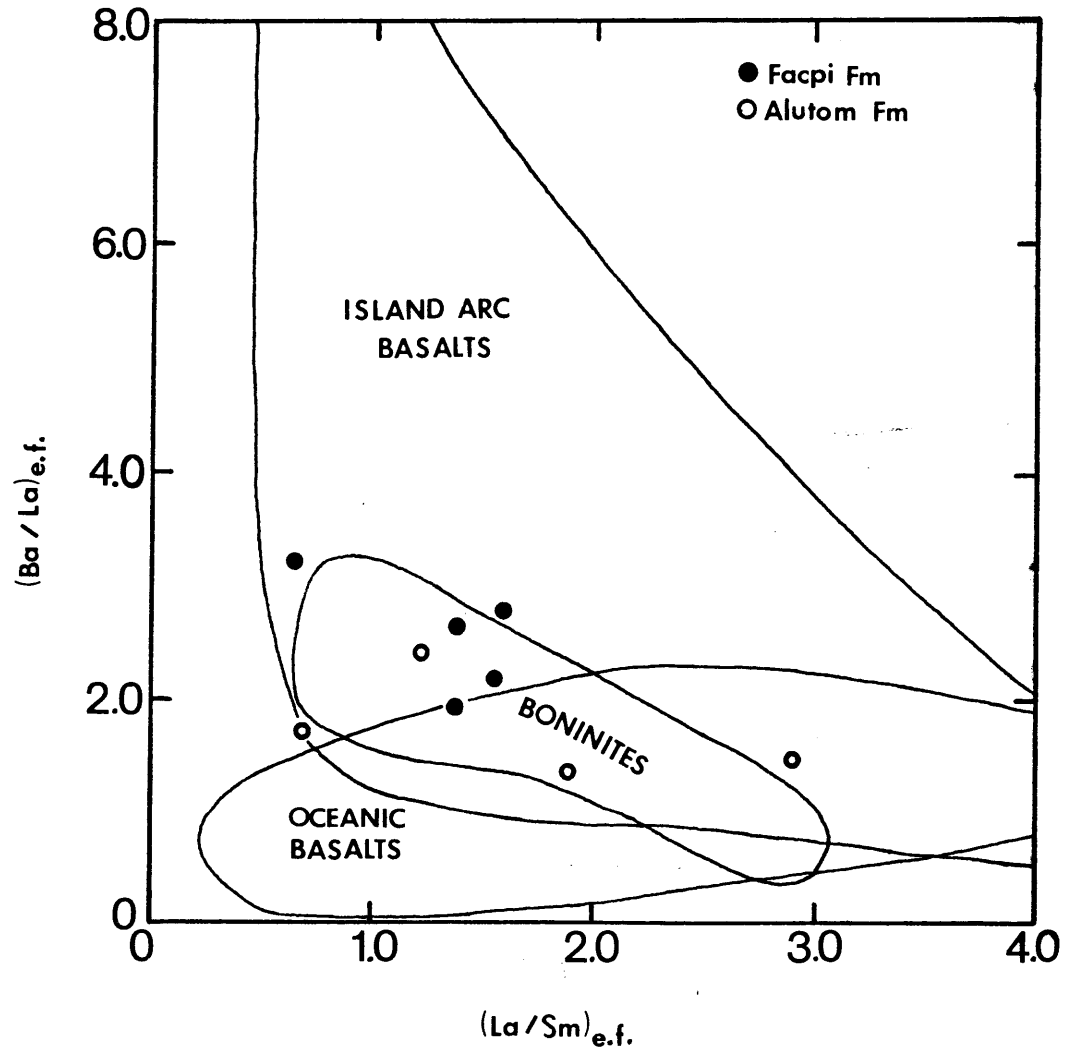
8.0
6.0
4.0
2.0
0
0
1.0
2.0
3.0
4.0
● Facpi Fm
O Alutom Fm
ISLAND ARC
BASALTS
BONINITES
OCEANIC
BASALTS
(Ba / La)e.f.
(La / Sm)e.f.

tholeiitic lava has less Zr enrichment relative to Ti and Sm than the LREE-enriched "boninite series" lava, but also has a lower Ti/Zr ratio (72) than is commonly found in oceanic volcanics. A correlation between low Ti/Zr and high La/Sm is also observed in boninites. In Fig. 4.6, Ti/Zr and La/Sm ratios in Facpi lavas are plotted with values of these ratios in boninites. The Facpi lavas plot with boninites from the Mariana - Bonin Arc, and the tholeiitic sample has lower (La/Sm) and higher Ti/Zr ratios than LREE-depleted boninites from DSDP Site 458.

Relative abundances of the elements K, Rb, Ba and Sr in Facpi "boninite series" and arc tholeiite series lavas are different from those in boninites. Ba/La ratios in these lavas, and all other Guam volcanics studied, are similar to those in boninites with similar La/Sm (Fig. 4.7). However, the Facpi "boninite series" samples studied have lower K/Ba and Rb/Ba ratios than those in boninites (K/Ba = 51-63 and Rb/Ba = 0.11-0.14, as compared to K/Ba = 86-340 and Rb/Ba = 0.15-0.70 in boninites), and the Facpi tholeiite has extremely low values of K/Ba = 27 and Rb/Ba = 0.05, and plots with the majority of island arc volcanics in Fig. 3.8. These K/Ba and Rb/Ba values are characteristic of the two Facpi lava types (Reagan and Meijer, 1982).

ISOTOPIC CHARACTERISTICS OF VOLCANICS FROM GUAM

Isotopic data for volcanic rocks from Guam are listed in Table 4.3. In Fig. 4.8, lavas from the Facpi Formation and other Guam volcanics are plotted on a Nd-Sr isotope correlation diagram. Four Facpi "boninite series" lavas have $^{143}Nd/^{144}Nd$ and $^{87}Sr/^{86}Sr$ ratios nearly within analytical error (Table 4.3) and average at $^{143}Nd/^{144}Nd = 0.51294$ and $^{87}Sr/^{86}Sr = 0.70358$. The Facpi Formation tholeiite has a similar

TABLE 4.3: Nd, Sr AND Pb ISOTOPIC DATA FOR VOLCANIC ROCKS FROM GUAM

	Age(1)	$(^{143}Nd/^{144}Nd)_o$(2)	$(\varepsilon_{Nd})_o$	$(^{87}Sr/^{86}Sr)_o$(3)	$(\varepsilon_{Sr})_o$	$^{206}Pb/^{204}Pb$	$^{207}Pb/^{204}Pb$
FACPI FORMATION:	44 m.y.						
"BONINITE SERIES"							
GM-68		0.512952 ± 17	+7.2	0.70357 ± 3	-15.3	18.927 ± 9	15.501 ± 8
GUM 79-11		0.512934 ± 20	+6.8	0.70354 ± 3	-15.8	--	--
GUM 79-19		0.512942 ± 20	+7.0	0.70365 ± 4	-14.2	--	--
GUM 80-39		0.512949 ± 16	+7.1	0.70355 ± 3	-15.6	--	--
THOLEIITE SERIES							
GUM 79-6		0.513044 ± 17	+8.8	0.70358 ± 4	-15.3	18.496 ± 9	15.512 ± 8
ALUTOM FORMATION:	35 m.y.						
THOLEIITE SERIES							
GSR-3		0.513054 ± 16	+9.0	0.70349 ± 3	-16.6	--	--
GUM 79-2		0.512977 ± 16	+7.4	0.70364 ± 4	-14.5	--	--
CALC-ALKALINE SERIES							
GM-75		0.513049 ± 16	+8.8	0.70355 ± 4	-15.8	--	--
UMATAC FORMATION:	13 m.y.						
71781-A-1		0.512917 ± 17	+5.7	0.70380 ± 3	-12.5	--	--
GM 65-3		0.512965 ± 16	+6.7	0.70375 ± 3	-13.2	--	--

(1) Reagan and Meijer (1982) and Reagan (personal communication).
(2) $^{143}Nd/^{144}Nd$ normalized to $^{146}Nd/^{144}Nd = 0.7219$, and BCR-1, $^{143}Nd/^{144}Nd = 0.51263$. $(\varepsilon_{Nd})_o$ calculated relative to present day chondritic $^{143}Nd/^{144}Nd = 0.51264$ and $^{147}Sm/^{144}Nd = 0.1936$.
(3) $^{87}Sr/^{86}Sr$ normalized to $^{86}Sr/^{88}Sr = 0.1194$ and Eimer and Amend $SrCO_3$, $^{87}Sr/^{86}Sr = 0.7080$. $(\varepsilon_{Sr})_o$ calculated relative to present day bulk earth $^{87}Sr/^{86}Sr = 0.7047$ and $^{87}Rb/^{86}Sr = 0.085$.

FIGURE 4.8: $(^{143}Nd/^{144}Nd)_o$ plotted vs $(^{87}Sr/^{86}Sr)_o$ for volcanic rocks from Guam, compared to the oceanic mantle array and boninites from the Bonin Islands. Data from Tables 4.3 and 3.3.

FIGURE 4.9: $(^{143}Nd/^{144}Nd)_o$ plotted vs La/Nd for volcanic rocks from Guam, compared to boninites from the Bonin Islands, Cape Vogel and DSDP Site 458. Data from Tables 4.2, 4.3, 3.2 and 3.3.

FIGURE 4.10: $^{206}Pb/^{204}Pb$ vs $^{207}Pb/^{204}Pb$ in a Facpi "boninite series" lava (filled circle) and a Facpi tholeiite series lavas (open circle) (Table 4.3), compared to Miocene Umatac Formation lavas and volcanics from Saipan (Meijer, 1976) and oceanic basalts and sediments (Meijer, 1976 and Hawkesworth, 1982).

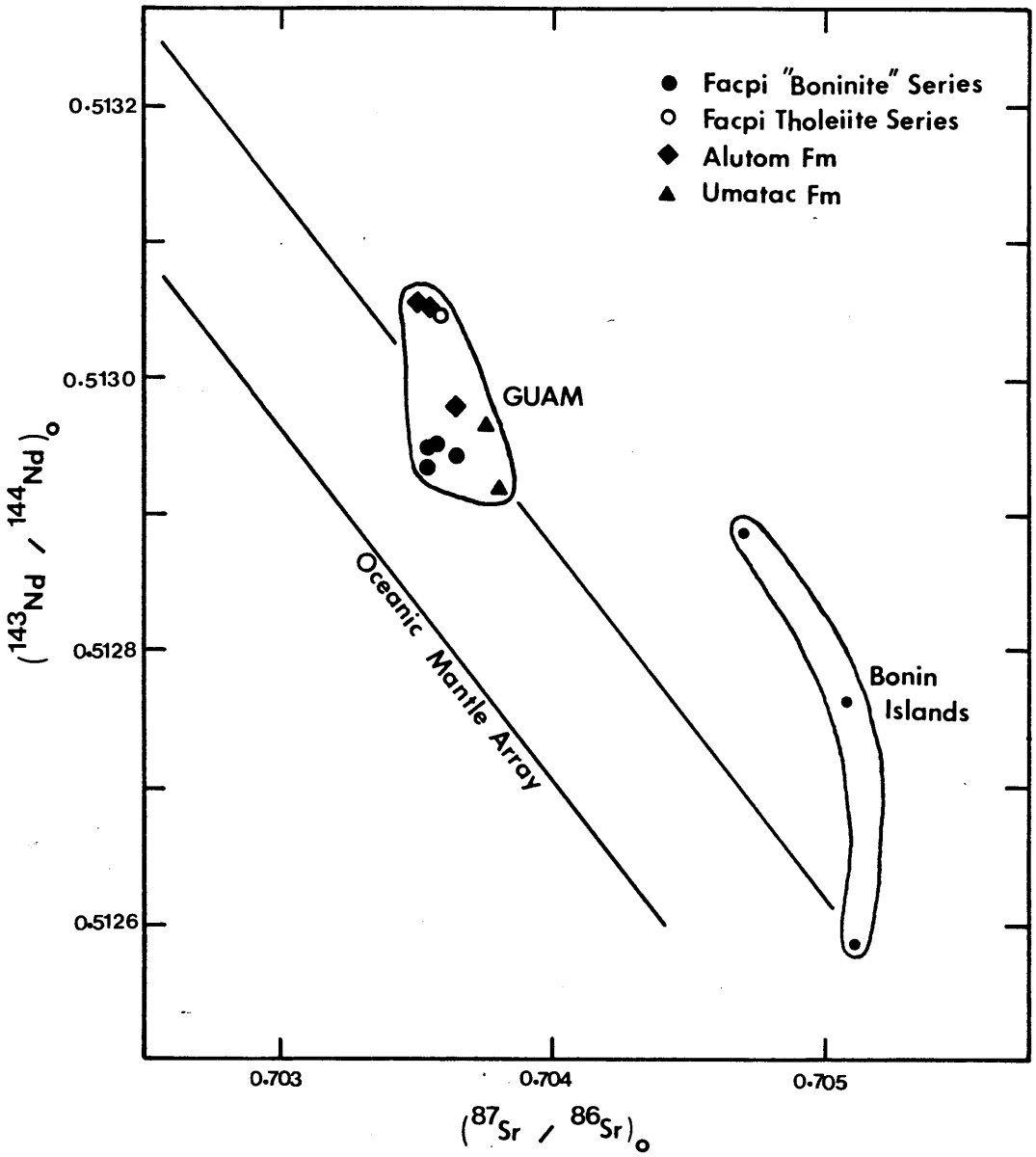
Facpi "Boninite" Series
Facpi Tholeiite Series
Alutom Fm
Umatac Fm
GUAM
Bonin Islands
Oceanic Mantle Array
0.5132
0.5130
0.5128
0.5126
0.703
0.704
0.705
$(^{143}Nd / ^{144}Nd)_o$
$(^{87}Sr / ^{86}Sr)_o$

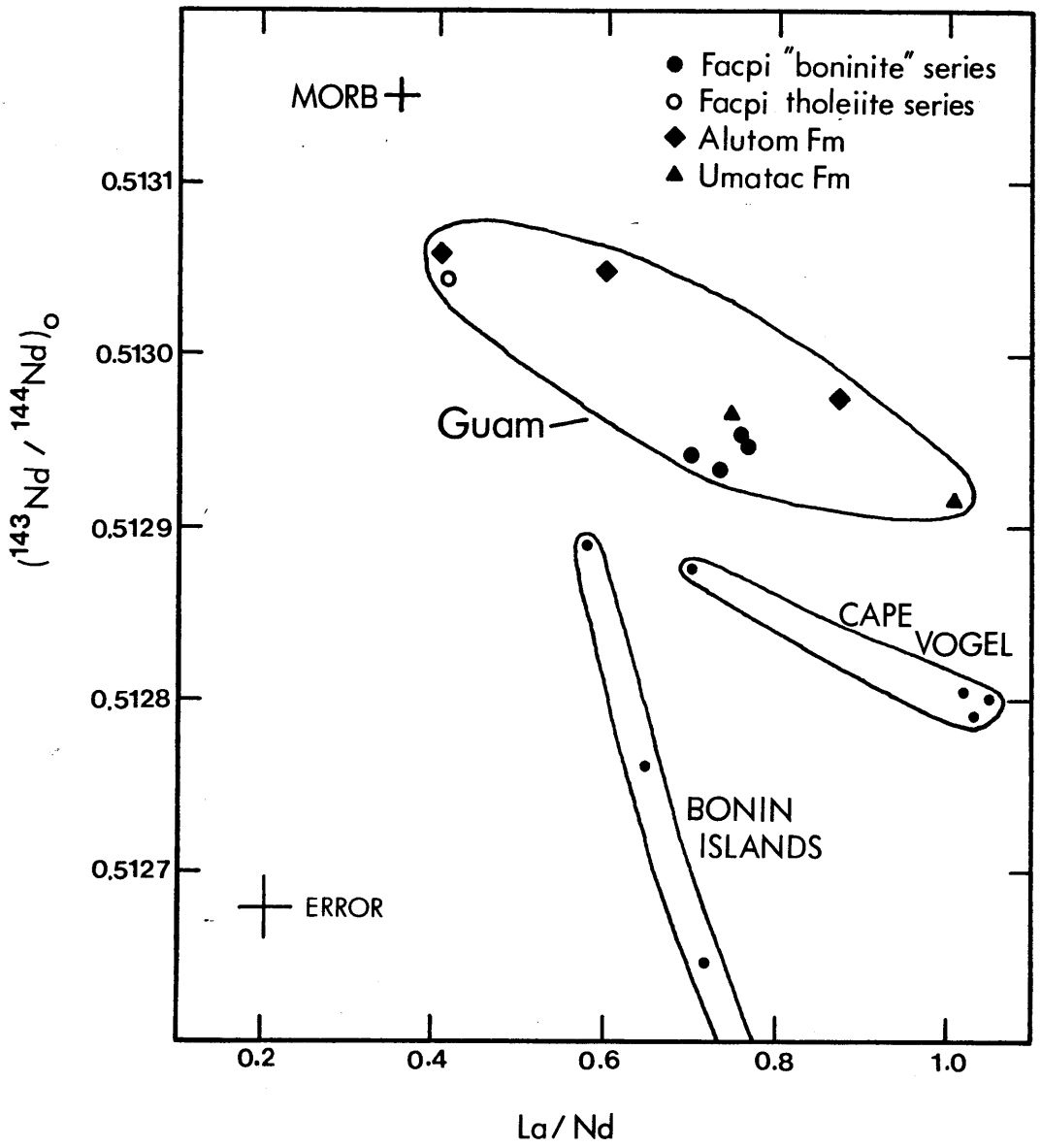
Facpi "boninite" series
Facpi tholeiite series
Alutom Fm
Umatac Fm
MORB
Guam
CAPE VOGEL
BONIN ISLANDS
ERROR
0.5131
0.5130
0.5129
0.5128
0.5127
0.2
0.4
0.6
0.8
1.0
$(^{143}Nd / ^{144}Nd)_o$
La/Nd

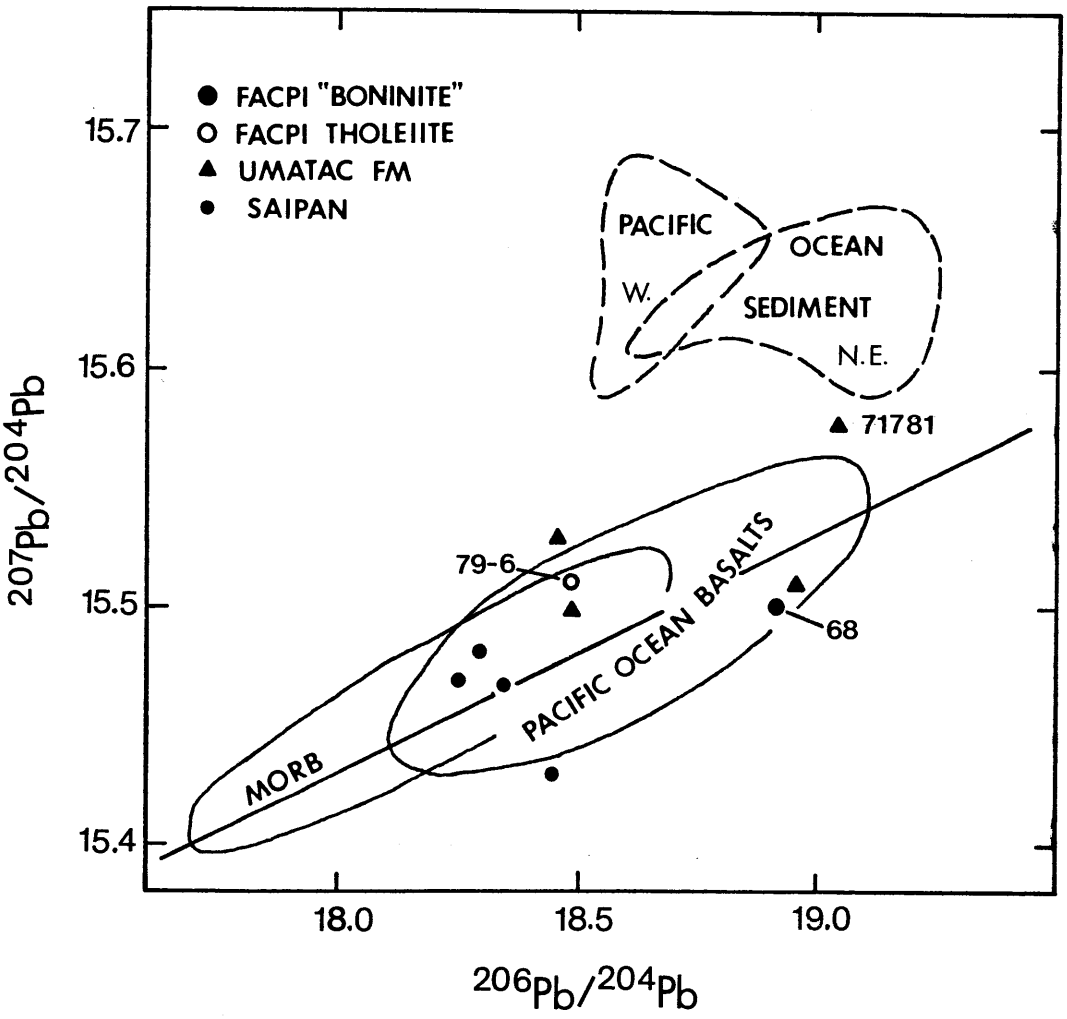
FACPI "BONINITE"
FACPI THOLEIITE
UMATAC FM
SAIPAN
PACIFIC
OCEAN
W.
SEDIMENT
N.E.
71781
79-6
68
MORB
PACIFIC OCEAN BASALTS
15.7
15.6
15.5
15.4
18.0
18.5
19.0
$^{207}Pb/^{204}Pb$
$^{206}Pb/^{204}Pb$

$^{87}Sr/^{86}Sr$ (0.70358) but higher $^{143}Nd/^{144}Nd$ (0.51304), and plots at higher 87Sr/86Sr than the oceanic mantle array (Fig. 4.8). Guam volcanics as a group vary in $^{87}Sr/^{86}Sr$ from 0.7035 to 0.7038 and $^{143}Nd/^{144}Nd$ from 0.51292 to 0.51306, and have a steeper slope on the Nd-Sr correlation diagram than the mantle array. Variations in $^{143}Nd/^{144}Nd$ and $^{87}Sr/^{86}Sr$ do not appear to be related to the ages of eruption or chemical types of the lavas, e.g., the Facpi Formation tholeiite and a calc-alkaline and tholeiitic Alutom Formation lava have similar $^{143}Nd/^{144}Nd$ and $^{87}Sr/^{86}Sr$ ratios, and the Facpi Formation "boninite series" lavas are similar to both a tholeiitic Alutom Formation sample and a Miocene Umatac Formation sample.

Increasing $^{143}Nd/^{144}Nd$ in the Guam volcanics correlates to some extent with decreasing LREE enrichment (Fig. 4.9). Andesitic and dacitic samples usually have higher La/Nd than high MgO samples with similar $^{143}Nd/^{144}Nd$ (Fig. 4.9), therefore, removal of mafic minerals during magma differentiation, which will increase La/Nd, could account for the scatter in the diagram. Like the correlation of $^{143}Nd/^{144}Nd$ and $^{87}Sr/^{86}Sr$ (Fig. 4.8), lavas of all ages and chemical types appear to plot along a similar trend in Fig. 4.9.

Fig. 4.10 is a Pb-Pb isotope correlation diagram, showing ratios in a Facpi "boninite series" lava and a Facpi tholeiite series lava, and lavas from the Umatac Formation analyzed by Meijer (1976). Both Facpi Formation lavas plot in the field for Pacific Ocean basalts, and the "boninite series" sample has a significantly higher $^{206}Pb/^{204}Pb$, but similar $^{207}Pb/^{204}Pb$ ratio compared to the Facpi tholeiite. Both samples have similar $^{207}Pb/^{204}Pb$ and $^{206}Pb/^{204}Pb$ ratios to Miocene Umatac Formation lavas.

DISCUSSION

COMPARISON OF FACPI FORMATION LAVAS AND BONINITES: EVIDENCE FOR A DEPLETED PERIDOTITE SOURCE

As shown in Fig. 4.4 and 4.6, relative abundances of Ti, Y and HREE in MgO-rich Facpi lavas, including both "boninite series" and tholeiite series samples, are similar to those in boninites, i.e., Ti is depleted relative to Y and Yb. Like boninites, MgO-rich Facpi lavas also have high Cr, Ni and Co abundances, and higher than chondritic Al_2O_3/TiO_2, CaO/TiO_2 and Sc/Ti ratios. These features suggest that the model proposed to explain abundances of these elements in boninites, i.e., that they are derived from peridotite sources which have been depleted in incompatible elements, is also applicable to the Facpi lavas.

Although relative abundances of Ti, Y and HREE in Facpi lavas and Bonin Island boninites are similar, the Facpi Formation lavas have higher absolute abundances of these elements by a factor of 2 to 3 (Fig. 4.4), and have lower Al_2O_3/TiO_2, CaO/TiO_2 and Sc/Ti ratios. In Chapter 3, variations in Al_2O_3/TiO_2, CaO/TiO_2, Sc/Ti and V/Ti ratios in boninites from different areas were attributed largely to the amount of Ti introduced into their depleted peridotite source by secondary enrichment. In boninites, variation in these ratios are also reflected in variation in the relative abundance of Ti compared to Y and Yb, e.g., boninites from Cape Vogel, with high Ti/Sc (Fig. 3.4) also have higher than chondritic Ti/Y and Ti/Yb (Fig. 3.6), while boninites from the Bonin Islands, with low Ti/Sc (Fig. 3.4) have lower than chondritic Ti/Y and Ti/Yb ratios (Fig. 3.6, Fig. 4.4). Since the Facpi lavas have similar relative abundances of Ti, Y and Yb to Bonin Island boninites, their higher absolute abundances are unlikely to result from secondary enrichment processes.

Although Facpi lavas have lower MgO contents than many boninites, their relatively high Ni and Sc abundances (Fig. 4.3) indicate that their higher abundances of moderately incompatible elements is unlikely to result from removal of olivine and clinopyroxene from a parental magma with absolute abundances of these elements similar to boninites. For example, Fig. 4.11 shows Ti plotted vs Sc for Facpi lavas and boninites, with crystallization vectors for varying proportions of olivine and clinopyroxene. Removal of about 40% olivine or olivine plus small amounts of clinopyroxene from a parental magma like MgO-rich boninites from the Bonin Islands and Dredge Site 1403 could produce the Ti and Sc abundances in primitive Facpi lavas, but would also result in Ni contents of less than 50 ppm, as compared to Ni contents of 134-199 ppm in the Facpi lavas.

The Facpi lavas may have been derived by lower degrees of partial melting than boninites and/or from a less depleted source peridotite. In Fig. 4.11, the Sc and Ti contents of partial melts derived from depleted peridotites from Ronda (Table 3.4), such that clinopyroxene is exhausted during partial melting (see caption, Fig. 4.11), are plotted. Partial melts of the most depleted peridotites R771 and R893 (points C and E in Fig. 4.11) could be parental compositions for boninites from the Bonin Islands and Dredge Site 1403. Lower degrees of partial melting of these sources (e.g., point D in Fig. 4.11) do not produce compositions with Ti and Sc contents high enough to be parental magmas for the Facpi lavas. Partial melts of more fertile peridotite R856 (points A and B) have similar Ti contents to primitive Facpi lavas, but lower Sc abundances. The Facpi lavas could be derived from parental magmas similar to these partial melts by 10-15% olivine crystallization, which is consistent with their Ni contents. Early crystallization of olivine in the Facpi lavas is supported

FIGURE 4.11: Ti plotted vs Sc for Facpi Formation lavas and boninites. MgO-rich Facpi Formation lavas have higher Sc contents than most boninites. Points A, B, C, D and E are partial melts derived from harzburgites from Ronda (Table 3.4) such that clinopyroxene is exhausted during partial melting: A) R856, 6% partial melting with melting proportions 50 cpx : 50 opx; B) R856, 10% partial melting with melting proportions 30 cpx : 70 opx; C) R893, 4% partial melting with melting proportions 50 opx : 50 cpx; D) R771, 1.4% partial melting with melting proportions 80 cpx : 20 opx; and E) R771, 3% partial melting with melting proportions 50 cpx : 50 opx. Melting with high opx/cpx melting proportions may occur under hydrous, low pressure conditions (Green, 1973). Ti and Sc partition coefficients from Sun et al. (1979).

Partial melts with Sc contents greater than 40 ppm cannot be produced from these peridotites. Facpi lavas may be derived from parental magmas similar to partial melts of peridotite R856 by fractional crystallization of 10 - 15% olivine. The resulting liquids would have 109 - 172 ppm Ni, similar to abundances in the MgO rich Facpi lavas, assuming 400 ppm Ni in the initial melts and $D_{Ol}^{Ni} = 9$ (Hart and Davis, 1978).

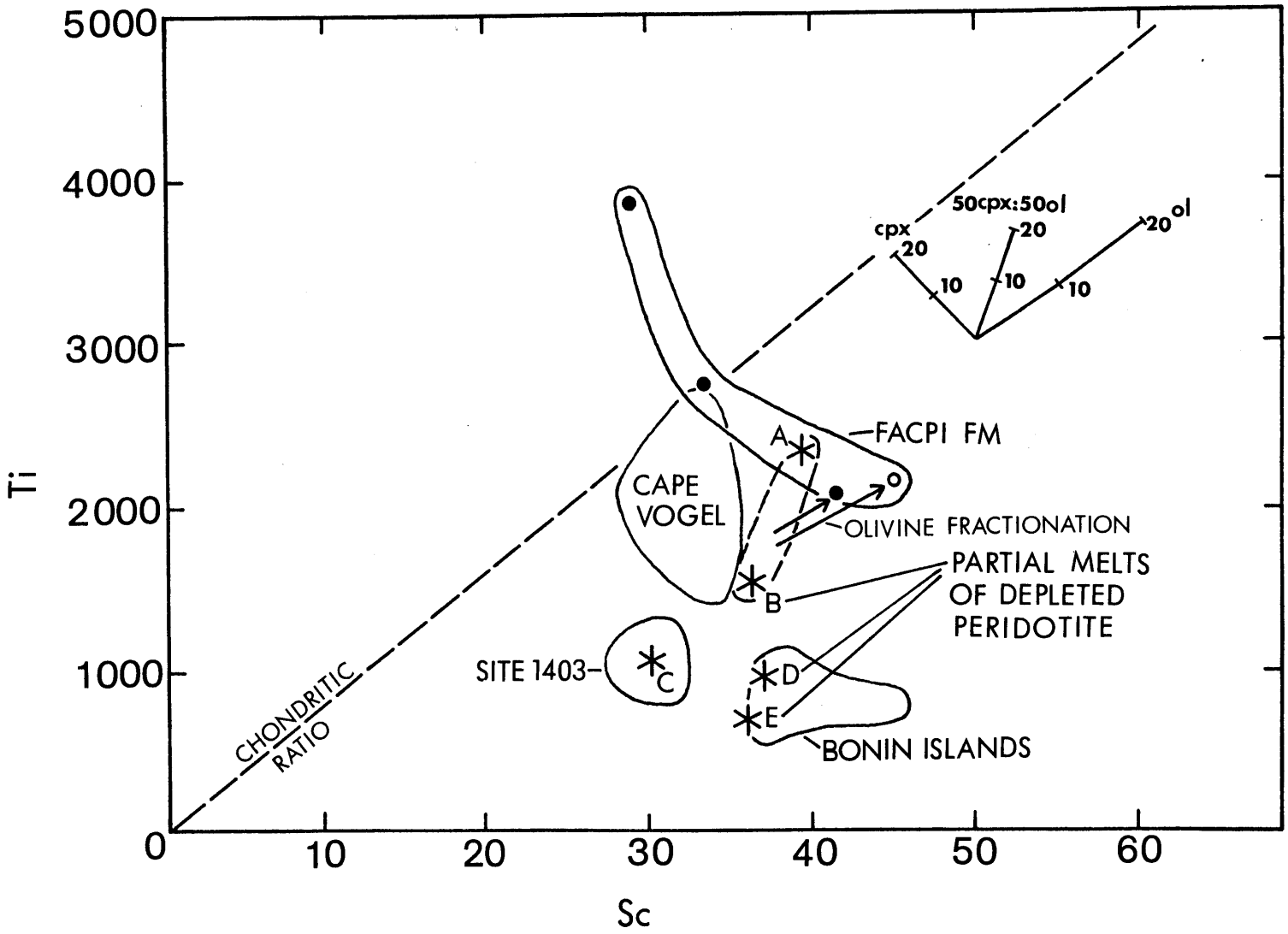
5000
4000
3000
2000
1000
0
Ti
10
20
30
40
50
60
Sc
CHONDRITIC RATIO
CAPE VOGEL
FACPI FM
A
OLIVINE FRACTIONATION
PARTIAL MELTS OF DEPLETED PERIDOTITE
B
SITE 1403
C
D
E
BONIN ISLANDS
50cpx:50ol
cpx
20
10
10
10
20
20ol

by the presence of chromite inclusions in olivines, but rarely in clinopyroxene. The Ronda harzburgites 771 and 893 cannot yield melts with initial Sc contents of 41-45, like those in the Facpi lavas, and low Ti contents. Therefore, the Facpi lavas may differ from boninites in being derived from a slighly more fertile peridotite source (such as Ronda 856), followed by olivine fractionation.

COMPARISON OF FACPI LAVAS AND BONINITES: EVIDENCE FOR SECONDARY ENRICHMENT IN LREE AND ZR

Like many boninites, Facpi Formation "boninite series" lavas are LREE-enriched, which is inconsistent with an incompatible element depleted peridotite source. If Facpi "boninite series" and arc tholeiite series lavas arc considered together, Facpi Formation lavas exhibit correspondence between LREE enrichment, and low $^{143}Nd/^{144}Nd$ and Ti/Zr ratios, which is also a characteristic of boninites (Fig. 4.6 and 4.9). For boninites (Chapter 3), this trend was interpreted to reflect mixing of a LREE and Zr enriched mantle derived fluid or melt with low $^{143}Nd/^{144}Nd$ with a LREE depleted peridotite with high $^{143}Nd/^{144}Nd$, residual from MORB generation. Since "boninite series" and tholeiite series Facpi lavas differ in major element composition and timing of eruption, it may not be valid to assume that their sources are composed of the same materials. However, since the Facpi tholeiite and "boninite series" lavas have extremely similar relative and absolute abundances of Ti, Y and HREE, and since both series show enrichment in Zr relative to Ti and Sm (Fig. 4.4b), which is unusual in other rocks, it is possible that a single mixing process can explain the REE and HFS element and Nd-isotopic characteristics of both series.

On Nd-normalized diagrams, such as Fig. 3.12, Facpi "boninite series" lavas plot as a cluster, with overlapping error, as they do on plots of $^{143}Nd/^{144}Nd$ vs La/Nd and $^{87}Sr/^{86}Sr$, while the Facpi tholeiite plots in a different position. Mixing lines drawn through these two points on plots of La/Nd, Yb/Nd and Ti/Nd vs Sm/Nd (e.g., Fig. 3.12), reach a maximum Sm/Nd of 1.55 and La/Nd = 0, and a minimum Sm/Nd of 0.4 at Ti/Nd = 0.

Relative abundances of La, Sm, Yb and Ti in possible mixing endmembers inferred from these plots as described for Fig. 3.13 are shown in Fig. 4.12, compared to possible mixing endmembers inferred for boninites from the Bonin Islands and Cape Vogel (Fig. 3.13). The LREE-depleted endmember has similar relative La, Sm, Yb and Ti abundances to those in LREE-depleted endmembers for Cape Vogel and Bonin Island boninites, and is consistent with a LREE-depleted peridotite source. Relative La, Sm, Yb and Ti abundances in the LREE-enriched endmember is similar to, but more LREE-enriched than that for Bonin Island boninites. The minimum $^{143}Nd/^{144}Nd$ inferred for this material (i.e., at Sm/Nd = 0.4 and La/Nd = 1.45) is 0.51275, and is similar to that inferred for the LREE-enriched endmember for Cape Vogel boninites. Therefore, source materials with similar REE and HFS element abundances and Nd-isotopic characteristics are indicated for Facpi lavas and boninites.

Like boninites, Pb-isotopic data for Facpi lavas supports an oceanic mantle vs sedimentary source for the LREE and Zr-enriched, low $^{143}Nd/^{144}Nd$ endmember. Compared to oceanic basalts with similar $^{206}Pb/^{204}Pb$ (e.g., the oceanic trend, Fig.4.11), the LREE-enriched Facpi "boninite series" lava has low $^{207}Pb/^{204}Pb$. The variation in $^{206}Pb/^{204}Pb$ between the LREE-depleted Facpi tholeiite series lava and the LREE-enriched Facpi "boninite series" lava (Fig. 4.11) is qualitatively consistent with mixing between a

FIGURE 4.12: Relative La, Sm, Yb and Ti abundances in possible LREE-enriched and LREE-depleted mixing endmembers for Facpi Formation lavas, inferred from plots of La/Nd, Yb/Nd and Ti/Nd vs Sm/Nd as described for Fig. 3.13. Possible LREE-enriched and LREE-depleted mixing endmembers for boninites, inferred in the same way (Figs. 3.12 and 3.13) are shown for comparison.

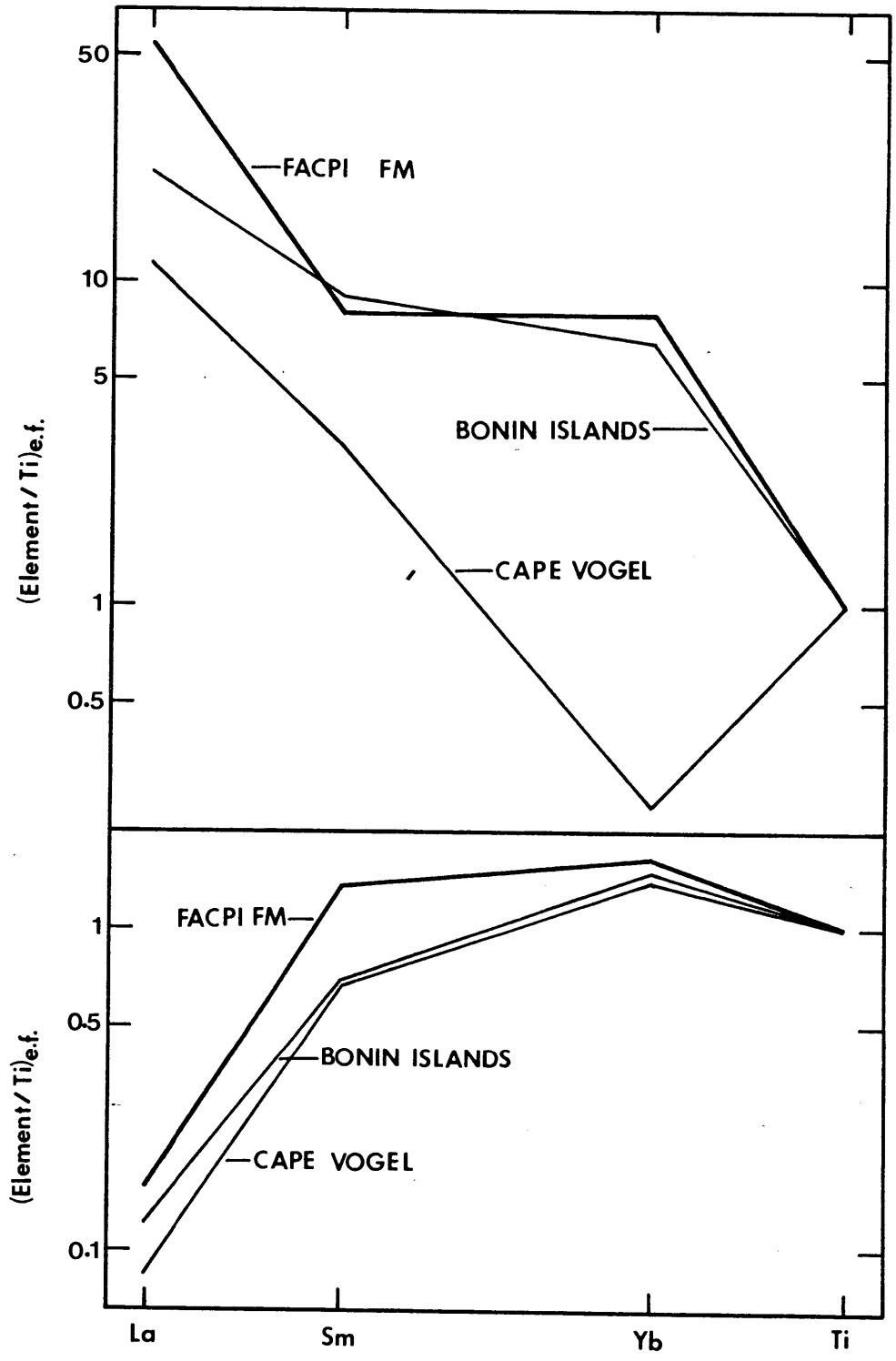
50
10
5
1
0.5
(Element / Ti)e.f.
FACPI FM
BONIN ISLANDS
CAPE VOGEL
1
0.5
0.1
(Element / Ti)e.f.
FACPI FM
BONIN ISLANDS
CAPE VOGEL
La
Sm
Yb
Ti

peridotite residue from MORB generation and a LREE-enriched material derived from mantle sources like those for oceanic island volcanics. Later in this chapter and in Chapter 7 an alternate interpretation will be proposed to explain the Pb-isotopic composition of these samples. However, in general, the low $^{207}Pb/^{206}Pb$ of the LREE-enriched Facpi "boninite series" lava does not support a sedimentary source for LREE in these lavas.

SOURCES FOR K, Rb, Ba AND Sr IN FACPI LAVAS

Relative abundances of K, Rb, Ba and Sr in Facpi lavas are different from those in boninites. Sr/Nd and Ba/La ratios in Facpi lavas are similar to those in boninites (Fig. 4.4, Table 4.2), but in Facpi "boninite series" lavas K and Rb abundances relative to Ba, Sr and La are lower than boninites, and in Facpi tholeiites, K and Rb have lower normalized abundances than Ba and Sr (Fig. 4.4b). For boninites (Chapter 3), high K/Ba and Rb/Ba ratios were interpreted to result from addition of a component from subducted "seawater" (i.e., from the dehydration of basaltic alteration products with high K/Ba and Rb/Ba like seawater) to the peridotite sources of boninites. To account quantitatively for the $^{87}Sr/^{86}Sr$ ratios in boninites, it was suggested that their sources included a component with high Sr/Nd (and Ba/La) also derived from subducted oceanic crust, with intermediate $^{87}Sr/^{86}Sr$ depending on the relative amounts of MORB, seawater and sediment Sr it contained. According to this scheme, Facpi "boninite series" lavas, which have similar Ba/La and Sr/La ratios to boninites but lower K/Ba and Rb/Ba, may have a smaller "seawater" component than boninites, but a similar subducted crustal component, while the Facpi tholeiite series lavas may have no "seawater" component contribution.

Relative abundances of K, Rb, Ba and Sr in the Facpi tholeiite are characterisitic of tholeiitic arc volcanics from many island arcs. Normalized abundances of these elements and La in arc tholeiites from the Aleutians; Tonga; and Manam Island, Bismarck Arc (Chapter 5) are compared to the Facpi tholeiite in Fig. 4.13. These lavas are characterized by enrichment of K, Rb, Ba and Sr relative to La, but low K/Ba and Rb/Ba ratios compared to those in boninites (Fig. 3.8). Lavas from Manam Island have low $^{87}Sr/^{86}Sr$ and plot in the mantle array. In Chapter 5, it will be argued based on possible mixing relationships in the Manam lava data, that these isotopic characteristics can result from mixing of components with high K, Rb, Ba and Sr abundances relative to REE, derived from subducted MORB and sediment, in which the MORB component predominates. The Facpi tholeiite, which has similar K, Rb, Ba and Sr abundances to the Manam lavas and other arc tholeiites, and a slightly higher $^{87}Sr/^{86}Sr$ than the mantle array, is also consistent with this model. The Pb-isotopic composition of this sample, which was earlier interpreted as reflecting its derivation from a MORB-residue peridotite, could also reflect mixing of components from subducted MORB and sediment, in which the MORB component dominates, or most likely, a mixture of Pb derived from MORB-residue peridotite, subducted MORB and sediment. Since the Pb concentration of this sample is unknown, this interpretation cannot be quantitatively evaluated.

For boninites from DSDP Site 458 (Chapter 3), and the Facpi "boninite series" lava (Fig. 4.10), Pb-isotopic compositions do not indicate a component from subducted sediment, although a subducted MORB component is permissible. It is unlikely, however, that the subducted oceanic crustal component for these lavas is derived exclusively

FIGURE 4.13: Normalized abundances of Rb, Ba, K, La and Sr in tholeiitic island arc volcanics from the Aleutians; Manam Island, Bismarck Arc; Tonga; and the Facpi Formation, Guam. Data for Tongan and Aleutian tholeiites from Kay (1977); Manam Island (Chapter 5, this study).

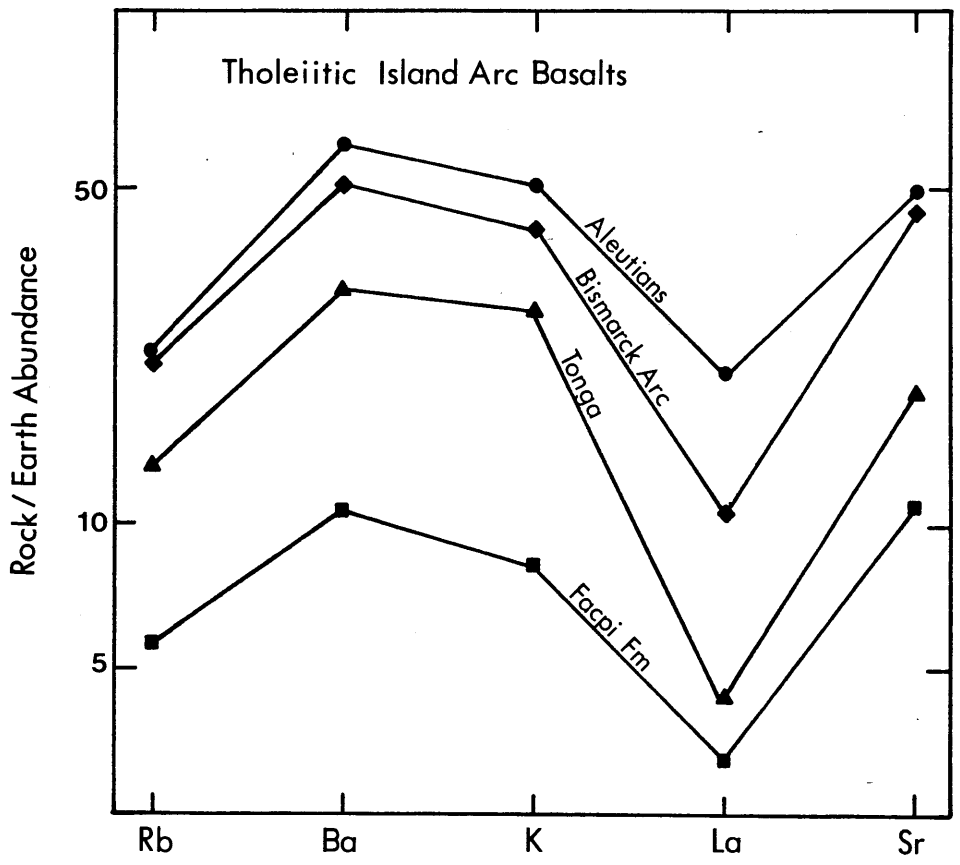
Tholeiitic Island Arc Basalts
Rock / Earth Abundance
50
10
5
Aleutians
Bismarck Arc
Tonga
Facpi Fm
Rb
Ba
K
La
Sr

from subducted MORB, while that for the Facpi tholeiite (and other arc tholeiites) is derived from MORB and sediment. This suggests that the subducted oceanic crustal (i.e., MORB and sediment) contribution to Pb in boninites and Facpi "boninite series" lavas may be very small compared to the contribution from their mantle peridotite sources. The Pb-isotopic compositions of these lavas will be discussed in more detail in Chapter 7.

Boninites (Chapter 3), Facpi "boninite series" lavas and Facpi tholeiite series lavas differ in their K/Ba and Rb/Ba ratios. This difference can be interpreted as the result of variations in the amount of a component derived by dehydration of basaltic clays which is introduced into their mantle peridotite sources from the subducted oceanic crust. Boninites have the greatest evidence for this component, while the Facpi tholeiites have the least. In partial melting experiments of peridotite (e.g., Green, 1973; 1976; Nicholls, 1974), high-SiO_2 liquids are produced under H_2O-saturated conditions or at very low pressures, while liquids with lower SiO_2 and higher Al_2O_3 and CaO contents are produced under H_2O-undersaturated conditions or under H_2O-saturated conditions at higher pressure. In these three groups of low TiO_2 lavas (boninites, Facpi "boninite series" lavas and tholeiites), decreasing SiO_2 and increasing CaO and Al_2O_3 (Tables 3.1 and 4.1) is accompanied by decreasing K/Ba and Rb/Ba. Since the lavas are geographically and temporally distinct, this could be coincidental. Alternatively, the K and Rb abundances in the lavas, and their major element composition may be related, particularly since both these chemical variables can be linked to H_2O content or to pressure.

Based on these concepts, a model for the geochemical characteristics of Facpi lavas can be outlined:

1) generation of a MORB-residue peridotite at a spreading ridge, and subsequent enrichment of this peridotite to varying degrees in LREE and Zr by a mantle derived fluid or melt with low $^{143}Nd/^{144}Nd$.
2) metasomatism of this mantle source by a fluid or melt with high K, Rb, Ba and Sr abundances relative to REE derived from subducted ocean crust, including a "seawater" component with high K/Ba and Rb/Ba derived by dehydration of basaltic clays. Peridotite containing larger amounts of the "seawater" component yields high SiO_2 "boninite series" lavas, with high K/Ba and Rb/Ba ratios, while peridotite containing smaller amounts of the "seawater" component yields tholeiite series lavas with low K/Ba and Rb/Ba. The relationship between major element composition and K and Rb content could be related to the amount of H_2O added to the sources of these two lava types, or to their depth of magma generation compared to the depth of dehydration of basaltic clays within the subducted oceanic crust.

RELATIONSHIP BETWEEN MAGMA TYPES ON GUAM

Lavas from the Facpi Formation, the calc-alkaline and tholeiitic series of the Alutom Formation, and the Umatac Formation on Guam have overlapping Pb, Nd and Sr-isotopic compositions (Fig. 4.8 and 4.10). In addition, these lavas overlap on a plot of $^{143}Nd/^{144}Nd$ vs La/Nd (Fig. 4.9). Although more data is required to confirm such a conclusion, the similar isotopic compositions of Guam volcanics suggests that changes with time in the type of magma generated were not caused by major changes in the nature of source materials. Major differences in source materials for these magma

types would be expected to result in large isotopic differences between magma types. The concept of similar source materials for Guam volcanics is consistent with the conclusion of Reagan and Meijer (1982) that distinct calc-alkaline and tholeiitic series of the Alutom Formation were generated from similar parental magmas through differences in fractional crystallization and magma chamber processes. Based on the data presented here, the sources of Facpi "boninite series" and tholeiite series lavas are predominantly metasomatized, refractory mantle peridotite, with minor addition of material from the subducted oceanic crust, and differ from each other in their H_2O content or depth of melting. MgO-rich Alutom and Umatac Formation lavas have higher TiO_2 and HREE contents that Facpi lavas, and may be derived from more fertile mantle peridotite. Therefore, the major factors determining magma type on Guam may be peridotite fertility, H_2O content or depth of melting and fractional crystallization history, rather than major differences in relative proportions of source materials derived from subarc mantle peridotite, subducted basalt and sediment.

SUMMARY AND CONCLUSIONS

Low TiO_2 lavas from the Facpi Formation, Guam, have relative REE and HFS element abundances and Nd-isotopic characteristics similar to those in boninites. Specifically, they have lower than chondritic Ti/Y, Ti/Yb and Ti/Sc ratios, indicating depletion of their peridotite sources in less compatible elements relative to more compatible elements, but are variably enriched in the highly incompatible LREE and Zr compared to HREE, Y and Ti. Lavas with high La/Sm and Zr/Ti have lower $^{143}Nd/^{144}Nd$ than a lava with low La/Sm and Zr/Ti. These characteristics suggest that, like boninites, Facpi lavas are derived from a refractory peridotite residue from MORB

generation, which has been enriched in LREE and Zr by a mantle derived fluid or melt with low $^{143}Nd/^{144}Nd$. The $^{206}Pb/^{204}Pb$ ratio in a LREE-enriched Facpi lava is higher than most oceanic sediments, while its $^{207}Pb/^{204}Pb$ is low compared to oceanic lavas with similar $^{206}Pb/^{204}Pb$, and supports a mantle rather than subducted sediment source for the low $^{143}Nd/^{144}Nd$, high La/Sm material.

Like most island arc volcanics, abundances of K, Rb, Ba and Sr in Facpi lavas are high relative to REE and HFS elements. Relative abundances of K and Rb compared to Ba, Sr and La are higher in "boninite series" Facpi lavas compared to tholeiitic Facpi lavas, but are lower than in boninites. The high K/Ba and Rb/Ba in Facpi "boninite series" lavas suggests that they, like boninites, contain a "seawater" component, derived by dehydration of basaltic alteration products with high K/Ba and Rb/Ba within the subducted oceanic crust, while the Facpi tholeiite series lavas lack this component. The difference in major element composition between Facpi "boninite series" and tholeiite series lavas may also be related to the absence or presence of this component.

Volcanics from Guam, including the Facpi Formation, calc-alkaline and tholeiitic lavas from the Oligocene Alutom Formation, and calc-alkaline to alkaline Miocene Umatac Formation lavas, have overlapping Pb, Sr and Nd isotopic compositions, and, as a group, define a trend of increasing LREE enrichment with decreasing $^{143}Nd/^{144}Nd$. This suggests that changes in magma type on Guam were not related to major changes in their source materials. Trace element and isotopic variations in each magma series may result from differing proportions of source materials, while the major controls on magma type may be peridotite fertility, H_2O content or depth of melting, and crystallization history.

CHAPTER 5: GEOCHEMISTRY OF LOW TiO_2 LAVAS FROM MANAM ISLAND, BISMARCK ARC

GEOLOGICAL BACKGROUND

Manam Island is located in the Bismarck Arc, approximately 12 km from the north coast of Papua New Guinea (Fig. 5.1). The Bismarck Arc is an east - west trending chain of islands, extending from New Britain (east) to the Schouten Islands (west). Volcanism in the eastern part of the Bismarck Arc started in the early Tertiary, while arc volcanism in the north coast islands starting the in late Pliocene (Johnson and Jaques, 1980), and has continued to the present throughout the arc.

The Bismarck Arc is close to margins of the Bismarck Sea plate and the Australian continental plate in the west (north coast islands) and the Bismarck Sea and Solomon Sea plates in the east (New Britain). A well defined subduction zone is not present beneath the western north coast islands. East of Karkar (Fig. 5.1) intermediate depth earthquakes define a steeply northward dipping slab from 120 to 200 km depth, with dip increasing to 80° (Johnson, 1976). West of Karkar, intermediate depth earthquakes are absent. There is also no trench between the north coast islands and Papua New Guinea. The lack of an identifiable subduction zone beneath the volcanically active north coast islands, the steeply northward dipping slab present east of Karkar, and the lack of a trench between the islands and Papua New Guinea led Johnson and Jaques (1980) to conclude that the volcanically inactive Coastal Ranges of Papua New Guinea (Fig. 5.1) represent an older island arc, equivalent in age to New Britain, which formed the southern margin of the Bismarck Sea plate, collided with the Papua New Guinean continent in the late Oligocene - early Miocene, and became inactive. Volcanic activity in the north coast islands began behind

FIGURE 5.1: Map of eastern Papua New Guinea showing the main tectonic features related to the Bismarck Arc and the position of Manam and other north coast islands. After Johnson (1977), Johnson et al. (1978), and Taylor (1979).

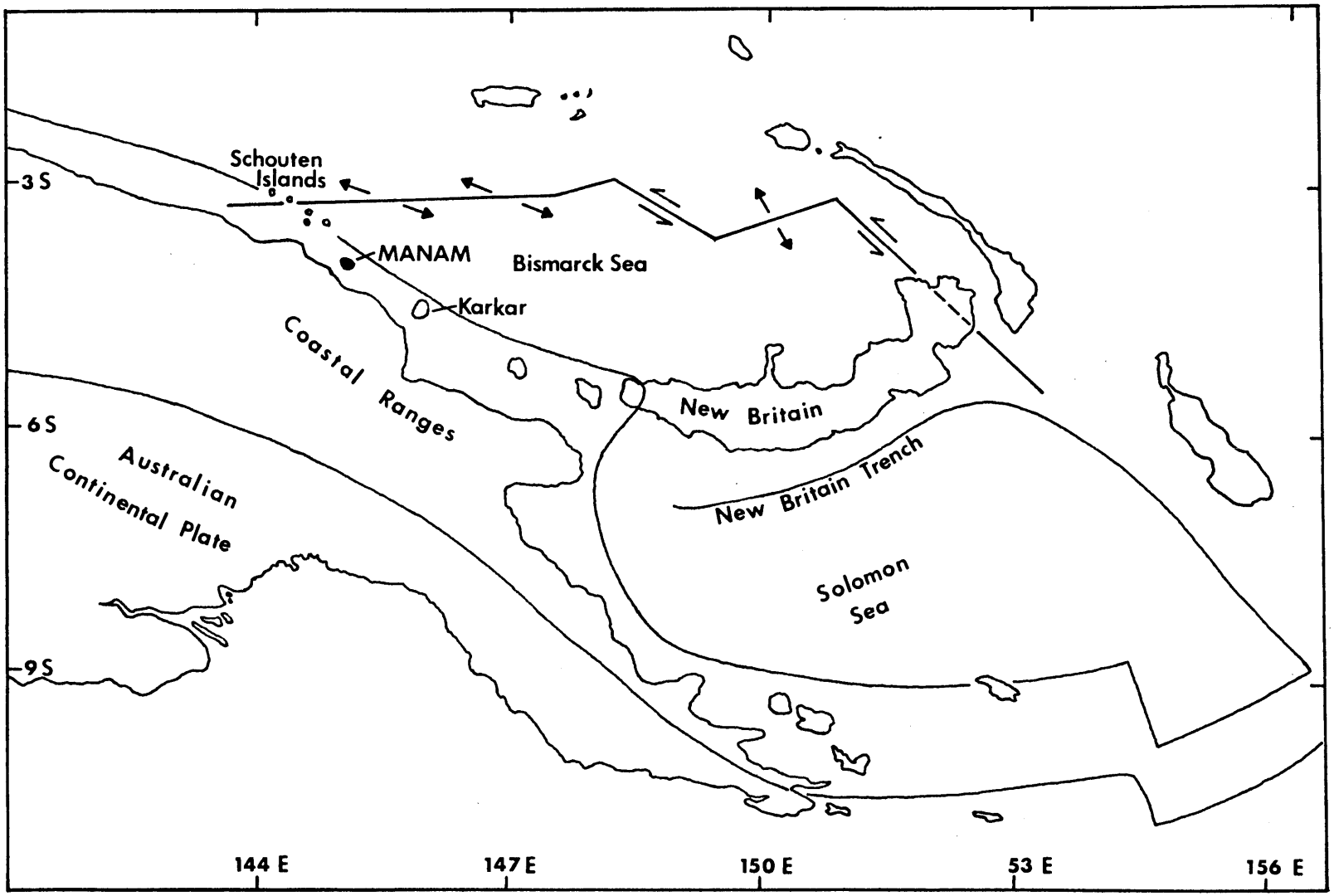
Schouten
Islands
3 S
MANAM
Bismarck Sea
Karkar
Coastal Ranges
New Britain
6 S
Australian
Continental Plate
New Britain Trench
Solomon
Sea
9 S
144 E
147 E
150 E
53 E
156 E

this arc in the late Pliocene, and may be associated with a northward dipping, near vertical subducted slab, similar to that defined east of Karkar.

The Bismarck Sea plate (Fig. 5.1), on which the Bismarck Island Arc is located, is bounded on the east and north by areas of active ocean floor spreading and transform fractures (Taylor, 1979). The northeastern margin, as defined by seismic activity, is within 100 km of Manam Island, and passes beneath the Schouten Islands at the westernmost end of the arc. The nature of this section of the plate boundary is unclear, but was described by Taylor (1979) as a possible transform with small component of spreading.

The major element geochemistry of volcanic rocks from the Bismarck Arc was studied in detail by Johnson (1977). Based on these analyses the arc was divided into western (the north coast islands from the Schouten Islands to the western part of New Britain) and eastern (New Britain) chemical zones. Basaltic lavas from all western zone volcanic centers are characterized by exceptionally low TiO_2 contents (<0.5%, Johnson, 1977; Morgan, 1966). For a given SiO_2 content, lavas from the western zone increase in K_2O, Na_2O, K_2O/Na_2O, TiO_2 and P_2O_5 contents from west to east along the arc. This variation was explained by Johnson (1976) as a possible result of increasing rates of plate convergence from west to east along the arc. Lavas from the Schouten Islands are predominantly andesitic, therefore, the lowest TiO_2 contents are found in basaltic lavas from other western north coast islands, including Manam Island.

PETROGRAPHY AND MAJOR ELEMENT COMPOSITION OF MANAM LAVAS

Lavas from Manam Island are mainly olivine-bearing quartz tholeiites and low SiO_2 andesites. The samples discussed in this study have 51 to 54% SiO_2, 6 to 9% MgO, and Mg/(Mg + ΣFe) from 0.55 to 0.66 (Table 5.1), and were taken from lavas erupted in 1946, 1964 and 1974, and older, unobserved flows. The samples were taken from subaerial flows, and both phenocrysts and groundmass are very fresh.

A major characteristic of rocks from Manam and most other north coast island is their high content of phenocrysts and xenocrysts. The samples analyzed contain 19 to 53% phenocrysts and xenocrysts, mainly plagioclase (9-31%), clinopyroxene (4-16%), small amounts of olivine (1-4%), and traces of opaques (<1%) and orthopyroxene (<0.5%). Plagioclase phenocrysts have cores of An 86 to 82 (Johnson et al., 1981), and are typically euhedral or fragmented, although large phenocrysts in some samples are rounded and partially resorbed. Olivine phenocrysts have Fo contents of 87 to 81 and olivine xenocrysts from Fo 92 to 90 (Johnson et al., 1981), and are typically embayed and resorbed. Clinopyroxene is mainly Ca-augite (Johnson et al., 1981) and is euhedral. Orthopyroxene is found in the groundmass and in some polymineralic aggregates (En 83, Johnson et al., 1981). Spinel occurs as tiny crystals of chromite in xenocrystal and phenocrystal olivine, and as titanomagnetite included in pyroxenes, in the groundmass, and as microphenocrysts in fractionated samples (Johnson et al., 1981).

In spite of their high phenocryst content, Manam lavas may approach liquid compositions at least with respect to olivine and clinopyroxene. In Fig. 5.2a, compositions of Manam samples are plotted on the projection quartz - olivine - clinopyroxene, along with the 1 atm plagiclase saturated

TABLE 5.1: MAJOR ELEMENT AND MODAL ANALYSES OF VOLCANIC ROCKS FROM MANAM ISLAND, BISMARCK ARC

	(1)	(2)	(3)	(4)	(5)	(6)	(7)	(8)
SiO_2	51.01	51.19	51.96	52.42	52.6	52.9	53.5	53.93
TiO_2	0.35	0.39	0.30	0.33	0.37	0.32	0.49	0.35
Al_2O_3	17.05	15.39	14.74	15.59	16.9	15.1	16.6	17.02
Fe_2O_3	4.78	4.01	3.34	4.04	4.60	4.65	4.40	4.55
FeO	4.60	5.29	5.19	4.70	4.10	4.10	3.95	3.70
MnO	0.18	0.17	0.17	0.17	0.16	0.16	0.16	0.15
MgO	6.63	7,83	9.00	7.89	6.70	8.60	6.40	5.70
CaO	11.31	11.76	11.28	11.20	10.7	11.2	9.7	10.29
Na_2O	2.41	2.44	2.37	2.41	2.65	2.40	2.75	2.66
K_2O	0.55	0.63	0.60	0.62	0.73	0.63	1.03	0.83
P_2O_5	0.12	0.13	0.10	0.11	0.12	0.10	0.20	0.15
H_2O^+	0.41	0.42	0.52	0.09	0.04	0.04	0.41	0.22
H_2O^-	0.07	0.01	0.13	0.03	0.04	<0.01	0.14	0.04
CO_2	0.05	--	--	0.05	0.05	<0.05	<0.05	0.05
Total	99.52	99.65	99.80	99.65	99.76	100.20	99.73	99.64
Plag.	21.0	31.0	9.0	14.5	23.5	24.5	21.0	13.5
Olivine	2.5	4.5	3.0	2.5	1.5	4.0	2.5	1.0
Opx.	<0.5	0.5	0.5	<0.5	nil	0.5	<0.5	0.5
Cpx.	7.5	15.5	16.0	11.0	8.5	13.0	8.0	3.5
Opaques	0.5	1.0	<0.5	<0.5	<0.5	1.0	<0.5	<0.5
Total	31.5	52.5	28.5	38.0	33.5	43.0	31.5	18.5

Analyses supplied by Australian Mineral Development Laboratories (Adelaide) (R. W. Johnson, personal communication).

(1) BMR sample NGV 75710007
(2) BMR sample NGV 78710015
(3) BMR sample NGV 78710009
(4) BMR sample NGV 75710013 (1974 flow)
(5) BMR sample NGV 74710028 (1964 flow)
(6) BMR sample NGV 74710025
(7) BMR sample NGV 74710030
(8) BMR sample NGV 77710025 (1946 flow)

FIGURE 5.2: Plot of Manam Island volcanic rocks on the projections:

a) Qtz - Oliv - Cpx, along with the main features of the phase diagram determined by Grove et al. (1982) for calc-alkaline rocks.

b) Qtz - Oliv - Plag, along with phase boundaries determined by Stolper (1980) for MORB's and Grove et al. (1982) for calc-alkaline rocks. The three circled points contain less than 15% plagioclase.

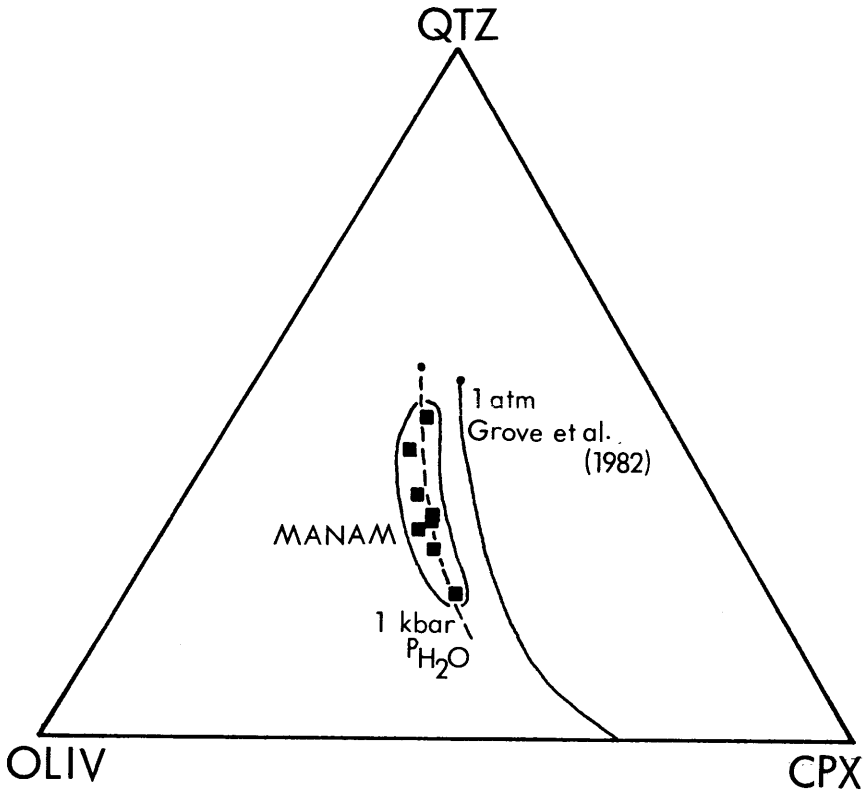
QTZ
1 atm
Grove et al.
(1982)
MANAM
1 kbar
P_{H_2O}
OLIV
CPX

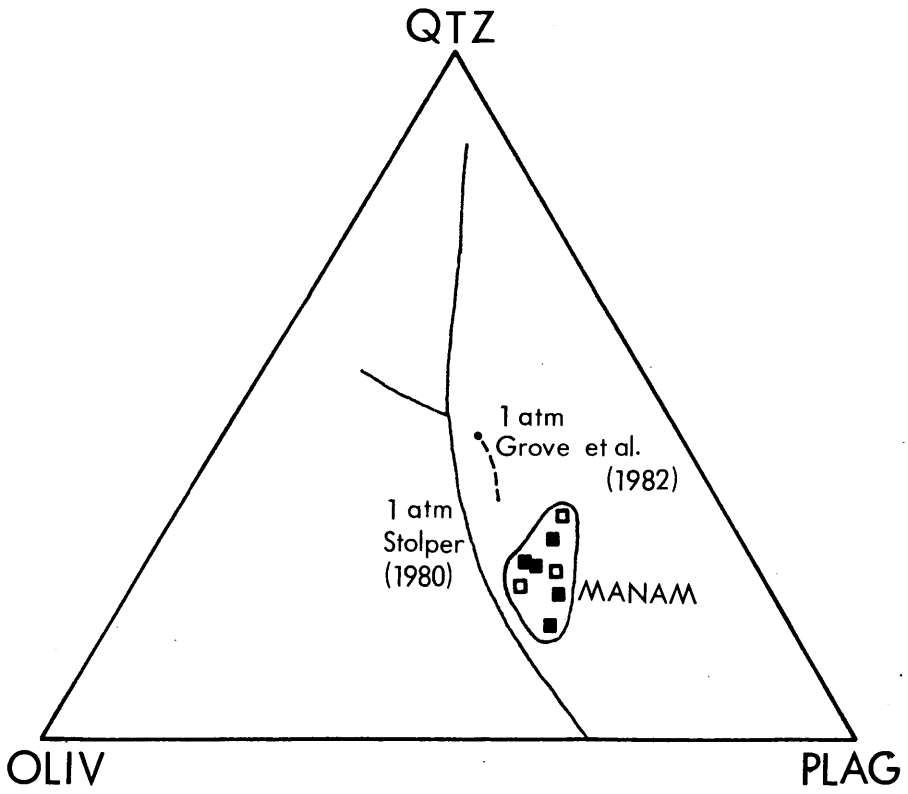
QTZ
1 atm
Grove et al.
(1982)
1 atm
Stolper
(1980)
MANAM
OLIV
PLAG

liquidus determined by Grove et al. (1982) for calc-alkaline lavas, and its inferred position at 1 kbar P-H_2O. The Manam lavas plot in a narrow field parallel to the 1 atm multiple saturation curve and coincide with the 1 kbar position. Although conditions of crystallization may not be rigorously interpreted from this diagram, the Manam lavas appear to be liquid compositions related by crystallization of olivine and clinopyroxene. Significant accumulation of olivine or clinopyroxene in the lavas would be expected to displace points toward the olivine or clinopyroxene apices, or at least produce greater scatter than is observed.

In Fig. 5.2b, Manam lavas are shown on the projection quartz - olivine - plagioclase, with the 1 atm multiple saturation curve of Stolper (1980) for MORB's and the section of this curve determined by Grove et al. (1982) for calc-alkaline lavas. In this diagram Manam lavas plot in a cluster near the 1 atm olivine - plagioclase curve of Stolper (1980) and the curve of Grove et al. (1982) if extended. The clustering of points may indicate that the lavas have undergone variable amounts of plagioclase removal and accumulation. Alternatively, the clustering may result from crystallization over a range of P-H_2O conditions. In either case, the plagioclase component contents of the lavas do not correspond to their plagioclase phenocryst contents (e.g., the three circled samples have less than 15% plagioclase phenocrysts), therefore accumulation alone cannot account for the arrangement of the lava compositions on this diagram.

TRANSITION METAL AND Sc ABUNDANCES IN MANAM LAVAS

Trace element abundances in volcanic rocks from Manam Island are listed in Table 5.2.

Chondrite normalized abundances of transition metals and Sc in Manam lavas are shown in Fig. 5.3 along with normalized abundances of these elements in normal MORB's. Ni and Cr abundances (30-81 ppm and 79-325 ppm Table 5.2) are lower than those in MORB's, and are similar to abundances in other island arc lavas of similar MgO content (e.g., Ewart et al., 1977; Gorton, 1977). V and Sc abundances are similar to those in MORB's, and, like boninites (Fig. 3.4), the Manam lavas have low normalized Ti abundances compared to these elements.

In Fig. 5.4, Ti/V ratios in Manam lavas are plotted vs Ti/Sc, along with the fields for boninites from Fig. 3.4. Ti/V and Ti/Sc ratios in MgO-rich Manam lavas are less than chondritic and are similar to those in boninites. V/Sc ratios increase with decreasing MgO content (Fig. 5.5), therefore, samples with lower MgO contents are most displaced from the boninite trend in Fig. 5.4.

INCOMPATIBLE TRACE ELEMENT ABUNDANCES IN MANAM LAVAS

Normalized abundances of incompatible trace elements and Sc in Manam lavas are shown in Fig. 5.6. In general, the lavas have similar relative abundances of highly and moderately incompatible elements. Like many island arc lavas, they have extremely different relative abundances of these elements compared to MORB's and other oceanic volcanics rocks.

K, Rb, Ba, Sr and Pb:

Manam lavas are enriched in K, Rb, Ba, Sr and Pb relative to MORB's and relative to their own REE and HFS element abundances (Fig. 5.6, Table

TABLE 5.2: TRACE ELEMENT ABUNDANCES IN MANAM LAVAS

	(1)	(2)	(3)	(4)	(5)	(6)	(7)	(8)
Sc[1]	40.0	44.0	45.4	42.4	36.8	42.7	34.7	34.3
V [2]	292	285	275	276	301	280	320	295
Cr	78.6	205	325	220	89.0	229	154	91.3
Ni	30	51	81	59	31	55	48	51
Ti	210	2350	1810	1980	2220	1920	2950	2100
Zr	27	26	22	21	26	21	43	30
Hf	0.77	0.78	0.55	0.71	0.75	0.60	1.2	0.88
Y	11	11	10	10	11	9	15	12
Ba	120	135	180	145	170	165	220	200
Pb	3	8	8	3	9	7	10	8
Sr[3]	612	544	506	534	608	549	562	626
Rb	7.2	8.3	7.7	8.2	9.5	7.9	15.7	10.6
La	4.15	4.18	3.33	3.75	4.25	3.44	7.31	4.53
Ce	9.6	9.59	7.92	8.05	10.1	7.16	15.7	9.69
Nd	5.79	6.09	4.51	4.93	5.91	4.22	9.12	5.60
Sm	1.58	1.59	1.27	1.32	1.51	1.25	2.11	1.50
Eu	0.555	0.594	0.467	0.497	0.563	0.470	0.709	0.555
Tb	0.325	0.346	0.287	0.292	0.325	0.275	0.418	0.322
Yb	1.29	1.44	1.21	1.22	1.42	1.10	1.79	1.26
Lu	0.208	0.217	0.199	0.191	0.219	0.178	0.280	0.199

(1) Data for Sc, Cr, Hf and REE by INAA. Precision and accuracy given in Appendix II.

(2) Data for V, Ni, Ti, Zr, Y, Ba and Pb by XRF, provided by B. W. Chappell and R. W. Johnson.

(3) Data for Rb and Sr by isotope dilution (Appendix II).

FIGURE 5.3: Chondrite normalized Sc and transition metal abundances in Manam lavas compared to abundances in MORB's (Langmuir et al., 1977) and a boninite (Table 3.2). Normalizing values given in Table 3.2.

FIGURE 5.4: Ti/Sc plotted vs Ti/V for Manam lavas compared to values of these ratios in boninites, chondrites and MORB's. The effect of Rayleigh fractional crystallization of clinopyroxene and magnetite on Ti/Sc and Ti/V ratios is shown by mineral vectors plotted in the lower part of the diagram (see Table 5.5 for partition coefficients).

FIGURE 5.5: Covariation of V/Sc, Zr/Ti, Yb/Sc and La/Yb ratios with MgO content in Manam lavas.

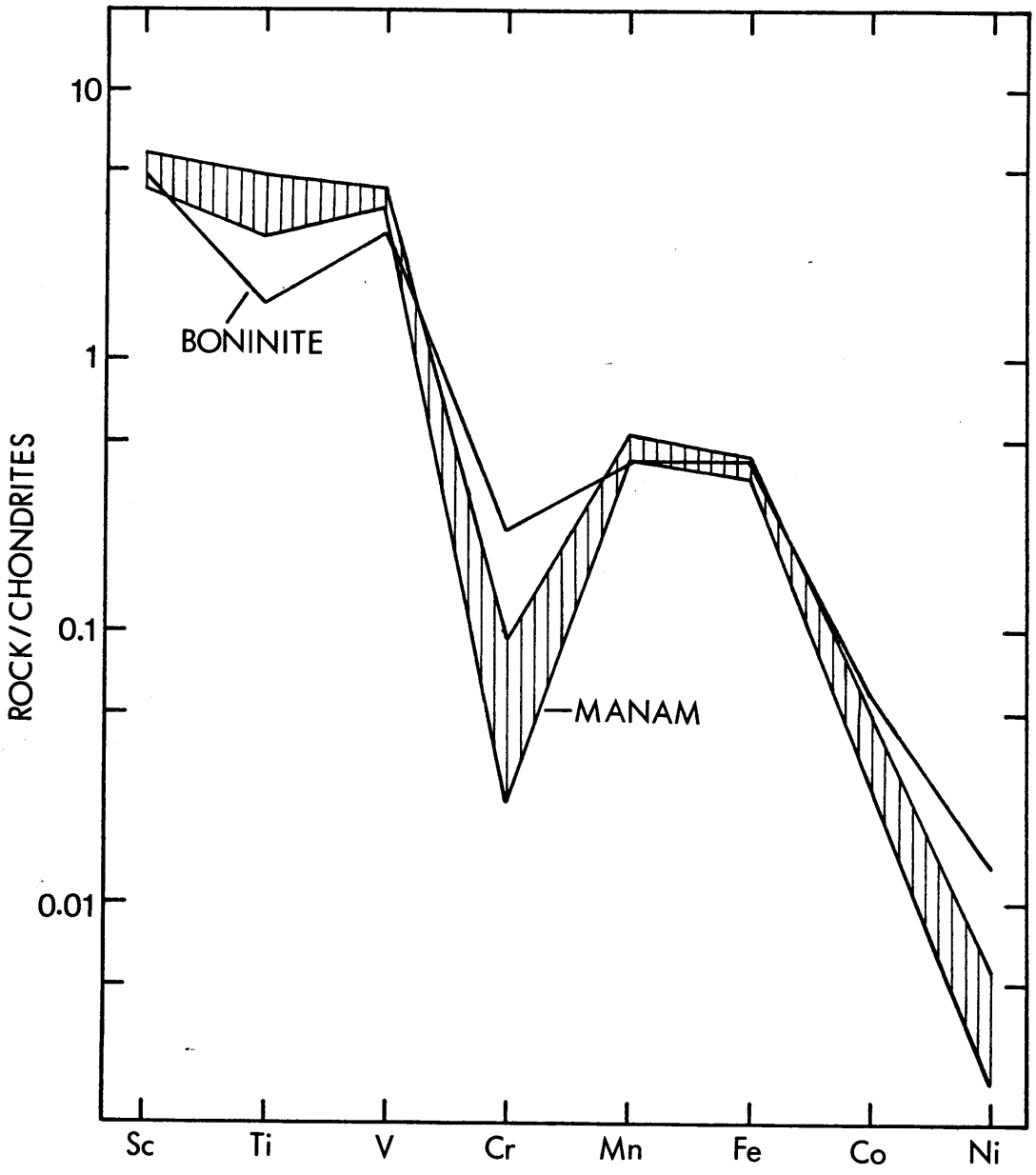
10
1
0.1
0.01
ROCK/CHONDRITES
BONINITE
MANAM
Sc
Ti
V
Cr
Mn
Fe
Co
Ni

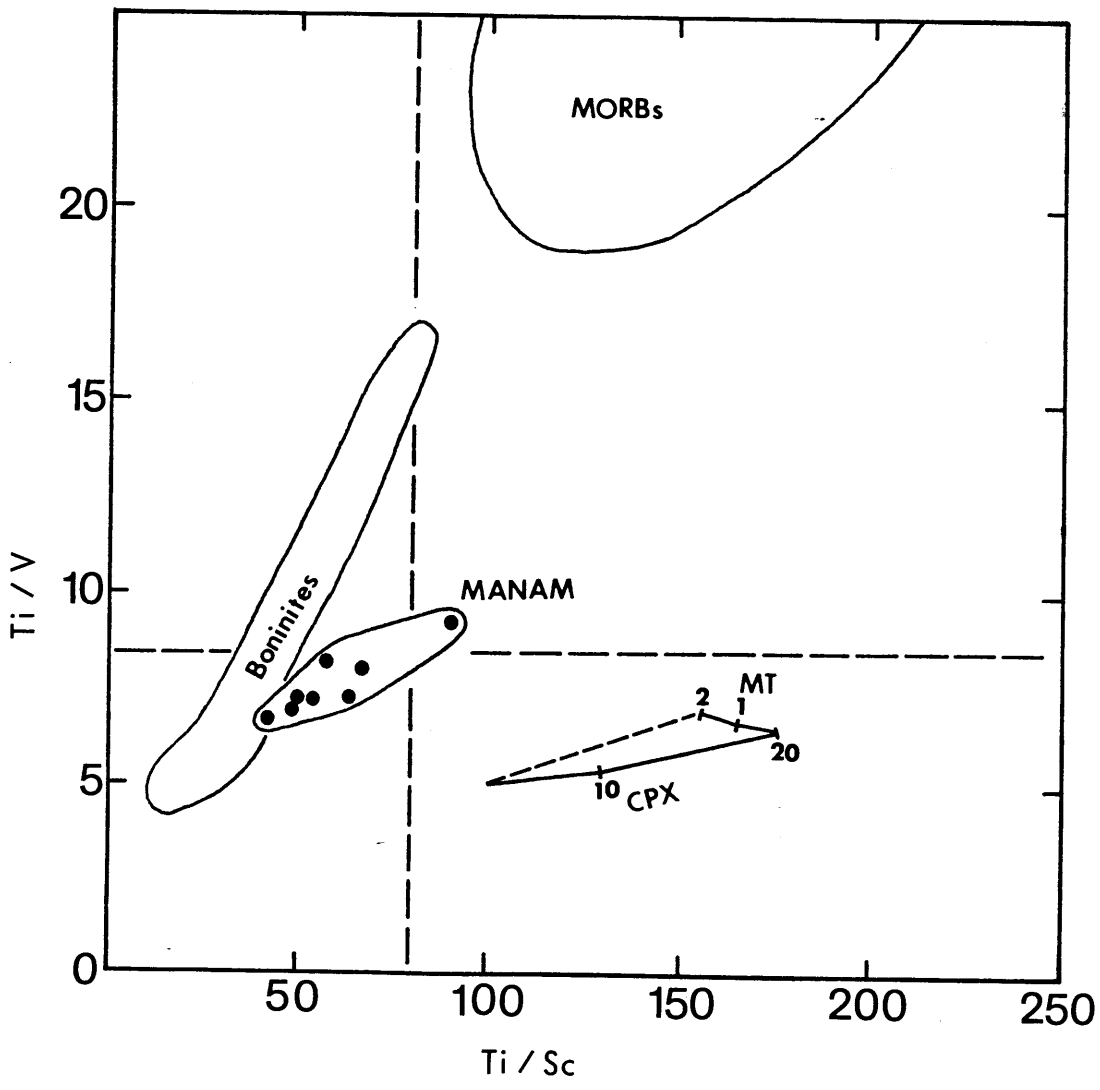
MORBs
Boninites
MANAM
MT
2
1
20
10
CPX
Ti / V
Ti / Sc
0
5
10
15
20
50
100
150
200
250

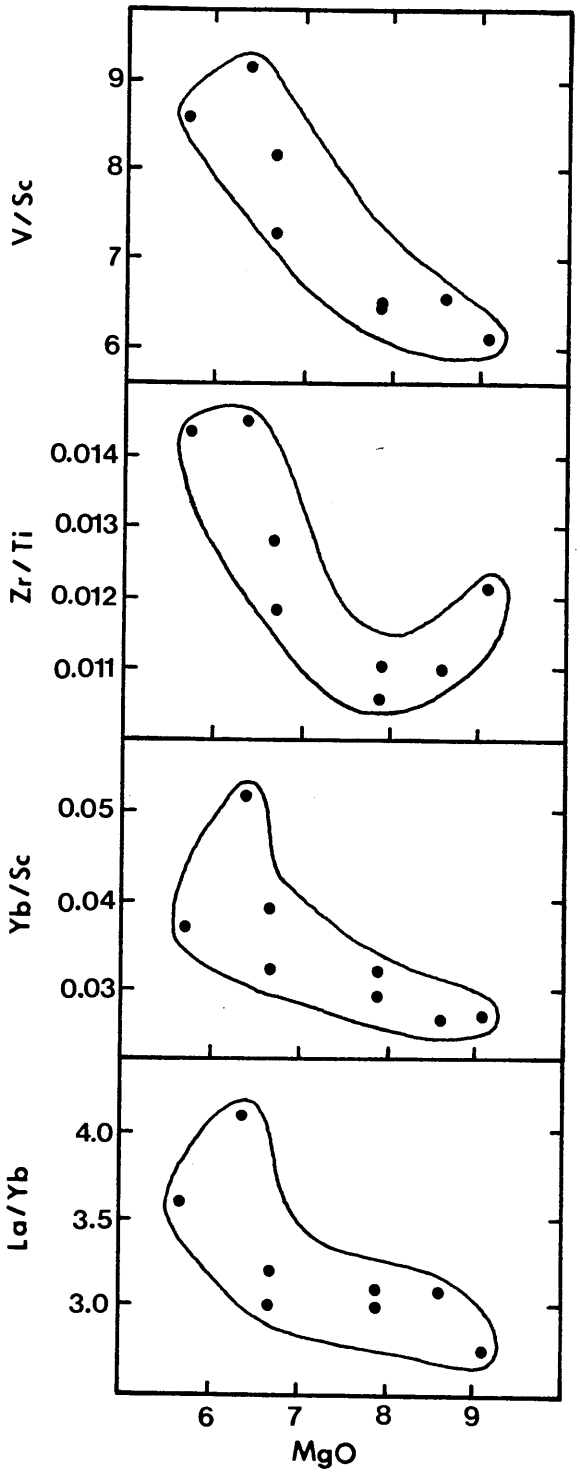
V/Sc
9
8
7
6
Zr/Ti
0.014
0.013
0.012
0.011
Yb/Sc
0.05
0.04
0.03
La/Yb
4.0
3.5
3.0
6
7
8
9
MgO

5.2). Sr (506-626 ppm) and Pb (3-10 ppm) abundances are especially high, and Sr/Nd (62-130) and Pb/Nd (0.5-1.8) ratios are among the highest found in island arcs (Fig. 5.8). Ba/La ratios (29-54) are also high compared to arc volcanics with similar La/Sm ratios (Fig. 5.8). K (4500-8600 ppm) and Rb (7.2-15.7 ppm) abundances and K/Rb ratios (550-660) are intermediate between those characteristic of calc-alkaline and arc tholeiitic volcanics, but Rb/Sr ratios (0.012-0.028) are low. Sr abundances in Manam lavas increase with increasing Al_2O_3 content, however, Sr/Nd, Sr/Ba and Rb/Sr ratios do not covary with Sr or Al_2O_3 contents.

REE and HFS Elements:

Manam lavas are LREE-enriched (Fig. 5.7), with $(La/Yb)_{e.f.}$ of 1.9 to 2.7, $(La/Sm)_{e.f.}$ of 1.7 to 2.2, and Sm/Nd of 0.30 to 0.23. HREE abundances (5 to 9 x chondrites) are low compared to MORB's. The lavas do not have Eu anomalies.

Unlike boninites, normalized Zr and Hf as well as Ti abundances in Manam lavas are lower than REE abundances (e.g., $(Zr/Sm)_{e.f.}$ = 0.6-0.7, Fig. 5.6). Zr/Hf ratios (30-40) are similar to those in chondrites and oceanic basalts (Bougault et al., 1980). Ti/Zr ratios (67-94) are lower than chondritic values, and overlap the with the highest values found in boninites.

Normalized abundances of Ti, Y and Yb increase in the order Ti<Y<Yb (Fig. 5.6), therefore, Ti/Y, Ti/Yb and Y/Yb ratios are less than chondritic. Sc/Yb ratios (19-39) range from lower than chondritic to chondritic values, and are lower than those in boninites.

The ratios La/Yb, Zr/Ti, and Yb/Sc in Manam lavas increase with decreasing MgO content (Fig. 5.5), while Zr/Sm and Ti/Yb ratios are relatively constant with varying MgO content.

FIGURE 5.6: Normalized trace element abundances in Manam lavas compared to abundances in a boninite (Table 3.2) and a MORB (Figure 3.6). Normalizing values given in Table 3.2.

FIGURE 5.7: Chondrite normalized REE abundances in Manam lavas. Normalizing values given in Table 3.2.

FIGURE 5.8: Plots of a) Sr/Nd vs SiO_2, and b) $(Ba/La)_{e.f.}$ vs $(La/Sm)_{e.f.}$ showing the enrichment of Manam lavas in Sr and Ba relative to REE elements compared to arc volcanics from the Aleutians (Kay, 1977; 1978), Antilles (Hawkesworth et al., 1979), New Hebrides (Gorton, 1977), New Britain (Johnson and Chappell, 1979; DePaolo and Johnson, 1979), Tonga (Ewart et al., 1973; Ewart et al., 1977), and boninites (Table 3.2).

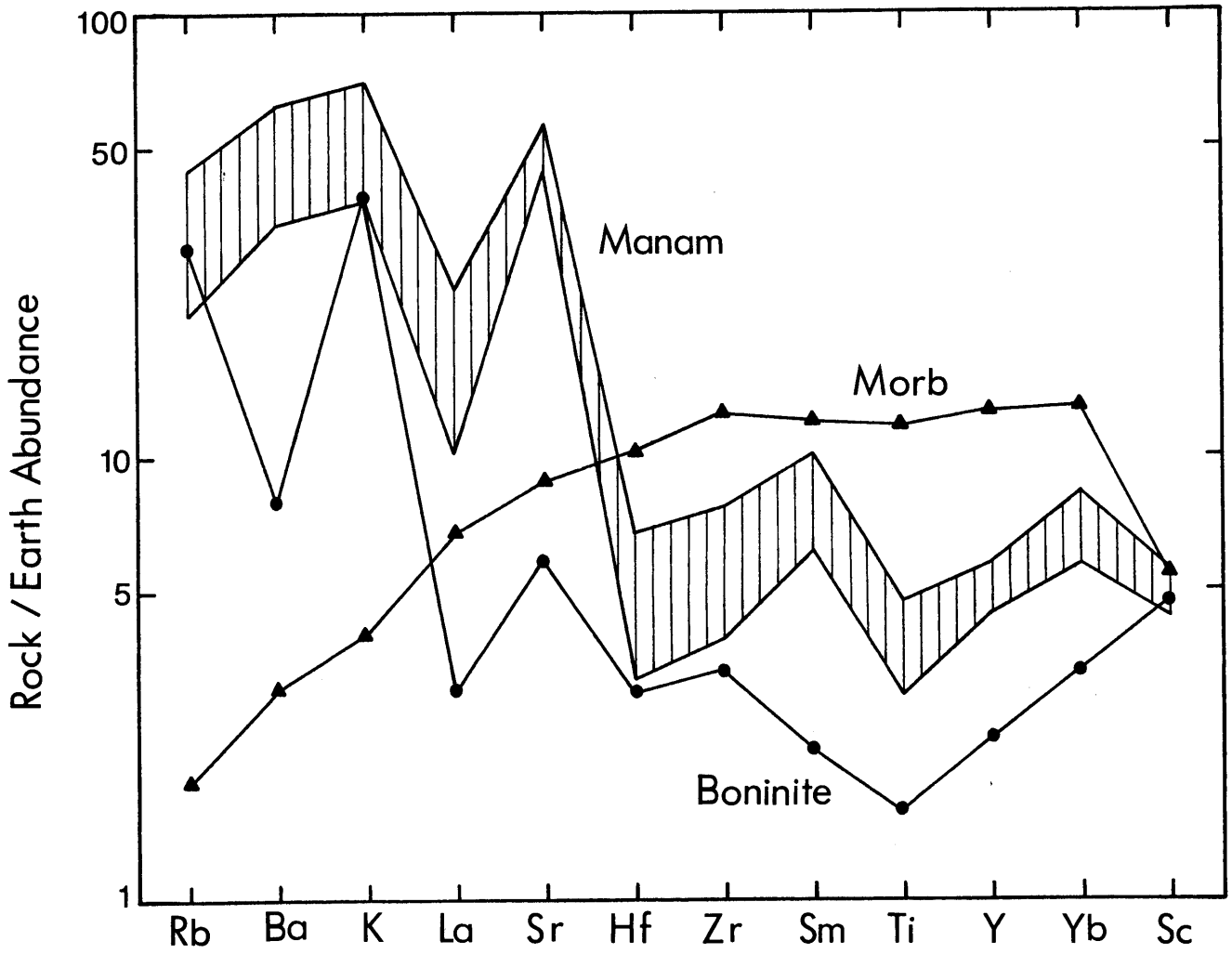
100
50
10
5
1
Rock / Earth Abundance
Manam
Morb
Boninite
Rb
Ba
K
La
Sr
Hf
Zr
Sm
Ti
Y
Yb
Sc

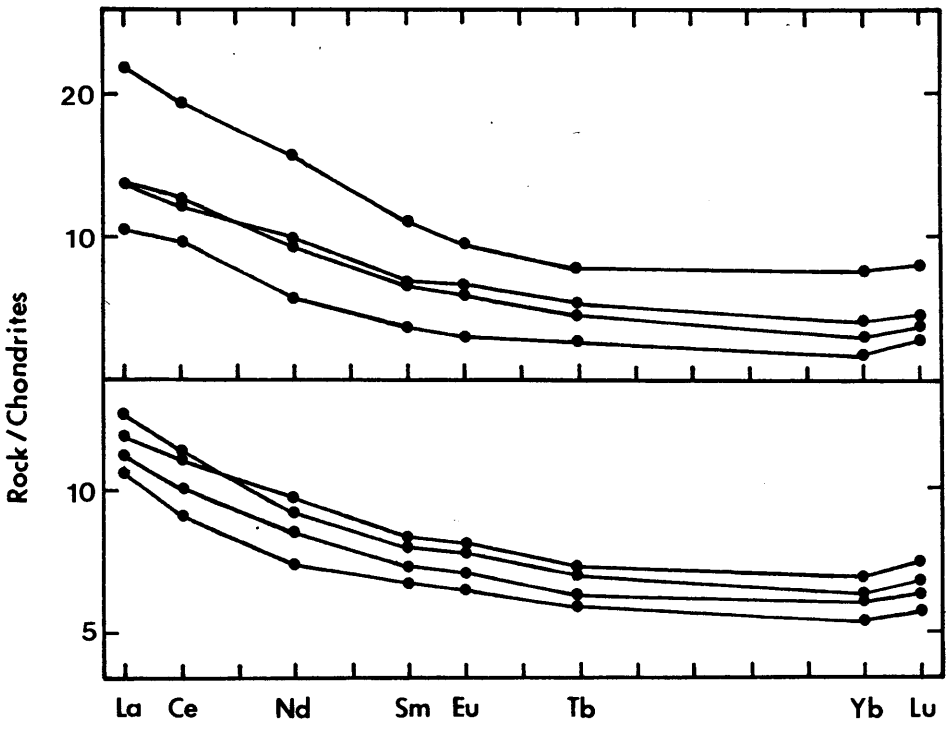
20
10
10
5
Rock / Chondrites
La
Ce
Nd
Sm
Eu
Tb
Yb
Lu

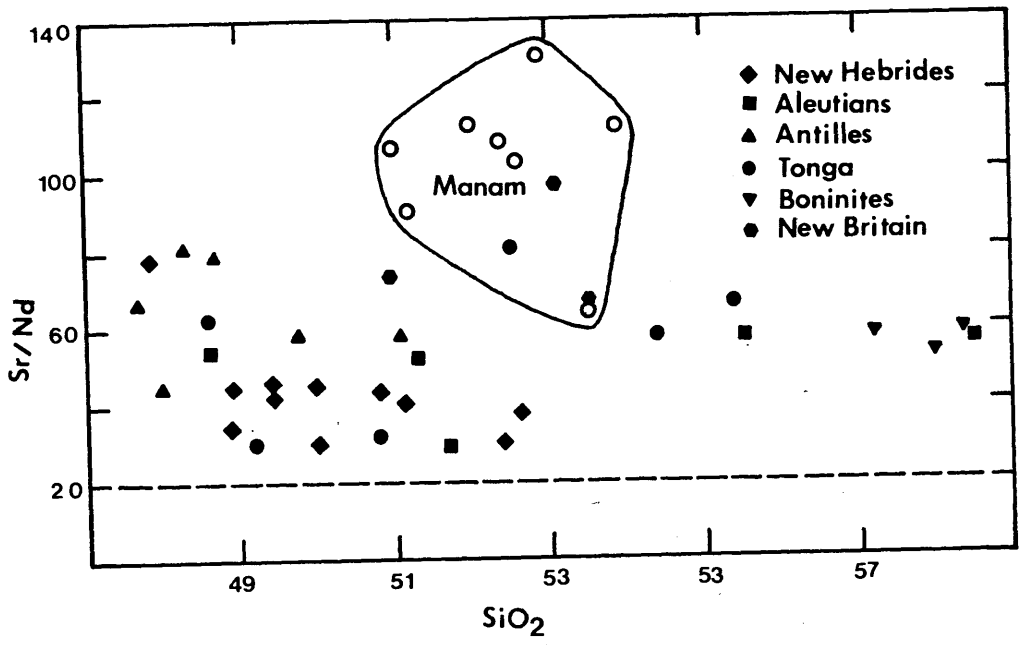
140
100
60
20
Sr/Nd
49
51
53
53
57
SiO2
Manam
New Hebrides
Aleutians
Antilles
Tonga
Boninites
New Britain

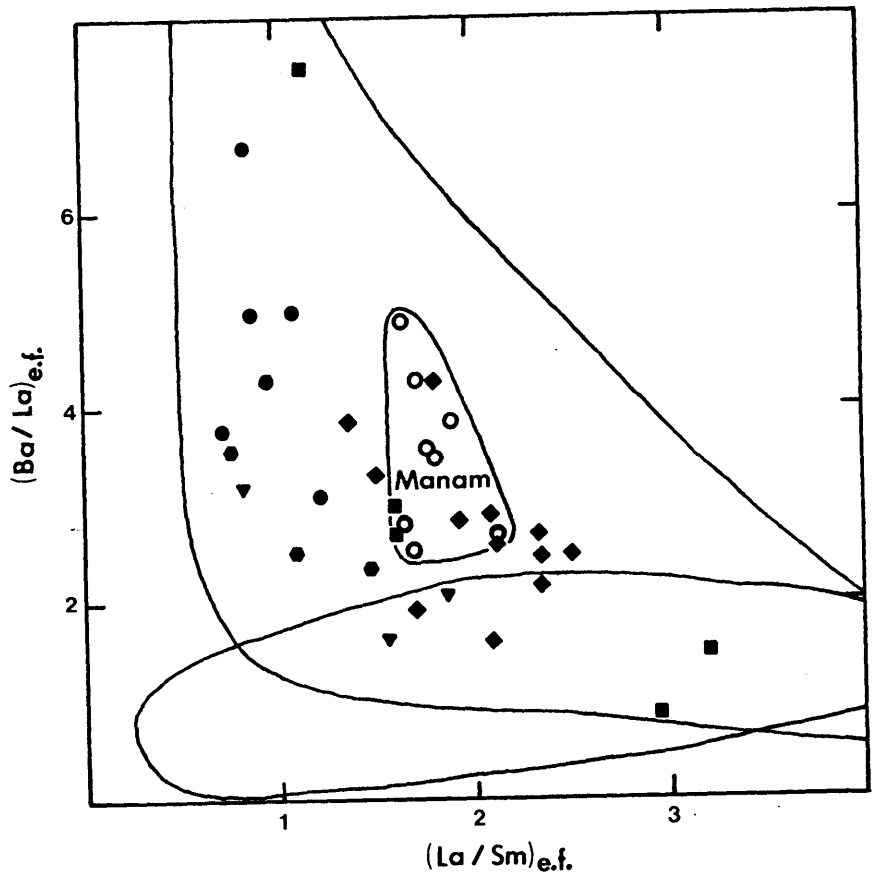
6
4
2
(Ba/La)e.f.
1
2
3
(La/Sm)e.f.
Manam

ISOTOPIC DATA FOR MANAM LAVAS

Sr, Nd and Pb isotopic data for Manam lavas are listed in Table 5.3. $^{87}Sr/^{86}Sr$ ratios vary from 0.70313 to 0.70338, and $^{143}Nd/^{144}Nd$ ratios from 0.51296 to 0.51303. All samples plot within the oceanic mantle array (Fig. 5.9).

$^{143}Nd/^{144}Nd$ ratios do not covary with $^{87}Sr/^{86}Sr$ ratios (Fig. 5.9), however K/La, Rb/La and Ba/La ratios in the lavas increase with increasing $^{87}Sr/^{86}Sr$ (Fig. 5.10). K/Ba and Rb/Ba ratios decrease with increasing $^{87}Sr/^{86}Sr$ (Fig. 5.10) and K/Rb ratios are constant (Table 5.2). Sr/Ba and Sr/La also covary with $^{87}Sr/^{86}Sr$ to some extent (Fig. 5.13).

$^{143}Nd/^{144}Nd$ ratios in the lavas increase with decreasing La/Nd (Fig. 5.11), but do not correlate with La/Yb, Ti/Zr or any ratios of the elements K, Rb, Ba, Sr or Pb to each other, or to REE and HFS elements. $^{87}Sr/^{86}Sr$ ratios and abundances of K, Rb, Ba, Sr and Pb appear to be completely decoupled from $^{143}Nd/^{144}Nd$ ratios and abundances of REE and HFS elements.

$^{206}Pb/^{204}Pb$ and $^{207}Pb/^{204}Pb$ ratios in three Manam samples plot within or close to the values found in MORB's (Fig. 5.12). Increasing $^{207}Pb/^{206}Pb$ in the three samples corresponds to increasing $^{87}Sr/^{86}Sr$, but does not appear to correlate with $^{143}Nd/^{144}Nd$. For example, the highest and lowest $^{207}Pb/^{204}Pb$ samples also have the highest and lowest $^{87}Sr/^{86}Sr$, but have similar, high $^{143}Nd/^{144}Nd$ ratios (Table 5.3). The third sample has intermediate $^{87}Sr/^{86}Sr$, but low $^{143}Nd/^{144}Nd$.

TABLE 5.3: Nd, Sr AND Pb ISOTOPIC ANALYSES OF MANAM ISLAND VOLCANICS

SAMPLE	$^{143}Nd/^{144}Nd$(1)	$^{87}Sr/^{86}Sr$(2)	$^{206}Pb/^{204}Pb$	$^{207}Pb/^{204}Pb$
1	0.513017 ± 13	0.70313 ± 3	--	--
2	0.513031 ± 16	0.70318 ± 3	15.500 ± 8	18.620 ± 9
3	0.513013 ± 15	0.70338 ± 3	15.535 ± 8	18.636 ± 9
4	0.512977 ± 15	0.70328 ± 3	--	--
5	0.512985 ± 17	0.70330 ± 3	--	--
6	0.512956 ± 16	0.70326 ± 3	15.513 ± 8	18.611 ± 9
7	0.512964 ± 20	0.70319 ± 3	--	--
8	0.512977 ± 14	0.70329 ± 3	--	--

(1) $^{143}Nd/^{144}Nd$ normalized to $^{146}Nd/^{144}Nd = 0.7219$, and BCR-1, $^{143}Nd/^{144}Nd = 0.51263$.

(2) $^{87}Sr/^{86}Sr$ normalized to $^{86}Sr/^{88}Sr = 0.1194$, and Eimer and Amend $SrCO_3$, $^{87}Sr/^{86}Sr = 0.7080$.

FIGURE 5.9: Plot of $^{143}Nd/^{144}Nd$ vs $^{87}Sr/^{86}Sr$ for Manam lavas compared to volcanic rocks from New Britain (DePaolo and Johnson, 1979) and the oceanic mantle array.

FIGURE 5.10: Variation of K/La, Rb/La, Ba/La and Rb/Ba with $^{87}Sr/^{86}Sr$ in volcanics rocks from Manam Island.

FIGURE 5.11: Variation of La/Nd with $^{143}Nd/^{144}Nd$ in Manam lavas, compared to trends for low TiO_2 volcanics from the Facpi Formation Guam (Tables 5.2 and 5.3) and boninites (Table 3.2 and 3.3).

FIGURE 5.12: $^{206}Pb/^{204}Pb$ and $^{206}Pb/^{204}Pb$ ratios in Manam lavas, along with fields for MORB's and Pacific Ocean sediments from Hawkesworth, 1982.

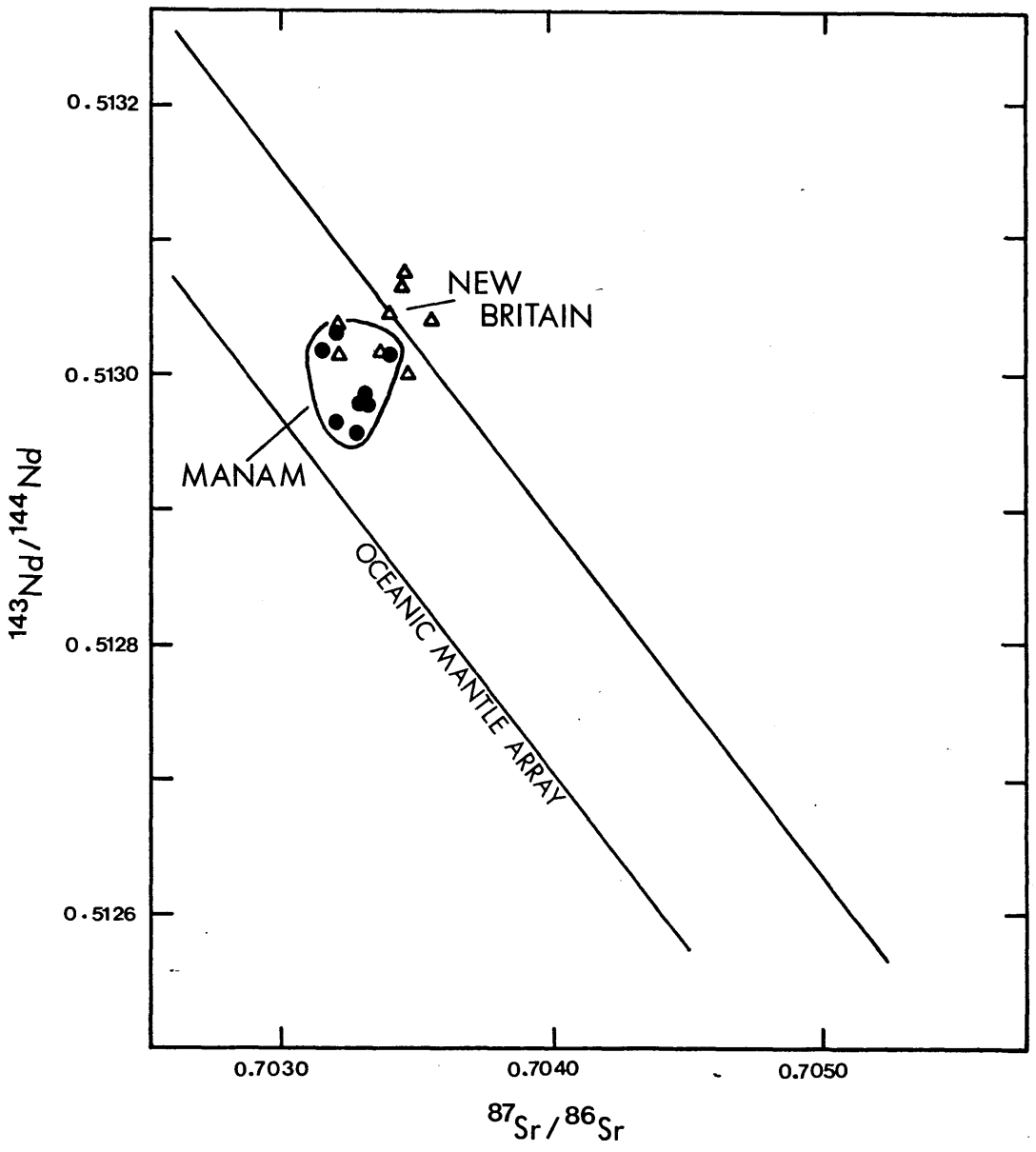
0.5132
0.5130
0.5128
0.5126
$^{143}Nd/^{144}Nd$
NEW
BRITAIN
MANAM
OCEANIC MANTLE ARRAY
0.7030
0.7040
0.7050
$^{87}Sr/^{86}Sr$

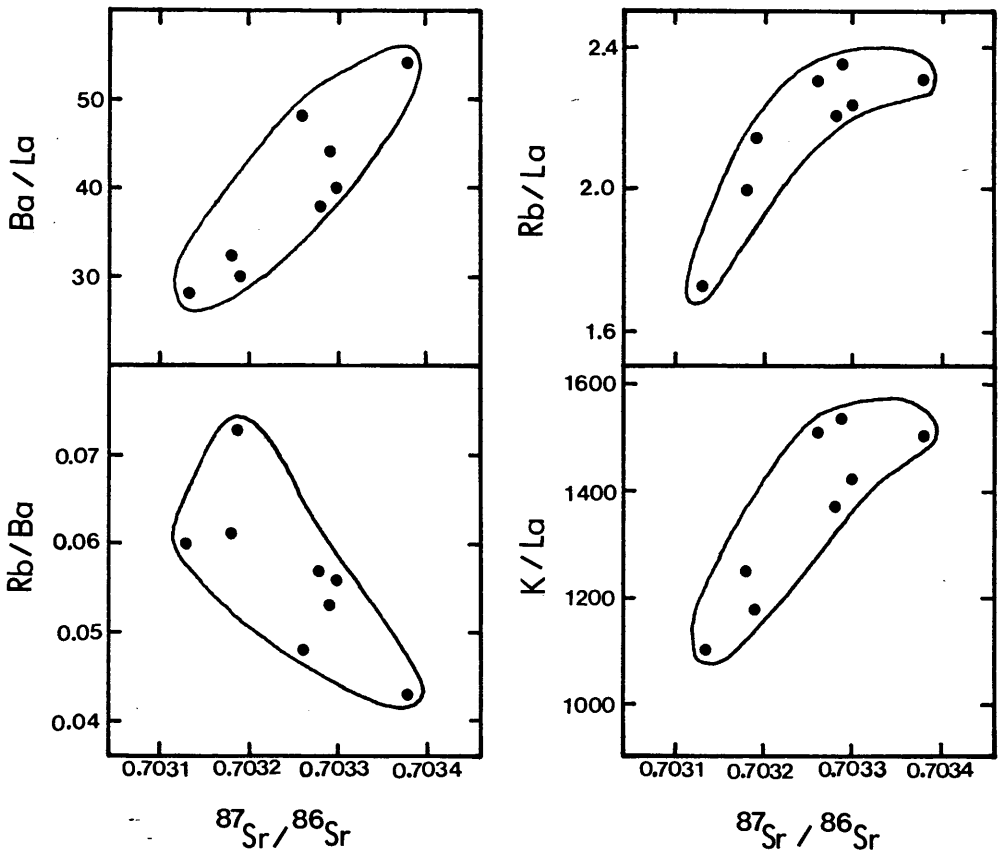
Ba / La
50
40
30
Rb/ La
2.4
2.0
1.6
Rb/Ba
0.07
0.06
0.05
0.04
K / La
1600
1400
1200
1000
0.7031
0.7032
0.7033
0.7034
87Sr / 86Sr
87Sr / 86Sr

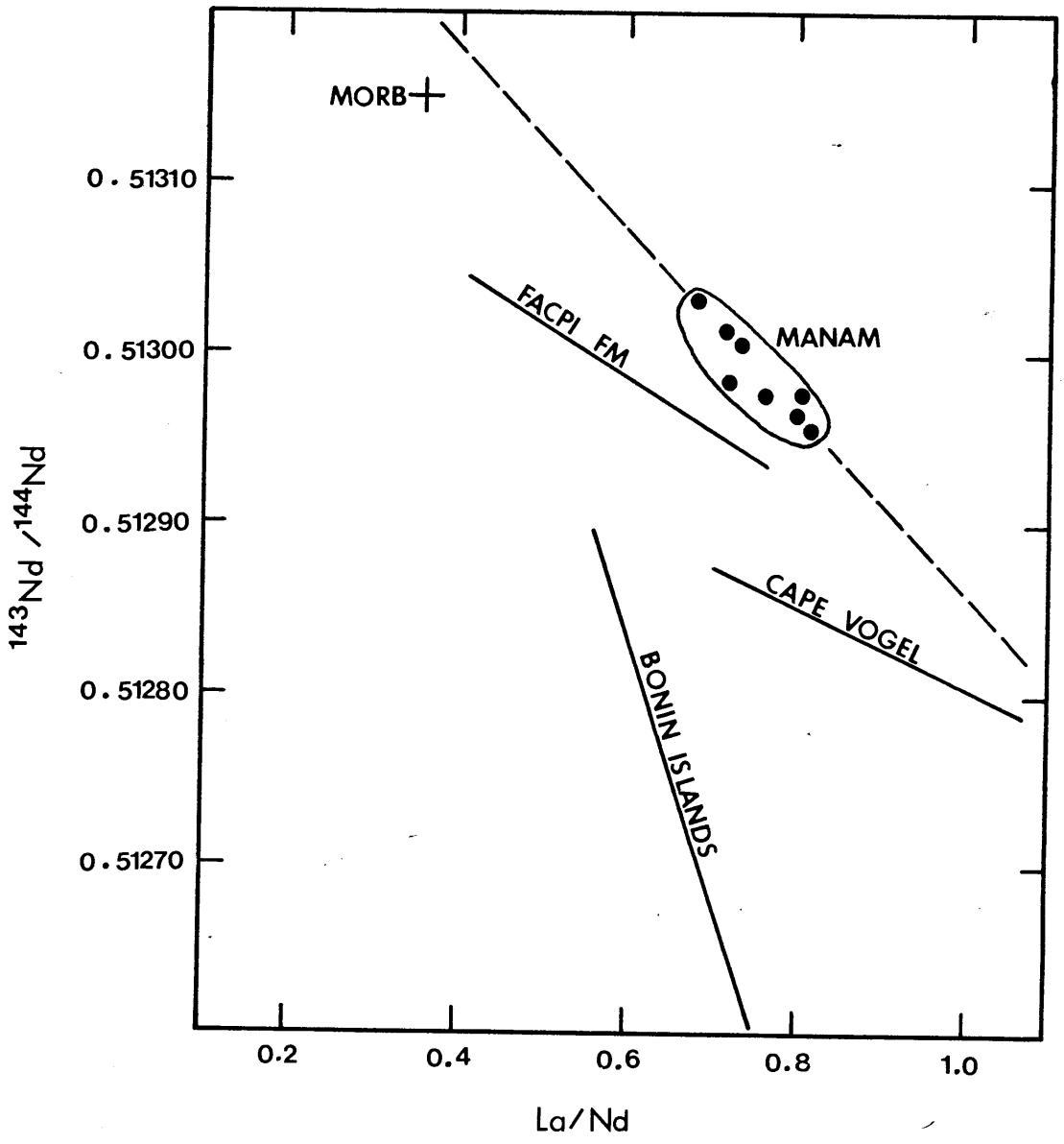
MORB
MANAM
FACPI FM
CAPE VOGEL
BONIN ISLANDS
0.51310
0.51300
0.51290
0.51280
0.51270
$^{143}Nd/^{144}Nd$
0.2
0.4
0.6
0.8
1.0
La/Nd

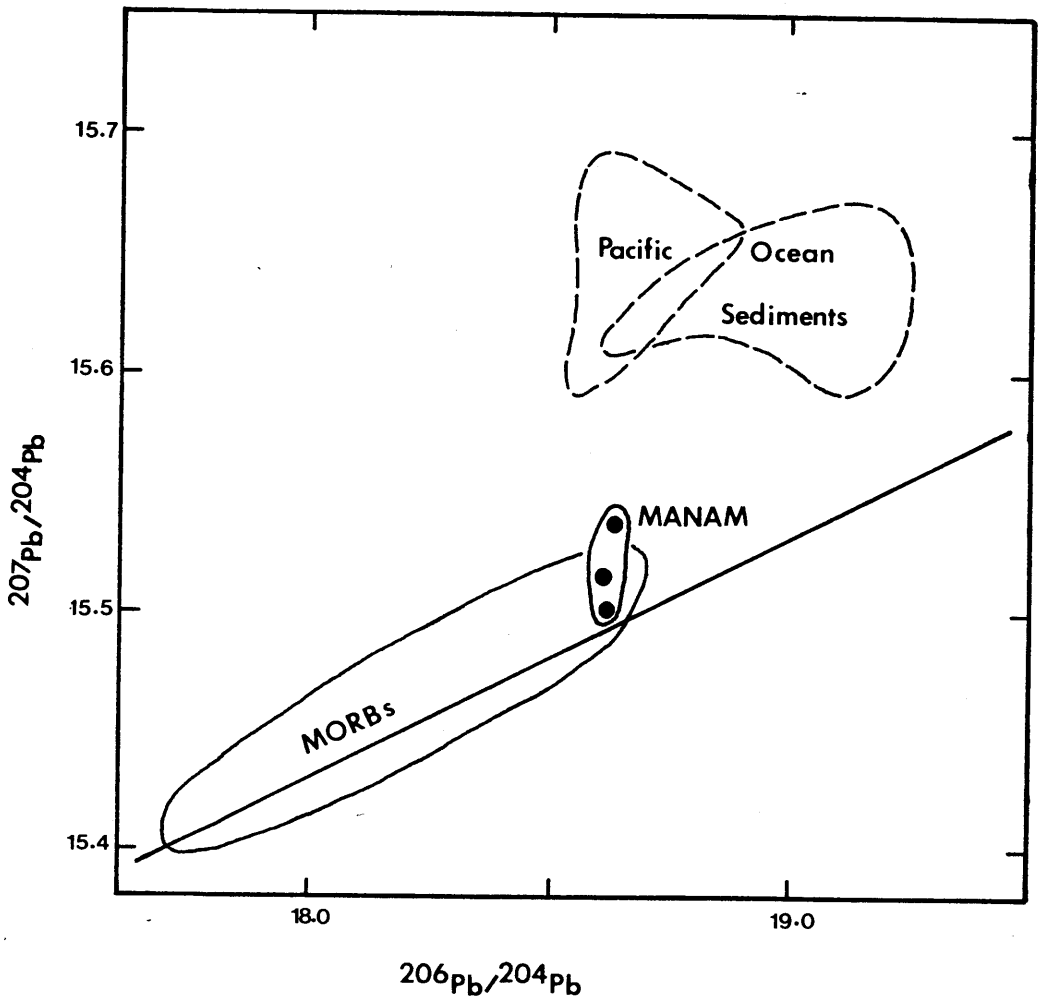
15.7
15.6
15.5
15.4
18.0
19.0
$^{207}Pb/^{204}Pb$
$^{206}Pb/^{204}Pb$
Pacific
Ocean
Sediments
MANAM
MORBs

SUMMARY OF KEY GEOCHEMICAL FEATURES

The key geochemical features of lavas from Manam Island can be summarized:

1) compared to MORB's, extremely high abundances of K, Rb, Ba, Sr and Pb relative to abundances of REE and HFS elements, and increasing ratios of K/La, Rb/La, Ba/La and Ba/Rb with increasing $^{87}Sr/^{86}Sr$.
2) enrichment in LREE compared to HREE, and correspondence between increasing La/Nd and decreasing $^{143}Nd/^{144}Nd$.
3) $^{87}Sr/^{86}Sr$ and $^{143}Nd/^{144}Nd$ which are similar to those in oceanic volcanic rocks, and $^{206}Pb/^{204}Pb$ and $^{207}Pb/^{204}Ob$ ratios similar to those in MORB's.
4) lower than chondritic ratios of Ti/Sc, Ti/V, Ti/Y and Ti/Yb, and also depletion of Zr relative to Sm.

DISCUSSION

SOURCES FOR K, Rb, Ba, Sr AND Pb IN ISLAND ARC VOLCANICS

The reason for enrichment in island arc volcanics of the elements K, Rb, Ba, Sr and Pb relative to abundances of REE and HFS elements is an unresolved problem in the understanding of island arc volcanism. Recent explanations for this characteristic involve addition of high K, Rb, Ba, Sr and Pb material to a mantle source or magma with "normal" (i.e., like oceanic lavas) abundances of these elements relative to REE and HFS elements. These postulated added materials include derivatives from subducted sediment and seawater (Kay, 1980), subducted oceanic basalt (DePaolo and Johnson, 1979), and the lower island arc crust (Arculus and Johnson, 1981). In Manam lavas, the decoupling of Sr and Pb from Nd

isotopic ratios supports different sources for REE vs Pb vs Sr, as suggested by these models. Although the Manam volcanics have one of the largest enrichments of K, Rb, Ba, Sr and Pb relative to REE and HFS elements found in island arc rocks, their isotopic composition is not significantly different from that of oceanic volcanics. Consequently, the dominant sources of these elements in Manam lavas may be materials recently removed from the oceanic mantle itself, consistent with the models of DePaolo and Johnson (1979) and Arculus and Johnson (1981). However, in Manam lavas, ratios such as Rb/Ba and Sr/Ba also covary with $^{87}Sr/^{86}Sr$, although all these elements have high abundances relative to REE and HFS elements. This suggests that the K, Rb, Ba, Sr and Pb contents of Manam lavas may represent a mixture of at least two materials having different relative abundances of these elements and different Pb and Sr isotopic compositions.

TWO COMPONENTS FOR K, Rb, Ba, Sr AND Pb

A multicomponent source for Sr is suggested by the positive correlation of Ba/La, Rb/La and K/La with $^{87}Sr/^{86}Sr$, but the negative correlation of Rb/Ba and K/Ba. Possible mixing relationships for two components are most easily examined on ratio-ratio plots using the same denominator element because linear trends of data points should be produced. Fig. 5.13a is a plot of Sr/Ba vs Rb/Ba for Manam lavas. Six of the eight Manam samples define a linear trend on this plot, and two of the samples (samples 1 and 7, Table 5.2) are displaced. Curves showing the effects of fractional crystallization and accumulation of plagioclase on Sr/Ba and Rb/Ba ratios are also plotted. The trend formed by the six samples is not a plagioclase fractionation line because it is nearly at

right angles to the predicted curves and has positive slope. The direction of displacement of sample 1 from the trend is consistent with ~20% plagioclase accumulation, and for sample 7, ~35% plagioclase removal. Since $^{87}Sr/^{86}Sr$ in the lavas decreases with increasing Rb/Ba (Fig. 5.10), returning the two samples, which both have low $^{87}Sr/^{86}Sr$, to the main trend along the crystallization and accumulation curves is also consistent with this variation. In Figs. 5.13b and c, samples 1 and 7 are also displaced from trends formed by other samples, and their relative distances from the trends are roughly the same in each diagram.

If the main trends in Figs. 5.13 a through c are interpreted as mixing lines, the following information can be obtained about the two possible mixing endmembers. In Fig. 5.13a, a line calculated through the Manam lavas extrapolates through zero, indicating that Rb/Sr is similar in the two components, as it is in the lavas themselves (0.015-0.017, excluding samples 1 and 7, Table 5.2). Since K/Rb ratios in the lavas are also constant, relative K, Rb and Sr abundances in the two endmembers are also similar. In Fig. 5.13b, $^{87}Sr/^{86}Sr$ decreases with decreasing Ba/Sr. At the extreme of Ba/Sr = 0, the minimum $^{87}Sr/^{86}Sr$ value for the low $^{87}Sr/^{86}Sr$ endmember is about 0.7026. The maximum value for the high $^{87}Sr/^{86}Sr$ endmember cannot be constrained because no ratio of K, Rb, Ba or Sr extrapolates to zero with increasing $^{87}Sr/^{86}Sr$.

Fig. 5.13c is a plot of Ba/La vs Sr/La. The linear trend of data points on this diagram may not be a two-component mixing line, because the decoupling of Ba and Sr abundances and $^{87}Sr/^{86}Sr$ ratios from LREE abundances and $^{143}Nd/^{144}Nd$ ratios indicates there is at least one other component for La. It appears on this diagram that Ba/La and Sr/La ratios

FIGURE 5.13: Ratio - ratio plots showing evidence for two component mixing for K, Rb, Ba and Sr in Manam lavas:

a) Variation of Sr/Ba vs Rb/Ba. Curves showing the effect of plagioclase accumulation and removal on Sr/Ba and Rb/Ba ratios are also shown.

b) Variation of Ba/Sr with $^{87}Sr/^{86}Sr$.

c) Variation of Sr/La with Ba/La.

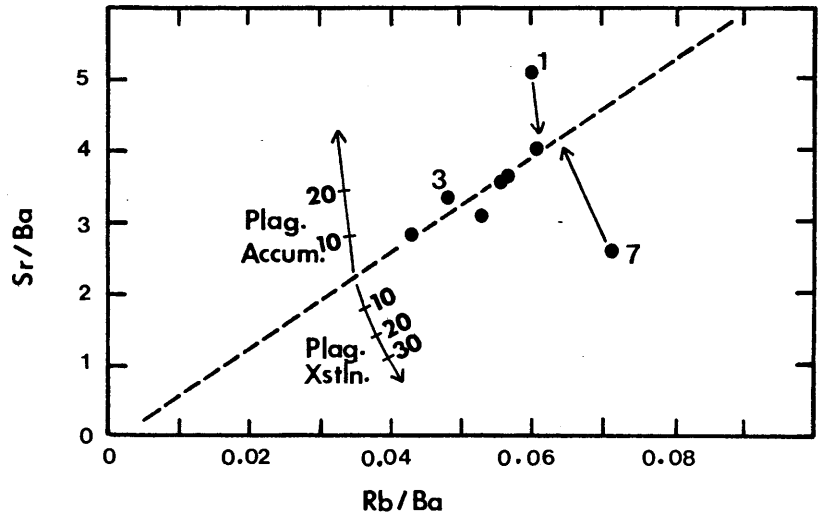
Sr/Ba
Rb/Ba
Plag.
Accum.
20
10
Plag.
Xstln.
10
20
30
1
3
7
0
1
2
3
4
5
0.02
0.04
0.06
0.08

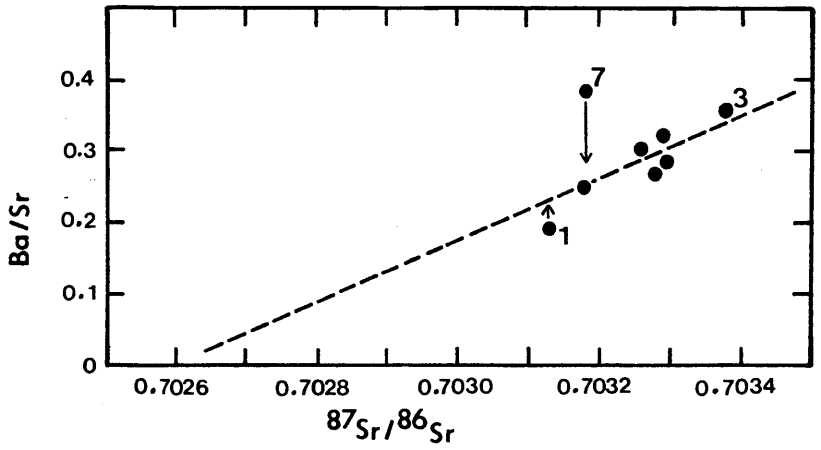
Ba/Sr
$^{87}Sr/^{86}Sr$
7
3
1
0
0.1
0.2
0.3
0.4
0.7026
0.7028
0.7030
0.7032
0.7034

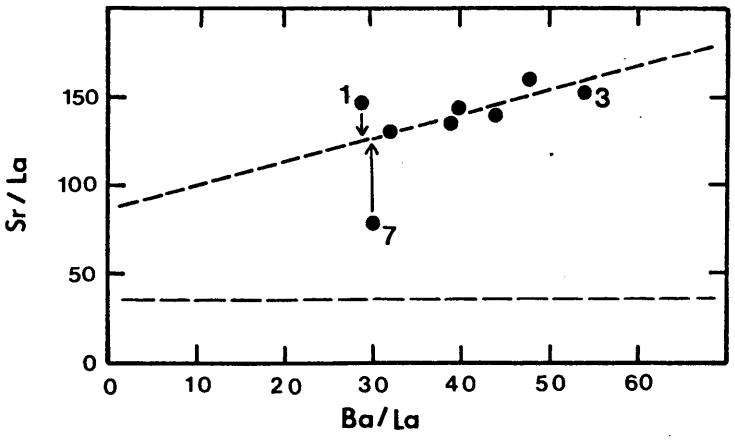
Sr/La
Ba/La
1
3
7
0
50
100
150
10
20
30
40
50
60

are higher in the $^{87}Sr/^{86}Sr$ endmember than in the low $^{87}Sr/^{86}Sr$ endmember, and this would be the case if La was derived from these two components alone. However, if much of the La in the Manam lavas comes from a third component, this trend (and the trends in Fig. 5.10a through c) could be produced if the high $^{87}Sr/^{86}Sr$ endmember had higher absolute concentrations of Ba, Sr, K and Rb than the low $^{87}Sr/^{86}Sr$ endmember, even if it had lower Ba/La, Sr/La, K/La and Rb/La ratios. Therefore, the relative Ba/La and Sr/La ratios in the two endmembers cannot be inferred from the plot. The Ba/La and Sr/La ratios in the lavas are the minimum values for these ratios in the two endmembers. At the extreme of Ba/La = 0, the Sr/La extrapolated from the lavas is significantly higher than the ratios for chondrites (85 vs 35). This means that in the absence of the high $^{87}Sr/^{86}Sr$ endmember, Sr/La ratios in the lavas would still be high, and indicates that both endmembers have high Sr/La ratios.

POTENTIAL SOURCES FOR K, Rb, Ba, Sr AND Pb IN MANAM LAVAS

Potential sources for enrichments in K, Rb, Ba, Sr and Pb in island arc lavas have been discussed and evaluated in several papers (e.g., DePaolo and Johnson, 1979; Kay, 1980; Arculus and Johnson, 1981). Since most of these discussions sought a single material to account for high abundances of these elements, it is worthwhile reviewing these sources with respect to their potential as endmembers of a mixture with the characteristics described for the Manam lavas. Geochemical characteristics of the endmembers inferred from Figs. 5.13a through c, Fig. 5.10 and Fig. 5.12 are listed in Table 5.4.

TABLE 5.4: COMPARISON OF INFERRED LOW $^{87}Sr/^{86}Sr$ AND HIGH $^{87}Sr/^{86}Sr$ ENDMEMBERS WITH SEDIMENTS, GRANULITES AND MORB

	Low $^{87}Sr/^{86}Sr$ Endmember	High $^{87}Sr/^{86}Sr$ Endmember	Average Sediment (1)	Carbonate Sediment (2)	50% Carbonate 50% Average Sediment
Rb/Sr	~0.016	~0.016	0.088	0.005	0.032
Sr/Ba	>4.0	<2.8	0.5	10.5	0.8
Rb/Ba	>0.06	<0.04	0.04	0.05	0.04
K/Ba	>36	<25	9.9	15.3	6.4
K/Rb	~600	~600	241	290	250
Ba/La	--	>60	100	19	74
Sr/La	>90	>150	47	200	96
K/La	>810	>1350	994	290	768
Rb/La	>1.4	>2.4	4.1	1.0	3.1
$^{87}Sr/^{86}Sr$	>0.7026 <0.7031	>0.7034	>0.7090	0.7090	0.7090
$^{207}Pb/^{204}Pb$	<15.50	>15.54	15.6	15.6	15.6

Mafic Granulites

	Lesotho (3)	Algeria (4)	France (5)	Scotland (6)	MORB
Rb/Sr	0.018	--	0.025	0.018	0.008
Sr/Ba	0.5	1.5	0.9	0.8	11.0
Rb/Ba	0.009	--	0.023	0.014	0.08
K/Ba	3.7	11.3	10	13	88
K/Rb	410	--	439	922	1000
Ba/La	280	32	31	25	3.9
Sr/La	142	46	27.2	19	43
K/La	1029	359	300	319	342
Rb/La	2.5	--	0.7	0.3	0.3
$^{87}Sr/^{86}Sr$	--	--	--	--	<0.7028
$^{207}Pb/^{204}Pb$	--	--	--	--	--

(1) Average sediment, Kay (1980).
(2) Carbonate sediment, Turekian and Wedepohl (1961).
(3) Lesotho granulites, Rogers (1977).
(4) Central Hoggar, Algeria (Leyreloup et al., 1982).
(5) Massif Central, France (Dostal et al., 1980).
(6) Lewisian gneisses, Scotland (Holland and Lambert, 1975).

Sediments: Kay (1980) suggested that the incorporation of subducted sediments into arc magmas could account for enrichment in K, Rb, Ba, Sr and Pb. For arc volcanics which have $^{87}Sr/^{86}Sr$ and $^{207}Pb/^{204}Pb$ within the range for oceanic volcanics, this model has been rejected because the combined high concentration of Sr and Pb in sediments and their radiogenic isotopic composition would cause them to dominate any mixture with a second component having normal Pb/Nd or Sr/Nd ratios (e.g., subducted MORB or oceanic mantle). The average sediment of Kay (1980) (Table 5.3) compares fairly well with the high $^{87}Sr/^{86}Sr$ endmember for Manam lavas, and critical features such as low Sr/Ba, Rb/Ba and isotopic characteristics match closely. The major discrepancy is the higher Rb/Sr, K/Sr and low Sr/La ratios in the average sediment. Carbonate sediments (Turekian and Wedepohl, 1961, Table 5.4), have values for these ratios similar to the high $^{87}Sr/^{86}Sr$ endmember, and a mixture of 50% carbonate and 50% average sediment (Table 5.4) is suitable as the high $^{87}Sr/^{86}Sr$ endmember. Therefore, a carbonate-rich sediment could be one source for the enrichment of K, Rb, Ba, Sr and Pb in the Manam lavas.

Lower Crust: Incorporation of a component from granulitic lower continental or island arc crust was suggested by Arculus and Johnson (1981) to account for enrichments in Ba, Sr and Pb in arc lavas which did not have high Rb/Sr or U/Pb ratios or radiogenic Sr or Pb isotopic compositions. They noted that many granulites have high Ba/La ratios, similar to those in island arc lavas. Comparison of the compositions of mafic granulites (Table 5.4) with the inferred Manam endmembers shows that several characteristics of granulites are similar to those in the high $^{87}Sr/^{86}Sr$ endmember, e.g., low Sr/Ba, Rb/Ba and K/Ba ratios. However, although the

mafic granulites have high Ba/La ratios, high Sr/La, Rb/La and K/La ratios are not characteristic of these rocks (Table 5.4, Fig. 5.14). Granulites which have high Sr/La ratios, for example, those from Hoggar, Algeria (Fig. 5.14), are plagioclase-rich rocks with Eu/Eu* = 3-4 (Leyreloup et al., 1982). Therefore, bulk assimilation or equilibration of magma with granulitic lower crust would not explain the high Sr/La, Rb/La and K/La in Manam lavas. Extraction of a partial melt from a granulitic source, leaving a plagioclase-free, REE accessory mineral bearing residue, and mixing of this melt with mantle derived magma could produce high Sr/La and Ba/La ratios. However, continental basalts, which must pass through continental crust, typically do not have high Sr/La, including lavas from Skye and Mull, Scotland, and the Taos volcanic field (Carter et al., 1978; Williams and Murthy, 1979; Lipman and Dungan, 1981; Fig. 5.14) which have isotopic evidence for lower crustal contamination. This suggests that interaction of crustal material and basaltic magma does not usually produce Sr-enrichment in the magma. Therefore, while lower continental or island arc crust has some features in common with the high $^{87}Sr/^{86}Sr$ endmember, many important features do not match.

Subducted MORB: DePaolo and Johnson (1979) proposed that a high Sr/Nd material derived from subducted MORB could be responsible for the high Sr/Nd but low $^{87}Sr/^{86}Sr$ ratios in volcanic rocks from New Britain. In order to the produce the high Sr/Nd ratios, which are not characteristic of MORB's, they suggested that Sr might be partitioned preferentially to Nd into volatile-rich fluids derived from subducted basalt, based on the higher solubility of Sr in seawater and higher concentration in marine carbonates. Relative abundances of K, Rb, Ba and Sr, and the isotopic

FIGURE 5.14: Ba/La and Sr/La ratios in lower crustal granulites and continental basalts compared to lavas from Manam Island. Granulite data from Rogers (1977), Leyreloup et al. (1982), Dostal et al. (1980) and Holland and Lambert (1975). Continental basalt data from Carter et al. (1978), Leeman and Vitaliano (1976), Lipman and Dungan (1981), Green (1981) and Haggerty and Irving (1981). Dashed lines are chondritic values.

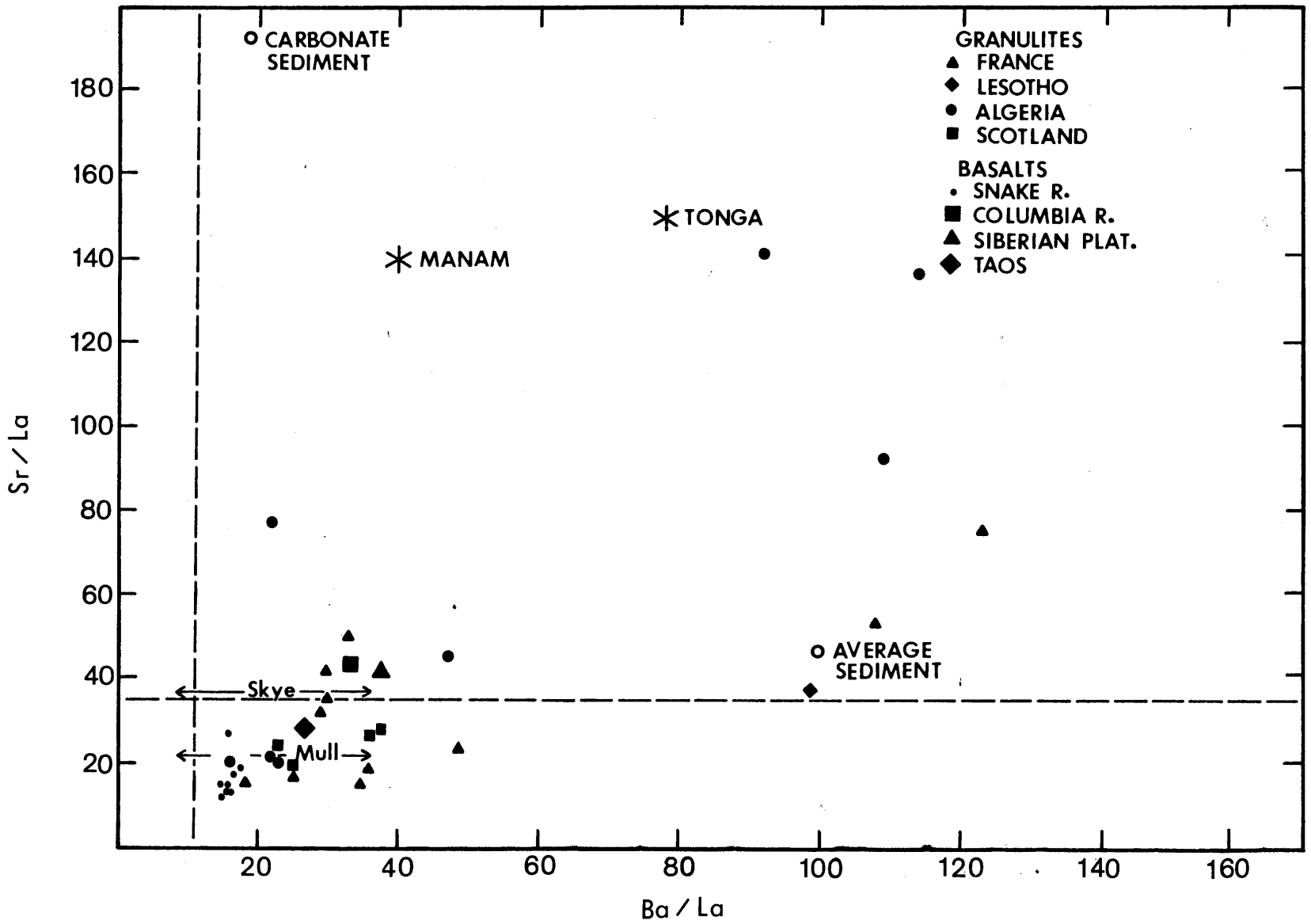
CARBONATE SEDIMENT
GRANULITES
FRANCE
LESOTHO
ALGERIA
SCOTLAND
BASALTS
SNAKE R.
COLUMBIA R.
SIBERIAN PLAT.
TAOS
TONGA
MANAM
AVERAGE SEDIMENT
Skye
Mull
Sr / La
Ba / La
180
160
140
120
100
80
60
40
20
20
40
60
80
100
120
140
160

composition of MORB's (Table 5.4) compare very well with the low $^{87}Sr/^{86}Sr$ endmember for Manam lavas. The only discrepancy is the higher Rb/Sr and lower K/Rb ratios in the low $^{87}Sr/^{86}Sr$ endmember which could reflect its derivation from MORB altered by seawater interaction. It should be noted however, that the low $^{87}Sr/^{86}Sr$ endmember does not have extremely high K/Ba and Rb/Ba ratios (>150 and >0.4, Table 3.5) characteristic of the "seawater" component proposed for boninites. The strong trace element and isotopic similarity between the low $^{87}Sr/^{86}Sr$ endmember and MORB's, and the lack of other low $^{87}Sr/^{86}Sr$ materials with comparable ratios of K, Rb, Ba and Sr, supports a subducted MORB source for this endmember.

Since MORB's do not have high abundances of K, Rb, Ba and Sr compared to LREE, these elements must be fractionated from the LREE by some process in order for MORB to be a source for the low $^{87}Sr/^{86}Sr$ endmember. Sr and LREE mineral/melt partition coefficients are similar for amphibole, garnet and clinopyroxene (Irving, 1978; Nicholls and Harris, 1980; Gill, 1978), which are the most abundant minerals comprising a basaltic composition at high pressures. Therefore, Sr and LREE should not be fractionated significantly by partial melting of subducted MORB. Partial melting in the presence of a residual accessory mineral with high partition coefficients for LREE but not Sr could produce a high Sr/LREE melt. In general, however, Sr partition coefficients for REE-rich accessory minerals are also high (e.g., apatite and perovskite, Irving, 1978).

DePaolo and Johnson (1979) proposed a vapor/solid partitioning process to derive a Sr-enriched material from subducted MORB. H_2O/mineral, CO_2-vapor/silicate melt and carbonate melt/silicate melt partition coefficients for REE have been determined by Mysen (1978) and Wendlandt and

Harrison (1979), and carbonate melt/silicate melt partition coefficients for Sr have been determined by Koster Van Groos (1975). According to Mysen (1978), REE partitioning into H_2O vapor vs silicate minerals is enhanced at high pressure. If the relative abundances of Sr and LREE in seawater indicates their relative preference for H_2O vs solid materials (silicate and carbonate sediments), then at high pressure H_2O-rich fluids released from subducted MORB could have high Sr and REE contents and high Sr/LREE ratios, as suggested for boninites.

The experiments of Wendlandt and Harrison (1979) and Koster Van Groos (1975) were performed at very different temperatures (1100-1300°C vs 600-800°C), and their results may not be comparable. Carbonate/silicate melt partition coefficients for Sr determined by Koster Van Groos (1975) are about 5, and exceed those for LREE determined by Wendlandt and Harrison (1979) by a factor of two. Since silicate solid/melt partition coefficients for Sr and LREE are approximately the same, a carbonate melt in equilibrium with a silicate solid might have high Sr/LREE ratios. Wendlandt and Harrison (1979) also found that LREE were strongly enriched in carbonate vapor compared to silicate melts. If the relative preference of Sr and LREE for carbonate melt vs silicate melt is the same in carbonate vapor, then high Sr/LREE ratios would also be expected in a carbonate vapor in equilibrium with a silicate solid. The enrichment of Sr vs LREE in carbonate fluids is consistent with the composition of carbonatites, which have high Sr/La ratios (140, Allegre et al., 1971; 170, Ridley and Dawson, 1975).

Both partial melting and H_2O or CO_2 fluid paritioning processes for producing a high Sr/La derivative from subducted MORB are speculative and unverifiable with available partitioning data. However, a high Sr/La

component derived from MORB and sediment endmembers provides the best fit to the mixing endmembers inferred from the data for Manam lavas. An alternative, lower crustal contamination, also requires unusual partial melting processes to explain high Sr/La ratios in arc magmas, but they are in this case less likely, because of the high plagioclase content of lower crustal rocks, and evidence that continental basalts, which must pass through continental crust, are not Sr-enriched. Therefore, a MORB-sediment mixture is preferred to explain the enrichment of K, Rb, Ba, Sr and Pb relative to REE in Manam lavas. Although contamination of arc magmas by crustal material probably occurs, the restriction of enrichment in these elements to island arcs supports a subduction related source for these elements.

Ti, Sc, V AND HREE ABUNDANCES IN MANAM LAVAS: EVIDENCE FOR A DEPLETED PERIDOTITE SOURCE

In Fig. 5.4, Ti/Sc and Ti/V ratios in Manam lavas were shown to be less than chondritic, and in MgO-rich samples similar to those in boninites. Low Ti/Sc and Ti/V ratios in primitive volcanic rocks imply a depleted peridotite source, because Ti is less compatible than Sc and V in common peridotite minerals such as olivine, pyroxenes, garnet and amphibole (Irving, 1978; Gill, 1978; Pearce and Norry, 1979; Le Roex, 1980). For the Manam lavas, which contain clinopyroxene and magnetite, the low ratios could also result from accumulation of these minerals in a parental magma with higher than chondritic Ti/V and Ti/Sc ratios. Since a clinopyroxene accumulation trend is not indicated in Fig. 5.2a, the low Ti/V and Ti/Sc ratios in MgO-rich lavas are probably characteristic of their parental liquid, and indicate a refractory peridotite source.

Ratios of V/Sc, Zr/Ti, Yb/Sc and La/Yb in Manam lavas increase with decreasing MgO content (Fig. 5.5), probably as the result of clinopyroxene and magnetite removal. Since the lavas have variable $^{143}Nd/^{144}Nd$ ratios which correlate with La/Nd, it is possible that ratios such as La/Yb and Zr/Ti were also variable in their parental magmas. The covariation of these ratios with the MgO content of the lavas indicates that fractional crystallization is the dominant process affecting these ratios, and that any preexisting variation with $^{143}Nd/^{144}Nd$, if present, has been destroyed.

In Table 5.5 the results of fractional crystallization calculations are summarized for a high and low MgO Manam sample with similar $^{143}Nd/^{144}Nd$. Relative and absolute concentrations of Ti, Sc, V, Zr, Yb and La in the low MgO lavas can be produced from the high MgO lava by 53% fractional crystallization of olivine $\pm$ plagioclase, clinopyroxene, and magnetite in the proportions 47:49:3.8 or 70:26:3.8 using higher partition coefficients for clinopyroxene (Table 5.5). Mineral vectors showing the effect of clinopyroxene and magnetite fractional crystallization on Ti/V, Ti/Sc and V/Sc ratios are shown in Fig. 5.4.

The results indicate that although Ti/Sc, Ti/V and Ti contents in primitive Manam magmas were low, significant amounts of Ti were also removed in magnetite during fractional crystallization, producing the high Zr/Ti ratios in differentiated samples. Based on the calculations, primitive liquids for the Manam lavas can be inferred to have lower than chondritic Yb/Sc ratios and lower V/Sc ratios than MORB's and komatiites (Table 5.5; Figure 3.4). For a peridotite mineralogy, low values of these ratios, and low values of Y/Yb and Y/Sc in the lavas themselves, indicate

TABLE 5.5: FRACTIONAL CRYSTALLIZATION CALCULATIONS FOR MANAM LAVAS

	Chondrites	Manam #6 8.6% MgO	- 53%: (Ol + Plag) 49 Cpx 47.2 Mt 3.8 Ewart K_d Cpx(1)	- 53%: (Ol + Plag) 69.8 Cpx 26.4 Mt 3.8 LeRoex K_d Cpx(2)	Manam #7 6.4% MgO
V		280	294	311	320
Sc		42.7	32.3	32.3	34.7
Ti		1920	2938	2957	2950
Zr		21	43	43	43
Yb		1.10	1.76	1.84	1.79
La		3.44	7.33	7.33	7.31
V/Sc	9.4	6.6	9.1	9.6	9.2
Yb/Sc	0.027	0.026	0.054	0.057	0.052
Zr/Ti	0.009	0.011	0.015	0.015	0.015
La/Yb	1.5	3.1	4.2	4.0	4.1

Partition Coefficients:

	Cpx(1)	Cpx(2)	Mt(3)
V	1.1	1.7	11
Sc	2.8	5.0	1.3
Ti	0.3	0.51	7.7
Zr	0.1	0.22	0.2
Yb	0.8	1.2	0.2
La	0	0	0

TABLE 5.5 CONT'D: FRACTIONAL CRYSALLIZATION CALCULATIONS FOR MANAM LAVAS

(1) V, Sc and Ti partition coefficients are phenocryst matrix values for basalts from Tonga from Ewart et al. (1973). The Zr partition coefficient is from Pearce and Norry (1978) and is within the range (0.06 - 0.22) reported by Dunn and McCallum (1982). This value was chosen to match the relative values of Zr and Ti partition coefficients given by LeRoex (1980) (see below). Dunn and McCallum (1982) report an increase in Zr partition coefficient with increasing Al_2O_3 content in clinopyroxene. This was interpreted as a charge balance effect by Dunn and McCallum (1982), therefore Ti should be influenced similarly. This is qualitatively consistent with relative values for Ti partition coefficients reported by Ewart et al. (1973) (2% Al_2O_3 in cpx) and LeRoex (1980) (4-5% Al_2O_3 in cpx). The Yb partition coefficient is the preferred value from Gill (1978).

(2) V, Sc, Ti and Zr partition coefficients are phenocryst matrix values for alkalic basalts from LeRoex (1980), and were tried because Ti and Zr partition coefficients were determined on the same minerals. The Yb partition coefficient is estimated from the value for Y given by LeRoex (1980) (0.7), the Y value given by Pearce and Norry (1978) and the Yb value given by Gill (1978).

(3) Sc and Ti partition coefficients are from Ewart et al. (1973). Using the V partition coefficient measured by Ewart et al. (1973) (24) variations in Ti, Sc and V abundances in the lavas cannot be modelled. A lower value from Leeman et al. (1978) was substituted and may be justified by the high Fe_2O_3/FeO ratios (~1.0), hence higher fO_2 in the Manam lavas compared to the Tongan lavas (Fe_2O_3/FeO = 0.4). Zr and Yb (estimated from Y) partition coefficients are from LeRoex (1980).

depletion in the less compatible elements and support a refractory peridotite source for the lavas. Zr/Ti ratios in the most MgO-rich Manam samples (Table 5.5) are slightly higher than chondritic, and are not consistent with an incompatible element depleted peridotite source. Therefore Zr-enrichment relative to Ti may have accompanied enrichment in LREE in the Manam lavas, as proposed earlier for boninites and Facpi Formation lavas (Chapters 3 and 4).

SOURCES FOR LREE IN MANAM LAVAS

The enrichment of LREE in Manam lavas, in addition to enrichment in K, Rb, Ba, Sr and Pb, is not consistent with a depleted peridotite source. Although the $^{143}Nd/^{144}Nd$ ratios of the lavas require a source with a time-integrated LREE depletion, i.e., $(Sm/Nd)_{e.f.} < 1$, the covariation of La/Nd with $^{143}Nd/^{144}Nd$ indicates that the LREE-enrichment is not a result of partial melting or fractional crystallization processes, but reflects the introduction of a LREE-enriched material into a LREE-depleted source. If this mixing or metasomatic process involved isotopically identical materials, the trend formed by the Manam lavas in Fig. 5.11 would have time significance. Measured Sm/Nd ratios in the Manam lava do not correlate with $^{143}Nd/^{144}Nd$. Since La/Nd ratios correlate with $^{143}Nd/^{144}Nd$ this is most likely due to a combination of fractional crystallization effects and the high analytical error in the Sm/Nd ratio (Appendix II) relative to its variation. Therefore, a possible age of metasomatism cannot be determined exactly. On the plot of La/Nd vs $^{143}Nd/^{144}Nd$ (Fig. 5.11) the trend formed by the Manam samples has an intermediate slope compared to boninites from the Bonin Islands and Cape Vogel. An intermediate age of 0.4 to 1.7

b.y.b.p. can be estimated roughly by this comparison, but is older than any tectonic reconstruction of northern Papua.

At the other extreme, the trend of La/Nd vs $^{143}Nd/^{144}Nd$ could be produced by recent mixing of materials with different La/Nd and $^{143}Nd/^{144}Nd$ ratios, i.e., one endmember with high $^{143}Nd/^{144}Nd$ and low La/Nd, and one endmember with low $^{143}Nd/^{144}Nd$ and high La/Nd (Fig. 5.11). For boninites, similar correlations between decreasing $^{143}Nd/^{144}Nd$ and increasing LREE enrichment were interpreted as reflecting recent mixing of a LREE-depleted peridotite with high $^{143}Nd/^{144}Nd$, and a LREE-enriched mantle derived fluid or melt with low $^{143}Nd/^{144}Nd$. Since a depleted peridotite source is also indicated for the Manam lavas, because of their low Ti/Sc and Ti/V ratios, a LREE-depleted peridotite with high $^{143}Nd/^{144}Nd$ is also a possible endmember for the source of the Manam lavas. At low La/Nd ratios like those in depleted peridotites (e.g., ~0.2 in harzburgites from Ronda, Frey and Suen, 1982), a $^{143}Nd/^{144}Nd$ value of ~0.5133 is indicated for the LREE-depleted endmember for Manam lavas (Fig. 5.11). This value is higher than values measured in most modern MORB's, but is consistent with a residual peridotite from earlier MORB generation, which has evolved a higher $^{143}Nd/^{144}Nd$ since the depletion event due to its higher Sm/Nd (Fig. 5.15a). Alternatively, the LREE-depleted endmember of the Manam lavas could be a peridotite with lower $^{143}Nd/^{144}Nd$, which has previously undergone an episode of LREE enrichment, as suggested for boninites from the Bonin Islands (Chapter 3).

One possible model for the source of the Manam lavas can be outlined: (Figs. 5.15a and 5.16a) metasomatism of a LREE-depleted peridotite residue from MORB generation by a LREE-enriched mantle derived fluid or melt with

low $^{143}Nd/^{144}Nd$, followed by addition of K, Rb, Ba, Sr and Pb from subducted MORB and sediment with insignificant addition of REE or HFS elements. This model is essentially identical to the model proposed for boninites, and readily explains the decoupling of K, Rb, Ba, Sr and Pb abundances and Sr and Pb isotopic composition from REE and HFS element abundances and Nd isotopic composition in the Manam lavas.

Independent of the boninite model, an interpretation which could be proposed to explain the correlation of $^{143}Nd/^{144}Nd$ and La/Nd in Manam lavas is that it simply represents mixing between subducted MORB (low La/Nd, high $^{143}Nd/^{144}Nd$, Fig. 5.15b) and subducted sediment (high La/Nd, low $^{143}Nd/^{144}Nd$, Fig. 5.15b), because these components have earlier been identified as probable sources for K, Rb, Ba, Sr and Pb in the lavas. In this case, the incompatible trace element abundances and Sr, Nd and Pb isotopic ratios of the lavas would represent a two-component mixture of derivatives from subducted MORB and sediment, superimposed on an incompatible element depleted peridotite source. The isotopic and incompatible element signature of the depleted peridotite could be swamped by the presence of the other two components.

Such a two-component mixing model is not feasible for the Manam lavas, because it does not account for the decoupling of $^{143}Nd/^{144}Nd$ ratios and LREE abundances from $^{87}Sr/^{86}Sr$ ratios and K, Rb, Ba, Sr and Pb abundances. Low $^{143}Nd/^{144}Nd$ samples, with a large sediment derivative contribution, would be expected to have high Ba/Sr, Ba/Rb and Ba/K ratios and high $^{87}Sr/^{86}Sr$ ratios, which is not true (Tables 5.2 and 5.3). In addition, it can be demonstrated that this mixture would not plot within the oceanic mantle array as in Fig. 5.9. If only two components are responsible

FIGURE 5.15: Possible explanations for the La/Nd vs $^{143}Nd/^{144}Nd$ correlation in Manam lavas:

a) The source of the lavas is formed by mixing of a LREE-depleted, MORB-residue peridotite and a LREE-enriched mantle derived fluid or melt with low $^{143}Nd/^{144}Nd$.

b) Two - component mixing between LREE-enriched derivatives from subducted MORB and sediment.

c) Four component mixing: 1) metasomatism of depleted peridotite by a LREE-enriched, low $^{143}Nd/^{144}Nd$ mantle derived fluid or melt, 2) mixing of the metasomatized mantle peridotite with a mixture derived from subducted MORB and sediment with low La/Nd and high $^{143}Nd/^{144}Nd$.

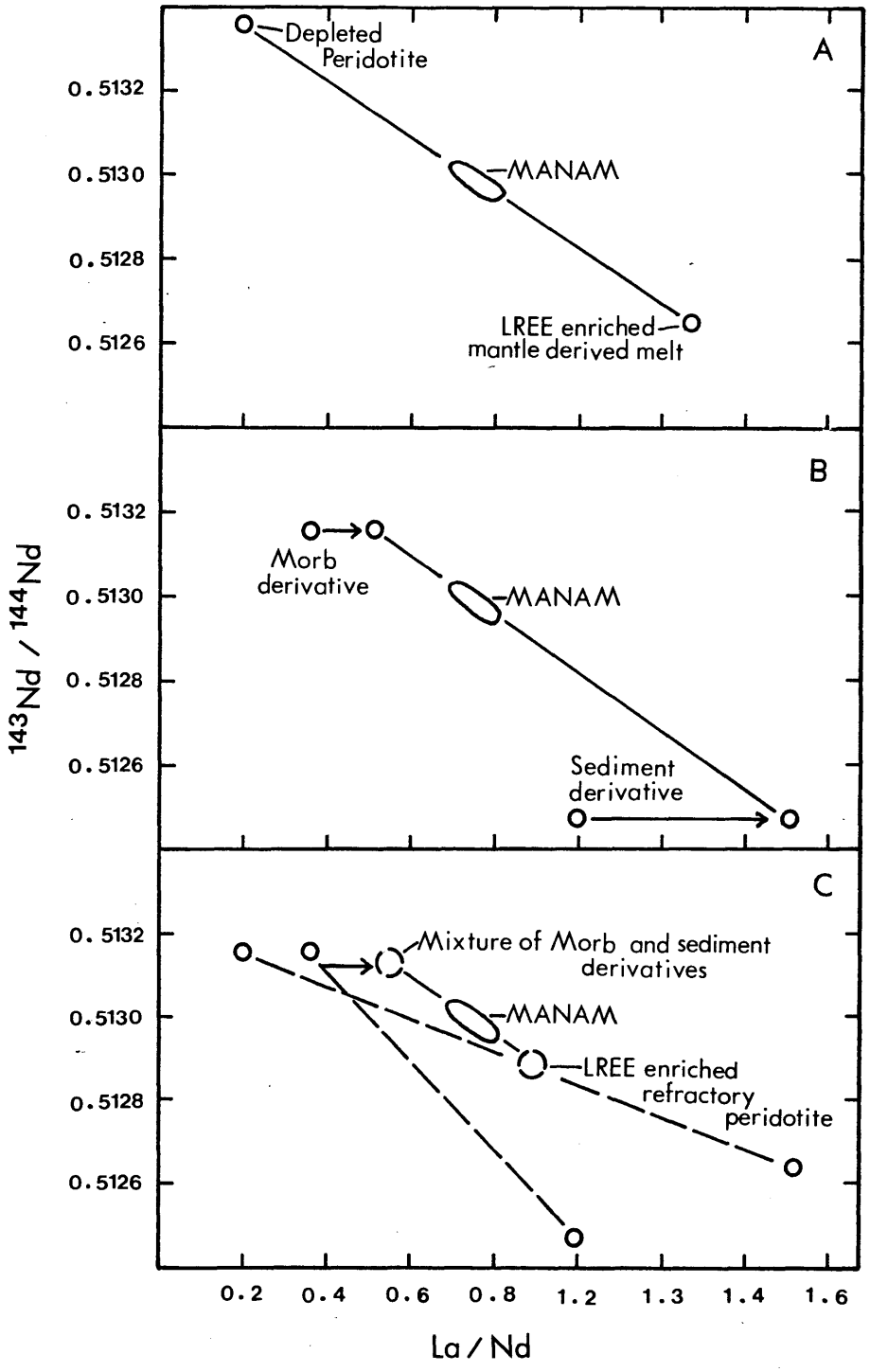
A
Depleted Peridotite
MANAM
LREE enriched mantle derived melt
B
Morb derivative
MANAM
Sediment derivative
C
Mixture of Morb and sediment derivatives
MANAM
LREE enriched refractory peridotite
0.5132
0.5130
0.5128
0.5126
143Nd / 144Nd
0.2
0.4
0.6
0.8
1.2
1.3
1.4
1.6
La / Nd

FIGURE 5.16: Sr - Nd isotope correlation diagrams showing:

a) Mixing of a LREE-depleted, MORB-residue peridotite with a LREE-enriched, mantle derived fluid or melt with low $^{143}Nd/^{144}Nd$ to produce the La/Nd vs $^{143}Nd/^{144}Nd$ correlation in Manam lavas, followed by addition of a material derived from subducted MORB and sediment which is virtually devoid of REE, similar to the model proposed for boninites (Fig. 3.16). $^{143}Nd/^{144}Nd$ ratios in the peridotite are not changed by addition of material from the subducted oceanic crust.

b) The composition of possible two component mixtures derived from MORB and sediment endmembers. The Sr/Nd in the MORB component is 45. For curve (1), the Sr/Nd for the sediment component is 600. These values are estimated from Figs. 5.10, 5.11 and 5.13c. For curve (2), the Sr/Nd ratio for the sediment component is 150 (slightly greater than those in the lavas).

c) Four component mixing model for Manam lavas. LREE-metasomatized mantle peridotite (Fig. 5.15c) mixes with a high Sr/Nd, high $^{143}Nd/^{144}Nd$ mixture derived from subducted MORB and sediment. Variation in $^{87}Sr/^{86}Sr$ is porduced by MORB - sediment mixing. Variation in $^{143}Nd/^{144}Nd$ is produced by mixing of the LREE-metasomatized peridotite with the MORB - sediment mixture. The mixing lines are curved because of the high Sr/Nd ratios in the MORB - sediment mixture.

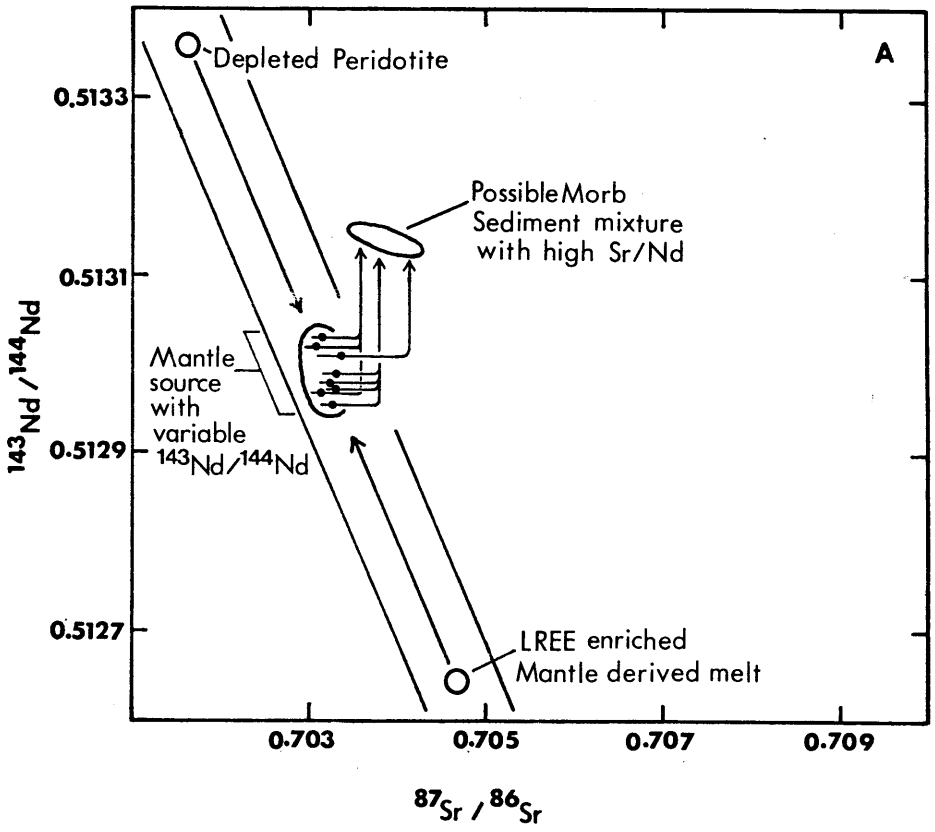
A
Depleted Peridotite
Possible Morb
Sediment mixture
with high Sr/Nd
Mantle
source
with
variable
143Nd/144Nd
LREE enriched
Mantle derived melt
0.5133
0.5131
0.5129
0.5127
143Nd / 144Nd
0.703
0.705
0.707
0.709
87Sr / 86Sr

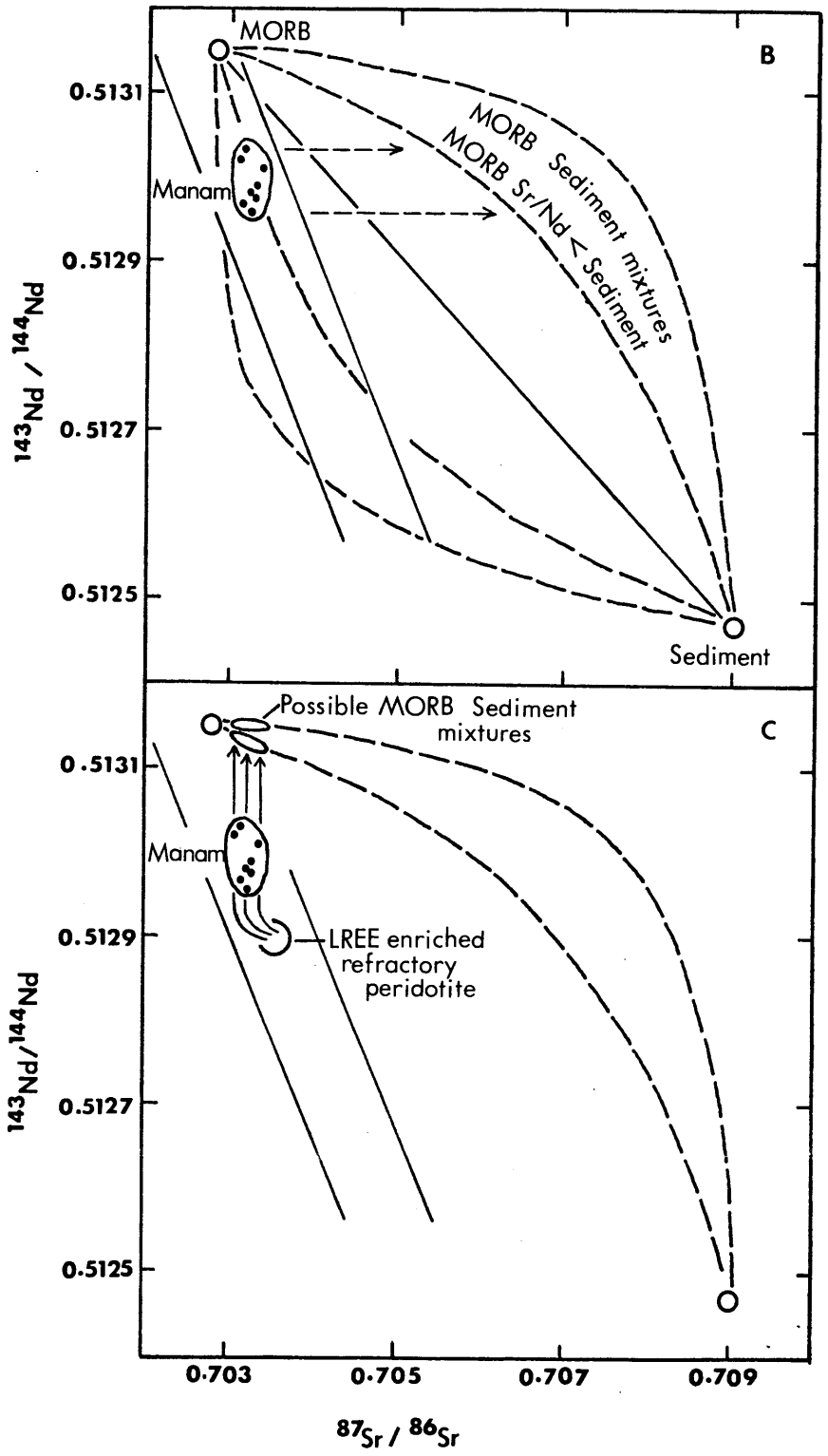
MORB
B
0.5131
0.5129
0.5127
0.5125
Manam
MORB Sediment mixtures
MORB Sr/Nd < Sediment
Sediment
Possible MORB Sediment mixtures
C
0.5131
0.5129
0.5127
0.5125
Manam
LREE enriched refractory peridotite
143Nd / 144Nd
143Nd/144Nd
0.703
0.705
0.707
0.709
87Sr / 86Sr

for the relative Sr, Ba and LREE abundances of the Manam lavas, then the relative Sr/Nd ratios of these components can be estimated from Figs. 5.10, 5.11 and 5.13c. The MORB component (at $^{87}Sr/^{86}Sr$ = 0.7028) has low Sr/La (Fig. 5.13c), low La/Nd (Fig. 5.11) and an estimated Sr/Nd ratios of 45. The sediment component (at $^{87}Sr/^{86}Sr$ = 0.7090) has high Ba/La (Fig. 5.10), high Sr/La (Fig. 5.13c), high La/Nd (Fig. 5.11) and an estimated Sr/Nd of 600. Although these values are only estimates, it is clear from Figs. 5.13c and 5.11, that the MORB component must have lower Sr/Nd than the sediment component. Mixing lines drawn from MORB to sediments on a Sr - Nd isotope correlation diagram will therefore be curved away from the mantle array, the magnitude of the curvature depending on the difference between the two ratios, and they do not pass through the $^{87}Sr/^{86}Sr$ and $^{143}Nd/^{144}Nd$ values for the Manam lavas (Fig. 5.16b).

Although a two-component MORB-sediment mixing model is inappropriate for the Manam lavas, it is possible that a mixture of the MORB and sediment components proposed to account for the Sr and Pb isotopic characteristics and K, Rb, Ba, Sr and Pb abundances of the lavas is <u>one</u> endmember for mixing of high $^{143}Nd/^{144}Nd$, low La/Nd and low $^{143}Nd/^{144}Nd$, high La/Nd materials. For example, the Sr-isotopic composition of the Manam lavas is dominated by a MORB-sediment mixture in which the MORB component is most abundant (i.e., relatively low $^{87}Sr/^{86}Sr$ in the lavas). In Fig. 5.16b, the $^{143}Nd/^{144}Nd$ of a MORB - sediment mixture at 0.70313 - 0.70338 (the range of $^{87}Sr/^{86}Sr$ in the Manam lavas), is higher than that in the lavas, and is relatively constant. The La/Nd of this mixture can not be predicted since the La/Nd of the two endmembers is unknown. However, the La/Nd ratios indicated for the high $^{143}Nd/^{144}Nd$ endmember (Fig. 5.15c) are

consistent with a mixture of LREE-enriched derivatives from MORB and sediment, dominated by the MORB endmember. In this case, the MORB-sediment mixture could be the low La/Nd, high $^{143}Nd/^{144}Nd$ endmember, while the high La/Nd, low $^{143}Nd/^{144}Nd$ endmember is a refractory, LREE-metasomatized mantle peridotite (Fig. 5.15c).

The MORB-sediment mixing lines drawn in Fig. 5.16b are based on the assumption that Fig. 5.13c depicts two component mixing, and that the MORB endmember has lower Sr/Nd than the sediment endmember. Since two component mixing has been ruled out, it is equally possible that the MORB endmember has higher Sr/Nd than the sediment endmember. In this case, in Fig. 5.16b, MORB component - sediment component mixing lines could curve toward the mantle array, and at $^{87}Sr/^{86}Sr$ = 0.70313 to 0.70338 such mixtures could have lower $^{143}Nd/^{144}Nd$ than the Manam lavas. A MORB-sediment mixture therefore could also be the high La/Nd, low $^{143}Nd/^{144}Nd$ endmember for Manam lavas, and a refractory peridotite could be the low La/Nd, high $^{143}Nd/^{144}Nd$ endmember. However, as can be seen in Fig. 5.16b, MORB component - sediment component mixtures in which the MORB endmember has higher Sr/Nd have large variations in $^{143}Nd/^{144}Nd$ within a small range of $^{87}Sr/^{86}Sr$ values. These mixtures probably could not appear as a single endmember, with relatively homogeneous La/Nd and $^{143}Nd/^{144}Nd$ ratios, as required by the relatively linear correlation of La/Nd and $^{143}Nd/^{144}Nd$ in the Manam lavas (Fig. 5.11) and still account for their variation in $^{87}Sr/^{86}Sr$.

A second possible model for the source of the Manam lavas can be described (Figs. 5.15c and 5.16c): 1) LREE metasomatism of an incompatible element depleted mantle peridotite by a mantle-derived LREE-enriched, low

$^{143}Nd/^{144}Nd$ fluid or melt, and 2) metasomatism of this source, or mixing of a partial melt derived from this source, with K, Rb, Ba, Sr and Pb enriched partial melts or fluids derived from subducted MORB and sediment which have higher $^{143}Nd/^{144}Nd$ and lower La/Nd ratios (i.e., are dominated by the MORB endmember) than the depleted peridotite plus LREE-enriched mantle metasomatic component.

Both models outlined above for the sources of Manam lavas can explain the decoupling of Sr and Nd isotopic systematics in the lavas, and their trace element characteristics. In model 1), endmembers for LREE are a LREE-depleted peridotite with high $^{143}Nd/^{144}Nd$, and a LREE-enriched mantle derived fluid or melt with low $^{143}Nd/^{144}Nd$, and endmembers for K, Rb, Ba, Sr and Pb are materials with very high abundances of these elements relative to REE and HFS elements derived from subducted MORB and sediments. In model 2), endmembers for K, Rb, Ba, Sr and Pb are the same as in model 1). However, endmembers for REE are a refractory, LREE-metasomatized mantle peridotite with high La/Nd and low $^{143}Nd/^{144}Nd$, and the mixture of MORB and sediment derived materials proposed to explain the Sr and Pb isotopic characteristics and K, Rb, Ba, Sr and Pb abundances of the lavas. In this model, endmembers for LREE are each actually mixtures of two materials.

COMPARISON OF MIXING MODELS 1) AND 2) FOR MANAM LAVAS

The two mixing models outlined above for lavas from Manam Island have advantanges and disadvantages which are discussed in this section. Although both models predict decoupling of K, Rb, Ba, Sr and Pb abundances and Sr and Pb isotopic composition from REE and HFS element abundances and Nd isotopic composition, the extent of this decoupling is different in the two models. For example, in model 1), a ratio such as Ba/La could increase either with increasing addition of the MORB-derived component, the sediment derived component or both components to the peridotite source of the lavas. According to this model, it is possible for a lava to have very low $^{87}Sr/^{86}Sr$ (high MORB endmember relative to sediment endmember contribution) and extremely high Ba/La (high total MORB plus sediment component contribution relative to mantle peridotite contribution). As shown in Fig. 5.10, Manam samples with low $^{87}Sr/^{86}Sr$ have low Ba/La and Ba/La increases with increasing $^{87}Sr/^{86}Sr$. This relationship can be explained if the sediment endmember has higher absolute Ba and Sr abundances than the MORB endmember, as discussed earlier in reference to Fig. 5.13c, and if the mantle peridotite and MORB plus sediment components of the Manam lava source mix in similar amounts. However, model 1) does not necessarily predict that $^{87}Sr/^{86}Sr$ should increase with Ba/La.

In model 2), Ba/La ratios also can increase with increasing addition of either the MORB or sediment derived components or both. However, since a mixture of the MORB and sediment components is one mixing endmember for LREE, Ba/La ratios in the lavas must lie between the Ba/La ratios of these components and that in the LREE-metasomatized peridotite source. According to this model, samples with the highest $^{143}Nd/^{144}Nd$ (highest MORB plus sediment endmember relative to LREE-metasomatized peridotite endmember

contribution) and the highest $^{87}Sr/^{86}Sr$ (highest sediment relative to MORB endmember contribution) should have the highest Ba/La, while samples with the lowest $^{143}Nd/^{144}Nd$ (smallest MORB plus sediment endmember relative to LREE-metasomatized peridotite endmember contribution) and the lowest $^{87}Sr/^{87}Sr$ (largest contribution of MORB endmember relative to sediment endmember) should have the lowest Ba/La. Samples with $^{143}Nd/^{144}Nd$ or $^{87}Sr/^{86}Sr$ between these extremes should have intermediate Ba/La. As shown in Fig. 5.10 and Table 5.2, this is true for the Manam lavas, i.e., sample 7, with low $^{87}Sr/^{86}Sr$ and low $^{143}Nd/^{144}Nd$ has the lowest Ba/La, and sample 3, with high $^{87}Sr/^{86}Sr$ and high $^{143}Nd/^{144}Nd$ has the highest Ba/La. However, two Manam samples with low $^{87}Sr/^{86}Sr$ and high $^{143}Nd/^{144}Nd$ (samples 1 and 2, Tables 5.2 and 5.3) also have low Ba/La like sample 7 (Fig. 5.13c). The similar Ba/La of these samples is not consistent with model 2) (e.g., Fig. 5.16c), but is consistent with model 1) with the restrictions that the sediment mixing component must have higher absolute Ba and Sr abundances than the MORB component, and that the mantle peridotite and MORB plus sediment components mix in similar amounts.

Model 1) also has an advantage over model 2) in that each mixing endmember is a single material, and each pair of endmembers is virtually devoid of the elements involved in mixing of the other pair. Such a scheme can easily explain the decoupling of K, Rb, Ba, Sr and Pb abundances from REE and HFS element abundances, as well as the well defined correlations which occur within each element group, e.g., Ba/Sr vs $^{87}Sr/^{86}Sr$ (Fig. 5.13b) and La/Nd vs $^{143}Nd/^{144}Nd$ (Fig. 5.11). In model 2) mixing endmembers for LREE are mixtures, therefore the feasibility of this model depends strongly on the homogeneity of these mixtures in relative LREE abundances and $^{143}Nd/^{144}Nd$. For the LREE-depleted endmember (MORB plus sediment

mixture), Fig. 5.16b shows that this mixture could be homogenous in $^{143}Nd/^{144}Nd$ because it is dominated by the MORB component. However, for the LREE-enriched endmember (LREE-depleted peridotite plus LREE-enriched metasomatic material), there is no reason to believe that such a mixture would be homogeneous. In fact, if the Sm/Nd vs $^{143}Nd/^{144}Nd$ correlations in boninites reflect mixing between depleted peridotite and LREE-enriched metasomatic materials, this would suggest that mantle metasomatism does not result in LREE homogeneity. This is also true of suites of refractory, LREE-metasomatized peridotite nodules, which often show variation in relative LREE-enrichment and/or $^{143}Nd/^{144}Nd$ (e.g., peridotites from Victoria, Australia, Frey and Green, 1974; Chen and Frey, 1981). Therefore, for model 2), a triangular field of $^{143}Nd/^{144}Nd$ and La/Nd values for the Manam lavas or no correlation at all might be expected rather than a linear trend in Fig. 5.11.

A third consideration in evaluating the two models is the effect of addition of different materials on the moderately incompatible element abundances of a depleted peridotite. Like boninites, the Manam lavas have relative HREE, Ti, Y, Sc and V abundances which indicate derivation from a depleted peridotite. In model 1), the preservation of these features in the lavas requires that the LREE-enriched mantle derived metasomatic melts or fluids have very low abundances of HREE, Ti, Y, Sc and V relative to LREE. Since the MORB and sediment endmembers in model 1) are considered to be virtually devoid of LREE, it is reasonable to assume that they would also have low abundances of more compatible elements such as HREE, Ti, Y, Sc and V. In model 2), both the LREE-enriched mantle derived metasomatic component and the MORB and sediment components must have low abundances of

HREE, Ti, Y, Sc and V relative to LREE, in order for the trace element characteristics of a depleted peridotite to be evident in the Manam lavas. For the MORB and sediment components, which form the low La/Nd endmember for mixing of LREE, this requires a materials with high La/Yb (>10 x chondrites), but relatively low La/Nd (<1.5 x chondrites, Fig. 5.11). A melt with these characteristics could be produced by partial melting of a chondritic or LREE-depleted material, with residual garnet retaining HREE, Ti, Y, Sc and V relative to LREE. This is consistent with partial melting of subducted MORB in the eclogite facies, and therefore is feasible within the model. However, that two materials in model 2), the LREE-enriched mantle metasomatic component and the subducted oceanic crustal component, must be added to a depleted peridotite source for the Manam lavas without significantly changing its relative abundances of HREE, Ti, Y, Sc and V is an additional complexity in model 2) compared to model 1).

Based on the considerations discussed above, model 1) is preferred over model 2) for the source of the Manam lavas.

COMPARISON WITH THE KAY (1980) MODEL FOR ARC VOLCANISM

The geochemical model outlined for lavas from Manam Island involves materials which have been traditionally considered as potential sources for island arc volcanics: oceanic mantle, subducted MORB and subducted sediment. In many respects it is similar to the general model of Kay (1980) for island arc volcanics. In Kay's model high Ba/La in arc volcanics resulted from a sedimentary component, high La/Sm from a partial melt derived from eclogite (subducted MORB) or garnet peridotite (oceanic mantle), and low HREE and HFS element abundances from a refractory peridotite source.

In the model proposed here, the low HREE and HFS element abundances, but relative LREE enrichment of Manam lavas also results from the mixing of a refractory peridotite with a LREE-enriched partial melt or fluid derived from the oceanic mantle. High Ba/La ratios are produced by a high Ba/La component derived from both subducted MORB and sediment. The advantage of this model is that it can explain high Ba/La ratios in arc volcanics which do not have radiogenic Sr or Pb isotopic compositions.

The critical feature of this model is the presence of a high Sr/La, Ba/La and Pb/La component derived from subducted MORB. As discussed earlier, this could be accomplished by partial melting of subducted MORB if an accessory mineral with high REE partition coefficients but low Sr partition coefficients was a residual phase, or by extaction of a H_2O and/or CO_2-rich fluid for which Sr, Ba and Pb had a greater preference than REE. Neither of these processes can be tested with the existing partitioning data. However, other potential sources for enrichment in these elements, such as lower crust, also require unverifiable partial melting processes to match the high Sr/La, Rb/La and K/La in island arc volcanics, and can be demonstrated not to occur during the interaction of continental magmas and lower continental crust.

Table 5.6 shows a calculation estimating the proportions of sediment and MORB Sr and Pb required to explain the Sr and Pb isotopic composition of the Manam lava (sample 3, Tables 5.2 and 5.3) with the highest apparent sediment contribution. In this calculation Sr and Pb in excess of that corresponding to Sr/Nd and Pb/Nd ratios for oceanic island basalts (e.g., Sr/Nd = 20, and Pb/Nd = 0.15, Table 5.6) is assumed to be derived from the MORB and sediment component, and the Pb and Sr isotopic composition of the samples is assumed to be dominated by this mixture (row 2, Table 5.6).

According to this calculation, 82% of the Sr in the Manam lavas is derived from MORB and sediment in the ratio 60:1, and 91% of the Pb in the ratio 110:1. The disparity between the two MORB - sediment proportions can be decreased if a higher $^{87}Sr/^{86}Sr$ or a lower $^{207}Pb/^{204}Pb$ is used for the MORB or the sediment endmember. The range of proportions estimated is 2 to 4 times higher than an estimate of the presubduction composition of the oceanic crust (30:1, Nohda and Wasserburg, 1981). Therefore, this model is feasible if the oceanic crust subducted under Manam had a small sediment component or if some sediments were not subducted.

TABLE 5.6: ESTIMATION OF A MORB - SEDIMENT RATIO FOR THE MANAM LAVA WITH HIGHEST $^{87}Sr/^{86}Sr$ and $^{207}Pb/^{204}Pb$

	Sr ppm	Pb ppm	$^{87}Sr/^{86}Sr$	$^{207}Pb/^{204}Pb$
Manam - 3:	506	8	0.7034	15.535
Manam - 3 minus mantle component(1):	411 (82%)	7.3 (91%)	0.7034	15.535
Oceanic sediment:	980(2)	37.5(2)	0.7090(3)	15.65(3)
MORB:	140(2)	0.75(2)	0.7028(3)	15.48(3)

	% Element from MORB	% Element from Sediment	MORB : Sediment by weight
Sr:	90	10	60:1
Pb:	68	32	110:1

(1) The mantle component has Sr and Pb concentrations corresponding to Sr/Nd and Pb/Nd ratios in oceanic island volcanics, i.e., Sr/Nd = 20 and Pb/Nd = 0.15 (for Hawaiian alkali basalts, Clague and Frey, 1982).

(2) Concentrations from Kay (1980).

(3) Endmember isotopic compositions estimated from Figs. 5.12 and 5.13. $^{87}Sr/^{86}Sr$ for seawater is used for sediment.

SUMMARY AND CONCLUSIONS

Low TiO_2 lavas from Manam Island have among the highest enrichments in K, Rb, Ba, Sr and Pb relative to REE and HFS elements found in island arcs, but have $^{87}Sr/^{86}Sr$, $^{143}Nd/^{144}Nd$, $^{206}Pb/^{204}Pb$ and $^{207}Pb/^{204}Pb$ ratios which are similar to those in oceanic volcanic rocks. $^{87}Sr/^{86}Sr$ ratios and $^{207}Pb/^{204}Pb$ ratios increase with increasing Ba/La, Sr/La and Ba/Sr, and suggest that the enrichment in these elements involves two high Sr/La materials. Relative K, Rb, Ba, Sr and Pb abundances and Sr and Pb isotopic compositions of these materials are consistent with components derived from subducted MORB and subducted sediments.

$^{143}Nd/^{144}Nd$ ratios in Manam lavas decrease with increasing La/Nd, but do not covary with $^{87}Sr/^{86}Sr$, or trace element ratios involving K, Rb, Ba, Sr or Pb. The lavas have less than chondritic ratios of Ti/Sc, Ti/V, Ti/Y and Y/Yb. Based on these features, an incompatible element depleted mantle peridotite also contributed to the source for the Manam lavas. This peridotite was enriched in LREE by a mantle derived partial melt or fluid, and enriched in K, Rb, Ba, Sr and Pb by melts or fluids derived from subducted MORB and sediment with high abundances of these elements compared to REE.

The isotopic similarity of Manam lavas to oceanic rocks, in spite of their enrichment in K, Rb, Ba, Sr and Pb relative to REE and HFS elements as compared to oceanic rocks, is explained by the incorporation of a high Sr/La and Pb/La material derived mainly from subducted MORB. This model is preferred to models for arc volcanism in which enrichment in K, Rb and Ba, and non-radiogenic Sr and Pb results from the interaction of mantle derived magma with lower crust, because most continental basalts and lower crustal granulites do not have high K, Rb and Sr abundances relative to REE.

CHAPTER 6: GEOCHEMICAL CHARACTERISTICS OF LOW TiO_2 OPHIOLITIC BASALTS: COMPARISON WITH BONINITES AND OTHER LOW TiO_2 ARC VOLCANICS

Low TiO_2 lavas from the Troodos Ophiolite and Arakapas Fault Belt, Cyprus, and the Betts Cove Ophiolite, Newfoundland, have been associated with boninites by the low TiO_2 contents, high Al_2O_3/TiO_2 and CaO/TiO_2 ratios (Sun and Nesbitt, 1978a), igneous petrographic features when preserved (Cameron et al., 1979), and the high Cr/(Cr + Al) ratios of their spinels (Cameron et al., 1979). As discussed in Chapter 2, only low TiO_2 lavas from the Arakapas Fault Belt have major element compositions which overlap those of boninites on the projection quartz - olivine - plagioclase (Fig. 2.3b). The other low TiO_2 ophiolitic lavas are similar compositionally to low TiO_2 island arc volcanics which are not boninites. Because these low TiO_2 ophiolitic basalts have some major element and petrographic features in common with boninites or other low TiO_2 island arc volcanics, their trace element characteristics may be useful in testing the geochemical models proposed for boninites and low TiO_2 arc volcanics in earlier chapters. In addition, since the tectonic environment of these ophiolites is a matter of controversy, evidence for a similar origin for these lavas and low TiO_2 island arc volcanics from the areas discussed earlier may also help to constrain the tectonic environment of the ophiolites.

LOW TiO_2 LAVAS FROM THE TROODOS OPHIOLITE AND ARAKAPAS FAULT BELT, CYPRUS

Extremely low TiO_2 lavas occur in two areas on Cyprus: the Troodos Ophiolite and the Arakapas Fault Belt (Smewing et al., 1975; Simonian and Gass, 1978). Lavas from the Troodos Ophiolite have been divided into two

groups: the stratigraphically lower Axis Sequence lavas, composed of strongly metamorphosed volcanics usually having normal TiO_2 contents (e.g., >0.8% TiO_2 in MgO rich lavas, Smewing and Potts, 1976), and the less strongly metamorphosed Upper Pillow Lavas, which typically have low TiO_2 contents (e.g., 0.3% TiO_2 in MgO rich lavas, Smewing and Potts, 1976). In order to explain the metamorphic and igneous characteristics of the Troodos lavas, Smewing et al. (1975) suggested that the Axis Sequence lavas were erupted and subsequently metamorphosed at high temperatures near a mid-ocean spreading center, while the low TiO_2 Upper Pillow Lavas were generated by higher degrees of partial melting, and metamorphosed in an off-axis, low temperature environment. This model was revised by Smewing and Potts (1976) on the basis of REE data to suggest that the Upper Pillow Lavas were derived by partial melting of the peridotite residua left after generation of the Axis sequence lavas, i.e., that the source of the Upper Pillow Lavas was more depleted in incompatible elements than the source of the Axis Sequence Lavas.

In the Arakapas Fault Belt, both Axis Sequence and Upper Pillow Lavas have extremely low TiO_2 contents (e.g., 0.2 - 0.3% TiO_2 in high MgO lavas, Simonian and Gass, 1978), similar to the Troodos Upper Pillow Lavas. Simonian and Gass (1978) linked this feature to high degrees of partial melting in an off-axis (transform fault) environment, and a smaller extent of fractional crystallization of the lavas due to easy magma egress to the surface through faults.

Normalized REE abundances in ophiolitic basalts reported by Smewing and Potts (1976) and Simonian and Gass (1978) are compared to REE abundances in some boninites in Fig. 6.1. Absolute HREE abundances in the

low TiO_2 Cyprus lavas (4-8 x chondrites) are higher than those in most boninites (<5 x chondrites), but are similar to those in low TiO_2 island arc volcanics from the Facpi Formation, Guam (6-11 x chondrites) and Manam Island, Bismarck Arc (5-8 x chondrites). Low TiO_2 Cyprus lavas have lower Ce/Sm than boninites and other low TiO_2 island arc lavas, and lower Ce/Sm and Sm/Yb than the Troodos Axis Sequence rocks (Fig. 6.1). Due to the small changes in intermediate REE/HREE ratios (e.g., Sm/Yb) during fractional crystallization and partial melting, Smewing and Potts (1976) concluded that the low intermediate REE/HREE ratios of the Troodos Upper Pillow Lavas were inherited from their sources which were peridotites residual from previous melting episodes.

Normalized abundances of REE and HFS elements in low TiO_2 Cyprus lavas are shown in Fig. 6.2. Like boninites and low TiO_2 island arc volcanics from all areas studied, these lavas are depleted in Ti and in most cases Y relative to Yb. Since Ti and Y are less compatible than Yb in common peridotite minerals (e.g., Irving, 1978), this characteristic is also consistent with an incompatible element depleted peridotite source for the low TiO_2 Cyprus lavas. In the most LREE depleted samples (e.g., 103A and 734, Fig. 6.2), all highly incompatible/moderately incompatible element ratios are less than chondritic (e.g., La/Ti, Zr/Ti). These lavas have relative abundances of La, Sm, Yb and Ti which are similar to those in calculated LREE-depleted mixing endmembers for boninites from the Bonin Islands and Cape Vogel (Chapter 3) and low TiO_2 volcanics from the Facpi Formation (Chapter 4) (Fig. 6.3), and have higher than chondritic Ti/Zr ratios (Fig. 6.4) which are also expected in LREE-depleted mixing endmembers for these rocks. In terms of the mixing model proposed to

FIGURE 6.1: Normalized REE abundances in low TiO_2 lavas from the Troodos Ophiolite (Smewing and Potts, 1976) and the Arakapas Fault Belt (Simonian and Gass, 1978), compared to boninites (Table 3.2) and tholeiitic lavas from DSDP Site 458 (Table 3.2, this study, and Hickey and Frey, 1981). Normalizing values given in Table 3.2.

FIGURE 6.2: Normalized REE and HFS element abundances in low TiO_2 lavas from Cyprus (Smewing and Potts, 1976; Simonian and Gass, 1978) compared to a boninite from the Bonin Islands (Table 3.2). La abundances for Cyprus lavas extrapolated from Ce and Nd. Normalizing values given in Table 3.2.

FIGURE 6.3: Normalized La, Sm, Yb and Ti abundances in extremely LREE-depleted low TiO_2 lavas from Cyprus (Smewing and Potts,, 1976; Simonian and Gass, 1978) compared to inferred LREE-depleted mixing endmembers for boninites from the Bonin Islands and Cape Vogel (Fig. 3.13) and the Facpi Fm., Guam (Fig. 4.12). La abundances for Cyprus lavas extrapolated from Ce and Nd.

FIGURE 6.4: $(La/Sm)_{e.f.}$ vs Ti/Zr ratio in low TiO_2 ophiolitic lavas from Cyprus (Smewing and Potts, 1976; Simonian and Gass, 1978), and the Betts Cove Ophiolite, Newfoundland (Coish et al., 1982). Fields for boninites and Facpi Formation lavas from Figs. 3.9 and 4.6.

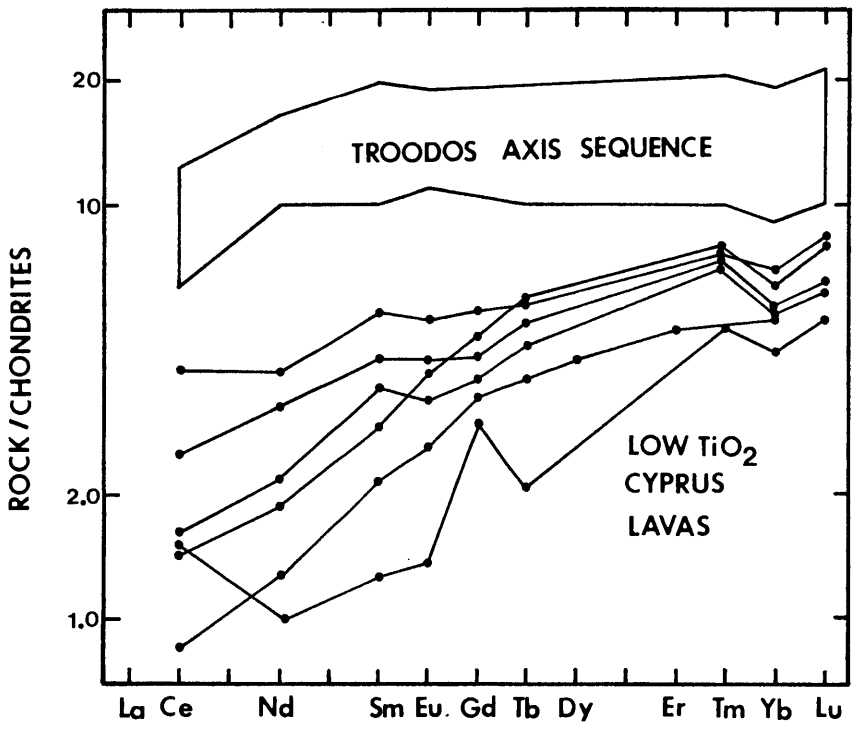
ROCK / CHONDRITES
20
10
2.0
1.0
TROODOS AXIS SEQUENCE
LOW TiO_2
CYPRUS
LAVAS
La Ce Nd Sm Eu. Gd Tb Dy Er Tm Yb Lu

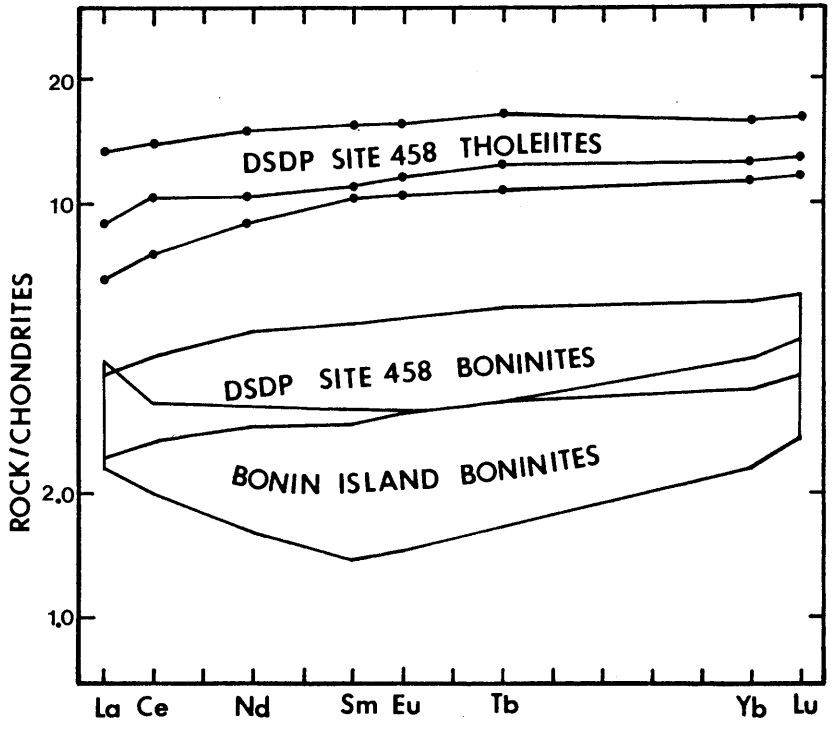
ROCK/CHONDRITES
20
10
2.0
1.0
DSDP SITE 458 THOLEIITES
DSDP SITE 458 BONINITES
BONIN ISLAND BONINITES
La Ce Nd Sm Eu Tb Yb Lu

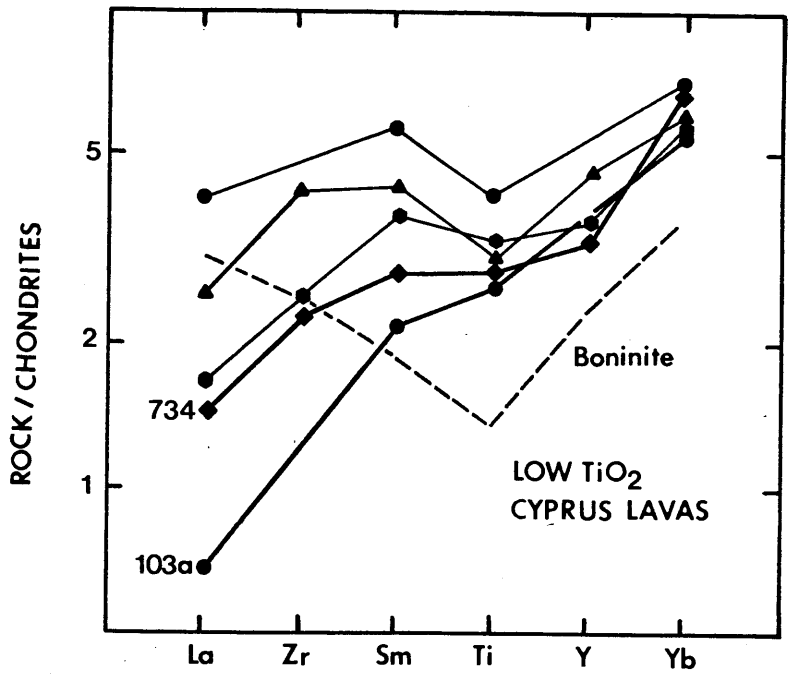
ROCK / CHONDRITES
5
2
1
734
103a
Boninite
LOW TiO2
CYPRUS LAVAS
La
Zr
Sm
Ti
Y
Yb

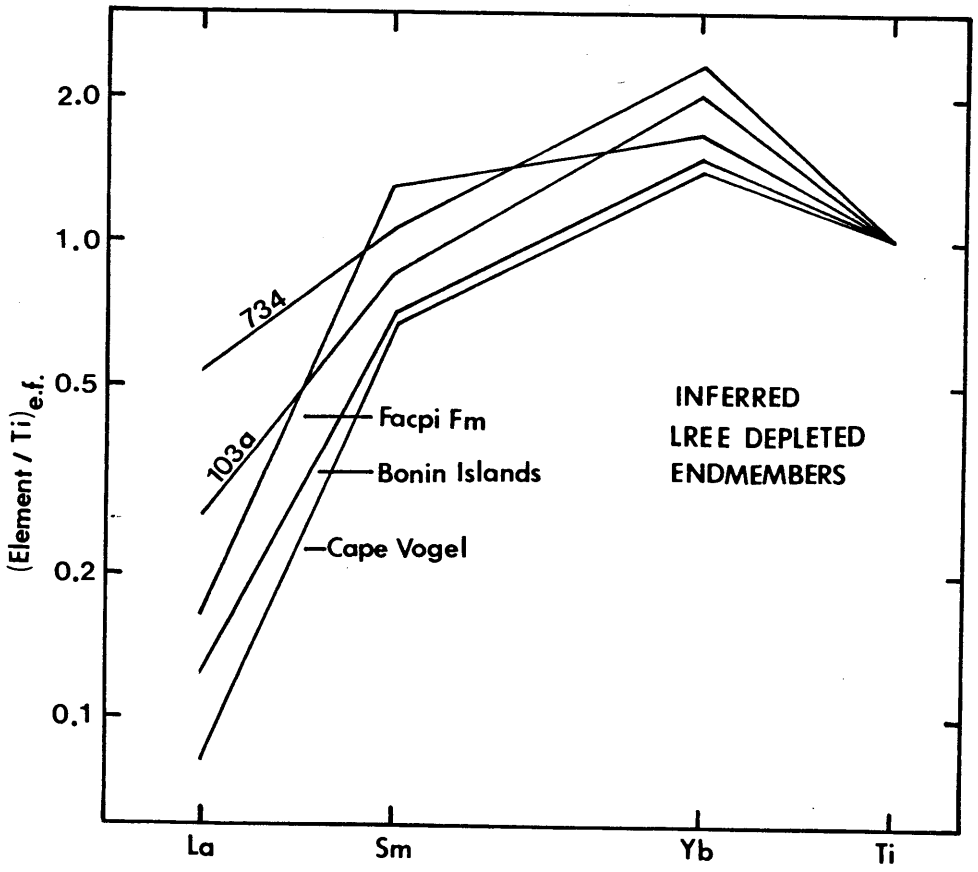
(Element / Ti)e.f.
2.0
1.0
0.5
0.2
0.1
734
103a
Facpi Fm
Bonin Islands
Cape Vogel
INFERRED
LREE DEPLETED
ENDMEMBERS
La
Sm
Yb
Ti

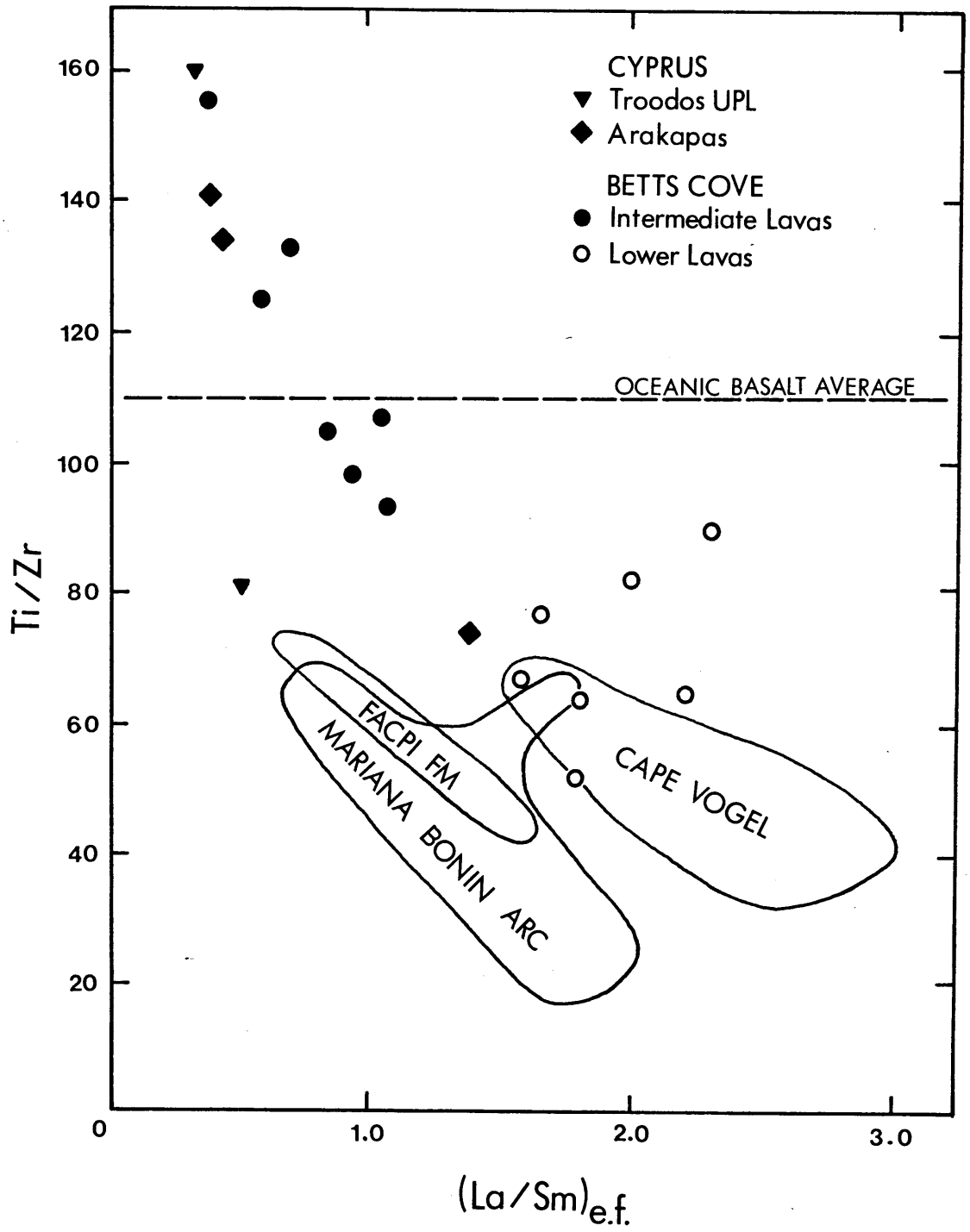
CYPRUS
Troodos UPL
Arakapas
BETTS COVE
Intermediate Lavas
Lower Lavas
OCEANIC BASALT AVERAGE
FACPI FM
MARIANA BONIN ARC
CAPE VOGEL
Ti/Zr
(La/Sm)e.f.
160
140
120
100
80
60
40
20
0
1.0
2.0
3.0

explain REE and HFS element abundances in boninites and Facpi Formation lavas, extremely LREE-depleted, low TiO_2 Cyprus lavas may represent partial melts of severely depleted peridotite which has not been metasomatically enriched in LREE and Zr.

The tectonic position of the Troodos Ophiolite is a controversial issue. The low TiO_2 contents of the Upper Pillow Lavas, which are characteristic of island arc volcanics, have led several workers to conclude that the ophiolite formed in an island arc. At DSDP Site 458, relatively high TiO_2 tholeiitic volcanics (e.g., ~0.8% TiO_2 in high MgO samples, Wood et al., 1981) are overlain by low TiO_2 boninites, which are overlain by sediments, comparable to the sequence at Troodos. As shown in Fig. 6.1, absolute and relative REE contents in Troodos Axis Sequence lavas and Site 458 tholeiitic basalts are also similar. This observation lends additional support to a subduction zone origin for the Troodos Ophiolite. Like the Site 458 lavas, the Troodos lavas may be a sequence of submarine island arc volcanics, formed in an area where volcancism ceased after generation of low TiO_2 lavas.

At Site 458, a direct genetic relationship between the tholeiite and boninite lavas is precluded by their different Nd-isotopic compositions (Table 3.3). Boninite lavas have lower $^{143}Nd/^{144}Nd$ (ε_{Nd} = +5.9 and +6.2) than a tholeiite (ε_{Nd} = +8.1), but values for both lava types are within the range typically found in island arcs. For Troodos, recent Nd-isotopic data reported by Hannah and Futa (1982) indicates that the boninite-like Upper Pillow Lavas have lower $^{143}Nd/^{144}Nd$ (initial ε_{Nd} = +6.4) than the Axis Sequence lavas (initial ε_{Nd} = +8.5). Values for the Upper Pillow Lavas are therefore not MORB-like, but values for both lava types are

within the range found in island arcs. This evidence also supports a subduction related origin for the Cyprus ophiolites, and strengthens the parallel between Troodos and the Mariana fore-arc lava sequence recovered at DSDP Site 458. A tectonic model for Site 458, which may also be applicable to the Cyprus ophiolites is discussed in Chapter 7.

LOW TiO_2 LAVAS FROM THE BETTS COVE OPHIOLITE

Trace and major element characteristics of lavas from the Betts Cove Ophiolite were studied by Coish and Church (1979) and Coish et al. (1982). Based on distinct groupings on plots of TiO_2 content vs FeO^t/MgO and Ni content, Coish and Church (1979) and Coish et al. (1982) divided Betts Cove lavas into three chemical groups: the Lower Lavas (0.1 - 0.3% TiO_2), the Intermediate Lavas (0.3 - 0.5% TiO_2), and the Upper Lavas (0.8 to >2.0% TiO_2). Ni contents and FeO^t/MgO in the three groups overlap, therefore it was concluded that the variation in TiO_2 content between these lavas groups did not result from fractional crystallization from a common parental magma (Coish and Church, 1979; Coish et al., 1982). Both Lower and Intermediate Betts Cove lavas have unusually low TiO_2 contents, which overlap with the low TiO_2 arc volcanics discussed earlier.

At Betts Cove, the stratigraphy of the compositional groups is inverse of that at Troodos, Cyprus. Low TiO_2 Lower and Intermediate Lavas form the lower part of the section and directly overlie the sheeted dike and gabbroic section of the ophiolite. Lower and Intermediate lavas are interfingered in some areas, while the high TiO_2 Upper Lavas always form the upper part of the section (Coish et al., 1982).

REE abundances in Betts Cove lavas from Coish et al. (1982) are compared to abundances in boninites from the Bonin Islands in Fig. 6.5. Betts Cove Lower Lavas have similar low absolute REE abundances to these boninites (2 - 5 x chondrites) and U-shaped REE patterns, which are also characteristic of boninites. Intermediate Betts Cove Lavas usually have $(LREE/HREE)_{e.f.} < 1$ (Coish et al., 1982), although some samples have $(LREE/HREE)_{e.f.} > 1$ (Fig. 6.5). Consistent with their higher TiO_2 contents, the Intermediate Lavas have higher HREE abundances (4 - 8 x chondrites) than the Lower Lavas and most boninites (Fig. 6.5; Coish et al., 1982). The most LREE-depleted Intermediate Lavas have similar LREE/HREE ratios to low TiO_2 lavas from Cyprus (Fig. 6.1). Coish et al. (1982) suggested that the variation in relative LREE enrichment in Intermediate and Lower Betts Cove Lavas may be the result of metamorphic alteration.

Normalized abundances of REE and HFS elements in Lower and Intermediate Lavas from Coish et al. (1982) are shown in Fig. 6.6. Lower Lavas, like boninites and all low TiO_2 island arc volcanics studied, have lower than chondritic Ti/Yb and Ti/Sc ratios, indicating depletion in less compatible relative to more compatible elements. Intermediate Lavas (Fig. 6.6) have variable Ti/Yb and Ti/Sc ratios, but at comparable MgO contents, have generally higher Ti/Yb and Ti/Sc ratios than boninites, other low TiO_2 island arc volcanics, and low TiO_2 ophiolitic lavas from Cyprus. Like boninites and low TiO_2 lavas from the Facpi Formation, Ti/Zr ratios in Lower Lavas are less than chondritic (Fig. 6.4), however, decreasing Ti/Zr ratios in the Lower Lavas do not correlate with increasing LREE enrichment (Fig. 6.4). Among the Intermediate Lavas, Ti/Zr ratios decrease with

FIGURE 6.5: Normalized REE abundances in Betts Cove Lower and Intermediate Lavas (Coish et al., 1982) compared to boninites (Table 3.2). Normalizing values given in Table 3.2.

FIGURE 6.6: Ranges of normalized REE and HFS element abundances in Betts Cove Lower and Intermediate Lavas (Coish et al., 1982) compared to a boninite from the Bonin Islands (Table 3.2) and low TiO_2 lavas from Cyprus (Fig. 6.2). Normalizing values given in Table 3.2.

FIGURE 6.7: $(La/Sm)_{e.f.}$ and Zr/Ti plotted vs Yb/Sc for Betts Cove Lower and Intermediate Lavas (Coish et al., 1982). Trends formed by the Intermediate Lavas oppose those expected from removal or accumulation of clinopyroxene.

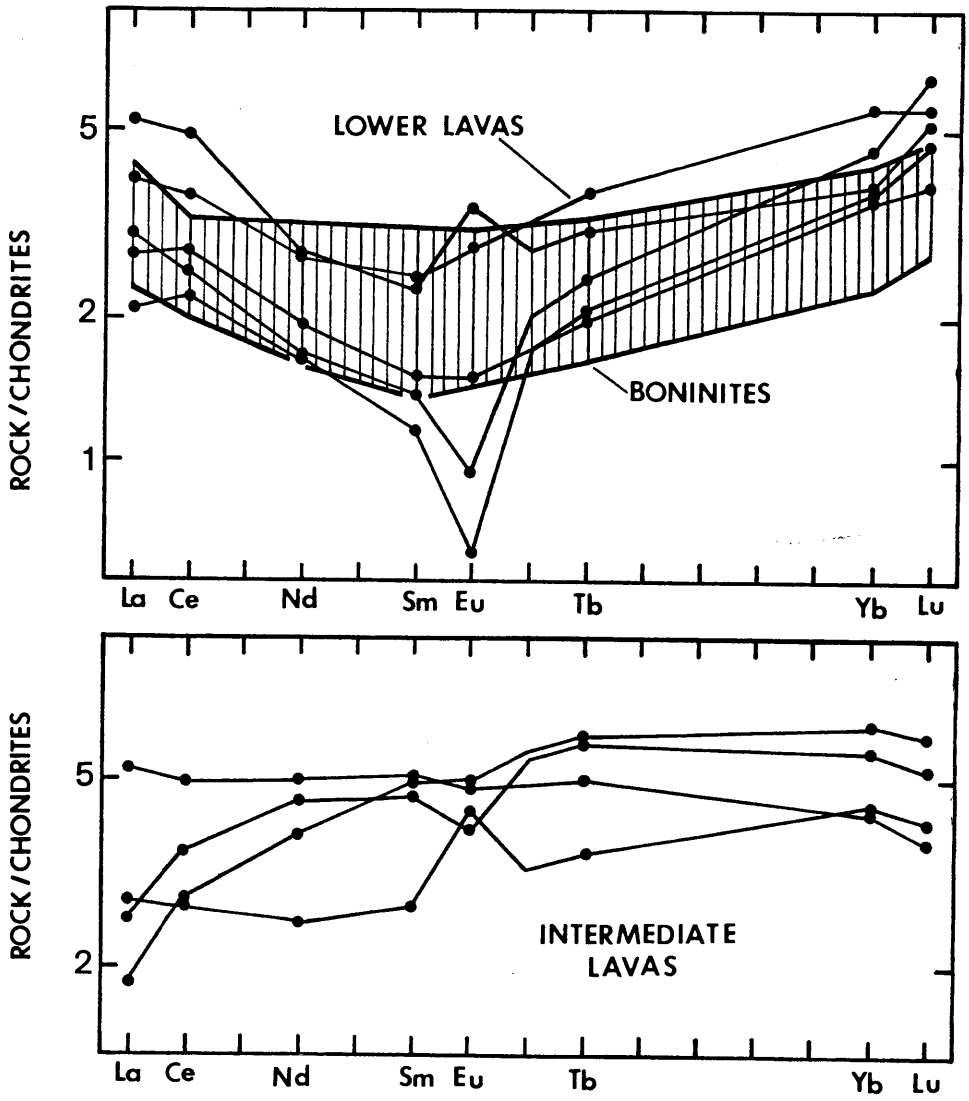
ROCK/CHONDRITES
5
2
1
LOWER LAVAS
BONINITES
La Ce Nd Sm Eu Tb Yb Lu
ROCK/CHONDRITES
5
2
INTERMEDIATE
LAVAS
La Ce Nd Sm Eu Tb Yb Lu

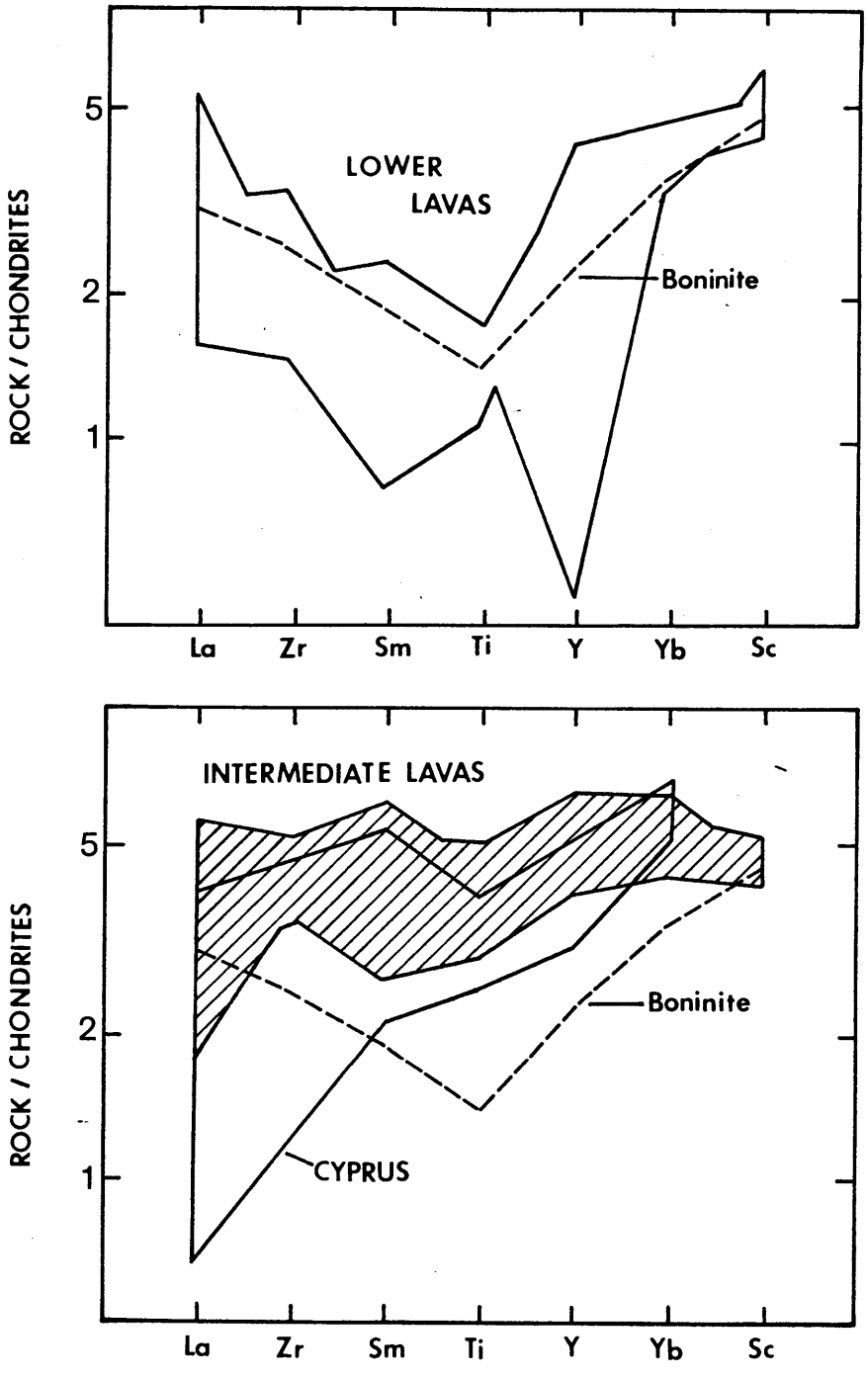
ROCK / CHONDRITES
5
2
1
LOWER
LAVAS
Boninite
La
Zr
Sm
Ti
Y
Yb
Sc
INTERMEDIATE LAVAS
Boninite
CYPRUS

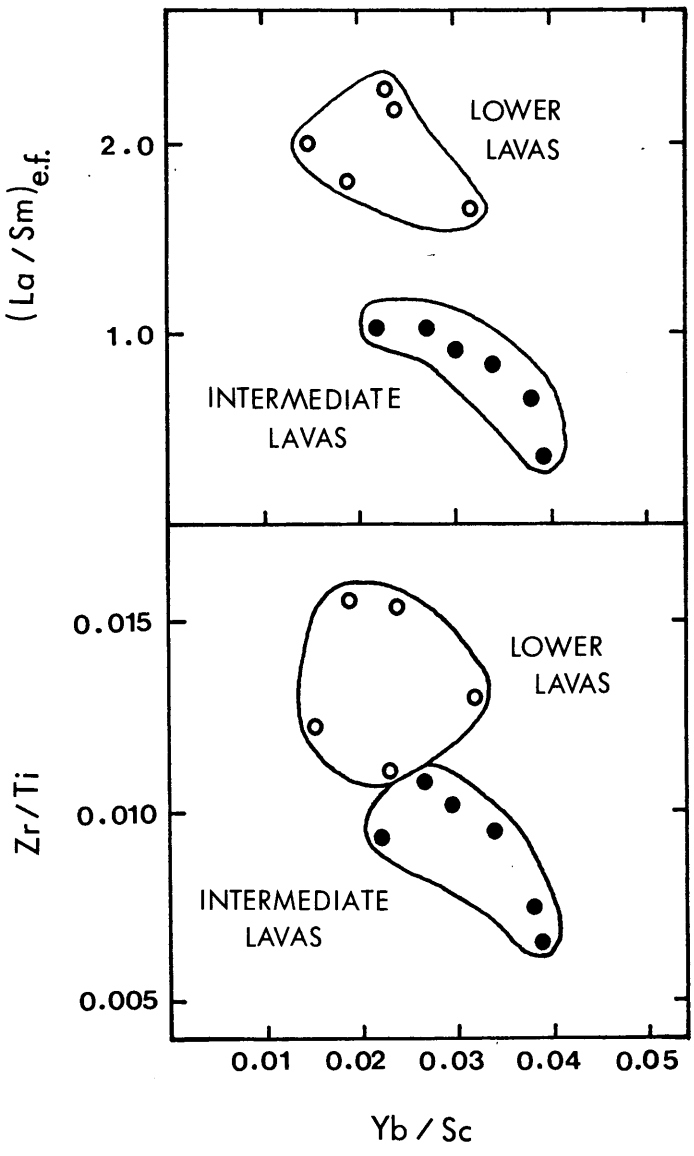
LOWER
LAVAS
INTERMEDIATE
LAVAS
2.0
1.0
(La / Sm)e.f.
LOWER
LAVAS
INTERMEDIATE
LAVAS
0.015
0.010
0.005
Zr / Ti
0.01
0.02
0.03
0.04
0.05
Yb / Sc

increasing La/Sm (Fig. 6.4). Since Ti and Zr are considered among the most immobile elements during alteration, this trend suggests that the variation in LREE abundance in these lavas may be a primary igneous feature, rather than an alteration effect as suggested by Coish et al. (1982).

Increasing La/Sm and decreasing Ti/Zr could be produced by fractional crystallization of clinopyroxene or by decreasing degrees of partial melting with clinopyroxene or garnet as residual minerals. Clinopyroxene fractionation as an explanation for this trend is not supported by the similar Ni, Cr and Sc contents in low La/Sm and high La/Sm Intermediate Lavas (31-37 ppm and 34-42 ppm respectively, Coish et al., 1982). In addition, La/Sm and Zr/Ti ratios in Intermediate Lavas increase with decreasing Yb/Sc ratio (Fig. 6.7). This is opposite to the trend expected for clinopyroxene fractionation, or decreasing degrees of partial melting with residual clinopyroxene or garnet. Therefore, it is unlikely that the variation in La/Sm and Ti/Zr in the Intermediate Lavas is the result of partial melting or fractional crystallization processes.

This trend could be explained if the sources of the Intermediate Lavas were mantle peridotites of variable fertility, which mixed with similar amounts of a LREE-enriched, low Ti/Zr material, like that proposed as one component of the sources of boninites. The variable Yb/Sc ratios in the Intermediate Lavas may reflect variations of this ratio in their peridotite sources. Lavas derived from more depleted peridotites (low Yb/Sc) could have higher La/Sm and Zr/Ti than lavas derived from more fertile peridotite (high Yb/Sc). The Betts Cove Lower Lavas form an extension to the trend in Fig. 6.7, and could also result from partial melting of a severely depleted peridotite (low Yb/Sc) which has been enriched in LREE and Zr. However, some Betts Cove Lower Lavas have higher

absolute LREE abundances than Intermediate Lavas, but similar Ni, Cr and Sc contents (Coish et al., 1982). Therefore, the Lower Lavas were probably formed by lower degrees of partial melting than the Intermediate Lavas.

Nd-isotopic data for lavas from Betts Cove are listed in Table 6.1. Initial $^{143}Nd/^{144}Nd$ for rim and core samples from a single Lower Lava pillow are within error. This indicates that if REE were mobilized during alteration, any change in Sm/Nd occurred very early, and that the Nd-isotopic composition of the lavas was significantly not affected. The Lower Lava has lower $^{143}Nd/^{144}Nd$ than the Intermediate and Upper Lavas, but has $\varepsilon_{Nd} > 1$, although it has $(Sm/Nd)_{e.f.} < 1$. The Intermediate and Upper lavas have similar, high $^{143}Nd/^{144}Nd$, which are in the range reported for lavas from the Bay of Islands Ophiolite (Jacobsen and Wasserburg, 1979), and similar to that expected in a normal MORB 500 m.y.b.p.. The Upper Lavas also have relative and absolute REE abundances similar to those in modern normal MORB's (Coish et al., 1982).

In the above discussion it was suggested that the source of Lower and Intermediate Betts Cove Lavas were mixtures of variably depleted peridotite and a high La/Sm, low Ti/Zr metasomatic material. In this case, the $^{143}Nd/^{144}Nd$ of a strongly LREE-depleted, high Ti/Zr lava (i.e., having a small metasomatic contribution) should be most similar to that of the peridotite. The Intermediate Lava analyzed for $^{143}Nd/^{144}Nd$ has high Sm/Nd (0.41), high Ti/Zr (125), and a high initial $^{143}Nd/^{144}Nd$, which is consistent with a depleted peridotite source residual from the generation of MORB-like magmas (i.e., magmas having a source with a time integrated history of LREE-depletion). Since the Upper Lavas overlie the Intermediate Lavas, the Intermediate Lavas cannot be generated from the residue of the

TABLE 6.1: Nd ISOTOPIC DATA FOR BETTS COVE LAVAS

	$^{143}Nd/^{144}Nd$(2)	$^{147}Sm/^{144}Nd$	$(^{143}Nd/^{144}Nd)_o$(3)	$(\varepsilon_{Nd})_o^{CHUR}$(4)
Upper Lava:				
BC-74-13b(1)	0.513024 ± 18	0.2054	0.512378	+6.8
Intermediate Lava:				
BC-74-57	0.513140 ± 17	0.2475	0.512362	+6.5
Lower Lavas:				
BC-74-101a	0.512791 ± 16	0.1749	0.512241	+4.1
BC-74-101b	0.512728 ± 19	0.1624	0.512217	+3.6

(1) Sample numbers from Coish et al. (1982).

(2) $^{143}Nd/^{144}Nd$ ratios normalized to $^{146}Nd/^{144}Nd = 0.7219$ and BCR-1, $^{143}Nd/^{144}Nd = 0.51263$.

(3) Initial ratios calculated assuming an age of 480 m.y..

(4) $(\varepsilon_{Nd})_o^{CHUR}$ calculated relative to present day CHUR, $^{143}Nd/^{144}Nd = 0.51264$ and $^{147}Sm/^{144}Nd = 0.1936$.

Upper Lavas. The similar $^{143}Nd/^{144}Nd$ of the Intermediate and Upper Lava may indicate that they are derived from a common mantle reservior, i.e., the Upper Lavas from a MORB-source peridotite, and the Intermediate Lavas from a MORB-residue peridotite which has not evolved significantly since its depletion. The similar $^{143}Nd/^{144}Nd$ of the Upper and Intermediate Lava also rules out mixing of the Upper and Lower Lavas as a possible origin for the Intermediate Lavas. The low $^{143}Nd/^{144}Nd$ of the Lower Lava indicates either that LREE enrichment of their depleted peridotite source occurred significantly before generation of the lavas (~200 m.y. before formation of the ophiolite), or that the LREE-enriched metasomatic material had low $^{143}Nd/^{144}Nd$, as suggested for boninites.

The sequence of lavas at Betts Cove is not observed in any low TiO_2 island arc volcanic area discussed. Although lavas from Guam also grade from extremely low TiO_2 lavas, probably derived from extremely refractory peridotite (Facpi Formation), to higher TiO_2 lavas, probably derived from more fertile peridotite (Alutom and Umatac Formations), the upper lavas are distinctly arc-like in character, and include calc-alkaline rocks. At Betts Cove, upper lavas are oceanic in character, including both the MORB-like Upper Lavas (Coish et al., 1982) and the Upper Snooks Arm Volcanics, which resemble oceanic island lavas and have TiO_2 contents of ~2% in basaltic samples (Jenner and Fryer, 1980). This sequence is inconsistent with thermal considerations, i.e., if the sources of all these volcanics were present in a single area, fertile peridotites, melting at lower temperatures than refractory peridotite, would yield high TiO_2 lavas before low TiO_2 lavas, like the sequences at Troodos and DSDP Site 458. The Betts Cove sequence is best explained if the low TiO_2 lavas are derived

from hydrous, refractory peridotite, while the Upper Lavas are derived from anhydrous, fertile peridotite. In this case, heat conducted from the source peridotite diapirs for the Upper Lavas could initiate partial melting of hydrous, refractory peridotite sources for the Lower and Intermediate lavas, as proposed in the model of Crawford et al. (1979) for boninites. The superposition of hydrous, refractory peridotite and fertile oceanic mantle peridotite indicated by this model is consistent with formation of the Betts Cove Ophiolite within a subduction zone which became the site of back-arc spreading, and eventually fully oceanic volcanism (Coish et al., 1982).

SUMMARY

Chemical features of low TiO_2 lavas from Cyprus and the Betts Cove Ophiolite generally support geochemical models for low TiO_2 island arc volcanics discussed in Chapters 3 through 5. Lavas from Cyprus and the Betts Cove Lower Lavas have lower than chondritic Ti/Yb ratios, and Betts Cove Lower Lavas also have lower than chondritic Ti/Sc and Yb/Sc ratios, supporting a refractory peridotite source for these lavas. Extremely LREE-depleted lavas from Cyprus have relative La, Sm, Yb and Ti abundances similar to those in inferred LREE-depleted mixing endmembers for boninites, and higher than chondritic Ti/Zr ratios. These lavas may be partial melts of refractory peridotite which had not been metasomatically enriched in LREE and Zr. Betts Cove Lower Lavas have U-shaped REE patterns and lower than chondritic Ti/Zr ratios, like those in boninites. However, in the Lower Lavas decreasing Ti/Zr does not correlate with increasing La/Sm, as expected in mixing between and LREE-depleted peridotite with high Ti/Zr and

LREE-enriched, low Ti/Zr material. Betts Cove Intermediate Lavas, which have Ti/Sc and Yb/Sc ratios ranging from less than chondritic to greater than chondritic, show a correlation between increasing La/Sm and decreasing Ti/Zr. La/Sm ratios in these lavas also increase with decreasing Yb/Sc ratio. This trend cannot be explained by fractional crystallization of clinopyroxene, or varying degrees of partial melting with clinopyroxene or garnet bearing residua, but is consistent with mixing of a variably depleted source peridotite with a LREE-enriched, low Ti/Zr material.

A LREE-depleted Betts Cove Intermediate Lava has high $^{143}Nd/^{144}Nd$, similar to that expected in MORB's at the time of ophiolite formation, and supports a residual peridotite from MORB generation as the source of the Intermediate and probably the Lower Lavas. One of the MORB-like Betts Cove Upper Lavas has a similar high $^{143}Nd/^{144}Nd$, but cannot be related to the peridotite source of the Intermediate and Lower Lavas, because the Upper Lavas are apparently younger than both Intermediate and Lower Lavas. A LREE-enriched Lower Lava has lower $^{143}Nd/^{144}Nd$, and suggests that LREE metasomatism occurred significantly before generation of the lavas, or that it involved a low $^{143}Nd/^{144}Nd$ material.

The sequence at Troodos, Cyprus, i.e., extremely low TiO_2 lavas overlying high TiO_2 lavas, overlain by sediment, is similar to DSDP Site 458 in the Mariana Fore-arc. This supports the theory that the Troodos Ophiolite lavas may represent a sequence of submarine island arc lavas, rather than mid-ocean ridge volcanics. Lavas from the Betts Cove Ophiolite

have the inverse sequence: low TiO_2 lavas are overlain by high TiO_2 lavas of oceanic character. This sequence is not found in the low TiO_2 island arc areas studied, but could result from partial melting of depleted hydrous peridotite within a subduction zone, leading to low TiO_2 volcanism, by heat conducted from anhydrous MORB-source peridotite diapirs, which later give rise to the upper oceanic lavas within a back-arc spreading center.

CHAPTER 7: GEOCHEMICAL AND TECTONIC REGULARITIES IN LOW TiO_2 VOLCANICS: IMPLICATIONS FOR THEIR SOURCES AND GENERATION

In Chapters 3, 4, and 5, the geochemical characteristic of boninites and low TiO_2 island arc lavas from the Facpi Formation, Guam and Manam Island, Bismarck Arc, were modelled in terms of four basic source components: 1) incompatible element depleted mantle peridotite, with high $^{143}Nd/^{144}Nd$, which may be the residue of MORB generation; 2) a mantle derived fluid or melt with low $^{143}Nd/^{144}Nd$, enriched in LREE relative to HREE and Ti, and enriched in Zr relative to Ti and in some cases intermediate REE; 3) a component enriched in K, Rb, Ba, Sr and possibly Pb relative to REE and HFS elements, derived from subducted MORB and sediment; and 4) a "seawater" component enriched in K and Rb compared to Ba, Sr, REE and HFS elements, derived from alteration products resulting from seawater - MORB interaction. In Chapter 6 it was shown that the REE and HFS element characteristics of low TiO_2 ophiolitic basalts from the Troodos Ophiolite and Arakapas Fault Belt, Cyprus, and the Betts Cove Ophiolite, Newfoundland are also consistent with mixing of components 1) and 2). In this chapter geochemical evidence for each of these components in low TiO_2 volcanics from different areas will be compared and a general geochemical and tectonic model for the origin of low TiO_2 island arc volcanics will be developed.

EVIDENCE FOR A DEPLETED PERIDOTITE SOURCE

Unlike many island arc volcanics, most low TiO_2 lavas studied in this thesis have characteristics of liquids which have equilibrated with peridotite. MgO-rich (>8% MgO) boninites from the Bonin Islands, Cape

Vogel and Dredge Site 1403 and lavas from the Facpi Fm., Guam have $MgO/(MgO + \Sigma FeO) = 0.66 - 0.76$, and Ni contents of 111 to 334 ppm. Many of these samples contain less than 10% olivine and/or orthopyroxene phenocrysts and should represent near-liquid compositions. Olivine and orthopyroxene (or clinoenstatite) compositions reach Fo 92 and En 92 in boninites (Jenner and Green, in prep.), and Fo 92 in Facpi Fm. lavas (Reagan and Meijer, 1982), and are consistent with the derivation of these lavas from mantle peridotite.

Lavas from Manam Island are more phenocryst rich, and have lower $MgO/(MgO + \Sigma FeO)$ (0.57 - 0. 66) and Ni contents (30 to 81 ppm) than other low TiO_2 volcanics studied. Major element compositions of these lavas suggest that, in spite of their high phenocryst content, they are close to liquid compositions which are related by fractional crystallization of olivine and clinopyroxene (e.g., Fig. 5.2a). The lavas contain olivine xenocrysts with Fo 93, which is evidence that they may have evolved from parental magmas which equilibrated with mantle peridotite.

A depleted peridotite source for low TiO_2 island arc lavas is suggested by their low absolute abundances of Ti, Y and HREE (1 to 8 x chondrites), as proposed by Green (1973) and Kay (1980) to explain the low abundances of these elements in arc volcanics in general. This interpretation is supported by relative abundances of Ti, Y, Yb, Sc and V in low TiO_2 arc volcanics. Based on bulk partition coefficients for peridotite mineral assemblages, these elements can be ordered in terms of increasing compatibility as $Ti < Y < Yb < V \leq Sc$. The low TiO_2 volcanics studied exhibit depletion in less compatible elements relative to more compatible elements. For example, Ti/Sc ratios are less than chondritic in

high-MgO samples from all areas studied (Figs. 3.4, 4.11, 5.4 and 6.6), Ti/V ratios are less than chondritic in boninites from the Bonin Islands and Dredge Site 1403, and low TiO_2 basalts from Manam Island (Figs. 3.4 and 5.4), Yb/Sc ratios are lower than chondritic in all samples studied except those from the Facpi Fm. (Figs. 3.6, 4.4, 5.6, and 6.7) and Ti/Yb ratios are lower than chondritic in all samples except those from Cape Vogel (Figs. 3.6, 4.4, 5.6 and 6.6). This information is summarized in Fig. 7.1, on which samples from all areas are plotted.

Lower than chondritic Ti/Sc, Ti/V, Yb/Sc and Ti/Yb ratios are expected in peridotites from which a partial melt has been extracted, and extremely low values of these ratios are observed in harzburgitic peridotites (Fig. 7.1, Table 3.4). Low values of these ratios in melts are not consistent with retention of Ti and HREE in residual garnet, clinopyroxene or amphibole, as a possible explanation of their low abundances, because Sc and V have higher solid/melt partition coefficients than Ti and HREE in these minerals. For boninites, retention of Ti and HREE in a residual accessory mineral is also unlikely because experimental studies indicate that these magmas separate from extremely refractory residual peridotite, consisting only of olivine and orthopyroxene. Therefore it is concluded that boninites and low TiO_2 arc volcanics from the Facpi Fm., Guam, and Manam Island, and low TiO_2 ophiolitic basalts from Cyprus and the Betts Cove Ophiolite are derived in part from a mantle peridotite depleted in incompatible elements due to a prior episode of melt extraction, and that the low absolute abundances of Ti, Y and HREE, and low Ti/Sc, Ti/V, Yb/Sc and Ti/Yb ratios in these rocks reflect the low abundances and low ratios of these elements in this source component.

FIGURE 7.1: Ti/Sc plotted vs Yb/Sc for low TiO_2 volcanics compared to chondrites, primitive mantle-derived liquids, and peridotites. MORB data from Frey et al. (1974), Langmuir et al. (1977) and Sun et al. (1979). Komatiite data from Sun and Nesbitt (1978b). Peridotites from Ronda, data from Frey and Suen (1982).

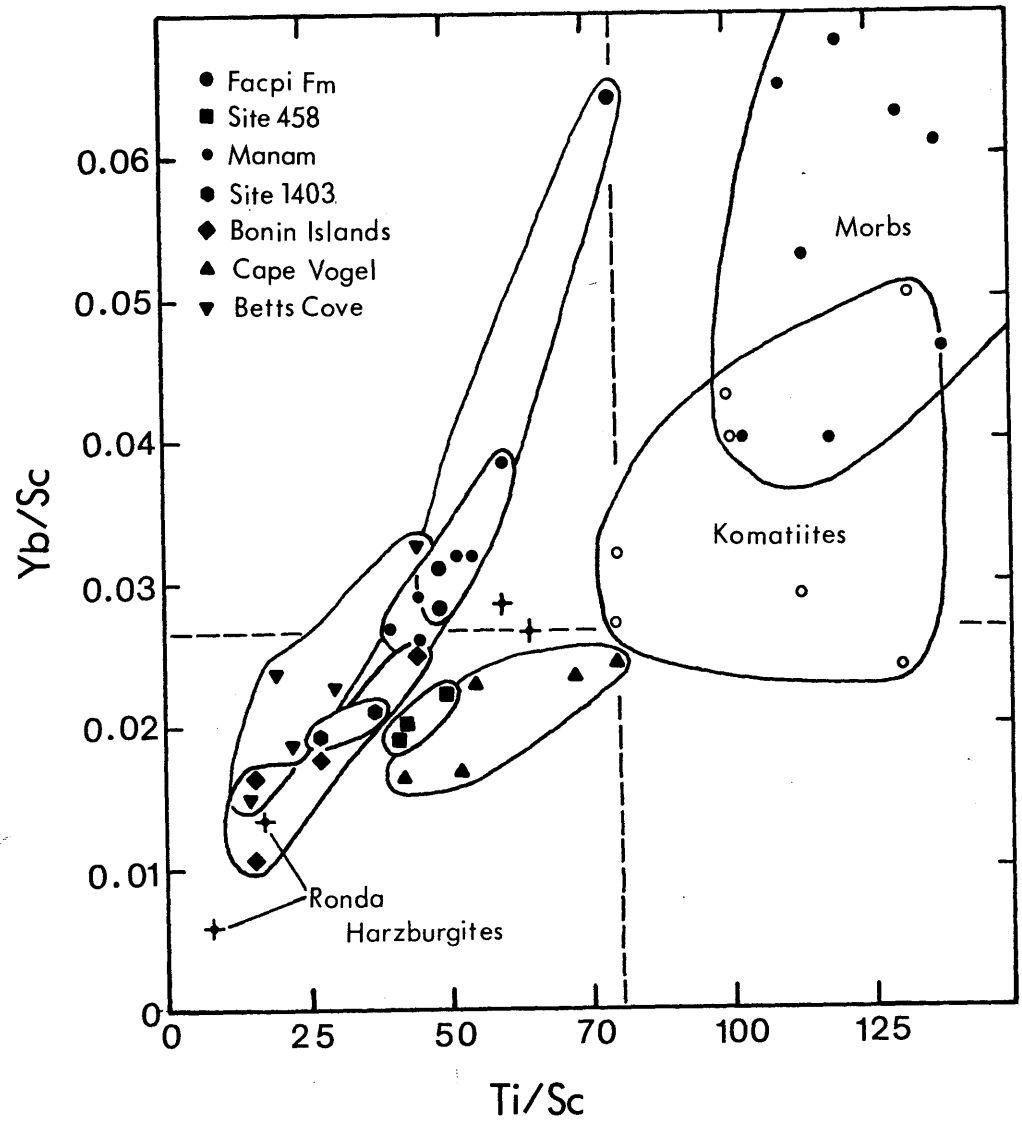
Facpi Fm
Site 458
Manam
Site 1403
Bonin Islands
Cape Vogel
Betts Cove
Morbs
Komatiites
Ronda
Harzburgites
Yb/Sc
Ti/Sc
0.06
0.05
0.04
0.03
0.02
0.01
0
0
25
50
70
100
125

The derivation of low TiO_2 island arc volcanics by partial melting of refractory peridotite is difficult to reconcile with thermal models of subduction zones. In calculated P-T profiles of subduction zones, partial melting of fertile, hydrous peridotite can occur at depths of about 100 km beneath volcanic arcs (Wyllie, 1979). However, under such conditions, significant partial melting of subducted oceanic crust is also expected (Gill, 1981). Although a metasomatic component derived from subducted oceanic crust is proposed for low TiO_2 arc volcanics (this chapter), the presence of a large melt fraction derived from subducted crust is unlikely because it would obscure the trace element characteristics of the peridotite. For boninites, experimental results suggest shallow depths of derivation (e.g., 1200°C, <10 kbar, under water-saturated conditions, Green, 1973; 1976; >1200°C, <5-10 kbar, water-undersaturated conditions, Jenner and Green, in prep.). These P-T conditions are not found in any subduction zone model. Since the geochemical evidence that boninites and other low TiO_2 volcanics are derived from refractory peridotite is strong, it must be assumed that the conditions under which they are generated are different from those generally inferred for subduction related volcanism. Because of the relatively widespread occurrence of low TiO_2 arc volcanics, these conditions must also be fairly common. Models which might explain the derivation of boninites and low TiO_2 volcanics from refractory peridotite will be discussed in a later section of this chapter.

EVIDENCE FOR ENRICHMENT IN LREE THROUGH MANTLE METASOMATISM

Enrichment in LREE compared to HREE or intermediate REE is characteristic of boninites from the Bonin Islands, Cape Vogel, and Dredge Site 1403, and low TiO_2 lavas from the Facpi Fm., Guam, Manam Island, and the Betts Cove Ophiolite (Figs. 3.5, 4.5, 5.7, and 6.5). In each of these areas high La/Sm is correlated with low $^{143}Nd/^{144}Nd$ (Figs. 3.10, 4.9, 5.11, and Table 6.1). Since enrichment in LREE relative to HREE and intermediate REE is not consistent with an incompatible element depleted peridotite source for these rocks, this was interpreted in Chapters 3 through 6 as the result of mixing of a LREE-enriched material with the LREE-depleted peridotite source inferred from relative abundances of Ti, HREE, Sc and V. Mixing of two materials to explain this feature is supported by the covariation of Nd-isotopic composition and relative LREE abundances, along with trace element ratios such as Ti/Zr (Figs. 3.9, 4.6).

That the refractory peridotite source of these volcanics is the LREE-depleted mixing endmember is indicated by several factors: 1) for boninites from the Bonin Islands and Cape Vogel, and low TiO_2 volcanics from Guam, relative REE and Ti abundances in LREE-depleted endmembers calculated from data for these lavas (Figs. 3.13 and 4.12), are similar to those reported in harzburgitic peridotites (Fig. 3.13); 2) some low TiO_2 ophiolitic lavas from Cyprus are extremely LREE-depleted and have been modelled as partial melts of peridotite which has previously lost a melt fration (Smewing and Potts, 1976). These Cyprus lavas have relative REE and Ti abundances similar to the calculated LREE-depleted mixing endmembers for boninites from the Bonin Islands and Cape Vogel and low TiO_2

lavas from the Facpi Fm. on Guam, and have similar absolute HREE and Ti abundances to boninites and Facpi Fm. lavas. In terms of the mixing scheme proposed for boninites and low TiO_2 arc lavas, the extremely LREE-depleted Cyprus lavas may be partial melts of peridotite which has not been metasomatized; 3) while many harzburgitic peridotites are severely LREE-depleted (Frey, 1982; Frey and Suen, 1982), as predicted by most values of REE partition coefficients for peridotite minerals, enrichment in LREE relative to HREE or intermediate REE is a common feature of these rocks (Kurat et al., 1980; Stosch and Seck, 1980; Hickey, in Frey, 1982; Tanaka and Aoki, 1981). Leaching experiments on some of these harzburgites indicate that LREE-enriched materials are concentrated on grain boundaries or in inclusions (Stosch and Seck, 1980; Kurat et al., 1980), and that LREE-enrichment in these peridotites does not reflect high mineral/melt equilibrium partition coefficients for LREE in olivine or orthopyroxene. Therefore, secondary LREE-enrichment of LREE-depleted, refractory peridotite, as suggested for the sources of low TiO_2 lavas, may be a common process in the mantle.

The correlation of increasing relative LREE abundances and decreasing $^{143}Nd/^{144}Nd$ found in low TiO_2 volcanics was interpreted in earlier chapters in terms of recent mixing of a LREE-depleted peridotite with high $^{143}Nd/^{144}Nd$, and a LREE-enriched material with low $^{143}Nd/^{144}Nd$, i.e., mixing of isotopically distinct materials with little isotopic evolution between the metasomatic event and generation of the lavas. This was in part because the consideration of subduction related sources for LREE-enriched materials implies recent mixing. Correlation between increasing LREE-enrichment and decreasing $^{143}Nd/^{144}Nd$ could also result from ancient mixing of LREE-enriched and LREE-depleted materials

and subsequent evolution of $^{143}Nd/^{144}Nd$ with time, or an intermediate between these two extremes.

Assuming recent mixing, sources for LREE-enriched, low $^{143}Nd/^{144}Nd$ mixing endmembers for low TiO_2 arc volcanics can be broadly classified as: 1) subducted sedimentary sources, and 2) mantle sources similar to the sources of oceanic island volcanics. These sources are evaluated for each area studied in earlier chapters. Based on the following criteria, a mantle source rather than a subducted sedimentary source is preferred for all areas studied: 1) low TiO_2 volcanics for all areas studied exhibit decoupling or lack of correlation between relative and absolute K, Rb, Sr and Ba abundances and relative LREE-enrichment. Since K, Rb, Sr and Ba have high abundances in various types of sediments, their abundance patterns are expected to correlate with LREE-enrichment if sediments contribute LREE to the sources of these lavas; 2) of all areas studied, only boninites from the Bonin Islands have $^{143}Nd/^{144}Nd$ values supporting sedimentary versus oceanic mantle sources, i.e., they have $^{143}Nd/^{144}Nd$ lower than commonly found in oceanic island volcanics (Table 3.3). However, similar low $^{143}Nd/^{144}Nd$ values are observed in LREE-enriched alkalic basalts from Takashima and Oki Islands, southwestern Japan (Allegre et al., in press) which are located near the probable original position of the Bonin Islands. Thus a suitable mantle source for LREE-enrichment of the source of Bonin Island boninites is present; and 3) Pb isotopic compositions of LREE-enriched, low TiO_2 lavas from the Bonin Islands, the Facpi Fm., Guam, and Manam Island do not indicate a large sediment contribution (Figs. 3.15, 4.10 and 5.12). Since sediments have high Pb/Nd ratios (e.g., Kay, 1980), a sediment source for LREE-enrichment and low

$^{143}Nd/^{144}Nd$ should be strongly evident in the Pb isotopic composition of the lavas, which is not the case.

If mantle derived metasomatic materials are responsible for the LREE-enrichment of the source of low TiO_2 arc volcanics, then the assumption of recent mixing for the sources of these rocks is not necessarily valid because the metasomatism could be unrelated to subduction. Metasomatism of depleted peridotites in the oceanic mantle could occur at any time between the event causing depletion and generation of low TiO_2 lavas within a subduction zone. Isochron ages and initial ratios for low TiO_2 vocanics from the Bonin Islands, Cape Vogel, Guam and Betts Cove are listed in Table 7.1. For low TiO_2 volcanics from the Bonin - Mariana Arc (Bonin Islands and Guam), ages of >200 m.y. before eruption of the lavas exceed the age of initiation of subduction along the arc (~50 m.y.b.p.), and therefore do not limit LREE enrichment to a post-subduction event. Since times of initiation of subduction for other areas are not known, similar observations can not be made. Initial ratios for all areas except the Bonin Islands are greater than chondritic, but slightly less than those in a hypothetical LREE-depleted MORB-type mantle source at the isochron age. For these areas it is conceivable that mixing of LREE-enriched and LREE-depleted materials occurred significantly before eruption of the lavas. For Bonin Island boninites, initial $^{143}Nd/^{144}Nd$ ratios exceed those in a LREE-depleted MORB-type mantle source at their isochron age of 1.7 b.y.b.p. and are outside the range of initial values measured in terrestrial rocks. For these lavas, mixing must have occurred more recently than 1.7 b.y.b.p. and must have involved isotopically distinct LREE-enriched and LREE-depleted materials. These calculations do not favor either recent mixing of isotopically distinct materials or

TABLE 7.1: Nd-ISOTOPE "AGES" AND INITIAL RATIOS FOR LOW TiO_2 VOLCANICS

	AGE(1)	$(^{143}Nd/^{144}Nd)_o$	$(\varepsilon_{Nd})_o^{CHUR}$(2)	$(\varepsilon_{Nd})_o^{D.M.}$(3)
Bonin Islands:	1.7×10^9	0.51076	+6.2	+5.2
Facpi Fm., Guam:	2.4×10^8	0.51264	+7.1	-1.3
Cape Vogel, PNG:	3.6×10^8	0.51246	+6.2	-1.8
Betts Cove:	2.6×10^8	0.51202	+4.7	-1.5

(1) Years before eruption of volcanic rocks.

(2) Calculated relative to present day CHUR, $^{143}Nd/^{144}Nd = 0.51264$, and $^{147}Sm/^{144}Nd = 0.1936$.

(3) "Depleted mantle" reservoir, calculated relative to present day MORB, $^{143}Nd/^{144}Nd = 0.51315$, and $^{147}Sm/^{144}Nd = 0.234$.

ancient mixing and isotopic evolution, however, they demonstrate that LREE-enrichment may have occurred significantly before generation of the lavas, and for Bonin - Mariana Arc lavas, before initiation of subduction. Mantle metasomatism of the depleted peridotite sources of low TiO_2 arc volcanics before the initiation of subduction is easier to conceive of geometrically, because the subducted oceanic lithosphere would tend to isolate the subarc peridotite "wedge" from surrounding mantle sources for metasomatic fluids.

Based on this information, the following time sequence is proposed for the generation of sources for low TiO_2 arc volcanics (Fig. 7.2a): 1) generation of LREE-depleted peridotite within the oceanic lithosphere at mid-ocean ridges by extraction of MORB magma; 2) metasomatism of this depleted peridotite by LREE-enriched fluids derived from mantle sources similar to the sources of oceanic island volcanics, away from the spreading ridge; and 3) entrapment of the refractory, LREE-metasomatized peridotite within the underthrust plate of a subduction zone, addition of materials derived from subducted oceanic crust (next section), and initiation of partial melting, in part, through addition of H_2O. The metasomatism of the depleted peridotite sources of low TiO_2 volcanics during transit between mid-ocean ridges and entrapment in subduction zones may be related to oceanic island volcanism. Oceanic islands form where magmas rising from deep mantle sources invade and are erupted through older oceanic lithosphere. In areas which are not the site of oceanic island volcanism fluids or melts derived from the same sources may also invade oceanic lithosphere but precipitate within the mantle, possibly owing to smaller volume, low temperature, or the refractoriness of the host peridotite.

FIGURE 7.2: Cartoon depicting the development of sources for low TiO_2 arc volcanics:

A) Events related to the REE, HFS and compatible element characteristics of low TiO_2 volcanics:
   1) generation of depleted peridotite, residual from MORB extraction at a spreading ridge;
   2) LREE-enrichment of depleted peridotite within the oceanic lithosphere by mantle-derived metasomatic fluids, possibly arising from sources similar to those for oceanic island volcanics;
   3) entrapment of LREE-enriched, refractory peridotite in the overthrust mantle wedge of a subduction zone.

B) Enrichment in K, Rb, Ba, Sr and Pb: volatile rich-fluids enriched in these elements relative to REE and HFS elements derived from the subducted oceanic crust, including "seawater", basalt and sediment, are added to the LREE-enriched, refractory peridotite.

Boninite sources are formed at shallow depths, where basaltic clays dehydrate, leading to enrichment in K and Rb relative to Ba and Sr. Pb contents in shallow level fluids may be low.

Low TiO_2 basalt sources are formed at greater depths and have lower K and Rb contents compared to Ba and Sr, and higher Pb contents than the shallow level peridotites.

DEVELOPMENT OF SOURCES FOR LOW TiO_2 ISLAND ARC VOLCANICS

A) REE, HFS AND COMPATIBLE ELEMENTS

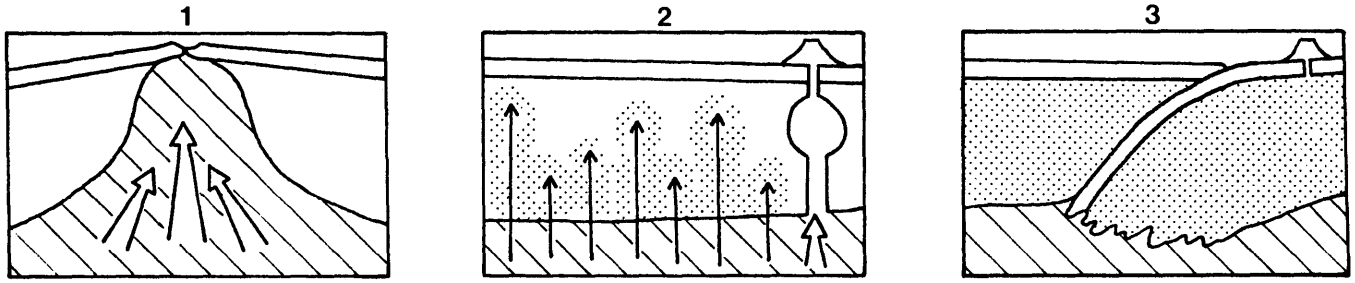

B) ENRICHMENT IN K, Rb, Ba, Sr AND Pb

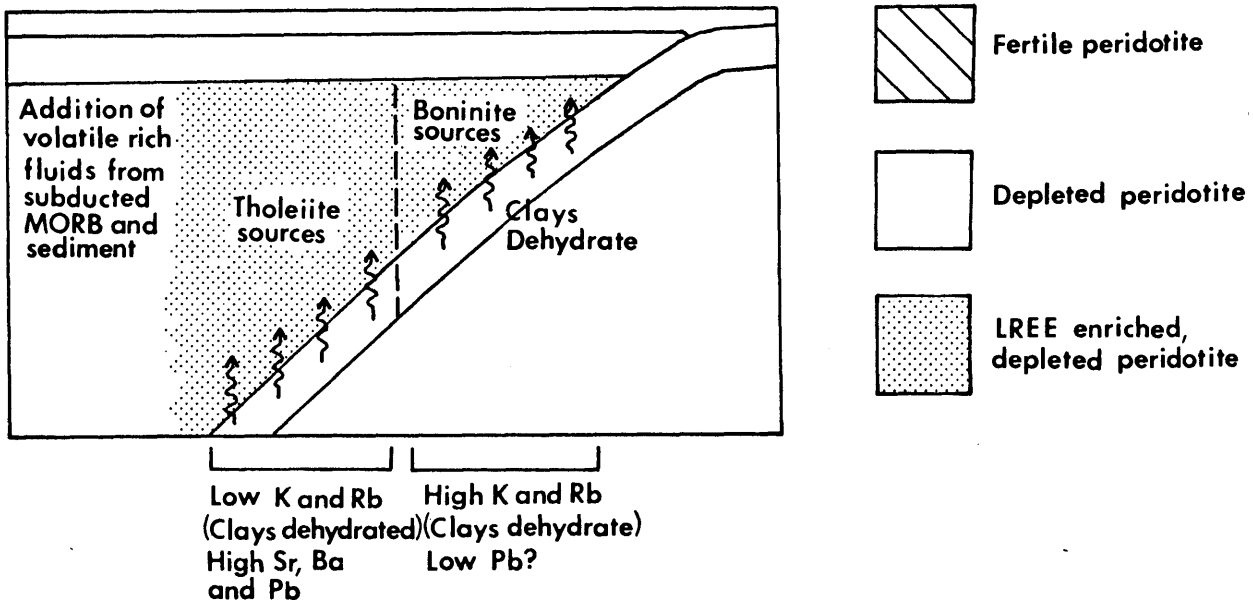

The resulting mantle would be a source for low TiO_2 island arc volcanics. This process would explain the Nd-isotopic similarity between low TiO_2 arc volcanics and oceanic island volcanics, and the similar REE abundance patterns in low TiO_2 arc volcanics and metasomatized harzburgite nodules from alkalic basalts.

This model for metasomatism of the refractory peridotite sources of low TiO_2 volcanics is similar to the model proposed by Frey and Green (1974) for refractory but LREE-enriched peridotites from Victoria, Australia. Like low TiO_2 volcanics, these peridotites have $^{143}Nd/^{144}Nd$ ratios which decrease with increasing LREE-enrichment (Chen and Frey, 1981). Unlike the low TiO_2 arc volcanics studied, these peridotites are not enriched in Sr relative to Nd (Chen, unpublished data; Burwell, 1974), and $^{87}Sr/^{86}Sr$ and Rb/Sr ratios are correlated. Therefore, while mantle metasomatism of refractory peridotite may explain the REE and HFS element characteristics of low TiO_2 volcanics, other sources or processes are required to explain their Sr abundance and isotopic characteristics.

ENRICHMENT IN Zr

One major difference between the REE and HFS element abundances in mantle derived volcanics and low TiO_2 arc volcanics is the low Ti/Zr ratios and particularly the high Zr/Sm ratios found in boninites, low TiO_2 lavas from Guam, and the Betts Cove Ophiolite. Higher than chondritic Zr/Sm ratios are not observed in oceanic volcanics, alkalic basalts from continental regions or in kimberlites. For example, in Figs. 7.3 and 7.4 Ti/Zr, La/Sm and Zr/Sm ratios in alkalic basalts from several tectonic regimes and in kimberlites are plotted along with low TiO_2 arc volcanics.

Several of these rock suites have lower than chondritic Ti/Zr ratios (e.g., kimberlites, and alkalic basalts from Victoria, Australia and the Antilles, Fig. 7.3), but in contrast to boninites and low TiO_2 volcanics from Guam and the Betts Cove Ophiolite, none of these rocks suites has significantly higher than chondritic Zr/Sm (Fig. 7.4). In kimberlites and Hawaiian lavas, decreasing Ti/Zr is correlated with increasing La/Sm and decreasing Zr/Sm (Fig. 7.4), therefore the phases responsible for low Ti/Zr and high La/Sm in these lavas cannot explain the high Zr/Sm in boninites.

The correlation of high La/Sm and low Ti/Zr observed in kimberlites, and alkalic basalts from the Hawaiian Islands; Victoria, Australia; and the Antilles is not difficult to explain. The capacity for garnet and clinopyroxene, which are commonly inferred residual minerals for these magmas, to retain intermediate REE and HREE relative to LREE is well established. Zr partition coefficients for clinpyroxene have been demonstrated to vary with compositional factors (Dunn and McCallum, 1981), however, as discussed in Chapter 5, Ti partition coefficients for clinopyroxene are likely to be influenced similarly to Zr partition coefficients by these compositional changes. The relative values of Ti and Zr partition coefficients calculated from the same specimens should therefore be correct, and are higher for Ti than Zr (Le Roex, 1980). Zr partition coefficients for garnet have not been determined directly, but values relative to Ti can be estimated using Zr and Ti concentration data for coexisting clinopyroxene - garnet pairs reported by LeRoex (1980) and Shimizu and Allegre (1978). For example, Le Roex (1980) reports $D_{Ti}^{cpx/liq} / D_{Zr}^{cpx/liq} = 3$, and this value is also given by Pearce and Norry (1979) based on individually measured Ti and Zr partition coefficients. $D_{Ti}^{gt/cpx}$ and $D_{Zr}^{gt/cpx}$ obtained by Le Roex (1980) are 3 and

FIGURE 7.3: Ti/Zr plotted vs $(La/Sm)_{e.f.}$ for: (a) low TiO_2 volcanics compared to (b) kimberlites, alkalic basalts, differentiated rocks and LREE-enriched peridotites. Kimberlite data from Fesq et al. (1975) and Kable et al. (1975). Basalt data from Frey et al. (1978) (Victoria); Arculus (1976) and Shimizu and Arculus (1975) (Antilles); Clague and Frey (1982) (Hawaii); and Baker et al. (1977) (Kenya). Data for Tuolumne granites from Frey et al. (1978). Data for Lashaine peridotite from Ridley and Dawson (1975) and Rhodes and Dawson (1975); Ronda peridotites from Frey and Suen (1982); and Kaptenstein peridotite (Kal67) from Kurat et al. (1980). Zr for Kal67 estimated from Hf (see text).

FIGURE 7.4: Zr/Sm plotted vs $(La/Sm)_{e.f.}$ for: (a) low TiO_2 volcanics compared to (b) kimberlites, alkalic basalts, differentianted rocks and LREE-enriched peridotites. Kimberlite data from Fesq et al. (1975) and Kable et al. (1975). Basalt data from Frey et al (1978) (Victoria); Arculus (1976) and Shimizu and Arculus (1975) (Antilles); Clague and Frey (1982) (Hawaii); and Baker et al (1977) (Kenya). Data for Tuolumne granites from Frey et al. (1978). Data for Lashaine peridotite from Ridley and Dawson (1975) and Rhodes and Dawson (1975); Ronda peridotites from Frey and Suen (1982), and Kaptenstein peridotite (Kal67) from Kurat et al. (1980). Zr for Kal67 estimated from Hf (see text).

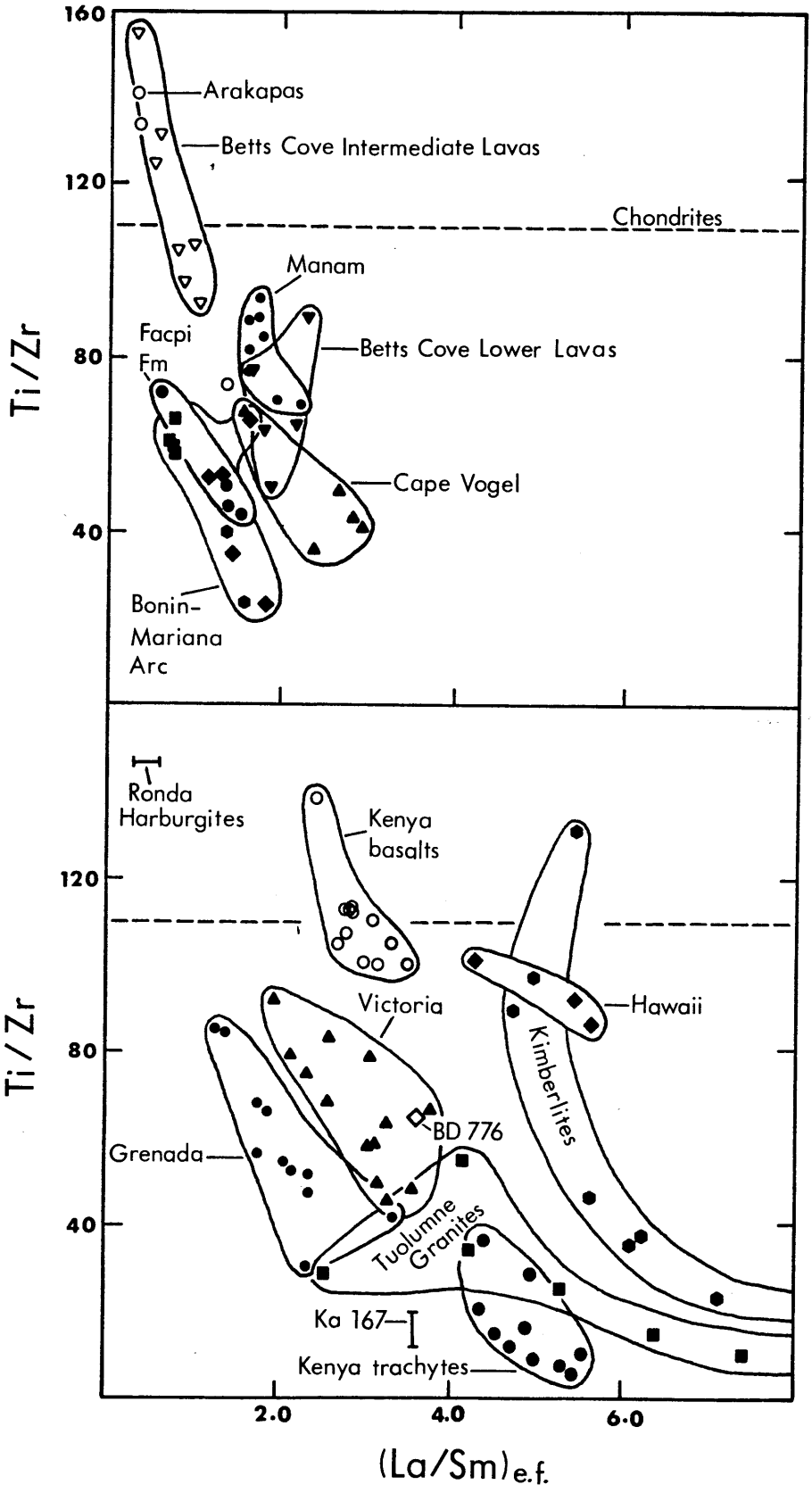
160
120
80
40
Ti/Zr
Arakapas
Betts Cove Intermediate Lavas
Chondrites
Manam
Facpi
Fm
Betts Cove Lower Lavas
Cape Vogel
Bonin-
Mariana
Arc
Ronda
Harburgites
Kenya
basalts
Victoria
Hawaii
Kimberlites
BD 776
Grenada
Tuolumne
Granites
Ka 167
Kenya trachytes
2.0
4.0
6.0
(La/Sm)e.f.

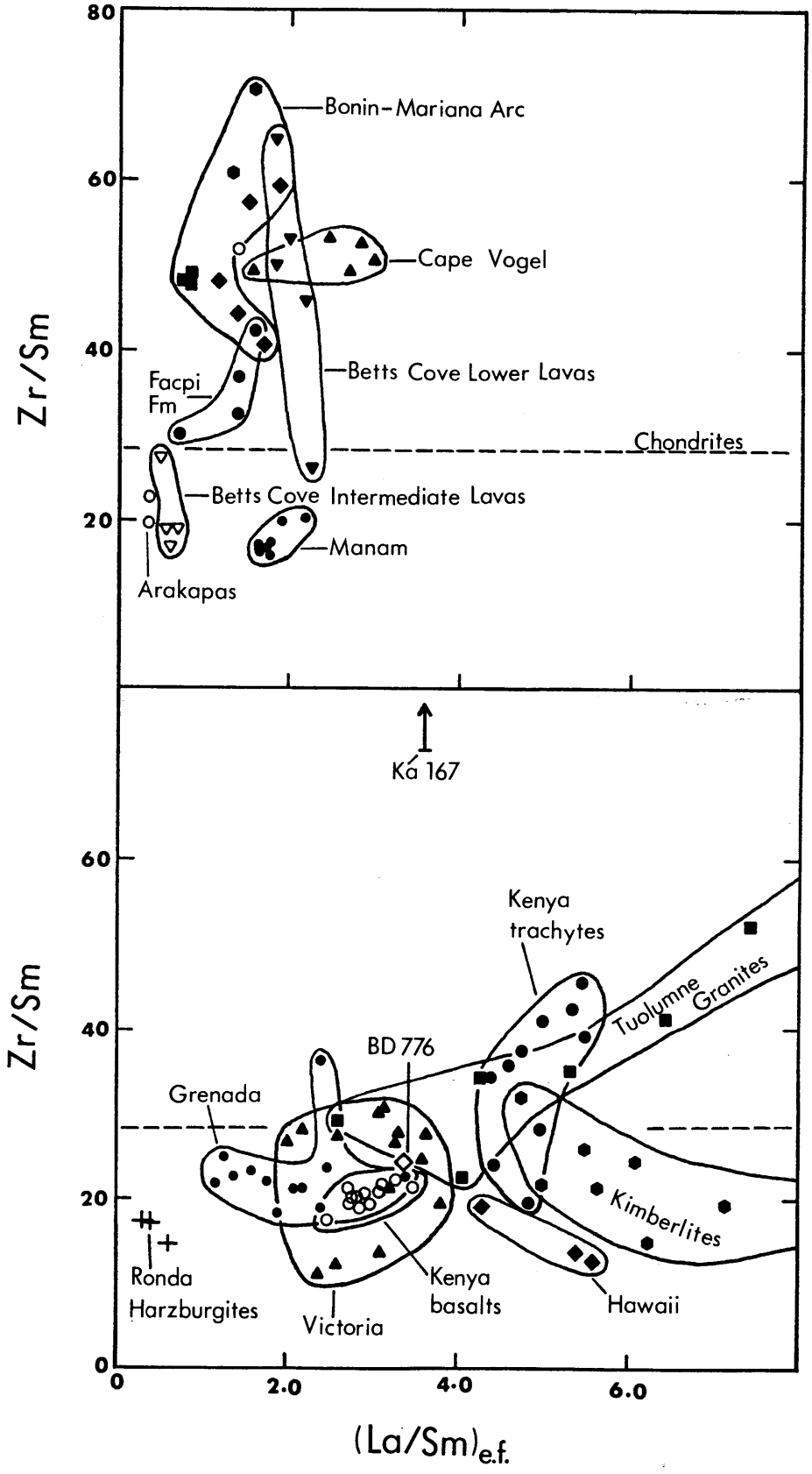
Zr/Sm
80
60
40
20
Bonin-Mariana Arc
Cape Vogel
Betts Cove Lower Lavas
Facpi Fm
Chondrites
Betts Cove Intermediate Lavas
Manam
Arakapas
Ká 167
Zr/Sm
60
40
20
0
Kenya trachytes
Tuolumne Granites
BD 776
Grenada
Kimberlites
Ronda Harzburgites
Victoria
Kenya basalts
Hawaii
0
2.0
4.0
6.0
(La/Sm)e.f.

5 respectively, and 2.7 and 5.4 using data from Shimizu and Allegre (1978). Using both sets of data, $D_{Ti}^{gt/liq}$ / $D_{Zr}^{gt/liq}$ can be estimated to be 1.5 to 1.8. Therefore, both garnet and clinopyroxene retain Ti preferentially to Zr, and as residual minerals, can result in the generation of low Ti/Zr, high La/Sm liquids during partial melting of mantle peridotite.

Relative partition coefficients for Sm and Zr are more difficult to estimate for garnet and clinopyroxene because these elements are virtually never measured on the same specimens. The range of $D_{Zr}^{cpx/liq}$ reported by Dunn and McCallum (1981) is 0.05 to 0.22. Using the average $D_{Zr}^{gt/cpx}$ from LeRoex (1980) and Shimizu and Allegre (1978), $D_{Zr}^{gt/liq}$ can be estimated to be 0.26 to 1.1. Preferred partition coefficients for Sm in clinopyroxene and garnet suggested by Frey et al. (1978) are 0.14 to 0.26 (cpx) and 0.08 to 0.22 (gt). According to these values, clinopyroxene is not expected to significantly fractionate Zr from Sm, while garnet is expected to retain Zr preferentially to Sm. This is borne out by Zr/Sm ratios in clinopyroxenes and garnets from lherzolite inclusions (Shimizu, 1975; Shimizu and Allegre, 1978), which are 8.5 - 14.9 in clinopyroxenes, similar to values for alkalic basalts, and 54 - 79 in garnets, significantly higher than values in alkalic basalts and chondrites. The lower than chondritic Zr/Sm in many alkalic basalts, and the correlation of decreasing Zr/Sm with increasing La/Sm and Zr/Ti in alkalic basalts from the Hawaiian Islands and kimberlites can also be explained by this partitioning behavior. Therefore, residual garnet and clinopyroxene can explain high La/Sm and low Ti/Zr ratios in the metasomatic material which affected the sources of boninites, but cannot account for their high Zr/Sm.

High Zr/Sm ratios are occasionally but not invariably present in highly differentiated rocks. For example, five granites used as

geochemical reference standards (Flanagan, 1973) have Zr/Sm ranging from 15 to 41. Figs. 7.3 and 7.4 show Zr/Sm, La/Sm and Ti/Zr ratios in two suites of silicic rocks in which Zr/Sm ratios reach values significantly higher than chondrites with increasing degree of differentiation: the Tuolumne Intrusive Series and trachytes and benmoreites from the Gregory Rift, Kenya. Because of the variety of minor or accessory minerals which can affect REE, Ti and Zr abundances in these rocks (e.g., hornblende, magnetite and sphene in the Tuolumne Intrusive Series, Bateman and Chappell, 1979; apatite and magnetite in the Kenyan trachytes, Baker et al., 1977), it is difficult to determine which phase or combination of phases is responsible for the increase in Zr/Sm. However, most of these minerals have been found in minor amounts in mantle peridotites. A possible explanation for the high Zr/Sm in boninites is that the LREE-enriched fluid or melt which mixed with their depleted peridotite sources separated from a residue bearing the minor or accessory minerals responsible for high Zr/Sm in the Tuolumne granites or Kenyan trachytes.

An important feature of the high Zr/Sm ratios in boninites and other low TiO_2 volcanics is that they do not correlate with La/Sm or Ti/Zr ratios. For example, in Fig. 7.4 Zr/Sm and La/Sm ratios in low TiO_2 volcanics from different areas plot in clusters or in elongate fields, but these fields do not have consistent slopes as in Fig. 7.3. As discussed in reference to Fig. 3.12d (Sm/Nd vs Zr/Nd), the lack of correlation between Zr/REE ratios and relative abundances of REE and Ti, which correlate with each other (Figs. 3.12 a-c), could result by mixing of two components with constant relative abundances of REE and Ti, but variable relative abundances of Zr. Variable abundances of Zr relative to REE and Ti in the

LREE-enriched component also points to a residual accessory mineral as the source of Zr enrichment. For example, if the residue of the LREE-enriched component included dominantly garnet and clinopyroxene but minor and variable amounts of an accessory which incorporated Sm preferentially to Zr, relatively constant La/Sm and Ti/Zr but variable Zr/Sm could result if the accessory fractionated La from Sm and Ti from Zr similarly to garnet or clinopyroxene (amphibole?), or if the accessory did not significantly fractionate La from Sm and Ti from Zr (apatite?).

According to this scheme the Ti/Zr, La/Sm and Zr/Sm ratios observed in Figs. 7.3 and 7.4 could be explained as follows. The correlation of decreasing Ti/Zr and increasing La/Sm in boninites and other low TiO_2 volcanics may result from mixing of refractory peridotite (low La/Sm and high Ti/Zr) with LREE-enriched, low Ti/Zr mantle derived fluids or melts. The La/Sm and Ti/Zr ratios in these fluids or melts are relatively constant within individual areas, but vary from area to area. The lack of correlation between La/Sm and Zr/Sm in Fig. 7.4 may result from variation of relative Zr contents in the LREE-enriched fluids or melts within individual areas, due to variable amounts of an accessory mineral which fractionates Zr from Sm in the source of the metasomatic material. Low La/Sm, high Ti/Zr lavas like those from Cyprus and some Betts Cove Intermediate Lavas (Fig. 7.3) have chondritic or less than chondritic Zr/Sm (Fig. 7.4) and may be derived from unmetasomatized depleted peridotite. LREE-enriched, low Ti/Zr lavas have Zr/Sm ranging from higher than chondritic (boninites from Site 1403) to lower than chondritic (Manam Island). The Zr/Sm ratio in these lavas varies with the Zr/Sm ratio in the LREE-enriched, low Ti/Zr metasomatic material, and the relative amounts of refractory peridotite and metasomatic component mixed.

A possible line of evidence which could support the existence of Zr-enriched mantle derived materials would be the presence of high Zr/Sm ratios in refractory peridotites which are suitable sources for low TiO_2 volcanics with respect to their REE and other HFS element abundances. Unfortunately, most analyses of these peridotites do not include Zr. Ti/Zr ratios in LREE-depleted peridotites from Ronda range from 100 to 240, and Zr/Sm from 14 to 24 (Frey and Suen, 1982) and support the conclusion that low Ti/Zr and high Zr/Sm are not characteristic of refractory peridotites. Extremely LREE-enriched peridotites from Lashaine, Tanzania have variable Ti/Zr ratios (39-159), but a low Ti/Zr samples also analyzed for REE has near chondritic Zr/Sm (Figs. 7.3 and 7.4), as do the host lavas (Rhodes and Dawson, 1975; Ridley and Dawson, 1975). Harzburgites studied by Kurat et al. (1980), Stosch and Seck (1980) and Tanaka and Aoki (1981), which have U-shaped REE patterns, may be the most useful for evaluating the source of Zr enrichment in boninites. Zr data is not reported for these peridotites. However, using Zr/Hf ratios in the range reported in chondrites and MORB's (30-50), which is similar to the range found in Zr-enriched, low TiO_2 volcanics (33-51), a harzburgite analyzed for Hf and REE by Kurat et al. (1980) would be predicted to have low Ti/Zr (12-20) and Zr/Sm (73-121) (Figs. 7.3 and 7.4).

No definite conclusions can be formed on the basis of this data. More and better Zr data for peridotites and Zr partitioning data is required to resolve the source of Zr-enrichment in boninites and other low TiO_2 volcanics. Based on the geochemically coherent behavior of Zr with REE and other HFS elements, and the lack of correlation between Zr enrichment and other chemical variables, the tentative conclusion of this thesis is that

Zr is introduced into the refractory peridotite sources of low TiO_2 volcanics with LREE by mantle derived fluids or melts. Fractionation of LREE from intermediate and HREE, and of Zr from Ti in this material could result from separation from garnet and/or clinopyroxene bearing residua. Fractionation of Zr from Sm requires an unkown accessory phase.

DERIVATION OF K, Rb, Ba AND Sr FROM SUBDUCTED MORB AND SEDIMENT

The low TiO_2 arc volcanics studied in this thesis, as well as many other arc volcanics, are characterized by high abundances of K, Rb, Ba and Sr relative to REE and HFS elements (Figs. 3.6, 4.5, and 5.6). Lavas from Manam Island (Chapter 5) have high abundances of Pb relative to REE and elements, but Pb concentrations in other low TiO_2 volcanics have not been measured. Except for some boninites, which have exceptionally high $^{87}Sr/^{86}Sr$ compared to oceanic volcanics, Sr, Nd and Pb isotopic compositions in the low TiO_2 volcanics studied are not significantly different from those in oceanic volcanics (Figs. 3.11, 3.15, 4.8, 4.10, 5.9 and 5.12). The source of enrichment in K, Rb, Ba and Sr and in some cases Pb, which is not characteristic of oceanic volcanics, combined with isotopic compositions similar to oceanic volcanics, is a problem with implications for nearly all island arc volcanics.

The simplest explanation for enrichment in K, Rb, Sr and Ba is that these elements are derived from mantle sources by some process which fractionates K, Rb, Ba and Sr from REE and HFS elements. Several lines of evidence, discussed in earlier chapters, suggest that mantle sources are not involved: 1) absolute and relative abundances of K, Rb, Ba and Sr are decoupled from absolute and relative abundances of REE and HFS elements,

which are best explained by mantle metasomatism of refractory peridotite. In lavas from Manam Island, $^{87}Sr/^{86}Sr$ ratios do not correlate with $^{143}Nd/^{144}Nd$, although the lavas plot within the mantle array, and although the $^{87}Sr/^{86}Sr$ ratios correlate with trace element ratios involving K, Rb, Ba and Sr. Therefore, if mantle metasomatism is responsible for high abundances of K, Rb, Ba and Sr in these low TiO_2 volcanics, at least two metasomatic episodes are required, one involving LREE and another involving K, Rb, Ba and Sr; 2) extremely high abundances of K, Rb and Sr relative to REE and HFS elements are restricted to island arc volcanics and in island arc volcanics it is an extremely common feature (e.g., Arculus and Johnson, 1981). This points to a subduction related source for these elements. Among mantle derived liquids, enrichment in Sr and Ba are found only in carbonatites (high Sr/Nd) and kimberlites (high Ba/La). Mantle metasomatism by liquids such as these could account for enrichment in K, Rb, Ba and Sr in arc volcanics. However, since enrichment in these elements is not characteristic of oceanic volcanics, and high Sr/Nd is not characteristic of continental volcanics, this implies that there is a relationship between kimberlitic and/or carbonatitic metasomatism and subduction; 3) enrichments in K, Rb, Ba and Sr relative to REE and HFS elements are not common in metasomatized peridotite nodules. This situation is different from that discussed earlier for Zr enrichment, because K, Rb, Ba and Sr data are available for these rocks. Like continental basalts (Fig. 5.14), high Ba/La ratios have been reported in LREE enriched peridotite nodules (Tanaka and Aoki, 1981), but high Sr/Nd is extremely uncommon, e.g., values of 9-19 are found in LREE-enriched peridotites from Victoria, Australia (Chen, unpublished data; Burwell, 1974); Dreiser Weiher, West Germany (Jagoutz et al., 1979) and two samples

from Lashaine, Tanzania (Ridley and Dawson, 1975). Two Lashaine peridotites have high Sr/Nd of 26 and 50, as does the carbonatite host lava (170, Ridley and Dawson, 1975).

Therefore, in arc volcanics the decoupling of K, Rb, Ba and Sr abundances from abundances of elements more clearly related to mantle metasomatism, and the rarity of enrichment in K, Rb, Ba and Sr relative to REE and HFS elements in oceanic volcanics and metasomatized peridotite nodules indicates that this enrichment does not result from mantle metasomatism. A subduction related source is preferred for these elements.

The hypothesis of this thesis is that enrichment in K, Rb, Ba and Sr in low TiO_2 volcanics results from a component enriched in K, Rb, Ba and Sr relative to REE and HFS elements, derived from subducted MORB and sediment, in which the MORB contribution is dominant. In boninites, which have exceptionally high K/Ba and Rb/Ba ratios, in addition to high Ba/La and Sr/Nd, and some cases extremely high $^{87}Sr/^{86}Sr$, another component, derived by dehyration of basaltic alteration products with trace element and isotopic characteristics resembling seawater, is also suggested. This model is essentially a combination of models proposed by other researchers to explain high abundances of K, Rb, Ba and Sr in arc volcanics: Kay (1980), subducted seawater and sediment; DePaolo and Johnson (1979), a high Sr/Nd volatile phase derived from subducted MORB. These models individually cannot explain high abundances of these elements and the Sr, Nd and Pb isotopic compostions observed in low TiO_2 volcanics.

Arguments against derivation of enrichment in K, Rb, Ba and Sr in arc volcanics by interaction of mantle derived magmas with lower continental or island arc crust, as proposed by Arculus and Johnson (1981), are given in Chapter 5. An additional observation against such a source which can be made at this point is that while all low TiO_2 arc volcanics studied have enrichments in K, Rb, Ba and Sr relative to REE and HFS elements, many, and in particular Facpi Formation lavas, which are among the oldest in the Mariana Arc system, are from areas where well developed lower crust is unlikely to be present.

The choice of mixing of components with high K, Rb, Ba and Sr derived from subducted MORB and sediment to explain the high abundances of these elements in arc volcanics is thus based in part on arguments against other source materials. Positive arguments for this model are: 1) evidence from Manam Island lavas that mixing of two high Sr/Nd materials with the geochemical characteristics of MORB and sediments are involved in the generation of these lavas (Chapter 5), and that relative abundances of K, Rb, Ba and Sr to each other and to REE and HFS elements in Manam lavas are typical of island arc tholeiites (Fig. 4.13); and 2) that mixing of MORB and sediment can explain Sr and Pb isotopic characteristics of many island arc volcanics (e.g., Kay, 1980; Hawkesworth, 1982). Such MORB - sediment mixing models are frequently rejected because they cannot explain Nd isotopic characteristics or elemental abundances in island arc volanics. Derivation of Sr and Pb in arc volcanics from high Sr/Nd and Pb/Nd components derived from subducted MORB and sediment is a possible solution to these problems.

For the low TiO_2 volcanics studied, this model rests on two untested processes: 1) that K, Rb, Ba and Sr can be fractionated from

REE and HFS elements in subducted materials, and 2) that the proportion of these elements derived from subducted MORB can be high relative to the contribution from subducted sediment. Possible processes for the generation of K, Rb, Ba and Sr enriched materials from subducted basalt and sediment are discussed in Chapters 3 and 5. Basically, it is suggested that volatile rich fluids or melts released from the subducted oceanic crust may preferentially concentrate these elements relative to REE and HFS elements. Although there is little experimental evidence to support this proposal, the occurrence of high abundances of these elements compared to REE and HFS elements in volatile rich, mantle derived fluids such as kimberlites and carbonatites may indicate that volatile transport is a viable process for enrichment in these elements.

A high MORB - sediment ratio is a critical feature of this model, especially for volcanics such as those from Manam Island which plot within the mantle array. In Chapter 5 it was estimated that a MORB component: sediment component proportion of 60:1 to 110:1 was required to explain the Sr and Pb isotopic composition of the Manam sample with the largest apparent sediment contribution. This estimate is a factor of 2 to 4 higher than an estimate of the presubduction composition of the oceanic crust (30:1, Nohda and Wasserburg, 1981), but is explicable if some oceanic sediments are not subducted, as has been proposed by numerous island arc researchers.

An important observation supporting this model is that many arc volcanics lie on MORB - sediment mixing lines on Pb - Pb isotope diagrams, as noted by Sun (1980), Kay (1980) and Hawkesworth (1982). Such volcanics include tholeiitic low TiO_2 lavas from Manam and the Facpi Fm., Guam, and

tholeiites from the Aleutians and Tonga, which have similar relative K, Rb, Ba and Sr abundances to those in the Facpi and Manam tholeiites (Fig. 4.13). Aleutian lavas, like Manam, plot within the mantle array (Perfit et al., 1981). Interpretations of these lavas which suggest that they are derived wholly or predominantly by partial melting of MORB and sediment, during which Pb, Sr and Nd are not fractionated, cannot simultaneously explain Pb - Pb isotope diagrams, which suggest MORB - sediment mixing, and Sr - Nd isotope diagrams, which suggest mantle derivation, and the relative abundances of these elements. On Nd - Sr isotope correlation diagrams, MORB - sediment mixing lines will diverge significantly from the mantle array (e.g., Fig. 7.5), unless the sediment endmember has lower Sr/Nd than the MORB endmember (e.g., has no carbonate component). In this case, simple MORB - sediment mixing could not account for enrichment in Sr relative to Nd, which is characteristic of these volcanics.

The model suggested here is that components with high K, Rb, Ba, Sr and Pb abundances compared to REE and HFS elements are derived from both subducted MORB and sediment, and mix with mantle peridotite with trace element and isotopic characteristics of the sources of oceanic island lavas. Nd-isotope, and REE and HFS element abundances are dominated by the mantle source, while Sr and Pb isotope, and K, Rb, Ba, Sr and Pb abundances are dominated by MORB - sediment mixes. On Nd - Sr isotope correlation diagrams volcanics derived from such sources will plot on strongly curved mixing lines between their mantle component, and points on mixing lines between MORB and sediment (Fig. 7.5). Since the process by which high Sr/Nd components are derived from subducted MORB and sediment is poorly characterized, there is no basis for determining the relative Sr/Nd ratios in MORB and sediment components. This feature could also vary from

subduction zone to subduction zone, or with changes in P - T conditions within a single subduction zone. Therefore, MORB - sediment mixing lines could curve in either direction around a straight line between MORB and sediment (Sr/Nd equal, Fig. 7.5). In one case (MORB Sr/Nd < sediment Sr/Nd, curve 3, Fig. 7.5), lava compositions plotting within the mantle array could result from near coincidence of the Sr-isotopic compositions of the mantle and MORB plus sediment components. In the second case (sediment Sr/Nd < MORB Sr/Nd, curve 1, Fig. 7.5), both Sr- and Nd-isotopic compositions of the mantle and MORB plus sediment components could coincide. The important feature of this model is that, unlike two component mixing, Sr-isotopic composition will not necessarily correlate with enrichment in K, Rb, Ba and Sr relative to REE, either within a single arc suite or between suites, as is observed in arc volcanics (Arculus and Johnson, 1981), because both MORB and sediment components are enriched in K, Rb, Ba and Sr relative to REE. Enrichment in K, Rb, Ba and Sr relative to REE may vary with addition of either component or both together.

On Pb - Pb isotope diagrams, according to this model, arc volcanics should plot on mixing lines between their mantle sources and points on MORB - sediment mixing lines. Since Pb-isotope compositions for possible mantle sources overlap significantly with hypothetical MORB - sediment mixtures, and do not necessarily correlate with Nd- or Sr-isotopic composition, the interpretation of the Pb-isotope compositions of arc volcanics in terms of these three components is more difficult than on Sr - Nd isotope correlation diagrams. Low TiO_2 arc tholeiites from Manam Island and the Facpi Fm., and many arc volcanics, plot directly on possible MORB - sediment mixing lines (Fig. 7.6). This could result if nearly all the Pb

FIGURE 7.5: Mixing of high Sr/Nd materials derived from MORB and sediment, with an oceanic mantle component, to account for the high Sr/Nd but variable Sr and Nd isotopic characteristics in island arc volcanics.

Example MORB - sediment mixing lines are calculated: (1) MORB Sr/Nd = 4 X Sediment Sr/Nd; (2) MORB Sr/Nd = Sediment Sr/Nd; and (3) MORB Sr/Nd X 4 = Sediment Sr/Nd.

Mixing lines are drawn between a mantle component with Sr/Nd = 20 and MORB-sediment mixtures with: (1) MORB Sr/Nd = 600, Sediment Sr/Nd = 150; and (3) MORB Sr/Nd = 150, Sediment Sr/Nd = 600. Such mixtures may or may not coincide with the mantle array, but all will have high Sr/Nd. For example, all points marked on mixing lines all have Sr/Nd = 50.

FIGURE 7.6: Pb - Pb isotope diagram showing range of possible MORB - sediment mixtures, tholeiitic arc basalts, including samples from Manam Island and the Facpi Fm., Guam, and boninites and a "boninite series" lava from the Facpi Fm., Guam. Tholeiitic arc basalts plot within the range of MORB-sediment mixtures, therefore the oceanic crustal component may be dominant in the Pb isotopic composition of these volcanics volcanics. Boninites and the Facpi "boninite series" lava plot outside the range of MORB - sediment mixtures, and may contain a smaller contribution to Pb from the oceanic crustal component, and a larger contribution from the mantle component than tholeiitic lavas.

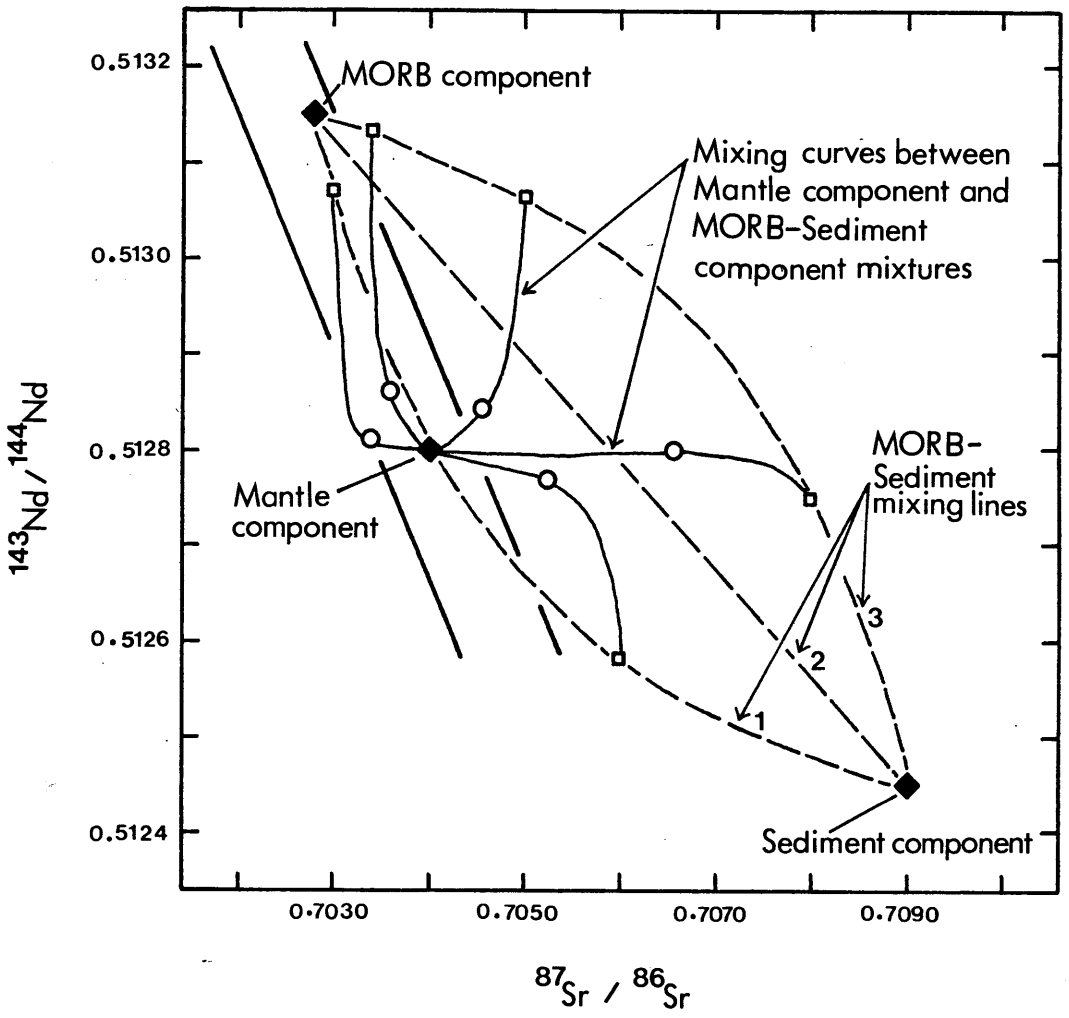
0.5132
0.5130
0.5128
0.5126
0.5124
$^{143}Nd / ^{144}Nd$
0.7030
0.7050
0.7070
0.7090
$^{87}Sr / ^{86}Sr$
MORB component
Mixing curves between Mantle component and MORB-Sediment component mixtures
MORB-Sediment mixing lines
Mantle component
Sediment component
1
2
3

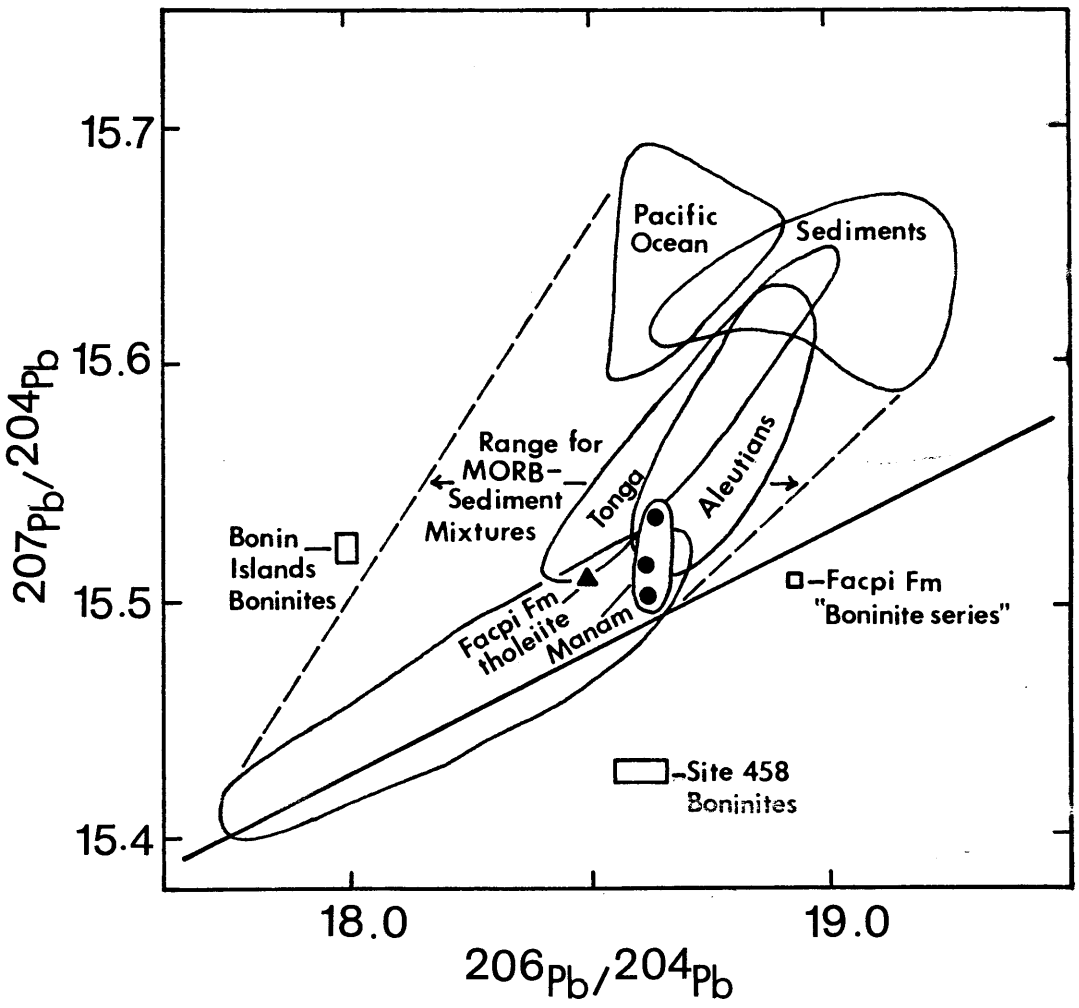
15.7
15.6
15.5
15.4
18.0
19.0
$^{207}Pb/^{204}Pb$
$^{206}Pb/^{204}Pb$
Pacific Ocean
Sediments
Range for MORB–Sediment Mixtures
Tonga
Aleutians
Bonin Islands Boninites
Facpi Fm tholeiite
Manam
Facpi Fm "Boninite series"
Site 458 Boninites

in these volcanics is contributed by the MORB plus sediment component, or if the Pb-isotopic composition of their mantle sources is similar to MORB's, or both of these possibilities. In the case of Manam, for which Pb concentration data are available, it was estimated that more than 90% of the Pb in these volcanics is derived from the MORB - sediment mixture (Chapter 5), which is consistent with the first interpretation above, but does not necessarily contradict the second.

A potential problem with this model is demonstrated by boninites from the Bonin Islands, DSDP Site 458, and a "boninite series" lava from the Facpi Fm., which do not plot on MORB - sediment mixing lines. If the MORB plus sediment component contributes most of the Pb in these volcanics (e.g., if they are found to have high Pb/REE), the Pb-isotopic compositions of these volcanics could be explained by this model, but with difficulty. For example, Bonin Island boninites could lie on a mixing line between an extremely non-radiogenic MORB (i.e., less radiogenic than the MORB field shown in Fig. 7.6) and sediments, although this would imply a similar origin for Pb in alkalic basalts from Oki Dogo and Takashima (Fig. 3.15). Site 458 boninites could contain a Pb component derived virtually entirely from a MORB endmember with Pb-isotopic composition similar to that measured in a basalt from the eastern side of the Mariana Trench (Fig. 3.15; Meijer, 1976). A high contribution from MORB compared to sediment in Site 458 boninites is qualitatively consistent with the low average $^{87}Sr/^{86}Sr$ of their "anomalous" Sr component (Table 3.6). The Pb-isotopic composition of the Facpi "boninite series" lava can be explained by this model only if the Pb-isotopic composition of its "MORB" component is more radiogenic than in MORB's, e.g., like that in seamount basalts from the east Pacific Ocean (Church and Tatsumoto, 1975).

A more general solution to this problem is that the Pb-isotopic compositions of boninites and the "boninite series" Facpi lava are dominated by the Pb-isotopic composition of their mantle components. This suggestion would be borne out if Pb/REE ratios in these volcanics are found to be low. Since these lavas also differ from other arc volcanics in having much higher K/Ba and Rb/Ba, which is interpreted as the result of a difference in the composition of fluids derived from the subducted oceanic crust for these lavas, a possible connection between these two features will be suggested and incorporated into the model in the next section. However, if Pb concentrations in boninites and Facpi "boninite series" lavas are found to be very high relative to REE and HFS elements, earlier interpretations of their Pb-isotope characteristics in terms of MORB - sediment mixing, or possible mantle sources for enrichment in Pb relative to REE will have to be reconsidered.

ENRICHMENT IN K AND Rb IN BONINITES

A major trace element characteristic of boninites which distinguishes them from other island arc volcanics is their enrichment in K and Rb compared to Ba and Sr (Fig. 3.8). In Chapter 3, this feature was linked to a contribution to the sources of these lavas from fluids released through the breakdown during subduction of basaltic alteration products which, like seawater, have high K/Ba, K/Sr, Rb/Ba and Rb/Sr ratios (Staudigel et al., 1978; Staudigel et al., 1981). A "seawater" contribution to these lavas is also supported by the high $^{87}Sr/^{86}Sr$ in some boninites. Additional evidence is the atmospheric $^{3}He/^{4}He$ ratio measured in a boninite not studied in this thesis (Bloomer et al., 1979), which supports a seawater source for volatile elements in boninites.

In Chapter 4 it was observed that enrichment in K and Rb relative to Ba could be correlated with differences in major element composition between the two groups of Facpi Fm. lavas, and boninites. K/Ba and Rb/Ba ratios are highest in boninites, lower in Facpi "boninite series" lavas, and lowest in Facpi tholeiite series lavas, which are like the majority of island arc tholeiites. Decreasing values of these ratios therefore correspond to decreasing SiO_2 content and increasing CaO and Al_2O_3 content in rocks of similar MgO content and Mg/(Mg + ΣFe). According to experimental studies on melting conditions required to generate boninites, these major element changes could be produced in several ways, e.g., at similar pressures, the boninites could be produced by hydrous partial melting, and the basalts by low-H_2O to anhydrous partial melting, or, at similar degree of water saturation, the boninites could be produced by partial melting at low pressure, and basalts by partial melting at higher pressure. The correspondence between major element changes related to water content or pressure of melting, and trace element variable linked to seawater or the dehydration of hydrous minerals is extremely important, and could be related in the following ways: 1) the peridotite source of boninites, which have high K/Ba and Rb/Ba ratios, could contain a larger amount of the "seawater" component (including H_2O) than the sources of basaltic low TiO_2 arc lavas, or 2) the sources of boninites may be located in a specific part of the mantle wedge, overlying the point where the high K/Ba, high Rb/Ba component is released by dehydration of basaltic clays, while the sources of basaltic low TiO_2 arc lavas are located at greater depths where H_2O is released by dehydration of other phases. Since a refractory peridotite source is indicated for all low TiO_2 arc volcanics,

the second model above is preferred, because the presence of H_2O will facilitate and may be essential for partial melting.

If the difference in K/Ba and Rb/Ba ratios in boninites and Facpi "boninite series" lavas, and basaltic low TiO_2 lavas (Manam Island and the Facpi tholeiite series lavas) results from changes in the composition of fluids released from the subducted oceanic crust at different pressures, then it is also possible that the smaller Pb component derived from subducted MORB and sediment proposed to explain the Pb-isotopic characteristics of boninites and the Facpi "boninite series" lava also could be related to such a process. Fluids relaeased at low pressure (boninite sources) may have lower Pb contents than fluids released at high pressures (basalt sources). This suggestion is purely speculation, but is a possible explanation of the data.

A general model for the development of sources for low TiO_2 arc volcanics is shown in Fig. 7.2. The sequence of events leading to the formation of these sources can be summarized: 1) the generation of depleted peridotite at a midocean spreading center (Fig. 7.2a-1); 2) metasomatic enrichment in LREE and in some cases Zr, by fluids or melts derived from mantle sources similar to the sources of oceanic island volcanics (Fig. 7.2a-2); 3) entrapment of this peridotite within the overlying plate of a subduction zone (Fig. 7.2a-3); 4) metasomatism of this peridotite by H_2O-rich fluids with high abundances of K, Rb, Sr and Ba relative to REE, derived from subducted MORB and sediment (Fig. 7.2b). Fluids released at shallow depths have high K/Ba and Rb/Ba ratios, resulting from the breakdown of basaltic clays with these trace element characteristics, and may have low Pb contents. Fluids released at greater

depths have lower K/Ba and Rb/Ba ratios and high Pb contents. Shallow level peridotites have trace element and isotopic characteristics appropriate for boninites, and should give rise to SiO_2-rich liquids if partially melted. Deeper lever peridotites have trace element and isotopic compositions appropriate for tholeiitic low TiO_2 volcanics and should give rise to basaltic partial melts.

TECTONIC MODELS FOR THE GENERATION OF LOW TiO_2 ISLAND ARC VOLCANICS

REQUIREMENTS FOR PARTIAL MELTING OF REFRACTORY PERIDOTITE:

The basic geochemical model proposed in this thesis for low TiO_2 arc volcanics is that they are derived by partial melting of mantle peridotite with minor addition of material from the subducted oceanic crust (e.g., volatiles, volatile-rich melts). This conclusion is at odds with current thermal models of subduction zones. As noted by Wyllie (1979) and Gill (1981), partial melting of the peridotite wedge overlying a subducted oceanic plate without partial melting of the oceanic plate is not likely under normal conditions. According to Gill (1981), partial melting of peridotite alone could occur at about 80 km depth, but only if the peridotite contains an extremely H_2O-rich vapor and the adjacent subducted oceanic slab is unusually cool. This requires an extremely high thermal gradient between the slab and mantle peridotite.

The conclusion that low TiO_2 arc volcanics are derived from refractory peridotite is an additional difficulty. For example, hydrous fertile peridotite solidi can be as low as about 1000° C at 10-30 kbar pressure (e.g., Wyllie, 1979). The water-saturated liquidus determined by Green (1973; 1976) for experimental liquids similar to boninites produced by high degrees of partial melting at 10 kbar was 1200° C. Since water-saturated partial melting is not likely in a natural environment, 1200° C probably represents the minimum possible melting temperature for liquids derived from refractory peridotite (i.e., generated at high degrees of partial melting). Therefore, derivation of low TiO_2 arc volcanics from refractory peridotite without significant slab involvement requires unusually high

temperature in the subarc peridotite wedge, in addition to unusually low temperatures in the subducted oceanic plate.

For basaltic low TiO_2 volcanics, like lavas from Manam Island and tholeiites from the Facpi Formation, Guam, a subduction zone model with the restrictions described above could be feasible since the major element composition of these lavas is consistent with moderate to high pressure melting. For boninites, experimental evidence suggests low pressure melting (<10 kbar, Green, 1973; 1976; Jenner and Green, in prep.). This requires peridotite temperatures of >1200° C within 30 km of the surface, and is inconsistent with normal geotherms inferred for oceanic plates (Solomon, 1976).

THERMAL MODELS FOR LOW PRESSURE MELTING IN SUBDUCTION ZONES:

Two models have been proposed to explain the generation of boninites at low pressures: that of Meijer (1980) and Crawford et al. (1981). Both these models were proposed specifically to explain the occurrence of boninites in the Mariana Arc region between 28 and 34 m.y.b.p., and to explain the change from tholeiitic to boninitic volcanism observed at DSDP Site 458.

In the model of Meijer (1980), high temperatures required to produce partial melting of refractory peridotite were present at shallow depths in the subarc mantle wedge because the Philippine Basin, which formed the overlying plate of the Palau-Kyushu subduction zone, was extremely young (37-60 m.y.b.p., Scott et al., 1980). Meijer (1980) suggested that in the early stages of subduction of the Pacific plate under the Philippine Sea at about 45 m.y.b.p., tholeiitic volcanics were generated by anhydrous

partial melting. After sufficient water from the subducted Pacific plate had infiltrated the peridotite residue of the early tholeiitic volcanism, boninites were generated by hydrous partial melting.

The plate configuration proposed in this model includes the requirements outlined above for generation of partial melting from depleted peridotite. The overlying peridotite wedge is abnormally hot because of its youth, the older (150 m.y.) subducted Pacific plate is cold, and volcanism occurs shortly after the initiation of subduction, such that the two plates may not have equilibrated thermally. The age of the Philippine Basin is not well constrained, but using the 37-60 m.y. range suggested by Scott et al. (1980), an age of about 7-30 m.y. can be inferred at the time of boninite generation. Using the cooling oceanic plate model of Forsyth (1976), the minimum 1200° C temperature for boninite generation could have been present at depths of 30 to 70 km (10-20 kbar). Therefore Meijer's (1980) model has the minimum essential elements required to explain boninite volcanism in the Mariana Arc.

In the model of Crawford et al. (1981), boninites are generated by partial melting of refractory, hydrous peridotite at shallow depths by heat conducted from rising MORB-source peridotite diapirs in the incipient stages of back arc spreading. Arc tholeiites are generated earlier by "normal" arc volcanism, and boninites are generated from the peridotite residue of the tholeiites plus volatiles derived from the subducted oceanic crust.

Crawford et al. (1981) based their model on the possible correlation in time between boninite volcanism (28-34 m.y.b.p.) and the rifting of the Palau-Kyushu Arc (about 29 m.y.b.p.). Thermally this model

is an effective way to generate boninites. Contact of hot dry peridotite with cooler, hydrous peridotite could produce partial melting in the hydrous peridotite. A possible difficulty in this scheme is that experimental studies on MORB's suggest formation of MORB magma at depths of 60-70 km (Duncan and Green, 1980) or 50 km (Wyllie, 1979). Passage of MORB magma, or partially molten peridotite through hydrous peridotite at the 30 km depth inferred for boninites could also result in partial melting, but it is unclear if this process would result in two discrete magma types.

A third model with possible importance in understanding the generation of boninites is the model of Duncan and Green (1980), which was proposed mainly to explain the existence of low TiO_2 lavas in ophiolites. In Duncan and Green's (1980) model, low TiO_2 lavas are generated directly by anhydrous partial melting of the peridotite residue of earlier normal MORB extraction at mid ocean ridges, due to the continued uprise of these refractory peridotite diapirs to extremely shallow depths. Duncan and Green (1980) propose that uprise of the MORB-residue diapirs results in "second stage melting" at 5-25 km depths, and generates low TiO_2 lavas in an off-axis position relative to the main spreading ridge. Because of low pressure melting these second stage lavas have high SiO_2 contents, like those in the Troodos Upper Pillow Lavas. Duncan and Green (1980) do not present experimental evidence that second stage melting occurs, but suggest this process as a possible explanation for the presence of low TiO_2 lavas and extremely refractory cumulate sequences in some ophiolites.

COMPARISON OF THERMAL MODELS WITH OCCURRENCES OF LOW TiO_2 VOLCANICS:

The processes suggested above to explain the generation of partial melts from refractory peridotite can be outlined: 1) addition of H_2O to recently formed (hot) oceanic upper mantle due to the subduction of old oceanic crust under or near an oceanic spreading center (Meijer, 1980); 2) passage of hot, anhydrous peridotite through a region of hydrous peridotite in the initial stages of backarc spreading; and 3) anhydrous remelting of rising refractory peridotite diapirs generated at mid ocean ridges due to decompression. When compared to actual occurrences of boninites and low TiO_2 volcanics each of these models contain elements which are useful in explaining the generation of these rocks.

Mariana - Bonin Arc: Because of the correspondence in time between the rifting of the Palau-Kyushu Arc and K/Ar and stratigraphic ages of boninites in the Bonin - Mariana Arc, the model of Crawford et al. (1981) is the most convincing explanation for these boninites. The model of Meijer (1980), although feasible, does not account in detail for the eruption of boninites along the length of the arc within a relatively restricted period of time. In Meijer's (1980) model boninites are generated by addition of water to hot mantle peridotite, while in Crawford et al.'s (1981) model boninites are generated by heating of hydrous peridotite. Therefore, in Meijer's (1980) model, the generation of boninites at 28-34 m.y.b.p. would be associated with an influx of water to the subarc mantle wedge along the length of the Palau-Kyushu Arc. While there is no evidence that this did not occur, the initiation of backarc spreading along the Palau-Kyushu Arc at this time is better established.

The potential problem with the model of Crawford et al. (1981) mentioned above, that of the depth of MORB magma separation, may be resolvable using the model of Duncan and Green (1980). If diapirs of refractory, MORB-residue peridotite continue to rise through the upper mantle after MORB magma separation these may also be potential sources of heat for melting of refractory, hydrous peridotite at shallow depths within a subduction zone. This modification of the Crawford et al. (1981) model also might explain why MORB basalts (or back-arc basin basalts) do not overlie boninites at DSDP Site 458.

Although less convincing than the model of Crawford et al. (1981) for generation of boninites in the Mariana - Bonin Arc system at 28-34 m.y.b.p., the model of Meijer (1980) provides a better explanation for the occurrence of boninite-like lavas of the Facpi Formation on Guam at 44 m.y.b.p.. According to tectonic reconstructions of the Philippine Sea region, the West Philippine Basin formed by spreading around a center now marked by the Central Basin Fault Zone (e.g., Karig, 1975). In the tectonic reconstructions of Meijer (1980) and Karig (1975), Guam is located at the point at which the Philippine Basin spreading center intersected the Palau-Kyushu subduction zone. At the time of eruption of the Facpi Formation lavas this locale would be characterized by underthrusting of the old Pacific plate beneath extremely young oceanic upper mantle, possibly an active spreading center (Scott et al., 1980).

Using the models of Meijer (1980) and Crawford et al. (1981), a possible scenario for generation of boninites and other low TiO_2 lavas in the Bonin - Mariana Arc system could be:

1) early generation of Facpi Formation lavas on Guam at 44 m.y.b.p., shortly after the initiation of subduction of the Pacific plate beneath the extremely young, hot oceanic upper mantle near the Philippine basin spreading center. Partial melting is initiated by the infiltration of volatiles released from the subducted plate into the hot peridotite;

2) generation of boninites at 28-34 m.y.b.p. on the Bonin Islands and at various locations between DSDP Site 458 at 18° N and Dredge Site 1403 at 13° N, by uprise of hot peridotite diapirs, which eventually led to rifting of the Palau-Kyushu Arc and formation of the Shikoku and Parece Vela Basins, into the peridotite wedge beneath the Palau-Kyushu Arc, which had been hydrated by volatiles released from the subducted Pacific plate since the initiation of subduction at about 45 m.y.b.p.

Papuan Low TiO_2 Volcanics: Comparison of the Papuan low TiO_2 volcanics of the western Bismarck Arc (Manam Island) and Cape Vogel with the thermal models discussed above is more difficult because the tectonics of this area are not as well constrained as the Philippine Sea - Mariana Arc region.

For Manam Island, which is currently active, the situation is more amenable to interpretation. According to Johnson and Jaques (1980), the island and other north coast islands may be situated on Bismarck Sea crust, northward of an older island arc represented by the Coastal Ranges of Papua New Guinea which collided with the Australian continental plate in the Oligocene - Miocene. The plate subducted during this earlier phase of arc

volcanism is not well defined geophysically and may be vertical. In this situation, the geochemical problems associated with partial melting of peridotite without melting of the subducted slab are not present. A two - stage model could be proposed for Manam: 1) addition of materials derived from the subducted slab (but not large scale melting) during the earlier stage of active subduction, and 2) later melting of the "preconditioned" mantle peridotite at a significant distance from the subducted slab after collision of the older arc with the continent and steepening of the slab. This model is similar to that proposed by Johnson et al. (1978) to explain Quaternary volcanism in eastern Papua where there is no active subduction, and chemically it is similar to that of Crawford et al. (1981), in that the chemical characteristics of the sources of the volcanics are formed during subduction, but melts are generated only during a later heating event unrelated to subduction.

The critical aspect of the model, therefore, is the reason for the initiation of melting of the preconditioned peridotite after subduction had ceased. Johnson et al. (1978) also were confronted with this question in their model for volcanism in eastern Papua and suggested that diapirism and partial melting were initiated by heat from radioactive decay of K, Th and U in the enriched peridotite sources. For Manam and the north coast islands, proximity to a divergent plate margin in the Bismarck Sea (Fig. 5.1) suggests that the models of Meijer (1980) or Crawford et al. (1981) may be applicable. For example, the Bismarck Sea upper mantle beneath the islands may be young and hot such that migration of volatile-rich fluids released from the subducted slab during the earlier period of subduction into this region would produce partial melting. Alternatively, diapirism

along the northwestern segment of the divergent margin (Fig. 5.1), may have heated preconditioned mantle beneath the islands sufficiently to initiate partial melting. The late Pliocene age of the volcanoes (Johnson and Jaques, 1980) at least corresponds in age to a period of active spreading in the eastern part of the Bismarck Sea, beginning at ~3.5 m.y.b.p. (Taylor, 1979). A better understanding of the tectonic evolution of this area is necessary to test the veracity of these models. However, the general location of the north coast islands, at the edge of a young marginal basin with a possibly active divergent margin in close proximity is comparable to occurrences of low TiO_2 volcanics in the Mariana - Bonin Arc system.

Explanation of the generation of boninites at Cape Vogel, Papua New Guinea is difficult, in part, because the age of these volcanics is disputed. The K/Ar age obtained from one sample of 28 m.y.b.p. places the eruption of the Cape Vogel boninites and other Dabi volcanics in a tectonically poorly-characterized period between emplacement of the PUB (Papuan Ultramafic Belt) in the Eocene (Davies, 1977) and the opening of the Woodlark Basin at ~20 m.y.b.p. (Lydendyk et al., 1973). Current volcanism in southeastern Papua is also unaccompanied by subduction, but is of a different chemical character (calc-alkaline to alkaline) (Johnson et al., 1978).

Jaques and Chappell (1980) noted that Eocene (50-55 m.y.) tonalites which intrude the gabbroic section of the PUB were chemically similar to boninites from Cape Vogel, and suggested that the two rock types were related chemically and in timing of eruption. Similarities between the tonalites and Cape Vogel boninites include low TiO_2 contents (0.26-0.33%) and nearly identical absolute and relative REE abundances (Jaques and

Chappell (1980). In addition, the tonalites have high Mg/(Mg + ΣFe) (~0.6), Cr and Ni contents (~185 ppm and ~35 ppm respectively) compared to tonalites from other areas (Jaques and Chappell, 1980). Basalts from the PUB are LREE-depleted and MORB-like in character.

Both Jaques and Chappell (1980) and Karig (1972) interpreted the presence of tonalites in the PUB as evidence of island arc volcanism prior to or accompanying emplacement of the PUB. If an Eocene age is accepted for the Cape Vogel boninites, a more suitable tectonic situation can be proposed, i.e., that they were generated in a subduction zone by hydrous partial melting of peridotite, possibly the residue from generation of the MORB-like basalts which form the basaltic section of the ophiolite (Jaques and Chappell, 1980). The extremely refractory peridotites which characterize the tectonite section of the PUB (Table 3.4) may be the sources or in some cases the residua from generation of boninites and tonalites. Recent $^{40}Ar/^{39}Ar$ dating by Walker and McDougall (1982) establishes the age of the Dabi volcanics as ~55 m.y.b.p.

Reasons for shallow level melting of refractory peridotite for the Cape Vogel boninites, with regard to the thermal requirements for boninite generation outlined above, can only be speculated on. The PUB was originally interpreted as a section of Pacific Ocean crust and upper mantle (Davies, 1971), while others (Karig, 1972; Milsom, 1973; and Finlayson, 1977) have suggested that it was formed in a younger marginal basin. A marginal basin origin for the PUB, comparable to the West Philippine Sea and Bismarck Sea could explain elevated temperatures at shallow depths, such that the models of Meijer (1980) or Crawford et al. (1981) would be applicable.

In general, the thermal models of Crawford et al. (1981) and Meijer (1980) are consistent with occurrences of boninites and low TiO_2 volcanics in the areas studied, and particularly in the Mariana - Bonin Arc region, the tectonic evolution of which is well constrained. According to these models boninites and low TiO_2 volcanics would be expected to occur in areas where old oceanic lithosphere underthrusts very young oceanic lithosphere, and near young or incipient backarc spreading centers.

CHAPTER 8: CONCLUSIONS AND SUMMARY

There are many geochemical problems involved with explaining the origin of island arc volcanics. In this thesis it was attempted to explain one common geochemical characteristic of island arc basalts, i.e., their low TiO_2 contents compared to oceanic and continental basalts, by examining arc volcanics with this characteristic in the extreme. The conclusion of this thesis is that the low TiO_2 contents in these volcanics results from their derivation from extremely depleted peridotite, based on experimental petrological results, Cr-spinel compositions and abundance ratios of Ti, HREE, Y, Sc and V. Because the main group of arc volcanics studied are boninites, which have major element compositions distinct from the majority of island arc volcanics, it can be argued that this conclusion is not generally applicable. However, the similarity demonstrated in this thesis between abundance ratios of Ti, HREE, Y, Sc and V in boninites and low TiO_2 basalts from the Facpi Fm., Guam and Manam Island, Bismarck Arc indicate that the reason for the low Ti contents in these volcanics is essentially the same.

Nearly all low TiO_2 arc volcanics studied are characterized by enrichment in LREE compared to HREE or intermediate REE, and increasing LREE enrichment typically corresponds with decreasing $(^{143}Nd/^{144}Nd)_o$. After consideration of both subducted sediment and mantle sources for enrichment in LREE and low $^{143}Nd/^{144}Nd$, this feature is interpreted as the result of metasomatism of the depleted peridotite sources of low TiO_2 volcanics by mantle derived fluids or melts with low $^{143}Nd/^{144}Nd$, possibly originating in sources similar to the sources of oceanic island volcanics.

Because of the difficulty of introducing such fluids into an established subduction zone, and because "mantle isochron" ages for most areas studied permit this interpretation, it is suggested that LREE metasomatism occurs between the generation of depleted peridotite at mid-ocean ridges, but prior to the entrapment of the depleted, LREE-metasomatized peridotite sources of low TiO_2 volcanics within the overlying plate of a subduction zone. This conclusion is not proved or disproved by the data, but can explain the similarity of LREE and Nd-isotopic characteristics of low TiO_2 volcanics, oceanic island volcanics and LREE-enriched mantle peridotite inclusions.

One difference between boninites and Facpi Fm. lavas, and oceanic island volcanics is the high Zr/Sm ratios in boninites and Facpi Fm. lavas. This feature is not found in primitive mantle derived liquids from any other tectonic regime, but is found in some highly differentiated rocks, where increasing Zr/Sm accompanies increasing LREE-enrichment and decreasing Ti/Zr. These trends are attributable to an accessory or minor mineral in the differentiated rocks, possibly amphibole or apatite. Tentatively, the reason for Zr enrichment in boninites is ascribed to the presence of an unknown accessory mineral in the mantle sources of the LREE-enriched metasomatic fluids or melts. Evaluation of this hypothesis requires better and more complete Ti, Zr and Sm partitioning data for minor phases.

The geochemical feature of boninites and other low TiO_2 arc volcanics which is most similar to other arc volcanics is their high abundances of K, Rb, Sr and Ba compared to REE and HFS elements. The presence of this feature in boninites, for which experimental petrologic results, Cr-spinel compositions, and trace element abundance patterns support a depleted

peridotite source, strongly indicates that this phenomenon results from addition of K, Rb, Ba and Sr to a source poor in these elements, rather than subtraction of REE and HFS elements from partial melts of fertile peridotite by residual minerals rich in these elements.

Mantle, subducted oceanic crust, and lower arc crust have been evaluated as sources for enrichment in K, Rb, Ba and Sr. Mantle sources, and oceanic crustal sources, including both MORB and sediment, are most consistent with Nd, Sr and Pb isotopic data. Mantle sources are not favored because high abundances of K, Rb, Ba and Sr relative to REE and HFS elements are generally not observed in mantle derived liquids or peridotite nodules, and because the decoupling of abundances of K, Rb, Ba and Sr and Sr-isotopic composition, from abundances of REE and HFS elements and Nd-isotopic composition observed in low TiO_2 arc volcanics would require either two phases of mantle metasomatism, or disequilibrium partial melting processes.

The preferred model, that of derivation of materials with high abundances of K, Rb, Ba and Sr relative to REE and HFS elements from oceanic crustal sources consisting of both MORB and sediment, is equally speculative as mantle sources, i.e., fluids with these characteristics are also not observed. However, this model is capable of explaining isotopic and trace element data for the arc volcanics studied. Further study, particularly Pb-isotopic and concentration data for boninites is required for complete development of the model. As a general model for arc volcanics, derivation of K, Rb, Sr and Ba enriched materials from subducted MORB and sediment has essential features which are required to explain the variability of abundances and abundance ratios of the elements and isotopic compositions observed in island arc volcanics. At this point the model

needs to be tested against specific data for many island arcs in order to evaluate its potential and limitations.

An unusual feature of the geochemistry of boninites compared to other arc volcanics is their high K/Ba and Rb/Ba ratios. This feature, supported by their sometimes very high and variable $^{87}Sr/^{86}Sr$ ratios and an atmospheric $^{3}He/^{4}He$ ratio reported by other researchers, is interpreted as the result of addition to the sources of boninites of a material with the trace element and isotopic characteristics of seawater. This material is identified with fluids released from the subducted oceanic crust by dehydration of basaltic alteration products with trace element and isotopic compositions similar to seawater. A significant contribution from seawater or the dehydration products of hydrous minerals has been precluded for most arc volcanics by thermodynamic data indicating loss of volatiles at shallow depths. The presence of such a component in boninites, for which low pressure partial melting is indicated, is therefore consistent with thermodynamic dehydration data and the inferred environment of generation of boninites.

REFERENCES

Allegre C. J., Pineau F., Bernat M. and Javoy M. (1971) Evidence for the occurrence of carbonatites on the Cape Verde and Canary Islands. Nature 233, 103-104.

Allegre C. J., Richard P., Joron J.-L., Minster J.-F., Treuil M. and Tatsumoto M. Basalt genesis in subduction zones: the Japan case. (in preparation).

Arculus R. J. (1976) Geology and geochemistry of the alkali basalt - andesite association of Grenada, Lesser Antilles island arc. Bull. Geol. Soc. Amer. 87, 612-624.

Arculus R. J. and Johnson R. W. (1981) Island-arc magma sources: a geochemical assessment of the roles of slab-derived components and crustal contamination. Geochem. J. 15, 109-133.

Baker B. H., Goles G. G., Leeman W. P. and Lindstrom M. M. (1977) Geochemistry and petrogenesis of a basalt - benmoreite - trachyte suite from the southern part of the Gregory Rift, Kenya. Contrib. Mineral. Petrol. 64, 303-332.

Bateman P. C. and Chappell B. W. (1979) Crystallization, fractionation and solidification of the Tuolumne Intrusive Series, Yosemite National Park. Geol. Soc. Amer. Bull. 90 - Part 1, 465-482

Beccaluva L., Macciotta G., Savelli C., Serri G. and Zeda O. (1980) Geochemistry and K/Ar ages of volcanics dredged in the Philippine Sea (Mariana, Yap and Palau Trenches and Parece Vela Basin). In The Tectonic and Geologic Evolution of Southeast Asian Seas and Islands (ed. D. E. Hayes), Amer. Geophys. Union Monogr. 23, pp. 247-268.

Bloomer S. (1981) Marianas forearc ophiolite - structure and petrology. EOS, Trans. Amer. Geophys. Union 62, 1086-1087.

Bloomer S., Melchior J., Poreda R. and Hawkins J. (1979) Mariana arc-trench studies: Petrology of boninites and evidence for a "boninite series". EOS, Trans. Amer. Geophys. Union 60, 968.

Bougault H. and Hekinian R. (1974) Rift valley in the Atlantic Ocean near 35° 50' N: Petrology and geochemistry of basaltic rocks. Earth Planet. Sci. Lett. 24, 249-261.

Bougault H., Joron J.-L. and Treuil M. (1980) The primordial chondritic nature and large-scale heterogeneities in the mantle: Evidence from high and low partition coefficient elements in oceanic basalts. Phil. Trans. R. Soc. Lond. 297, 203-213.

Burwell A. D. M. (1975) Rb - Sr isotope geochemistry of lherzolites and their constituent minerals from Victoria, Australia. Earth Planet. Sci. Lett. 28, 69-78.

Cameron W. E., Nisbet E. J. and Dietrich V. J. (1979) Boninites, komatiites and ophiolitic basalts. Nature 280, 550-553.

Carter S. R., Evensen N. M., Hamilton P. J. and O'Nions R. K. (1978) Neodymium and strontium isotope evidence for crustal contamination of continental volcanics. Science 202, 743-747.

Chen C. Y. and Frey F. A. (1981) Multi-stage geochemical events in the upper mantle: evidence from geochemical studies of spinel lherzolites from Mount Leura, Australia. EOS, trans. Amer. Geophys Union 62, 415.

Church S. (1973) Limits of sediment involvement in the genesis of orogenic volcanic rocks. Contrib. Mineral. Petrol. 39, 17-32.

Church S. and Tatsumoto M. (1975) Lead isotope relations in oceanic ridge basalts from the Juan de Fuca - Gorda Ridge area, N. E. Pacific Ocean. Contrib. Mineral. Petrol. 53, 253-279.

Clague D. A. and Frey F. A. (1982) Petrology and trace element geochemistry of the Honolulu Volcanics, Oahu: Implications for the oceanic mantle below Hawaii. J. Petrol. 23 - Part 3, 447-504.

Coish R. A. (1977) Ocean floor metamorphism in the Betts Cove Ophiolite, Newfoundland. Contrib. Mineral. Petrol. 60, 255-270.

Coish R. A. and Church W. R. (1979) Igneous geochemistry of mafic rocks in the Betts Cove Ophiolite, Newfoundland. Contrib. Mineral. Petrol. 70, 29-40.

Coish R. A., Hickey R. L. and Frey F. A. (1982) Rare earth element geochemistry of the Betts Cove Ophiolite, Newfoundland: complexities in ophiolite formation. Geochim. Cosmochim. Acta 46, 2117-2134.

Coleman R. G. (1977) Ophiolites. Springer - Verlag.

Crawford A. J., Beccaluva L. and Serri G. (1981) Tectono - magmatic evolution of the west Philippine - Mariana region and the origin of boninites. Earth Planet. Sci. Lett. 54, 346-356.

Dallwitz W. B. (1968) Chemical composition and genesis of clinoenstatite - bearing volcanic rocks from Cape Vogel, Papua: A discussion. Proc. 23rd Int. Geol. Congr., Prague, Vol. 2, pp. 229-242.

Dallwitz W. B., Green D. H. and Thompson J. E. (1966) Clinoenstatite in a volcanic rock from the Cape Vogel area, Papua. J. Petrol. 7, 375-403.

Davies H. L. (1971) Peridotite - gabbro - basalt complex in eastern Papua an overthrust plate of oceanic mantle and crust. Aust. Bur. Min. Resour. Geol. Geophys. Bull. 128.

Davies H. L. (1977) Crustal structure and emplacement of ophiolite in southeast Papua New Guinea. Geol. Surv. Papua New Guinea Rpt. 77.

DePaolo D. J. and Johnson R. W. (1979) Magma genesis in the New Britain island-arc: Constraints from Nd and Sr isotopes and trace element patterns. Contrib. Mineral. Petrol. 70, 367-379.

DePaolo D. J. and Wasserburg J. G. (1977) The sources of island arcs as indicated by Nd and Sr isotopic studies. Geophys. Res. Lett. 4, 465-468.

Dick H. J. B. and Bullen T. (1983) Chromian spinel as a petrogenetic indicator in oceanic environments. Contrib. Mineral. Petrol. (in press).

Dietrich V., Emmermann R., Oberhansli R. and Puchelt H. (1978) Geochemistry of basaltic and gabbroic rocks from the West Mariana Basin and the Mariana Trench. Earth Planet. Sci. Lett. 39, 127-144.

Dixon T. H. and Batiza R. (1979) Petrology and chemistry of recent lavas in the northern Marianas: Implications for the origin of island arc basalts. Contrib. Mineral. Petrol. 70, 167-181.

Dosso L. and Murthy V. R. (1980) A Nd isotopic study of the Kerguelen Islands: inferences on enriched oceanic mantle sources. Earth Planet. Sci. Lett. 48, 268-276.

Dostal J., Dupuy C. and Leyreloup A. (1980) Geochemistry and petrology of meta-igneous granulitic xenoliths in Neogene volcanic rocks of the Massif Central, France - implications for the lower crust. Earth Planet. Sci. Lett. 50, 31-40.

Duncan R. A. and Green D. H. (1980) Role of multistage melting in the formation of the oceanic crust. Geology 8, 22-26.

Erlank A. J. and Kable E. J. D. (1976) The significance of incompatible elements in Mid-Atlantic Ridge basalts from 45o N, with particular reference to Zr/Nb. Contrib. Mineral. Petrol. 54, 281-291.

Evensen N. M., Hamilton P. J. and O'Nions R. K. (1978) Rare earth abundances in chondritic meteorites. Geochim. Cosmochim. Acta 42, 1199-1212.

Ewart A., Bryan W. B. and Gill J. B. (1973) Mineralogy and geochemistry of the younger volcanic islands of Tonga, southwest Pacific. J. Petrol. 13, 429-465.

Ewart A., Brothers R. N. and Mateen A. (1977) An outline of the geology and geochemistry, and the possible petrogenetic evolution of the volcanic rocks of the Tonga - Kermadec - New Zealand island arc. Jour. Volc. Geotherm. Res. 2, 205-250.

Fesq H. W., Kable E. J. D. and Gurney J. J. (1975) Aspects of the geochemistry of kimberlites from the Premier Mine, and other selected South African occurrences with particular reference to the rare earth elements. In Physics and Chemistry of the Earth (ed. L. H. Ahrens et al.), Vol. 9, pp. 687-707.

Finlayson D. M., Drummond B. J., Collins C. D. M. and Connelly J. B. (1977) Crustal structures in the region of the Papua Ultramafic Belt. Phys. Earth Planet. Inter. 14, 13-29.

Flanagan F. J. (1973) 1972 values for international geochemical reference samples. Geochim. Cosmochim. Acta 37, 1189-1200.

Forsyth D. W. (1977) The evolution of the upper mantle beneath mid-ocean ridges. Tectonophysics 38, 89-118.

Frey F. A. (1969) Rare earth abundances in a high-temperature peridotite intrusion. Geochim. Cosmochim. Acta 33, 1429-1447.

Frey F. A. (in press) Rare earth element abundances in upper mantle rocks. In Rare Earth Element Geochemistry (ed. P. Henderson). Chapt. 5., Elsevier.

Frey F. A. and Green D. H. (1974) The mineralogy and origin of lherzolite inclusions in Victorian basanites. Geochim. Cosmochim. Acta 38, 1023-1059.

Frey F. A. and Prinz M. (1978) Ultrmafic inclusions from San Carlos, Arizona: petrologic and geochemical data bearing on their petrogenesis. Earth Planet. Sci. Lett. 38, 129-176.

Frey F. A. and Suen C. J. (1982) The Ronda high temperature peridotite: geochemistry and petrogenesis (in prep.).

Frey F. A., Bryan W. B. and Thompson G. (1974) Atlantic Ocean floor: geochemistry and petrology of basalts from Legs 2 and 3 of the Deep-Sea Drilling Project. J. Geophys. Res. 79, 5507-5527.

Frey F. A., Chappell B. W. and Roy S. D. (1978) Fractionation of rare-earth elements in the Tuolumne Intrusive Series, Sierra Nevada batholith, California. Geology 6, 239-242.

Frey F. A., Green D. H. and Roy S. D. (1978) Integrated models of basalt petrogenesis: a study of quartz tholeiites to olivine melilites from southeastern Australia utilizing geochemical and experimental petrological data. J. Petrol. 19, 463-513.

Gill J. B. (1978) Role of trace element partition coefficients in models of andesite genesis. Geochim. Cosmochim. Acta 42, 709-724.

Gill J. B. (1981) Orogenic Andesites and Plate Tectonics. Springer Verlag.

Gorton M. P. (1977) The geochemistry and origin of quaternary volcanism in the New Hebrides. Geochim. Cosmochim. Acta 41, 1257-1270.

Green D. H. (1973) Experimental melting studies on a model upper mantle composition at high pressure under water-saturated and water-undersaturated conditions. Earth Planet. Sci. Lett. 19, 37-53.

Green D. H. (1976) Experimental testing of "equilibrium" partial melting of peridotite under water-saturated, high pressure conditions. Can. Mineral. 14, 255-268.

Green J. C. (1981) Pre-Tertiary continental flood basalts. In Basaltic Volcanism on the Terrestrial Planets (Basaltic Volcanism Study Project), Chapt. 1, pp. 30-77. Pergamon Press, New York.

Grove T. L., Gerlach D. C. and Sando T. W. (1982) Origin of calc-alkaline series lavas at Medicine Lake volcano by fractionation, assimilation and mixing. Contrib. Mineral. Petrol. 80, 160-182.

Haggerty S. E. and Irving A. J. (1981) Tertiary continental flood basalts. In Basaltic Volcanism on the Terrestrial Planets (Basaltic Volcanism Study Project), Chapt. 1, pp. 78-107. Pergamon Press, New York.

Hannah J. L. and Futa K. (1982) Nd, Sr and O isotope systematics in the Troodos Ophiolite, Cyprus. Geol. Soc. Amer. Abstr. with Prog. 14, 506.

Hart S. R. (1971) K, Rb, Cs, Sr and Ba contents and Sr isotope ratios of ocean floor basalts. Phil. Trans. R. Soc. Lond. 269, 573-587.

Hart S. R. and Davis K. E. (1978) Nickel partitioning between olivine and silicate melt. Earth Planet. Sci. Lett. 40, 203-219.

Hart S. R., Erlank A. J. and Kable E. J. D. (1974) Sea floor basalt alteration: some chemical and isotopic effects. Contrib. Mineral. Petrol. 44, 219-230.

Hart S. R. and Staudigel H. (1979) Ocean crust seawater interactions: Sites 417 and 418. In Initial Reports of the Deep-Sea Drilling Project, Vols. 51, 52 and 53, pp. 1169-1176. U. S. Government Printing Office.

Haskin L. A., Helmke P. A., Paster T. P. and Allen R. O. (1970) Rare earths in meteoritic, terrestrial and lunar matter. In Activation Analysis in Geochemistry and Cosmochemistry (eds. A. O. Brunfelt and E. Steinnes), pp. 201-219. Universitetsforlaget.

Hawkesworth C. J. (1982) Isotopic characteristics of magmas erupted along destructive plate margins. In Orogenic Andesites (ed. R. S. Thorpe), pp. - . J. Wiley and Sons.

Hawkesworth C. J., O'Nions R. K. and Arculus R. J. (1979) Nd and Sr isotope geochemistry of island arc volcanics, Grenada, Lesser Antilles. Earth Planet. Sci. Lett. 45, 237-248.

Hawkins J., Bloomer S., Evans C. and Melchior J. (1979) Mariana arc-trench system: petrology of the inner trench wall. EOS, Trans. Amer. Geophys. Union 60, 968.

Hawkins J. W., Bloomer S. H. and Evans C. (1982) Evolution of intra-oceanic island arc systems. EOS, Trans. Amer. Geophys. Union 63, 473.

Hellman P. L. and Green T. H. (1979) The role of sphene as an accessory phase in the high-pressure partial melting of hydrous mafic compositions. Earth Planet. Sci. Lett. 42, 191-201.

Hickey R. L. and Frey F. A. (1979) Petrogenesis of high-Mg amdesites: geochemical evidence. EOS, Trans. Amer. Geophys. Union 60, 413.

Hickey R. L. and Frey F. A. (1981) Rare earth geochemistry of Mariana fore-arc volcanics: Deep-Sea Drilling Project Site 458 and Hole 459B. In Initial Reports of the Deep-Sea Drilling Project, Vol. 60, pp. 735-741. U. S. Government Printing Office.

Hickey R. L. and Frey F. A. (1982) Geochemical characteristics of boninite series volcanics: implications for their source. Geochim. Cosmochim. Acta 46, 2099-2115.

Hickey R. L., Frey F. A. and Jenner G. (1980) Trace element and isotopic characteristics of boninites: implications for their source. EOS, Trans. Amer. Geophys. Union 61, 1140.

Hickey R. L. and Reagan M. K. (1981) REE and Nd- and Sr isotope geochemistry of Guam volcanic rocks: variation in time. EOS, Trans. Amer. Geophys. Union 62, 1091.

Holland J. G. and Lambert R. St. J. (1975) The chemistry and origin of the Lewisian gneisses of the Scottish mainland: the Scourie and Inver assemblages and sub-crustal accretion. Precamb. Res. 2, 161-188.

Howard A. H. and Stolper E. (1981) Experimental crystallization of boninites from the Mariana Trench. EOS, Trans. Amer. Geophys. Union 62, 1091.

Irving A. J. (1978) A review of experimental studies of crystal/liquid trace element partitioning. Geochim. Cosmochim. Acta 42, 743-770.

Jacobsen S. B. and Wasserburg G. J. (1979) Nd and Sr isotopic study of the Bay of Islands ophiolite comples and the evolution of the source of midocean ridge basalts. J. Geophys. Res. 84, 7429-7445.

Jagoutz E., Palme H., Baddenhausen H., Blum K., Cendales M., Dreibus G., Spettel B., Lorenz V. and Wanke H. (1979) The abundance of major, minor and trace elements in the earth's mantle as derived from rimitive ultramafic nodules. Proc. 10 Lunar Sci. Conf., Geochim. Cosmochim. Acta, Supplement II, 2, 2031-2050.

Jaques A. L. and Chappell B. W. (1980) Petrology and trace element geochemistry of the Papuan Ultramafic Belt. Contrib. Mineral. Petrol. 75, 55-70.

Jenner G. A. (1981) Geochemistry of high-Mg andesites from Cape Vogel, Papua New Guinea. Chem. Geol. 33, 307-332.

Jenner G. A. and Fryer B. J. (1980) Geochemistry of the upper Snooks Arm Group basalts, Burlington Peninsula, Newfoundland: evidence against formation in an island arc. Can. J. Earth Sci. 17, 888-900.

Jenner G. A. and Green D. H. High-Mg andesites: petrology and some constraints on their petrogenesis (in preparation).

Johannsen A. (1937) A Descriptive Petrography of Igneous Rocks. University of Chicago Press.

Johnson R. W. (1976) Late Cainozoic volcanism and plate tectonic at the southern margin of the Bismarck Sea, Papua New Guinea. In Volcanism in Australasia, (ed. R. W. Johnson), pp. 101-116. Elsevier.

Johnson R. W. (1977) Distribution and major element chemistry of late Cainozoic volcanoes at the southern margin of the Bismarck Sea, Papua New Guinea. Aust. Bur. Miner. Resour. Geol. Geophys. Rep. 188, 170 p.

Johnson R. W. and Chappell B. W. (1979) Chemical analyses of rocks from the late Cainozoic volcanoes of north-central New Britain and the Witu Islands, Papua New Guinea. Bur. Miner. Resour. Aust. Rpt. 209, 42 p.

Johnson R. W. and Jaques A. L. (1980) Continent-arc collision and reversal of arc polarity: new interpretations from a critical area. Tectonophysics 63, 111-124.

Johnson R. W., MacKenzie D. E. and Smith I. E. M. (1978) Delayed partial melting of subduction modified mantle in Papua New Guinea. Tectonophysics 46,197-216.

Johnson R. W., Jaques A. L., Hickey R. L., McKee C. O. and Chappell B. W. (1981) Manam Island, Papua New Guinea: petrologic development of a basaltic island arc volcano. I.A.V.C.E.I. Symposium on Arc Volcanism, Sept. 1981, Tokyo-Hakone, Japan.

Kable E. J. D., Fesq. H. W. and Gurney J. J. (1975) The significance of the interelement relationships of some minor and trace elements in South African kimberlites. In Physics and Chemistry of the Earth (ed. L. H. Ahrens et al.), Vol. 9, pp. 709-734.

Kaneoka I., Isshiki N. and Zashu S. (1970) K-Ar ages of the Izu-Bonin Islands. Geochem. Jour. 4, 53-60.

Kikuchi Y. (1890) On pyroxenic compounds in certain volcanic rocks from Bonin Island. J. Coll. Sci. Imp. Univ. Tokyo 3, 67-89.

Karig D. E. (1971) Structural history of the Mariana Island arc system. Bull. Geol Soc. Amer. 82, 323-344.

Karig D. E. (1972) Remnant arcs. Bull. Geol. Soc. Amer. 83, 1057-1068.

Karig D. E. (1975) Basin genesis in the Philippine Sea. In Initial Reports of the Deep-Sea Drilling Project, Vol. 31, pp. 857-879. U.S. Government Printing Office.

Kay R. W. (1977) Geochemical constraints on the origin of Aleutian magmas. In Island Arcs, Deep Sea Trenches and Back Arc Basins, Maurice Ewing Series, Vol. 1, pp. 229-242. Amer. Geophys. Union.

Kay R. W. (1978) Aleutian magnesian andesites: melts from subducted Pacific Ocean crust. Jour. Volc. Geotherm. Res. 4, 117-132.

Kay R. W. (1980) Volcanic arc magmas: implications of a melting - mixing model for element recycling in the crust - upper mantle. Jour. Geol. 88, 497-522.

Koster Van Groos A. F. (1975) The distribution of strontium between coexisting silicate and carbonate liquids at elevated pressures and temperatures. Geochim. Cosmochim. Acta 39, 27-34.

Kuno H. (1966) Lateral variation of basalt magma type across continental margins and island arcs. Bull. Volc. 29, 195-222.

Kurat G., Palme H., Spettel B., Baddenhausen H., Hofmeister H., Palme C. and Wanke H. (1980) Geochemistry of ultramafic xenoliths from Kapfenstein, Austria: evidence for a variety of upper mantle processes. Geochim. Cosmochim. Acta 44, 45-60.

Kuroda N. and Shiraki K. (1975) Boninite and related rocks of Chichi-jima, Bonin Islands, Japan. Rep. Fac. Sci. Shizuoka Univ. 10, 145-155.

Kushiro I. (1969) The system forsterite - diopside - silica with and without water at high pressures. Amer. J. Sci. 267A, 269-294.

Kushiro I. (1971) Effect of water on the composition of magmas formed at high pressures. J. Petrol. 13, 311-314.

Langmuir C. H., Bender J. F., Bence A. E., Hanson G. N. and Taylor S. R. (1977) Petrogenesis of basalts from the FAMOUS area: Mid-Atlantic Ridge. Earth Planet. Sci. Lett. 36, 133-156.

Leeman W. P. and Vitaliano C. J. (1976) Petrology of McKinney basalt, Snake River plain, Idaho. Bull. Geol. Soc. Amer. 87, 1777-1792.

Leeman W. P., Ma M. -S., Murali A. V. and Schmitt R. A. (1978) Empirical estimation of magnetite/liquid distribution coefficients for some transition elements: a correction. Contrib. Mineral. Petrol. 66, 429.

LeRoex A. P. (1980) Geochemistry and mineralogy of selected Atlantic Ocean basalts. Ph.D. Thesis. Univ. Cape Town, South Africa.

Leyreloup A., Bodinier J. L., Dupuy C. and Dostal J. (1982) Petrology and geochemistry of granulite xenoliths from Central Hoggar (Algeria) - implications for the lower crust. Contrib. Mineral. Petrol. 79, 68-75.

Lipman P. W. and Dungan M. A. (1981) Continental rift volcanism. In Basaltic Volcanism on the Terrestrial Planets (Basaltic Volcanism Study Project), Chapt. 1, pp. 108-160. Pergamon Press, New York.

Luyendyk B. P., MacDonald K. C. and Bryan W. B. (1973) Rifting history of the Woodlark Basin in the southwest Pacific. Geol. Soc. Amer. Bull. 84, 1125-1134.

Mason B. (1979) Meteorites. In Data of Geochemistry (ed. M. Fleischer), Chap. B, Part 1, U.S.G.S. Prof. Paper 440B-1. U.S. Government Printing Office.

McCulloch M. T. and Wasserburg G. J. (1978) Sm-Nd and Rb-Sr chronology of continental crust formation. Science 200, 1003-1011.

Meijer A. (1976) Pb and Sr isotopic data bearing on the origin of volcanic rocks from the Mariana island arc system. Geol Soc. Amer. Bull. 87, 1358-1369.

Meijer A. (1980) Primitve arc volcanism and a boninite series: examples from western Pacific island arcs. In The Tectonic and Geologic Evolution of Southeast Asian Seas and Islands (ed. D. E. Hayes), Amer. Geophys. Union Monogr. 23, pp. 269-282.

Meijer A., Anthony E. and Reagan M. (1981) Petrology of volcanic rocks from the fore-arc sites. In Initial Reports of the Deep-Sea Drilling Project, Vol. 60, pp. 709-730. U.S. Government Printing Office.

Meijer A., Reagan M., Shafiqullah M., Sutter J., Damon P. and Kling S. (1982) Chronology of volcanic events in the eastern Philippine Sea. In Amer. Geophys. Union Monogr. (in press).

Milsom J. S. (1973) Papuan Ultramafic Belt: gravity anomalies and the emplacement of ophiolites. Geol. Soc. Amer. Bull. 84, 2243-2258.

Morgan W. R. (1966) A note on the petrology of some lava types from east New Guinea. J. Geol. Soc. Aust. 13, 583-591.

Mysen B. O. (1979) Trace-element partitioning between garnet peridotite minerals and water-rich vapor: experimental data from 5 to 30 kbar. Amer. Mineral. 64, 274-287.

Nesbitt R. W. and Sun S. -S. (1976) Geochemistry of Archaean spinifex-textured peridotites and magnesian and low-magnesian tholeiites. Earth Planet. Sci. Lett. 31, 433-453.

Nicholls I. A. (1974) Liquids in equilibrium with peridotite mineral assemblages at high water pressures. Contrib. Mineral. Petrol. 45, 289-316.

Nicholls I. A. and Harris K. A. (1980) Experimental rare earth partition coefficients for garnet, clinopyroxene and amphibole coexisting with andesitic and basaltic liquids. Geochim. Cosmochim. Acta 44, 287-308.

Nicholls I. A. and Ringwood A. E. (1973) Effect of water on olivine stability in tholeiites and the production of silica-saturated magmas in the island-arc environment. Jour. Geol. 81, 285-300.

Nohda S. and Wasserburg G. J. (1981) Nd and Sr isotopic study of volcanic rocks from Japan. Earth Planet. Sci. Lett. 52, 264-276.

O'Nions R. K., Carter S. R., Cohen R. S., Evensen N. M. and Hamilton P. J. (1978) Pb, Nd and Sr isotopes in oceanic ferromanganese deposits and ocean floor basalts. Nature 273, 435-438.

O'Nions R. K., Hamilton P. J. and Evensen N. M. (1977) Variations in $^{143}Nd/^{144}Nd$ and $^{87}Sr/^{86}Sr$ ratios in oceanic basalts. Earth Planet. Sci. Lett. 34, 13-22.

Ottonello G. (1980) Rare earth ebundances and distribution in some spinel peridotite xenoliths from Assab (Ethiopia). Geochim. Cosmochim. Acta 44, 1885-1901.

Pearce J. A. and Norry M. J. (1979) Petrogenetic implications of Ti, Zr and Nb variations in volcanic rocks. Contrib. Mineral. Petrol. 69, 33-47.

Perfit M. R., Gust D. A., Bence A. E., Arculus R. J. and Taylor S. R. (1980) Chemical characterisitics of island-arc basalts: implications for mantle sources. Chem. Geol. 30, 227-256.

Peterman, Z. E., Hedge C. E. and Tourtelot H. A. (1970) Isotopic composition of strontium in sea water throughout Phanerozoic time. Geochim. Cosmochim. Acta 34, 105-120.

Petersen J. (1891) Beitrag zur Petrographie von Sulphur Island, Peel Island, Hachijo und Mijakeshima. Jahrb. Hamburg. Wiss. Anst. 8, 1-59.

Quinby-Hunt M. S. and Turekian K. K. (1983) Distribution of elements in seawater. EOS, Trans. Amer. Geophys. Union 64, 130-131.

Reagan M. K. and Meijer A. (1982) Geology and geochemistry of early arc volcanic rocks from Guam. Geol. Soc. Amer. Bull. (in press).

Reagan M. K., Meijer A. and Hickey R. L. (1981) Geology and geochemistry of volcanic rocks from Guam. EOS, Trans. Amer. Geophys. Union 62, 1091.

Rhodes J. M. and Dawson J. B. (1975) Major and trace element chemistry of peridotite inclusions from the Lashaine Volcano, Tanzania. In Physics and Chemistry of the Earth (ed. L. H. Ahrens et al.), Vol. 9, pp. 547-558.

Ridley W. I. and Dawson J. B. (1975) Lithophile trace element data bearing on the origin of peridotite xenoliths, ankaramite and carbonatite from Lashaine Volcano, N. Tanzania. In Physics and Chemistry of the Earth (ed. L. H. Ahrens et al.), Vol 9, pp. 559-569.

Rogers N. W. (1977) Granulite xenoliths from Lesotho kimberlites and the lower continental crust. Nature 270, 681-684.

Scott R. B., Kroenke L., Zakariadze G. and Sharaskin A. (1980) Evolution of the South Philippine Sea: Deep-Sea Drilling Project leg 59 results. In Initial Reports of the Deep-Sea Drilling Project, Vol. 59, PP. 803-816. U.S. Government Printing Office.

Sharaskin A. Y., Dobretsov N. L. and Sobolev N. V. (1980) Marianites: clinoenstatite-bearing pillow lavas associated with an ophiolite assemblage of the Mariana Trench. Proc. Int. Oph. Sym., Nicosia 1979, Cyprus.

Shimizu N. (1975) Rare earth elements in garnets and clinopyroxenes from garnet lherzolite nodules in kimberlites. Earth Planet. Sci. Lett. 25, 26-32.

Shimizu N. and Allegre C. J. (1978) Geochemistry of transition elements in garnet lherzolite nodules in kimberlites. Contrib. Mineral. Petrol. 67, 41-50.

Shimizu N. and Arculus R. J. (1975) Rare earth element concentrations in a suite of basanitoids and alkali olivine basalts from Grenada, Lesser Antilles. Contrib. Mineral. Petrol. 50, 231-240.

Shimokawa T., Masuda A. and Izawa K. (1972) Rare-earth elements in top samples of the cores from the Pacific Ocean floor. Geochem. Jour. 6, 75-81.

Shiraki K. and Kuroda N. (1977) The boninite revisited. J. Geol. Soc. Japan 86, 34-50.

Shiraki K., Kuroda N. and Urano H. (1979) Clino-enstatite bearing boninite of Muko-Jima, Bonin Islands. J. Geol. Soc. Japan 85, 591-594.

Simonian K. O. and Gass I. G. (1978) Arakapas fault belt, Cyprus: A fossil transform fault. Bull. Geol. Soc. Amer. 89, 1220-1230.

Smewing J. D. and Potts P. J. (1976) Rare-earth abundances in basalts and metabasalts from the Troodos Massif, Cyprus. Contrib. Mineral. Petrol. 57, 245-258.

Smewing J. D., Simonian K. O. and Gass I. G. (1975) Metabasalts from the Troodos massif, Cyprus: genetic implications deduced from petrography and trace element geochemistry. Contrib. Mineral. Petrol. 51, 49-64.

Smith I. E.. and Davies H. L. (1976) Geology of the southeast Papuan mainland. Aust. Bur. Miner. Resour. Geol. Geophys. Bull. 165, 86 pp.

Solomon S. C. (1976) Geophysical constraints on radial and lateral temperature variations in the upper mantle. Am. Mineral. 61, 788-803.

Stark J. T. (1963) Petrology of the volcanic rocks of Guam. U. S. Geol. Surv. Prof. Pap. 403-C, 32 pp.

Staudigel H. (1979) Chemical analyses of interlaboratory standards. In Initial Reports of the Deep Sea Drilling Project, Vols. 51, 52 and 53, pp. 1331-1333. U. S. Government Printing Office.

Staudigel H., Frey F. A. and Hart S. R. (1979) Incompatible trace-element geochemistry and 87Sr/86Sr in basalts and corresponding glasses and palagonites. In Initial Reports of the Deep-Sea Drilling Project, Vols. 51, 52 and 53, pp. 1137-1144. U.S. Government Printin Office.

Staudigel H., Hart S. R. and Richardson S. H. (1981) Alteration of the oceanic crust: processes and timing. Earth Planet. Sci. Lett. 52, 311-327.

Stern R. J. (1981) A common mantle source for Mariana and Volcano arc and Caroline and Kilauea "hotspot" magmas? A consideration of the trace element and isotopic evidence. EOS, Trans. Amer. Geophys. Union 62, 408.

Stolper E. (1980) Phase diagram for mid-ocean ridge basalts: preliminary results and implications for petrogenesis. Contrib. Mineral. Petrol. 74, 13-27.

Stosch H. G. and Seck H. A. (1980) Geochemistry and mineralogy of two spinel peridotite suites from Dreiser Weiher, West Germany. Geochim. Cosmochim. Acta 44, 457-470.

Sun S. -S. (1980) Lead isotopic study of young volcanic rocks from mid-ocean ridges, ocean islands and island arcs. Phil. Trans. R. Soc. Lond. A297, 409-445.

Sun S. -S. and Nesbitt R. W. (1977) Chemical heterogeneity of the Archaean mantle, composition of the earth and mantle evolution. Earth Planet. Sci. Lett. 35, 429-448.

Sun S. -S. and Nesbitt R. W. (1978a) Geochemical regularities and genetic significance of ophiolitic basalts. Geology 6, 689-693.

Sun S. -S. and Nesbitt R. W. (1978b) Petrogenesis of Archaean ultrabasic and basic volcanics: evidence from rare earth elements. Contrib. Mineral. Petrol. 65, 301-325.

Sun S. -S., Nesbitt R. W. and Sharaskin A. Y. (1979) Geochemical characteristics of mid-ocean ridge basalts. Earth Planet. Sci. Lett. 44, 119-138.

Takigama Y. and Ozima M. (1981) $^{40}Ar/^{39}Ar$ dating of rocks drilled at Site 458 and 459 in the Mariana fore-arc region during Leg 60. In Initial Reports of the Deep-Sea Drilling Project, Vol. 60, pp. 743-746. U. S. Government Printing Office.

Tanaka T. and Aoki K. (1981) Petrogenetic implications of REE and Ba data on mafic and ultramafic inclusions from Itinome-gata, Japan. Jour. Geol. 89, 369-390.

Tatsumoto M. (1969) Lead isotopes in volcanic rocks and possible ocean-floor thrusting beneath island arc. Earth Planet. Sci. Lett. 6, 369-376.

Taylor B. (1979) Bismarck Sea: evolution of a backarc basin. Geology 7, 171-174.

Tracey J. I., Schlanger S. O., Stark J. T., Doan D. B. and May H. G. (1964) General geology of Guam. U. S. Geol. Surv. Prof. Pap. 403-A, 104 pp.

Troger (1935) Spezielle Petrographie der Eruptivegesteine. Deutschen Mineralogischen Gesellschaft, Bonn, 1969.

Turekian K. K. and Wedepohl K. H. (1961) Distribution of the elements in some major units of the earth's crust. Bull. Geol. Soc. Amer. Bull. 72, 175-192.

Walker D., Shibata T. and DeLong S. E. (1979) Abyssal tholeiites from the Oceanographer fracture zone, II. Phase equilibria and mixing. Contrib. Mineral. Petrol. 70, 111-125.

Walker D. A. and McDougall I. (1982) $^{40}Ar/^{39}Ar$ dating of altered glassy volcanic rocks: the Dabi Volcanics, P. N. G. Geochim. Cosmochim. Acta 46, 2181-2190.

Wendlandt R. F. and Harrison W. J. (1979) Rare earth partitioning between immiscible carbonate and silicate liquids and CO_2 vapor: results and implications for the formation of light rare earth enriched rocks. Contrib. Mineral. Petrol. 69, 409-419.

Whitford D. J. and Jezek P. A. (1979) Origin of late Cenozoic lavas from the Banda arc, Indonesia: trace element and Sr isotope evidence. Contrib. Mineral. Petrol. 68, 141-150.

Whitford D. J., White W. M. and Jezek P. A. (1981) Neodymium isotopic composition of Quaternary island arc lavas from Indonesia. Geochim. Cosmochim. Acta 45, 989-995.

Williams S. and Murthy V. R. (1979) Sources and genetic relationships of volcanic rocks from the northern Rio Grande Rift: Rb-Sr and Sm-Nd evidence. EOS, Trans. Amer. Geophys. Union 60, 407.

Wood D. A., Marsh N. G., Tarney J., Joron J. -L., Fryer P. and Treuil M. (1981) Geochemistry of igneous rocks recovered from a transect across the Mariana Trough, Arc, Forearc and Trench, Sites 453 to 461, DSDP Leg 60. In Initial Reports of the Deep-Sea Drilling Project, Vol. 60, pp. 611-646. U.S. Government Printing Office.

Wyllie P. J. (1979) Magmas and volatile components. Am. Mineral. 64, 469-500.

Zindler A. (1980) Geochemical processes in the earth's mantle and the nature of crust - mantle interaction: evidence from studies of Nd and Sr isotope ratios in mantle derived rocks and lherzolite nodules. Ph.D. Thesis. Massachusetts Institute of Technology.

Zindler A., Hart S. R., Frey F. A. and Jakobsson S. P. (1979) Nd and Sr isotope ratios and rare earth element abundances in Reykanes Peninsula basalts: evidence for mantle heterogeneity beneath Iceland. Earth Planet. Sci. Lett. 45, 249-262.

Zonenshain L. P. and Kuzmin M. I. (1978) The Khan-Taishir ophiolite complex of Western Mongolia, its petrology, origin and comparison with other ophiolitic complexes. Contrib. Mineral. Petrol. 67, 95-109.

APPENDIX I: SAMPLE PREPARATION

Boninites: Boninite samples from the Bonin Islands (samples 2981, 2983, 1129-4 and 1127-5), Mariana Trench Site 1403 (samples 2980) and Cape Vogel, Papua New Guinea (samples 2984, 2985, 2986 and 2987) were provided as powders by D. H. Green. Obvious vesicle fillings and altered areas were discarded before crushing in agate (Green, personal communication, 1977).

Manam Island: The eight Manam Island samples were provided as powders by R. W. Johnson, and were crushed in tungsten carbide. Thin sections of these samples provided by C. O. McKee showed that alteration was minimal, restricted to oxidation of the glass or groundmass around vesicles.

DSDP Site 458: Samples from Site 458 were provided as small (1-3 g) rocks chips by A. Meijer. The samples used in this study were selected from a larger set (5 boninites and 3 tholeiites) analyzed for REE (Hickey and Frey, 1981) on the basis of their fresh appearance. The four boninites (samples 28-1, 30-1, 39-1 and 43-2) were glassy (<95% glass) and the tholeiite (samples 46-1) was fine grained and aphyric. The rocks chips were cleaned ultrasonically in deionized water, dried and crushed to mm sized chips. The crushed rock was examined microscopically and any vesicle fillings and/or vein material was removed manually. The samples were then cleaned for 1 hour in sub-boiling distilled, deionized water, dried and crushed to powder in an agate mortar.

Guam: Samples from Guam were provided as small chunks (10-50 g) by M. Reagan and A. Meijer. Facpi "boninite series" samples (samples GM-68, GUM-79-11, and GUM-79-19) were the smallest and consisted of glass and altered, fine grained rock, with sparse (<5%) phenocrysts. These samples were first prepared by crushing to <1 cm sized chunks and manually picking out glassy material. Large fine grained or glassy samples (samples GUM-79-6, GUM-79-2, 71781-A-1 and GM-65-3) were crushed to 1 cm sized chunks and fresh appearing pieces were separated manually from alteration rinds and/or vein material. Large medium grained samples (samples GSR-3 and GM-75) were trimmed with a saw, and then crushed to 1 cm sized chunks. All samples were cleaned ultrasonically in deionized water, dried and crushed to mm sized chips. The samples were split into two parts by cone and quartering. Approximately one half was crushed to powder in agate for Nd-and Pb isotope analysis and whole rocks trace element analysis.

Sr isotope analyses were performed on material separated from the second split. For samples containing plagioclase (samples GUM-79-19, GUM-79-2, GM-75, GSR-3, 71781-A-1 and GM-65-3) the second split was crushed to < 60 mesh and the size range 60-100 or 80-120 mesh removed for plagioclase separation. Samples with no plagioclase (samples GUM-79-11 and GM-68) or extremely fine grained plagioclase (sample GUM-79-6) were crushed through 40 mesh and the size range 40-60 mesh removed. A small amount of the freshest appearing rock was hand picked from this material, rinsed in sub-boiling deionized water, dried and crushed to powder. For samples GUM-79-11 and GM-68 this was dominantly glass, and for sample GUM-79-6 groundmass. Separate Rb and Sr concentration analyses were performed on this material for age correction of $^{87}Sr/^{86}Sr$.

Plagioclase was separated magnetically using a modification of the technique of Sando (personal communication, 1981). Samples were run down a piece a paper taped to the outside of the Frantz with settings: forward 12°, side 40°, 0.7 amps. The nonmagnetic fraction from this separation was run through the Frantz, one time with settings: forward 12°, side 7°, 0.7 amps and twice with settings: forward 12°, side 4°, 0.7 amps. The final non magnetic fraction was virtually pure plagioclase. This fraction was back-picked to remove altered plagioclase, rinsed in distilled, deionized water and dried. Comparisons of whole rock and plagioclase $(87Sr/86Sr)_o$ are listed below. Plagioclase values are 0.00003 (within error) to 0.00020 lower than whole rocks values.

GM 75	Whole rock:	0.70371 ± 2
	Plagioclase:	0.70355 ± 4
GSR-3	Whole rock:	0.70355 ± 3
	Plagioclase:	0.70349 ± 3
79-2	Whole rock:	0.70384 ± 3
	Plagioclase:	0.70364 ± 4
71781-A-1	Whole rock:	0.70383 ± 3
	Plagioclase:	0.70380 ± 3
GM 65-3	Whole rock:	0.70380 ± 3
	Plagioclase:	0.70375 ± 3

APPENDIX II: ANALYTICAL TECHNIQUES

A) Major Elements: All major element analyses except one sample (GM 65-3) were provided by other researchers. Techniques are listed in tables in each chapter.

Sample GM 65-3 was analyzed by XRF at U. Mass., Amherst along with several duplicates for samples from other researchers, and MORB standard AII-92-29-1. Values are given in Table A-II-1.

Agreement between analyses for MANAM-3 (both by XRF) are excellent. Agreement between analyses for 2987 and wet chemical values of Dallwitz, 1968, and values for GM 68 and microprobe analyses by Reagan and Meijer (1982) is less good. XRF analyses are lower in SiO_2 and higher in MgO. Statistics for duplicate XRF glasses were good (<1% for MgO and SiO_2). Since only one sample from each group was analysed it is unclear if these variations result from systematic differences between analytical techniques or are genuine chemical differences in the samples studied.

B) Trace Elements:

1) Ti, V, Mn, Ni, Y, Zr, Pb in addition to some data for Sr, Rb and Ba for rocks studied in this thesis were analyzed by other researchers. Techniques are listed in Tables in each chapter. Except for some Sr, Rb and Ba analyses by isotope dilution this data has not been duplicated for interlaboratory comparison.

2) INAA data for Sc, Cr, Co and Hf were obtained by INAA using the technique of Frey et al. (1974). In addition REE analyses for samples from Manam Island, and all Guam samples except GUM 79-19, GSR-3, and GUM 79-6 are also by INAA.

TABLE A-II-1: MAJOR ELEMENT ANALYSES OF STANDARDS AND DUPLICATES

	AII-92-29-1		MANAM 3	
SiO_2	50.09	48.89(1)	51.99	51.66(2)
TiO_2	1.77	1.78	0.32	0.30
Al_2O_3	15.73	15.84	14.56	14.65
Fe_2O_3	10.93	11.06	9.16	9.05
MnO	0.19	0.17	0.16	0.17
MgO	7.38	7.64	9.12	8.95
CaO	11.11	11.13	11.41	11.21
Na_2O	2.79	2.95	1.98	2.36
K_2O	0.16	0.16	0.59	0.60
P_2O_5	0.18	0.19	0.09	0.10
Total	100.29		99.38	99.05

	2987		GM 68	
SiO_2	56.57	57.12(3)	52.99	53.97(4)
TiO_2	0.23	0.24	0.37	0.34
Al_2O_3	8.12	8.43	14.43	14.92
Fe_2O_3	10.62	10.89	8.77	8.60
MnO	0.18	0.22	0.15	0.19
MgO	17.94	16.96	10.75	9.63
CaO	4.90	5.07	9.30	9.24
Na_2O	0.36	0.63	1.91	2.34
K_2O	0.41	0.37	0.64	0.61
P_2O_5	0.04	0.06	0.04	0.05
Total	99.37	99.99	99.35	99.89

(1) average from 10 laboratories (Staudigel, 1979).
(2) B. W. Chappell and R. W. Johnson (pers. comm.).
(3) Dallwitz (1968).
(4) Reagan and Meijer (1982).

Analytical precision for samples from Guam and Manam was monitored by analyzing MORB standard AII-92-29-1 with each irradiation. The average and standard deviation for three analyses is listed below. Standard deviations for REE, Co, Sc and Cr are less than 3%, Hf is 4%.

The values obtained compare favorably with the average of values reported by four other laboratories, reported by Staudigel (1979). Values for all elements are within the standard deviation of this average, except for Cr which is high by about 4%.

TABLE A-II-2: INAA ANALYSES OF AII-92-29-1

	AVERAGE AND STD DEVIATION OF TRIPLICATE INAA ANALYSES	AVERAGE 4 OF VALUES (Staudigel, 1979)
La	4.01 ± 0.03	4.18 ± 0.30
Ce	13.0 ± 0.1	12.6 ± 1.2
Nd	10.9 ± 0.3	11.7 ± 0.8
Sm	3.92 ± 0.12	4.10 ± 0.20
Eu	1.52 ± 0.04	1.47 ± 0.13
Tb	1.02 ± 0.03	0.92 ± 0.10
Yb	3.94 ± 0.08	3.81 ± 0.20
Lu	0.59 ± 0.02	0.58 ± 0.02
Co	58.6 ± 0.4	58.1 ± 2.8
Sc	38.77 ± 0.06	34.3 ± 4.6
Hf	3.17 ± 0.13	3.32 ± 0.4
Cr	243 ± 4	233 ± 2.6

Values for samples with concentrations significantly less than AII-92-29-1 are considered to have larger errors than those listed. Errors twice those listed for La and Nd were assumed for La/Nd ratios in Chapters 4 and 5.

3) REE abundances for all boninites, tholeiite 46-1 from DSDP Site 458, and Guam samples 79-19, GSR-3 and 79-6 were determined using a radiochemical technique developed by the author and C. Y. Chen which is described in Hickey and Frey (1981). The procedure involved two chemical steps: 1) separation of REE as a group from major cations, following irradiation and disolution, using ion exchange resin, and 2) removal of Sc and remaining Fe by solvent extraction with tri-n-butyl-phosphate. Chemical yields were determined using ^{144}Ce and ^{169}Yb tracers, which were added in equal quantitites to samples and standards before disolution. Since ^{169}Yb is also generated during irradiation, a second standard was spiked with ^{144}Ce only, and the ratio of areas of ^{169}Yb peaks to ^{175}Yb (used for Yb analysis) in this standard were used to correct Yb yields in samples and standards for reactor produced ^{169}Yb.

Early analyses during the development of this technique were performed using a liquid synthetic REE standard evaporated into poly vials. Duplicate analyses of BCR-1 from these analyses are listed in Table A-II-3. Except for Lu, values are consistent with other published data. Lu values are lower than those from other laboratories in both M.I.T. RNAA and INAA analyses.

Analysis of samples with low REE concentrations required a shift from poly vials to quartz vials, in order to use the high flux facilities at the M.I.T. reactor. Because of difficulties in inserting exact amount of liquid standards into these vials, small amounts of BCR-1 were used as the standard for analysis of samples. The values used for BCR-1 (Table A-II-3) are an average of values by different analytical techniques.

The average and average error for two samples analyzed for REE are listed in Table A-II-3. Reproducibility for all elements in these samples was

TABLE A-II-3: RNAA ANALYSES OF STANDARDS AND DUPLICATES

BCR-1

	RNAA	MIT INAA	I.D. AVERAGE	JACOBS & HASKIN	GORTON & TAYLOR	AVERAGE
La	25.5 ± 0.2	24.4	25.2	24.6	24.2	24.6
Ce	53.0 ± 0.4	52.0	54.1	53.7	53.7	53.2
Nd	28.2 ± 0.8	26.7	29.3	--	28.5	28.2
Sm	6.70 ± 0.06	6.54	6.75	6.80	6.70	6.70
Eu	2.03 ± 0.01	2.05	1.96	1.92	1.95	1.97
Tb	1.05 ± 0.01	1.14	--	1.10	1.08	1.11
Yb	3.33 ± 0.06	3.30	3.50	3.37	3.48	3.41
Lu	0.48 ± 0.01	0.48	0.56	0.52	0.55	0.53

Duplicate analyses and average deviations:

	32-2 (16-20)	2983
La	0.820 ± 0.006	0.95 ± 0.01
Ce	2.28 ± 0.04	2.16 ± 0.01
Nd	1.82 ± 0.08	1.47 ± 0.03
Sm	0.622 ± 0.006	0.429 ± 0.001
Eu	0.251 ± 0.007	0.150 ± 0.001
Tb	0.172 ± 0.001	0.109 ± 0.002
Yb	0.797 ± 0.009	0.663 ± 0.003
Lu	0.127 ± 0.002	0.115 ± 0.001

Comparison of RNAA and isotope dilution values:

Sample	Sm I.D.	Sm RNAA	Nd I.D.	Nd RNAA	Sm/Nd I.D.	Sm/Nd RNAA
2981	0.443	0.426	1.641	1.65	0.270	0.258
2982	0.278	0.266	0.983	0.97	0.283	0.274
2983	0.428	0.429	1.437	1.47	0.298	0.292
1129-4	0.635	0.623	2.01	1.95	0.316	0.319
1127-5	0.779	0.769	2.69	2.69	0.290	0.286
2984	0.607	0.602	2.10	2.09	0.280	0.288
2985	1.166	1.13	4.83	4.72	0.241	0.239
2986	0.968	0.972	4.11	4.44	0.235	0.219
2987	0.723	0.689	3.07	2.95	0.235	0.234
2980	0.491	0.508	1.787	1.85	0.275	0.275
28-1	0.313*	0.574	0.889*	1.72	0.353	0.334
30-1	0.619	0.633	1.737	1.88	0.356	0.337
39-1	0.613	0.604	1.753	1.76	0.350	0.343
43-2	0.847*	1.00	2.41*	2.93	0.351	0.341
46-1	1.233*	1.99	3.40*	5.41	0.363	0.368

* liquid splits

4% or better. Accuracy of the measurements can be estimated from the values listed for BCR-1, and also from comparison of RNAA values for Sm and Nd with later analyses of these elements by isotope dilution (Table A-II-3). Sm and Nd values by the two techniques agree withing 4%, except for one value (Nd for sample 2986, 8% difference), and are neither systematically high or low by either method. Sm/Nd ratios by the two techniques agree within 5% (except 2986 at 7%) and Sm/Nd ratios by RNAA are systematically low (12 out of 15 samples). This could be an error introduced by the choice of values for BCR-1.

C) Isotopic Analyses:

Isotopic analyses for Sr and Nd were performed using techniques described in Zindler (1980), and Pb-isotopic analyses were performed using the technique of Pegram (personal communication).

Nd isotopic analyses were performed on a minimum of 500 ng Nd, assuming 100% chemical yield. For some boninites this involved dissolution of up to 500 mg of rock powder. In order to lower blank levels, 10-15 ml pure 2-bottle HF was used in these dissolutions with ~1 ml Ultrex perchloric acid. Dissolved samples were split over 3 ion exchange columns and REE were collected earlier than the normal calibration, as suggested by Zindler (1980). The three REE collections were combined and run through Teflon columns for separation of Nd. Three whole procedure blanks for this technique measured from 10/80 to 9/81 were from 0.2 to 0.3 ng.

Nd isotopic data was usually collected until samples no longer yielded statistically good data, and values are based on an average of 200 to 500 ratios, except for sample 2982 (0.98 ppm Nd), for which only 120 ratios

were obtained. Because of variation in $^{143}Nd/^{144}Nd$ values noted after an alteration in the VRE, values measured after 9/80 are normalized to a value of BCR-1, $^{143}Nd/^{144}Nd = 0.51263$, reported by Zindler (1980) before the alteration. The normalizing value was calculated by averaging values for BCR-1 reported by all users. In addition, in order to ensure internal consistency in each data set, one sample from each data set was rerun at each session. Six of ten samples from Guam, six of eight Manam samples and two of twelve boninite samples were run on two different dates. Values measured on the same sample on different dates were always within statistical error, after correction for variations in BCR-1 in cases where the average of this value had changed between measurements.

Chemical duplicates were performed on two samples analyzed early in Nd-isotope data collection and are also within statistical error:

60-458-28-1	0.512996 ± 43	(120 ratios)
	0.512963 ± 16	(246 ratios)
60-458-46-1	0.513062 ± 26	(180 ratios)
	0.513053 ± 20	(246 ratios)

Chemistry for Sr-isotope analysis was performed using standard techniques. Three procedure blanks measured from 11/80 to 9/81 ranged from 0.09 - 0.34 ng.

Sr-isotope data is based on an average of 180 to 300 ratios, except for sample 2981 and two plagioclase separates for which 120-180 ratios were obtained. Analyses were repeated if resolution was less than 5K, and usually repeated if resolution was less than 10K. Reruns of samples with resolution 7-10K and 10-25K usually were within statistical error of each other. Reruns of samples with resolution <5K and 10-25K usually resulted in a lower $^{87}Sr/^{86}Sr$ value, by -0.00030 in the worst case.

$^{87}Sr/^{86}Sr$ ratios were normalized to a value of Eimer and Amend $SrCO_3$, $^{87}Sr/^{86}Sr = 0.7080$. The normalizing factor was calculated using values reported by all users, and also changed after 9/80.

D) Isotope dilution analyses:

Sm and Nd were analyzed by isotope dilution using techniques described in Zindler (1980) and using the Zindler-2 spike. Concentrations are based on an average of 2 to 5, 6-ratio blocks of data with total measurement errors in the range 0.03-0.09% for Nd, and 0.05-0.12% for Sm. The reproducibility of these values was not tested, but accuracy can be judged by comparison with values obtained by RNAA.

Rb and Sr concentrations for samples 1129-4, 2981, 2984, 2985, 28-1, 43-2, 46-1, 30-1, 39-1 and 2980 were determined using the Loiselle-2 spike. All Ba analyses, and Rb and Sr analyses for other samples were determined using MES III spike.

Sr and Ba concentrations are an average of values determined from 2 to 5, 6-ratio blocks of data with measurement errors for $^{84}Sr/^{88}Sr$ and $^{136}Ba/^{138}Ba$ in the range 0.02-0.08%. Rb data is based on 21 to 35 $^{85}Rb/^{87}Rb$ measurements with 2σ values in the range 0.02-0.04%.

Agreement between Sr and Rb data collected by isotope dilution and XRF analyses by other researchers was usually good. Differences between I.D. values and XRF data for Manam samples (Chappell, personal comm.) range from 0.28 to 2.7% for Sr and 0.11 to 5.3% for Rb. Differences between I.D. data and XRF data for boninites (Jenner, personal comm.) range from 0.33 to 4.0% for Sr and 0.33 to 8.11% for Rb.